Stereodivergent Approach to the Total Synthesis of Selected syn *trans* and anti *trans* Δ^{13}-9-isofurans

By

Calvin James Larson

Dissertation

submitted to the faculty of the

graduate school of Vanderbilt University

in partial fulfillment of the requirements

for the degree of

DOCTOR OF PHILOSOPHY

In

Chemistry

August 12, 2022

Nashville, Tennessee

Approved:

Gary Sulikowski, Ph.D.

Carmelo Rizzo, Ph.D.

Nathan Schley, Ph.D.

Steven Townsend, Ph.D.

James West, Ph.D.

For Danielle

"Cause tramps like us, baby, we were born to run”

Bruce Springsteen

Acknowledgements

When I came to Vanderbilt University, I knew earning a Ph.D. in chemistry would be a monumental task. Luckily, I was given the opportunity to work for Gary Sulikowski. His determination, passion and intelligence helped guide me through my graduate studies and transform me into the chemist I am today. Furthermore, his unwavering support to pursue my interest in gaining industry experience by allowing me to move to Boston for a year and work at GlaxoSmithKline in their Encoded Library Technology group. This experience was one of the best learning opportunities in my professional career and it would not have happened without his support.

I have also been blessed with a phenomenal dissertation committee containing Dr. Carmelo Rizzo, Dr. Steve Townsend, Dr. Nathan Schley, and Dr. James West. Their advice in my graduate studies was instrumental to my success as a chemist.

The best part of joining a chemistry lab is to get to know all the chemists in the lab and learn the ins and outs of organic chemistry. I would like to thank Dr. Robert Davis for being a great mentor and friend in the Sulikowski lab. Dr. Jennifer Kimbrough was my first mentor in graduate school, and I am forever grateful for the advice and support. Dr. Christopher Fullenkamp is a phenomenal chemist and I always admired and was inspired by his work ethic. Dr. Jason Hudlicky always could find a way to crack a joke and break ice in a room no matter the situation. Dr. Quinn Bumpers is a phenomenal chemist and a great benchmate who always made sure our shared equipment was working, plus he always had a great playlist to listen to on Friday afternoon. Dr. Zach Austin is a great chemist, I always enjoyed joking around with him, and it was a pleasure to work on the same project as him. I always enjoyed discussing my chemistry problems, along with collaborating on CBAS and talking about The Boys with Dr.

Alexander Allweil. Dr. Jade Williams is a great chemist and a phenomenal human being, I will always appreciate her advice and perspective. Finally, former lab mate Danielle Penk is wonderful to work with, her attention to detail and experimental care are matched by few.

Outside of the Sulikowski lab there are plenty of people who acknowledgment. The first is Johny Nguyen he is a great chemist, friend, and roommate. His late-night shower singing is memorable and always bring me cheer. Will Weeks was another great roommate and friend whose friendship I will cherish, plus he is always down to grab a beer and chat. Madison Wright was a great roommate, and his sarcasm is always appreciated. Joshua Elder is a great friend who always laughs at my jokes, even if they are bad. Chris Sharp always knows how to make me laugh and loves to teach me about building computers.

The Lindsley lab became a second home lab to me, Dr. Jeanette Bertron, Dr. Caitlin Kent, and Jacob Kalbfleisch whole heartedly welcomed me into their lab as an equal, they were always supportive, welcoming and took the time to let me give research updates to them. Their chemical intuition and advice were invaluable to my growth as a scientist.

In my time at GSK, I had the opportunity to work with a variety of talented scientists. I would like to thank Dr. Westley Tear for passing on his expertise in medicinal chemistry, DEL selections and scientific communication, he was a great mentor. I would like to also thank Dr. Minxue Huang for being a second mentor who taught me the importance of deep thought, how to develop DEL technology and her patience introducing me to new techniques I had not been exposed to beforehand. Other notable friends and colleagues at GSK are Dr. Adam Csaki, Dr. Jingyi Want, Dr. Lisa Marcaurelle, Dr. Melissa Grenier-Davies, Dr. Prolay Mondal, Alice Long, Sophie Op, Dr. Yun Ding, Jing Chai, Maureen Pontarelli, Dr. Logan Combee, Dr. Mark Mantell, Victoria Wu, Dr. Sarah Scott, Dr. Farhana Islam, Dr. Christopher Arico-Muendel, and Dr. Bing

Xia. Finally, I was blessed with a great group of other interns at GSK, Evgenia Semenova, Molly Hu and Patrick Neil are fantastic scientists, and they are even better friends I am glad for their friendship and look forward to seeing them in the future.

My family's support has been unwavering over the past five years, I would like to thank my parents, Jim, and Janelle Larson for encouraging me to pursue my higher academic interests and always let me blow off steam. My brother, Brad Larson, always reminded me about the importance of excellence and how hard work can pay off in the long run. Last, but certainly not least I would like to thank my Fiancée Danielle Penk for her unwavering love and support. She always holds me to the highest standards possible and she makes me a better man, I look forward to spending the rest of my life with her.

Table of Contents

List of Tables

List of Figures

List of Schemes

List of Abbreviations

2,2-DMP	2,2-dimethoxypropane
9-BBN	9-borbicyclo[3.3.1]nonane
AA	arachidonic acid
Ac	acetyl
AcOH	acetic acid
AcO_2	acetic anhydride
BMPR2	bone morphogenic protein receptor type 2
CBS	Corey-Bakishi-Shibata
d	doublet
Da	Dalton
DCC	dicyclohexylcarbodiimide
DDQ	2,3-dichloro-5,6-dicyano-1,4-benzoquinone
DEAD	diethyl azodicarboxylate
DIBAL	diisobutylaluminum hydride
DMAP	4-dimethylaminopyridine
DMF	N, N-dimethylformamide
DMP	Dess-Martin periodinane
Et	ethyl
Et_2O	diethyl ether
EtOAc	ethyl acetate
g	gram
GC-MS	gas chromatography-mass spectrometry
GPR55	G protein-coupled receptor 55
H_2O_2	hydrogen peroxide
ImH	imidazole
IsoF	isofuran
IsoP	isoprostane
L	liter
LDA	lithium diisopropylamide
LAH	lithium aluminum hydride
LC/MS	liquid chromatography/mass spectrometry
LRMS	low resolution mass spectrometry
m	multiplet
M	molar concentration
Me	methyl
MeCN	acetonitrile
MHz	megahertz
mol	mole
Ms	methanesulfonate
NaHMDS	sodium bis(trimethylsilyl)amide
n-BuLi	*n*-butyllithium
NCS	N-chlorosuccinimide
NEt_3	triethylamine
PAH	pulmonary arterial hypertension

PCC	pyridinium chlorochromate
$PGF_{2\alpha}$	prostaglandin $F_{2\alpha}$
PGG_2	prostaglandin G_2
PhH	benzene
PhMe	toluene
PMVEC	pulmonary microvascular endothelial cell
PNBA	4-nitrobenzoic acid
p-TSA	para-toluenesulfonic acid
ROS	reactive oxygen species
s	singlet
SAD	Sharpless asymmetric dihydroxylation
SAE	Sharpless asymmetric epoxidation
t	triplet
TBACl	tetrabutylammonium chloride
TBAF	tetrabutylammonium fluoride
TBDPSCl	*tert*-butyldiphenylchlorosilane
TBSCl	*tert*butyldimethylchlorosilane
TEMPO	2,2,6,6-Tetramethylpiperidin-1-yl)oxyl
Tf_2O	trifluoromethanesulfonic anhydride
TFA	trifluoroacetic acid
THF	tetrahydrofuran
$TMSCHN_2$	(trimethylsilyl)diazomethane
TMSCl	trimethylsilyl chloride
TrCl	trityl chloride

Chapter 1 Enzymatic and Non-Enzymatic Oxidation of Arachidonic Acid

Arachidonic Acid (AA) (**Figure 1.1**) is a non-essential polyunsaturated fatty acid with four sites of unsaturation obtained through consumption of meat, eggs, and seafood. Alternatively, AA can be produced *in vivo* from endogenous linoleic acid.[1] Of high physiological importance, arachidonic acid is enzymatically oxidized by cyclooxygenases, COX-1 and COX-2, to prostaglandin H_2 (PGH_2). The latter serves as a substrate of multiple enzymes leading to formation of several physiologically active oxidation products including prostacyclins, thromboxanes, Prostaglandin E 2 (PGE_2), and prostaglandin D 2 (PGD_2) (**Figure 1.1**).[2]

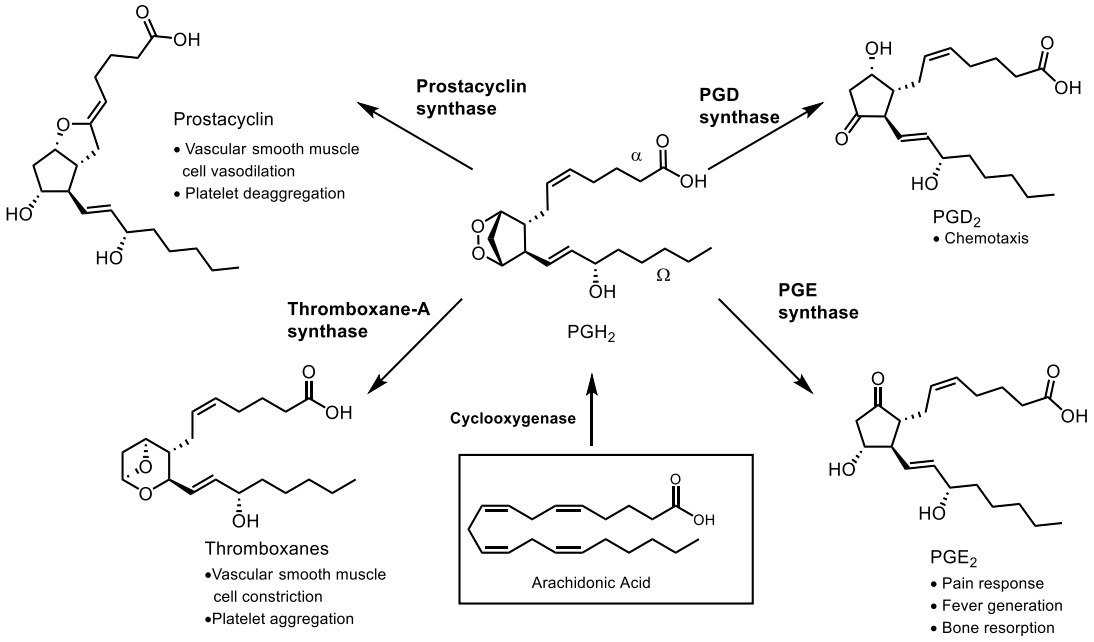

Figure 1.1 Cyclooxygenase mediated conversion of arachidonic acid to PGH_2 and enzyme mediated pathways to physiologically active metabolites.

The enzyme-derived arachidonic acid metabolites summarized in **Figure 1.1** have been studied extensively and shown to have significant biological activity.[2] Traditionally, enzyme-derived products of AA were thought to be the only arachidonic acid derived metabolites. This dogma stood because specific enzymes were assumed to have evolved to produce physiologically important metabolites with no other non-enzymatic metabolic pathways in existence.

It was later discovered arachidonic acid (AA) is also non-enzymatically oxidized by a sequence of events starting with abstraction of one of three bis-allyic hydrogen atoms by reactive oxygen species (ROS) such as hydroxyl radical, nitric oxide or superoxide. As reactive free-radicals, these ROS species readily abstract one of the three bi-allylic hydrogens (C7, C10 or C13).[3] Abstraction of bis-allylic hydrogen atoms readily occurs due to the relatively weak C-H bonds with a Bond Dissociation Energy (BDE) of approximately 73 kcal/mol. This is more than 10 kcal lower than a simple allylic C-H bonds with a BDE of *ca*. 84 kcal/mol and far lower in energy than isolated aliphatic C-H bond which has a BDE of *ca*. 100 Kcal/mol (**Figure 1.2**).[4] Abstraction of one of the three bi-allylic hydrogen atoms of the C-H bonds leads to generation of the corresponding carbon radical leading to series of events to produce cyclo-oxidized products.

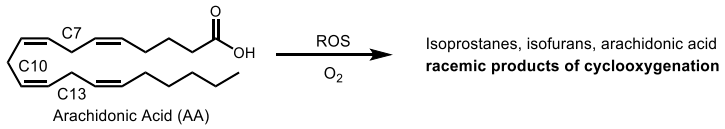

Figure 1.2 Bis-allylic C-H bonds C7, C10, and C13 subject to hydrogen abstraction leading to non-enzymatic cyclooxygenation products including isoprostanes and isofurans.

Isoprostanes

The first observation of arachidonic acid non-enzymatic oxidation was reported in 1967; however, it was largely ignored until isoprostanes were rediscovered by the Roberts group in 1990.[3,5] The first series of isoprostanes discovered by the Roberts group proved to have a cyclopentane ring core similar to $PGF_{2\alpha}$ (**Figure 1.3**), giving rise to the name "F-isoprostanes".[5] Based on the proposed synthesis of the isoprostanes and mass spectrometry data there are 8 possible substitution patterns of the cyclopentane ring in the isoprostanes with their name derived from prostaglandins nomenclature (**Figure 1.3**).

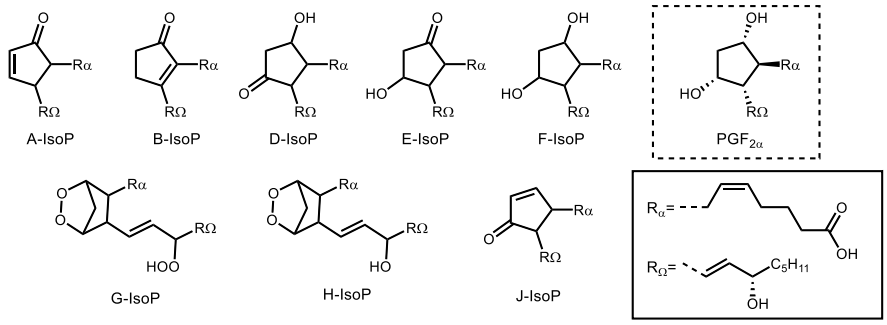

Figure 1.3 Classification of Isoprostanes based off the substitution pattern of the cyclopentane ring.

Autooxidation of Arachidonic Acid to Isoprostanes

Isoprostanes are derived from arachidonic acid following radical mediated hydrogen atom abstraction of the C7, C10, or C13 position (**Figure 1.4**) leading to radical intermediates **1.2-1.4.** The latter react with molecular oxygen to afford peroxy radical intermediates **1.5-1.7.** A 5-*exo-trig* cyclization of the intermediate radical onto a neighboring carbon-carbon double bond affords endoperoxides **1.8-1.10**. Then, a 5-*exo-trig* cyclization will forge the cyclopentane ring of the isoprostane giving rise to intermediates **1.11-1.13**.

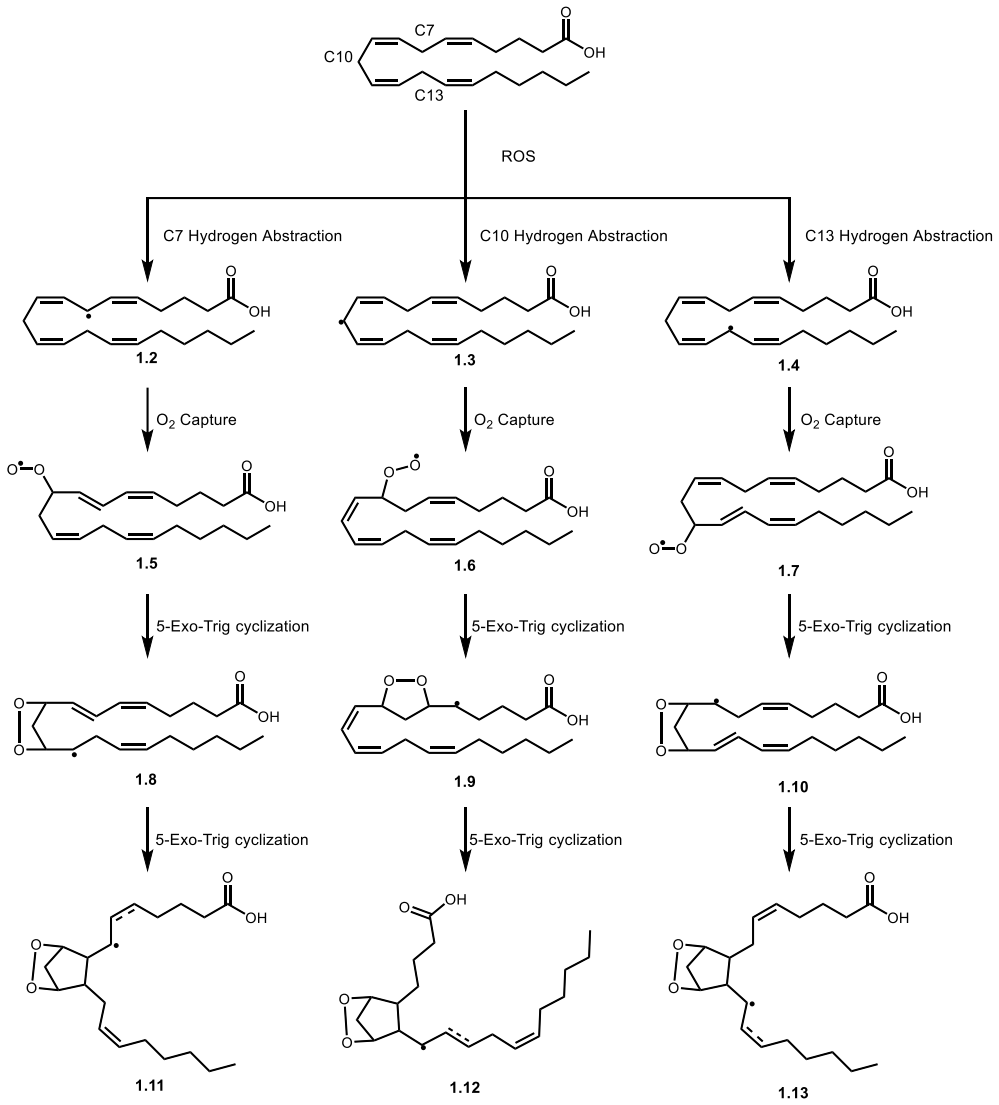

Figure 1.4 Oxidation of the C7, C10, and C13 CH bonds by ROS allows for conversion to endoperoxides **1.11**, **1.12** and **1.13**

The corresponding radical captures another molecule of oxygen, leading to peroxides **1.15-1.16 (Figure 1.5**). Finally, reduction of the peroxide affords F-2 isoprostanes (**1.17-1.19**), analogous pathways starting with abstraction of other bis-allylic hydrogen atoms are shown to lead to isomeric F-2 isoprostanes. For a thorough review of the synthesis of isoprostanes the reader is directed to the comprehensive review of Jahn *et al.*[3]

.

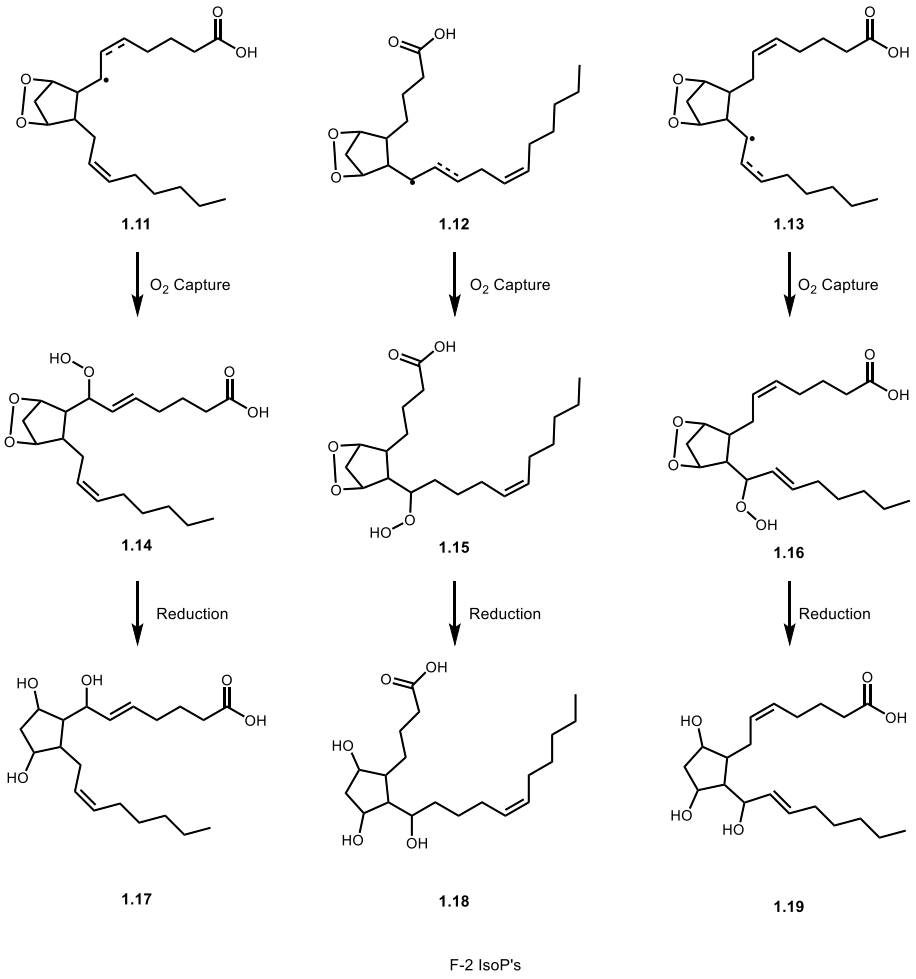

Figure 1.5 Conversion of endoperoxides **1.11**, **1.12**, and **1.13** to the final isoprostanes

Isofurans

In 2002 the Roberts group at Vanderbilt University discovered a second class of non-enzymatically oxidized AA metabolites called isofurans. Through the application of tandem MS-MS analysis, the structure of eight constitutional isomers termed isofurans was proposed, based on a common tetrahydrofuran core incorporating two side chains (**Figure 1.6**). The two side chains were proposed to be positioned across the tetrahydrofuran oxygen atom with one terminated in a carboxylic acid moiety (α side chain) and the second with an aliphatic group (Ω side chain).[6]

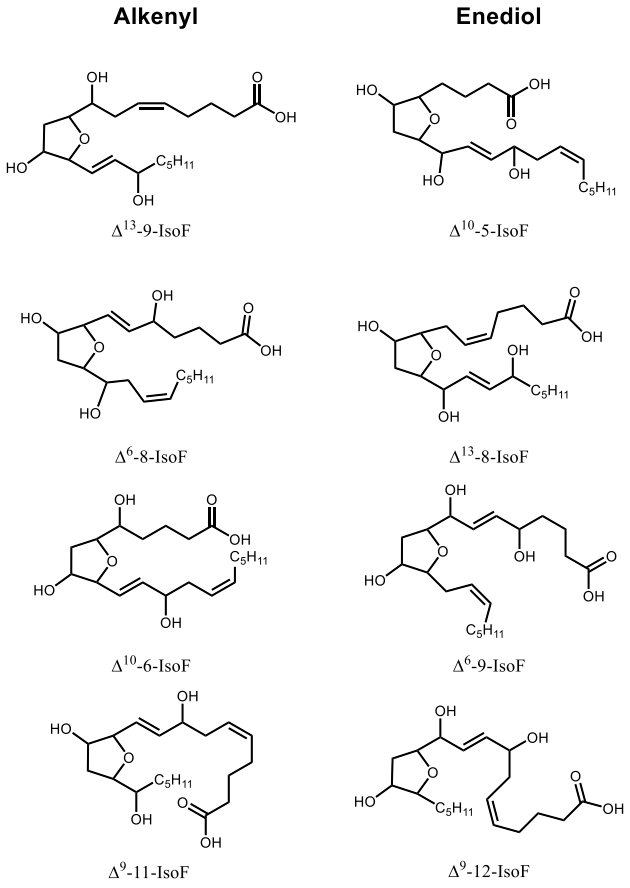

Figure 1.6. All eight stereoisomers of the isofurans are shown, they are separated by the alkenyl and the enediol class.

Isofurans can be further broken down into two classes, the alkenyl isofurans which have one hydroxyl group on each side chain and enediol isofurans incorporating a unique enediol on the side chain. Since the isofurans are synthesized non-enzymatically, all stereocenters are produced as a racemic mixture. Because there are five stereocenters in each constitutional isomer, each will consist of 32 stereoisomers. As eight constitutional isomers were identified by mass spectrometry-assisted analysis, 256 isomeric isofurans are possible.

With a total of 256 isomeric isofurans a nomenclature system was required to systematically identify each unique isofuran by name. The Roberts and Taber groups proposed a nomenclature system while the Taber group was developing a synthetic strategy to access individual isofurans.[7] Their nomenclature system started with the standard eicosanoid system of

numbering of carbons (1 to 20) with the carboxylic acid carbon assigned C1. In this nomenclature system the constitutional isomers of the isofurans are assigned by the number of the first furan associated carbon (cf. 9-isofuran, **Figure 1.7**). Isomers are further distinguished by the number of the first allylic alcohol E-alkene carbon and designate Δ as a site of unsaturation and the number of the carbon superscripts. (cf. Δ^{13}-9-isofuran, **Figure 1.7**). Nomenclature to indicate relative stereochemistry starts with the relative orientation of the two alkyl chains flanking the furan oxygen. If side-chains are oriented on the same side of the furan ring they are assigned "syn" and labeled with the prefix "S"; conversely alkyl chains opposite to each other are assigned the prefix A or "anti". The furan hydroxyl group is designated *cis* (C) or *trans* (T) depending on its relative orientation to the neighboring (vicinal) alkyl side-chain. Designation of stereochemistry of the first furan ring carbon and hydroxyl groups starts with both assigned S-configuration as "natural" by relation to the natural S-configuration of prostaglandin secondary alcohols. If the isofuran "first ring carbon" is of the R configuration that isofuran is assigned the prefix "ent". Similarly, if side-chain hydroxy groups are of the "unnatural" R configuration that carbon is assigned the prefix "epi" (cf. **Figure 1.8)**.

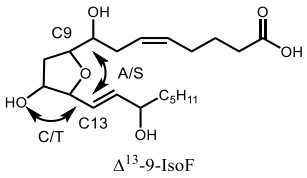

Δ^{13}-9-IsoF

Figure 1.7 Δ^{13}-9-isofuran highlighting the C9 carbon as the first carbon of the furan ring and the C13 carbon as the first olefin of the allylic alcohol. The two alkyl chains determine the A or S.

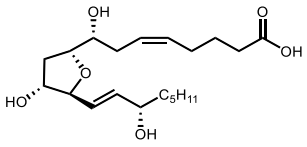

ent-15-epi-AT-Δ^{13}-9-IsoF

Figure 1.8 Example of a fully named isofuran.

Autooxidation of Arachidonic Acid to Isofurans

Intimately associated with the assignment of isofuran structure was Roberts group's study of their formation using oxygen-18 and H_2O^{18} labeling studies. Of course, this was necessary as isofurans like many human metabolites, are produced in small quantity as an unmanageable mixture of isomers. These labeling studies show that isofurans were synthesized with the incorporation of one atom of oxygen when using water and three atoms of oxygen based on studies using oxygen-18. An alternate pathway where isofurans could also be synthesized with four molecules of oxygen incorporated was also observed.[8] Using this information Roberts and co-workers suggested two unique pathways for isofurans synthesis either *in vivo* or *ex vivo*. The first pathway suggested is designated the "Cyclic Peroxide Cleavage Pathway (CPCP)" (**Figure 1.9** and **1.10**).

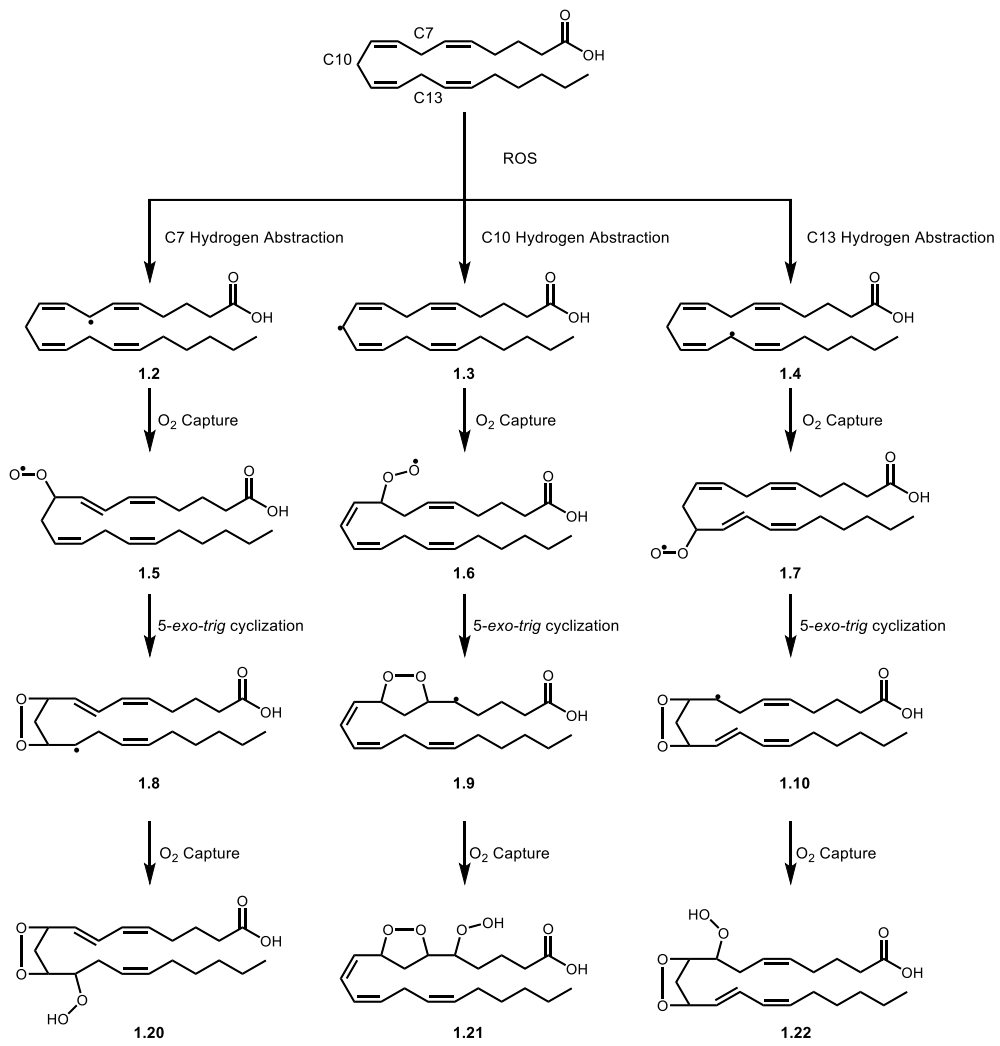

Figure 1.9. Oxidation of Arachidonic Acid *via* ROS to di-peroxides **1.20**, **1.21**, and **1.22** in route to isofurans through the CPCP pathway.

The Cyclic Peroxide Cleavage Pathway is proposed to start, like the isoprostanes, with ROS mediated hydrogen abstraction at either the C7, C10, or C13 positions of AA to afford bis-allylic radical intermediates **1.2-1.4**. The resulting free-radicals then capture a molecule of oxygen leading to peroxy radicals **1.5-1.7** which following a five-*exo-trig* cyclization yields endoperoxides **1.8-1.10**. Notably, the latter endoperoxides are proposed intermediates enroute to previously described isoprostanes. However, under high oxygen concentration free-radical intermediates (**1.8-1.10**) are proposed to capture a second molecule of oxygen to afford hydroperoxides **1.20-**

1.22 following hydrogen atom capture. Reductive cleavage of the endoperoxide releases an allylic oxygen radical which undergoes a 3-*exo-trig* cyclization (aka 1,3 S_Hi) to afford a series of allylic radical intermediates **1.23-1.25**, which capture a molecule of oxygen to give rise to allylic peroxides **1.26-1.28** (**Figure 1.10**). Reduction of the peroxides enables a 5-*exo-tet*-cyclization leading to the furan core structure common to the isofurans. As described this pathway can produce four of the constitutional isomers of the isofurans (Δ^6-8-IsoF, Δ^{10}-6-IsoF, Δ^9-11-IsoF, and Δ^9-11-IsoF).

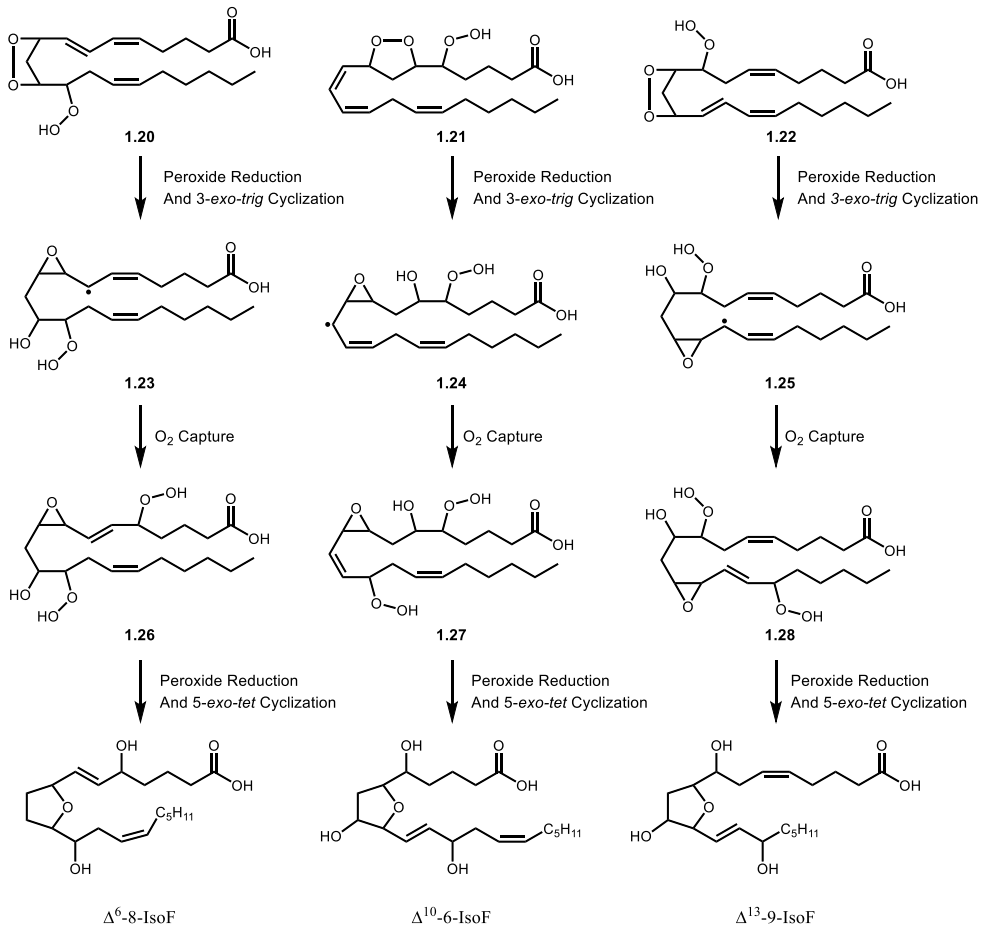

Figure 1.10. Continued synthesis of compounds **1.20**, **1.21**, and **1.22** to isofurans via the CPCP pathway.

The second proposed pathway, incorporating four molecules of oxygen, is called the Epoxide Hydrolysis Pathway (EHP) (**Figure 1.11**). This pathway begins from **1.8-1.10** which is

a common intermediate from the Cyclic Peroxide Cleavage (CPC) pathway and the proposed synthesis of the isoprostanes.

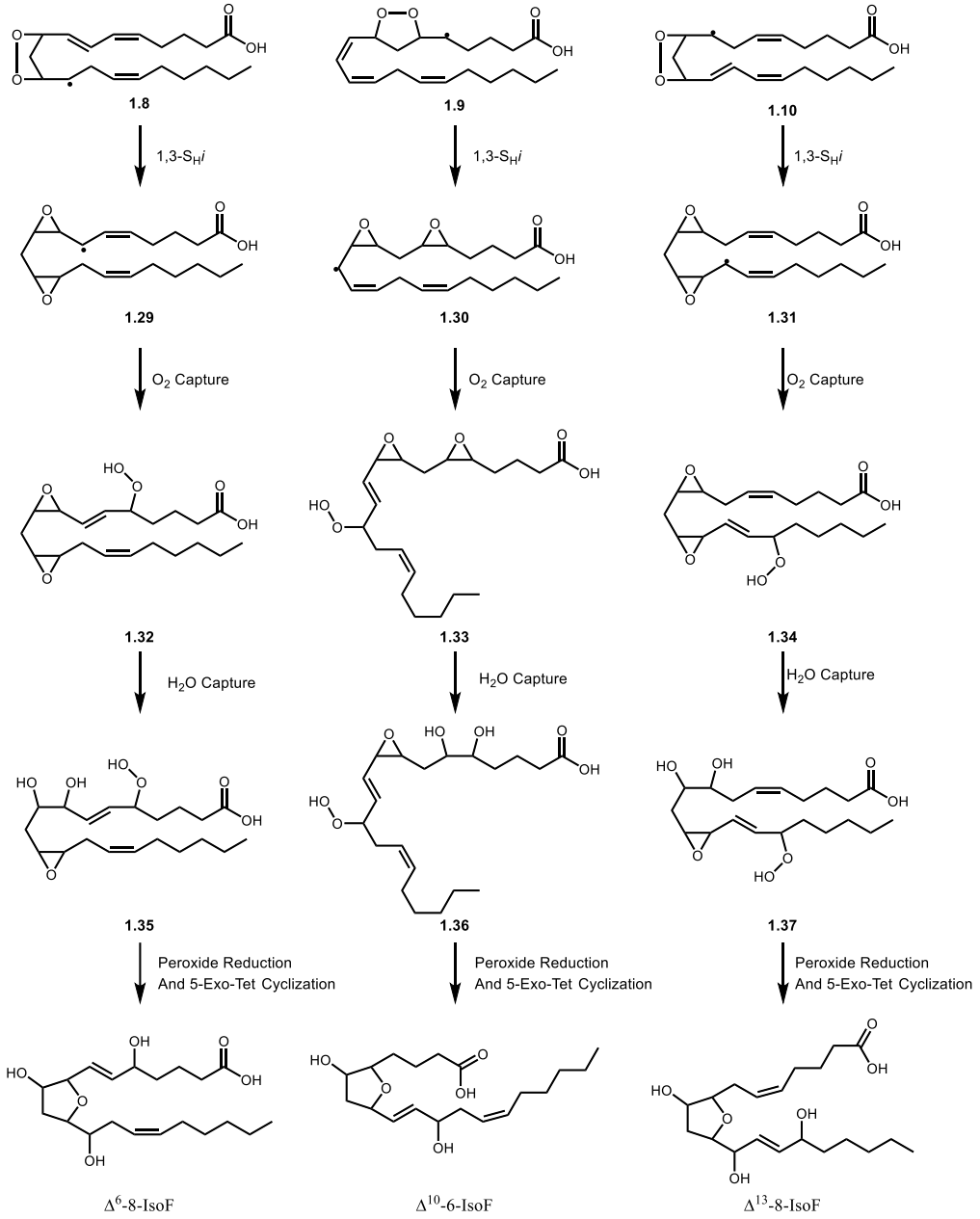

Figure 1.11. Synthesis of isofurans by the EHP from compounds **1.8**, **1.9**, and **1.10**.

With alkyl radicals **1.8-1.10** formed they will undergo an analogous 3-*exo-trig* cyclization (aka 1,3 S$_H$*i*) reaction to form bis-epoxide compounds **1.29-1.31**.[9,10] Then the corresponding alkyl radical will capture a molecule of oxygen to give rise to allylic peroxides **1.32-1.34**. Subsequently,

water initiates a nucleophilic epoxide opening to afford diols **1.35-1.37.** Finally, the peroxides are reduced to reveal a secondary hydroxyl group which will undergo a 5-*exo-tet* cyclization to install the furan core and give rise to the isofurans. The Epoxide Hydrolysis Pathway (EHP) can give rise to all 8 constitutional isomers of the isofurans whereas the Cyclic Peroxide Cleavage Pathway (CPC) can only access four of the isofuran stereoisomers.[3,6]

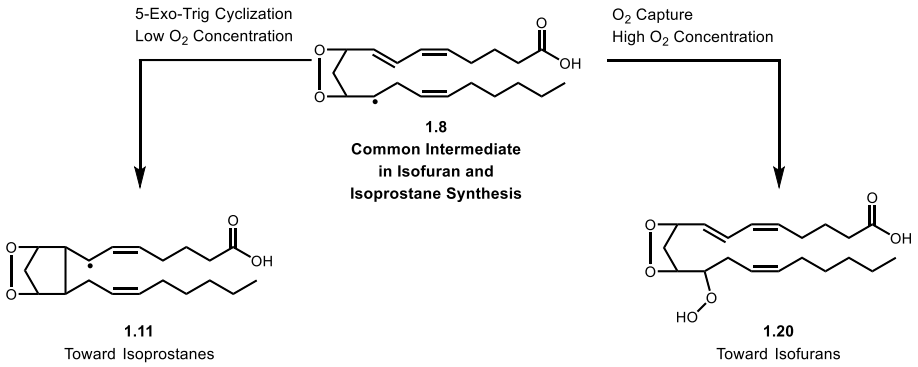

Figure 1.12. Endoperoxide **1.8** is a common intermediate for the synthesis of both isofurans and isoprostanes. Isofuran production is favored by high levels of oxygen which allows for radical capture of molecular oxygen creating intermediate **1.20**. Under low levels of oxygen intermediate **1.8** will undergo a 5-*exo-trig* cyclization to afford compound **1.11** which reacts further to become an isoprostane.

In accord with the isoprostane-isofuran oxygen mediated branching point (**Figure 1.5** and **Figure 1.12**) the Roberts group observed the effect of oxygen concentration on the ratio of isofurans verses isoprostanes. Given the difference of oxygenation in isofurans *verses* isoprostanes, they hypothesized that under low concentrations of oxygen isoprostanes would be favored, while under conditions of high oxygen the synthesis of isofurans would be favored. They tested this hypothesis *ex vivo* and discovered as oxygen tension increased, the isofurans were favored over the isoprostanes. Next, they studied the trend *in vivo*. Using rats treated with carbon tetrachloride, a known compound to induce oxidative stress and increase levels of ROS.[11,12] They discovered the liver, which is an oxygen-poor organ, favored the synthesis of isoprostanes. While analyzing isoprostanes and isofurans in the hippocampus and kidneys, which are oxygen rich

organs, they discovered higher levels of isofurans *verses* isoprostanes. This suggests that under high oxygen conditions isofurans formed are preferentially over isoprostanes while in low oxygen conditions isoprostanes are favored. This can be explained through the proposed synthesis of the isofurans and isoprostanes (**Figure 1.12**).

Isoprostane and Isofuran Relevance to Diseases of Oxidative Stress

Isoprostanes are currently the gold standard for measuring oxidative stress in the body.[13] This is because isoprostanes are stable, and produced independently of COX-1 and COX-2 rather than through lipid peroxidation pathways (**Figure 1.5 and 1.6**). They are naturally synthesized in the body, detectable in biological tissue and have a known normal physiological range. Isoprostane levels are known to increase upon oxidative injury, and their levels in the body are independent of lipid diet.[13,14]

Isoprostanes have also been shown to be one of the best indicators of carbon tetrachloride oxidative damage (oxidative stress). In an NIH study while exploring the best ways to measure oxidative damage by carbon tetrachloride, they discovered 8-*iso*-$PGF_{2\alpha}$ in blood plasma correlated with oxidative damage from carbon tetrachloride, showing 8-*iso*-$PGF_{2\alpha}$ is a good indicator of oxidative stress. Furthermore, 8-*iso*-$PGF_{2\alpha}$ is detectable in urine which offers a significant advantage over plasma because it allows a noninvasive way to measure levels of 8-*iso*-$PGF_{2\alpha}$ in the body. They also discovered that measuring oxidized proteins or DNA would not be indicative of oxidative damage from carbon tetrachloride, further showing that isoprostanes are currently the best indicator of oxidative damage.[15]

Oxidative stress is an imbalance between ROS in the body and antioxidants, where elevated levels of ROS will cause oxidative damage in the body. Some diseases associated with oxidative stress are aging, acute and chronic kidney disease, Alzheimer's, Parkinson's disease,

atherosclerosis, and pulmonary arterial hypertension. Isoprostanes have been shown to be elevated in chronic obstructive pulmonary disease (COPD), Parkinson's disease, Alzheimer's, and pulmonary arterial hypertension. Furthermore, isoprostanes have been shown to have increased levels in chronic kidney disease and as the disease progresses the levels of isoprostanes increases.[16] Isoprostanes have been studied significantly in diseases of oxidative stress because there is a strong correlation between levels of isoprostanes and diseases of oxidative stress. A drawback of using isoprostanes as a measure of oxidative stress is that under conditions of high oxygen tension the formation of isoprostanes is diverted to isofuran production. Given oxygen tension modulates the formation of isoprostanes and isofurans, it difficult to measure oxidative stress in conditions of high oxygen, like in the lungs after hypoxia.[13] It is possible isofurans may be a superior biomarker to isoprostanes for oxidative stress in highly oxygenated tissues because isoprostane synthesis is limited under conditions of high oxygen. Isofurans are preferentially formed making them superior biomarkers of oxidative stress in certain cases of high oxygen tension (in organs such as the kidney, or brain). Synthetically pure isofurans are needed to as internal standard so that more accurate and precise levels of isofurans can be measured in tissue to further examine their role in diseases of oxidative stress.

References

(1) Tallima, H.; El Ridi, R. Arachidonic Acid: Physiological Roles and Potential Health Benefits – A Review. *J. Adv. Res.* **2018**, *11*, 33–41. https://doi.org/10.1016/j.jare.2017.11.004.

(2) Funk, C. Prostaglandins and Leukotrienes: Advances in Eicosanoid Biology. *Science (80-.).* **2001**, *294*, 1871–1875.

(3) Jahn, U.; Galano, J. M.; Durand, T. Beyond Prostaglandins - Chemistry and Biology of Cyclic Oxygenated Metabolites Formed by Free-Radical Pathways from Polyunsaturated Fatty Acids. *Angew. Chemie - Int. Ed.* **2008**, *47* (32), 5894–5955. https://doi.org/10.1002/anie.200705122.

(4) Pratt, D. A.; Mills, J. H.; Porter, N. A. Theoretical Calculations of Carbon-Oxygen Bond

Dissociation Enthalpies of Peroxyl Radicals Formed in the Autoxidation of Lipids. *J. Am. Chem. Soc.* **2003**, *125* (19), 5801–5810. https://doi.org/10.1021/ja034182j.

(5) Morrow, J. D.; Harris, T. M.; Jackson Roberts, L. Noncyclooxygenase Oxidative Formation of a Series of Novel Prostaglandins: Analytical Ramifications for Measurement of Eicosanoids. *Anal. Biochem.* **1990**, *184* (1), 1–10. https://doi.org/10.1016/0003-2697(90)90002-Q.

(6) Fessel, J. P.; Porter, N. A.; Moore, K. P.; Sheller, J. R.; Roberts, L. J. Discovery of Lipid Peroxidation Products Formed in Vivo with a Substituted Tetrahydrofuran Ring (Isofurans) That Are Favored by Increased Oxygen Tension. *Proc. Natl. Acad. Sci. U. S. A.* **2002**, *99* (26), 16713–16718. https://doi.org/10.1073/pnas.252649099.

(7) Taber, D. F.; Fessel, J. P.; Roberts, L. J. A Nomenclature System for Isofurans. *Prostaglandins Other Lipid Mediat.* **2004**, *73* (1–2), 47–50. https://doi.org/10.1016/j.prostaglandins.2003.11.004.

(8) Fessel, J. P.; Roberts, L. J. Isofurans: Novel Products of Lipid Peroxidation That Define the Occurrence of Oxidant Injury in Settings of Elevated Oxygen Tension. *Antioxid. Redox Signal.* **2005**, *7*, 202–209.

(9) Bloodworth, A. J.; Courtneidge, J. L.; Davies, A. G. Rate Constants for the Formation of Oxiranes by γ-Scission in Secondary β-t-Butylperoxyalkyl Radicals. *J. Chem. Soc. Perkin Trans. 2* **1984**, No. 3, 523–527. https://doi.org/10.1039/p29840000523.

(10) Porter, N. A.; Nixon, J. R. Stereochemistry of Free-Radical Substitution on the Peroxide Bond. *J. Am. Chem. Soc.* **1978**, *100* (22), 7116–7117. https://doi.org/10.1021/ja00490a079.

(11) Morrow, J. D.; Awad, J. A.; Boss, H. J.; Blair, I. A.; Roberts, L. J. Non-Cyclooxygenase-Derived Prostanoids (F2-Isoprostanes) Are Formed in Situ on Phospholipids. *Proc. Natl. Acad. Sci. U. S. A.* **1992**, *89* (22), 10721–10725. https://doi.org/10.1073/pnas.89.22.10721.

(12) Karara, A.; Dishman, E.; Falck, J. R.; Capdevila, J. H. Endogenous Epoxyeicosatrienoyl-Phospholipids: A Novel Class of Cellular Glycerolipids Containing Epoxidized Arachidonate Moieties. *J. Biol. Chem.* **1991**, *266* (12), 7561–7569. https://doi.org/10.1016/s0021-9258(20)89484-8.

(13) Montuschi, P.; Barnes, P. J.; Roberts, L. J. Isoprostanes: Markers and Mediators of Oxidative Stress. *FASEB J.* **2004**, *18* (15), 1791–1800. https://doi.org/10.1096/fj.04-2330rev.

(14) Roberts, L. J.; Morrow, J. D. Measurement of F2-Isoprostanes as an Index of Oxidative Stress in Vivo. *Free Radic. Biol. Med.* **2000**, *28* (4), 505–513. https://doi.org/10.1016/S0891-5849(99)00264-6.

(15) Kadiiska, M. B.; Gladen, B. C.; Baird, D. D.; Germolec, D.; Graham, L. B.; Parker, C. E.; Nyska, A.; Wachsman, J. T.; Ames, B. N.; Basu, S.; Brot, N.; FitzGerald, G. A.; Floyd, R. A.; George, M.; Heinecke, J. W.; Hatch, G. E.; Hensley, K.; Lawson, J. A.; Marnett, L. J.; Morrow, J. D.; Murray, D. M.; Plastaras, J.; Roberts, L. J.; Rokach, J.; Shigenaga, M. K.; Sohal, R. S.; Sun, J.; Tice, R. R.; Van Thiel, D. H.; Wellner, D.; Walter, P. B.; Tomer, K.

B.; Mason, R. P.; Barrett, J. C. Biomarkers of Oxidative Stress Study II. Are Oxidation Products of Lipids, Proteins, and DNA Markers of CCl4 Poisoning? *Free Radic. Biol. Med.* **2005**, *38* (6), 698–710. https://doi.org/10.1016/j.freeradbiomed.2004.09.017.

(16) Tucker, P. S.; Dalbo, V. J.; Han, T.; Kingsley, M. I. Clinical and Research Markers of Oxidative Stress in Chronic Kidney Disease. *Biomarkers* **2013**, *18* (2), 103–115. https://doi.org/10.3109/1354750X.2012.749302.

Chapter 2: Association of Oxidative Stress, Disease and Arachidonic Acid Metabolites

Reactive Oxygen Species

Reactive Oxygen Species (ROS) are produced in elevated amounts when cells experience oxidative stress, often associated with an inflammatory response to a cellular insult such as a pathogen. Hydrogen peroxide/hydroxyl radicals, nitric oxides, and superoxide are the three major reactive oxygen species (ROS). Superoxide ($O_2^{-\bullet}$) is generated from single electron reduction of molecular oxygen to produce an oxygen in the form of a radical anion leading eventually to hydrogen peroxide, a precursor to hydroxyl and hydroperoxyl radicals. The conversion of superoxide to these ROS intermediates occurs in the mitochondria. Within this organelle, endogenous iron(II) reduces hydrogen peroxide to form hydroxyl (HO•) and hydroperoxyl (HOO•) by a process known as the Fenton reaction. These reactive oxygen species can react further in the body in a normal cellular process or cause damage to biomolecules such as proteins or DNA.[17] Normal functions of ROS include acting as secondary messengers in cell signaling or triggering of an immune response resulting in clearance of pathogens.[18] However, there is a fine balance between ROS acting as messengers and acting as a toxic oxidant leading to cellular damage. When the levels of ROS are too high, the body's antioxidants such as glutathione, superoxide dismutase or superoxide reductase cannot clear reactive oxygen species (ROS). This event will place the cell under oxidative stress and the resulting ROS will cause cellular damage.

Pulmonary Arterial Hypertension

A rare disease associated with oxidative stress and isoprostane and isofuran formation is pulmonary arterial hypertension (PAH). PAH is classified as a rare lung disease (500-1000 diagnoses per year) and characterized by high blood pressure in pulmonary artery (greater than 25 mmHg). Its symptoms include scarring and muscularization of the pulmonary arteries, elevated

blood pressure in the pulmonary circuit and ultimately heart failure.[19] PAH patients are found to produce unusually high amounts of isoprostanes and isofurans in comparison to healthy individuals. The relationship of these oxidative AA metabolites is an example of a correlation between an inflammatory disease state, oxidative stress and isoprostane/isofuran metabolites.[20,21] Currently the treatments for PAH are intravenous injection of prostacyclin because it will lower blood pressure by relaxing vascular smooth muscle cells; another treatment is endothelin-receptor antagonists. G-Protein receptor ET_A causes vasoconstriction and proliferation of vascular smooth muscle cells when activated. A second GPCR, ET_B is a receptor which mediates pulmonary endothelin clearance and induces the production of nitric oxide and prostacyclin by endothelial cells. Inhibitors of both proteins have been shown to slow the progress of PAH, unfortunately no cure for PAH exists. Patients are inevitably hospitalized and need lung transplants. In worst case scenarios the patient dies.[22,23] Since there are no cures for PAH there needs to be further study in to its pathology to discover its cause and eventually a cure for PAH.

A variety of factors contribute to the development of PAH. Some contributors include HIV infection, schistosomiasis, scleroderma, cocaine use, oxidative stress in the endoplasmic reticulum, altered estrogen metabolism, and a mutation in the gene Bone Morphogenic Protein Receptor 2 (BMPR2). Heterozygous genetic mutations in BMPR2 have been shown to be present in 70% of Heritable Pulmonary Arterial Hypertension (HPAH) and 10-20% of Idiopathic Pulmonary Arterial Hypertension (IPAH). However, 80% of patients with mutations in BMPR2 never develop PAH, showing other factors drive the disease state.[19]

Role of Isofurans and Isoprostanes in PAH

The West and Fessel groups at Vanderbilt University have conducted preliminary studies aimed at, in part, determining if isofurans and isoprostanes are causative in PAH and/or useful as

a biomarker of PAH. They discovered that mutations in $BMPR2^{R899X}$, which are known to cause HPAH, often lead to oxidative stress and oxidative injury.[24] When measuring the levels of isofurans and isoprostanes in the $BMPR2^{R899X}$ mutated mouse lung cells, they discovered isoprostane production increased by 50% while isofuran production increased by 100%, increasing the ratio of isofurans to isoprostanes from 2.2:3.2 in the control mice versus the $BMPR2^{R899X}$ mutated mice. This suggests there is mitochondrial disfunction in $BMPR2^{R899X}$ mutated mice which results in higher oxygen concentration in the cell, promoting the formation of isofurans over isoprostanes.[24]

The West and Fessel group also studied the role of hyperoxia (oxygen poisoning), and how $BMPR2^{R899X}$ mutated mice react to hyperoxia. In this study they discovered $BMPR2^{R899X}$ mutated mouse PMVEC cells had significantly altered isofuran to isoprostane ratios in the cell mitochondria. In both wild type and $BMPR2^{R899X}$ mutated cells the ratio of isofurans to isoprostanes remained about 1:1. However, in the $BMPR2^{R899X}$ mutated cells the levels of isofurans and isoprostanes increased, showing an increase of oxidative stress in the cells with BMPR2 mutations. Furthermore, when looking at mouse liver mitochondria they discovered the ratio of Isofurans to Isoprostanes in wild type mice is about 1.5:1. However, in the $BMPR2^{R899X}$ mutated mice the ratio of isofurans to isoprostanes shifted to 0.5:1. This suggests the amount of free oxygen in the mitochondria in $BMPR2^{R899X}$ mutated PMVEC cells is decreasing, which indicates that BMPR2 mutations are causing metabolic dysfunction throughout the body, even though the physiological symptoms are limited to the lungs.[25]

Furthermore, the West and Fessel groups studied the role BMPR2 mutations play in altering cellular metabolism. They discovered BMPR2 mutated endothelial cells shifted metabolism toward aerobic glycolysis and variations in the Citric Acid Cycle (TCA). This shows

metabolic reprogramming is a result of BMPR2 knockout or knockdown mutations and implies that BMPR2 induced PAH is a systemic disease which can effect multiple organs.[26] This is also exemplified by altered levels of isofurans and isoprostanes in liver tissue of BMPR2 mutated mice.[25]

Since there is a clear correlation between isofurans, isoprostanes, BMPR2 mutations and HPAH, the Fessel lab at Vanderbilt University accessed several, synthetically pure isofurans. Initial results showed if PVMEC's were treated with certain isofurans, they would induce a BMPR2 mutant phenotype in wild type cells. Also, isofurans were shown to induce abnormal aortic ring vascularization in rat hearts when treated with isofurans. This abnormal vascularization can be suppressed by silencing the protein (G Coupled Receptor 55) GPR55 with hairpin RNA, suggesting GPR55 is critical for the abnormal vascularization. GPR55 is an endocannabinoid receptor which couples to Gα13, which activates Rho, Rac1, and Cdc42 which are members of the Rho-GTPase family that modulates cytoskeletal organization and function.[27,28] Currently there are no known endogenous ligands to GPR55, classifying it as an orphan receptor.[29] Based on the preliminary work by the Fessel group, it is hypothesized that BMPR2 mutations put the body under oxidative stress which produces higher levels of isofurans and isoprostanes. Then the isofurans can activate GPR55 which activates Rho, Rac1 and Cdc42. This causes enhanced cellular proliferation, abnormal angiogenesis and altered cellular motility, thus causing the PAH phenotype. To further explore this hypothesis a flexible and readily divergent synthetic route must be established to access synthetically pure isofurans.

References

(17) Schieber, M.; Chandel, N. S. ROS Function in Redox Signaling and Oxidative Stress. *Curr. Biol* **2014**, *24* (10), R453–R462. https://doi.org/10.1016/j.cub.2014.03.034.

(18) Auten, R. L.; Davis, J. M. Oxygen Toxicity and Reactive Oxygen Species: The Devil Is in

the Details. *Pediatr. Res.* **2009**, *66* (2), 121–127. https://doi.org/10.1203/PDR.0b013e3181a9eafb.

(19) Rabinovitch, M. Molecular Pathogenesis of Pulmonary Arterial Hypertension. *J. Clin. Invest.* **2012**, *122* (12), 4306–4313. https://doi.org/10.1172/JCI60658.

(20) Cracowski, J.-L.; Cracowski, C.; Bessard, G.; Pepin, J.-L.; Bessard, J.; Schwebel, C.; Stanke-Labesque, F.; Pison, C. Increased Lipid Peroxidation in Patients with Pulmonary Hypertension. *Am. J. Respir. Crit. Care. Med* **2001**, *164*, 1038–1042.

(21) Hemnes, A. R.; Rathinasabapathy, A.; Austin, E. A.; Brittain, E. L.; Carrier, E. J.; Chen, X.; Fessel, J. P.; Fike, C. D.; Fong, P.; Fortune, N.; Gerszten, R. E.; Johnson, J. A.; Kaplowitz, M.; Newman, J. H.; Piana, R.; Pugh, M. E.; Rice, T. W.; Robbins, I. M.; Wheeler, L.; Yu, C.; Loyd, J. E.; West, J. A Potential Therapeutic Role for Angiotensin-Converting Enzyme 2 in Human Pulmonary Arterial Hypertension. *Eur. Respir. J.* **2018**, *51* (6). https://doi.org/10.1183/13993003.02638-2017.

(22) Tamura, Y.; Kimura, M. Treatment of Pulmonary Arterial Hypertension. *Japanese J. Chest Dis.* **2015**, *74* (3), 286–294. https://doi.org/10.1056/nejmra040291.

(23) Humbert, M.; Sitbon, O.; Simmonneau, G. Treatment of Pulmonary Arterial Hypertension. *N. Engl. J. Med.* **2004**, *351* (14), 1425–1436.

(24) Lane, K. L.; Talati, M.; Austin, E.; Hemnes, A. R.; Johnson, J. A.; Fessel, J. P.; Blackwell, T.; Mernaugh, R. L.; Robinson, L.; Fike, C.; Roberts, L. J.; West, J. Oxidative Injury Is a Common Consequence of BMPR2 Mutations. *Pulm. Circ.* **2011**, *1* (1), 72–83. https://doi.org/10.4103/2045-8932.78107.

(25) Fessel, J. P.; Flynn, C. R.; Robinson, L. J.; Penner, N. L.; Gladson, S.; Kang, C. J.; Wasserman, D. H.; Hemnes, A. R.; West, J. D. Hyperoxia Synergizes with Mutant Bone Morphogenic Protein Receptor 2 to Cause Metabolic Stress, Oxidant Injury, and Pulmonary Hypertension. *American Journal of Respiratory Cell and Molecular Biology*. 2013, pp 778–787. https://doi.org/10.1165/rcmb.2012-0463OC.

(26) Fessel, Joshua P, et al. Metabolomic Analysis of Bmpr2 Mutation in Human Pulmonary Endothelium Reveals Widespread Metabolic Reprogramming. *Pulm. Circ.* **2012**, *2* (2), 201–213.

(27) Sharir, H.; Abood, M. E. Pharmacological Characterization of GPR55, a Putative Cannabinoid Receptor. *Pharmacol. Ther.* **2010**, *126* (3), 301–313. https://doi.org/10.1016/j.pharmthera.2010.02.004.

(28) Lauckner, J. E.; Jensen, J. B.; Chen, H. Y.; Lu, H. C.; Hille, B.; Mackie, K. GPR55 Is a Cannabinoid Receptor That Increases Intracellular Calcium and Inhibits M Current. *Proc. Natl. Acad. Sci. U. S. A.* **2008**, *105* (7), 2699–2704. https://doi.org/10.1073/pnas.0711278105.

(29) Ryberg, E.; Larsson, N.; Sjögren, S.; Hjorth, S.; Hermansson, N. O.; Leonova, J.; Elebring, T.; Nilsson, K.; Drmota, T.; Greasley, P. J. The Orphan Receptor GPR55 Is a Novel Cannabinoid Receptor. *Br. J. Pharmacol.* **2007**, *152* (7), 1092–1101. https://doi.org/10.1038/sj.bjp.0707460.

Chapter 3: Previous Syntheses of Polyunsaturated Fatty Acid Metabolites

Selected Synthesis of Isoprostanes

A variety of syntheses of F-2 isoprostanes have been published either as accessing a few stereoisomers or, in the case of the Snapper group, all eight of the stereoisomers. These syntheses are relevant to the syntheses of isofurans because isoprostanes have similar alpha and omega side chains as both groups of natural products originate from arachidonic acid. Furthermore, both families consist of a mixture of stereoisomers and synthetic approaches need to address this unusual stereochemical diversity. Thus, these approaches inspire future approaches to polyunsaturated fatty acid metabolites.

The first reported synthesis of an isoprostane was disclosed by the Corey group in 1984 were they employed a biomimetic pathway to synthesize $PGF_{2\alpha}$.[30] Their chief challenge was to install the "F ring" substitution of four contiguous stereocenters within the cyclopentane structure. The difficulty arises from the *cis-anti-cis* relationship of hydroxyl and alkyl groups (**Scheme 3.1**). After the discovery of the isoprostanes by the Roberts group in 1992 it was realized the Corey group inadvertently published the first synthesis of 15-F_{2t}-IsoP eight years before the isoprostanes were discovered.

The synthesis began with alkyne **3.1** which was alkylated *via* generation of an acetylide in the presence of catalytic copper(I) chloride and propargyl iodide **3.2** to extend the carbon chain of the molecule (Scheme 3.1). Dihydroxylation of the terminal alkene using Upjohn conditions afforded diol **3.3**.[31] Next, both alkynes were semi-reduced to the *cis* olefin using Lindlar's catalyst followed by orthoester hydrolysis and ester exchange to give the corresponding methyl ester.[32] Finally, the diol was oxidatively cleaved with lead tetraacetate to provide aldehyde **3.4** in a 40% yield over six steps. At this point lithiated acetylide **3.5** was added to the aldehyde to install the

final carbon framework. Mesylation of the propargyl alcohol followed by treatment with hydrogen peroxide gave rise to allylic peroxide **3.6** in a 60% yield over 4 steps. This compound was the key substrate needed to attempt the biomimetic 5-*exo*-*trig* cyclization to install the cyclopentane core. To achieve the latter transformation, formation of peroxide **3.7**, hydroperoxide 3.6 was treated with mercury(II) chloroacetate to give **3.7** in 74-83% yield. Treatment of alkylmercury compound **3.7** with tributyltin hydride under an oxygen atmosphere led to a 5-*exo*-*trig* cyclization and capture of oxygen at the C15 position to afford the desired F ring stereochemistry and C15 hydroperoxide as a mixture of epimers. When treated with triphenyl phosphine the peroxides were reduced to afford 15-F_{2t}-IsoP's as a mixture of diastereomers at the C15 position in a three step sequence with a yield of 20% (**Scheme 3.1**).[30]

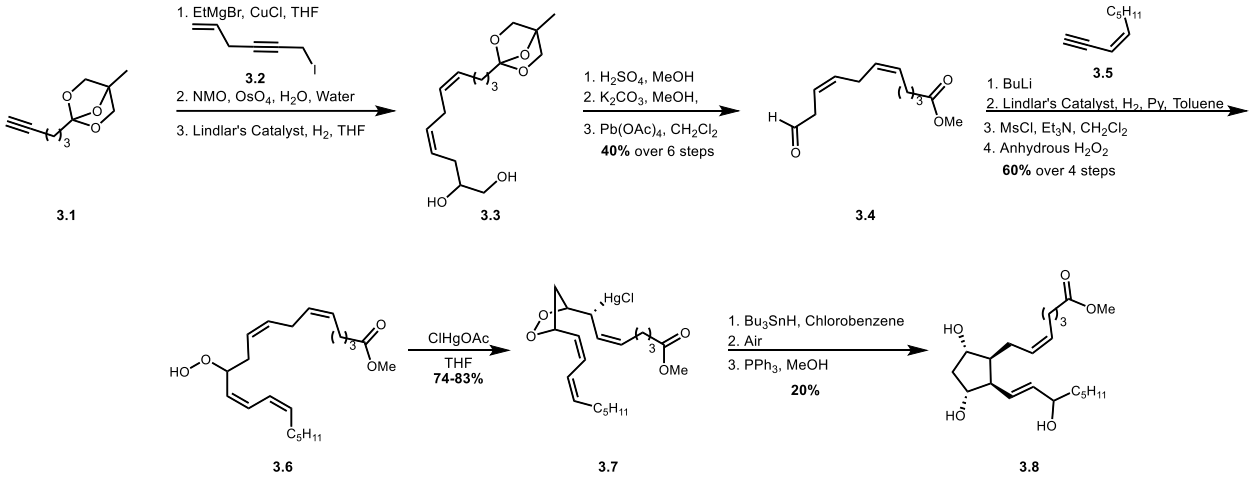

Scheme 3.1. Corey's synthesis of 15-F_{2t} isoprostanes.

In 2002 Rossi and co-workers published a synthesis of the F_{2T}-isoprostanes through a biomimetic cyclization like that employed by Corey. By employing modern methods, they accessed both enantiomerically pure diastereomers of the F_{2T}-Isoprostanes by using chiral starting material and separating the C15 diastereomer by HPLC purification.[33] Their synthesis began from known glucose bis-acetonide **3.9** which, in six steps, was advanced to ester **3.10** in a 30% overall yield (**Scheme 3.2**).[34] Triflation of the homopropargyl alcohol was achieved under standard

conditions, and the resulting triflate was converted to the iodide by Finkelstein exchange. The acetonide was deprotected with ethanethiol and zinc chloride to afford a thioacetal, which upon treatment with TESCl afforded compound **3.11** in good yields. Thioacetal removal was performed using mercury(II) mediated hydrolysis and the resulting aldehyde subjected to a Wittig olefination with phosphorous ylide **3.12**. This was followed by a second Wittig olefination with phosphorous ylide **3.13** to afford diene **3.14**, in a 60% yield over 3 steps, which is the substrate for the biomimetic 5-*exo*-*trig* ring closure to cyclopentane ring. The cyclization was attempted on two substrates, one featuring TES ethers and the other free diols. Treatment with tribuyltin hydride served to generate carbon centered radicals **3.15** and **3.16**, TES protected and free 1,3-diol, respectively. The stereochemistry of the cyclopentane ring was assigned based on proposed transition state structures **3.15** and **3.16** where the TES groups in **3.15** force a Beckwith-Houk chair transition state in which all substituents are in a thermodynamically favored equatorial position.[35,36] When the TES groups are removed, an envelope like transition state is proposed where the diols undergo hydrogen bonding to lock the envelope conformation (**3.16**) which then undergoes the 5-*exo*-*trig* cyclization to furnish the cyclopentane ring. In both cases, after the cyclization the subsequent radical was captured with molecular oxygen at the C15 position, while the C13 position observed no appreciable amount of oxygen capture. The subsequent peroxide was reduced with triphenylphosphine to afford either diol **3.17** or **3.18** as the TES ether as a mixture of diastereomers at the C15 position. If necessary, the TES groups were removed with tetrabutylammonium fluoride (TBAF); then the C15 diastereomers were separated by HPLC, and the alkynes were semi-reduced with P-2 nickel to afford methyl esters **3.19** and **3.20** as separated diastereomers in an 81% yield from compound **3.14**.[37] The goal of this study was to synthesize

F_{2T}-isoprostanes through a biomimetic 5-*exo-trig* cyclization which they discovered would give the desired stereochemistry of the cyclopentane ring, driven by the stereochemistry of the diols.

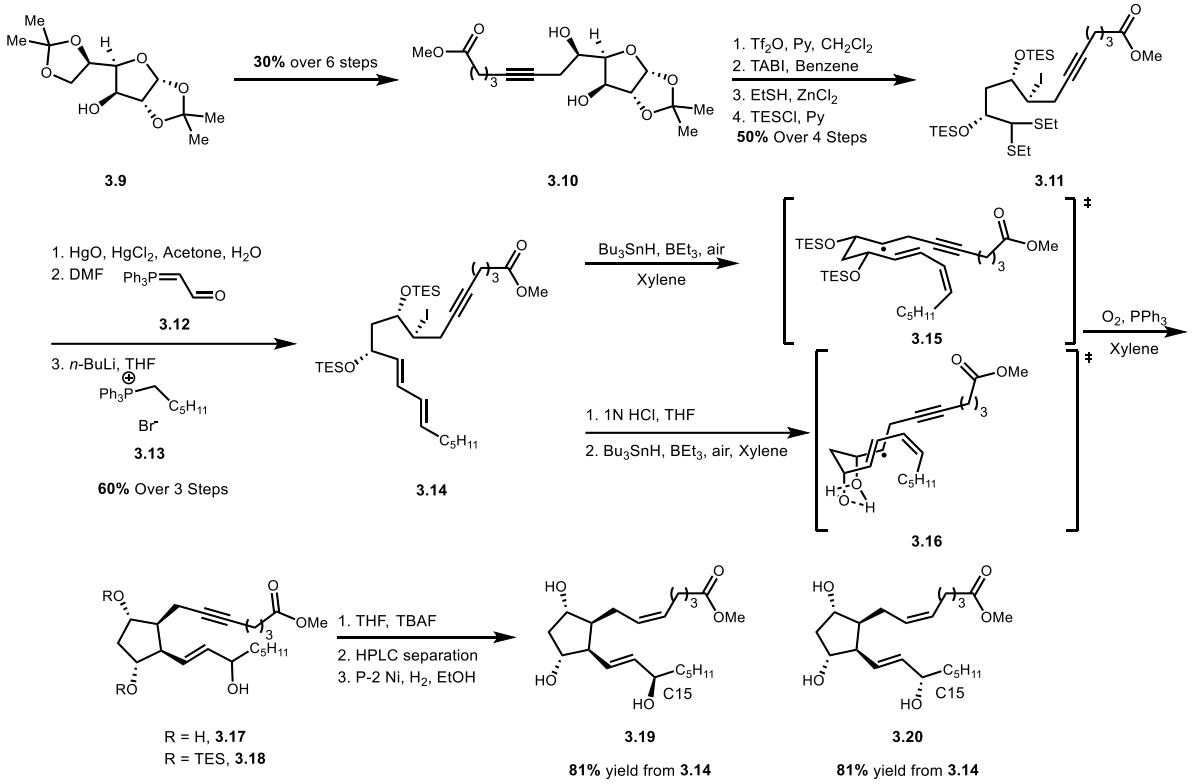

Scheme 3.2. Rossi's biomimmetic synthesis of F_{2T}-isoprostanes.

The two previous syntheses show the power of how radical cyclization chemistry can promote biomimetic cyclization's in the stereochemically desired sense. However, there are eight 15-F_{2t} isoprostanes and the previous syntheses only access two of the F-2 isoprostanes. To address this issue, the Snapper group employed a stereodivergent approach which started from racemic cyclopentenone **3.21 (Scheme 3.3)**. The first step in this sequence was a [2+2] cycloaddition of cyclopentenone **3.21** with acetylene to afford a mixture of diastereomers **3.22** and **3.23**, in a 39% and 21% yield respectively, which were reduced with DIBAL to afford compounds **3.24**, **3.25**, **3.26**, and **3.27** which were separated by flash chromatography. The desired isomers **3.26** and **3.27** were carried forward to the next step of TBS protection to give rise to compounds **3.28** and **3.29** (**Scheme 3.3**).

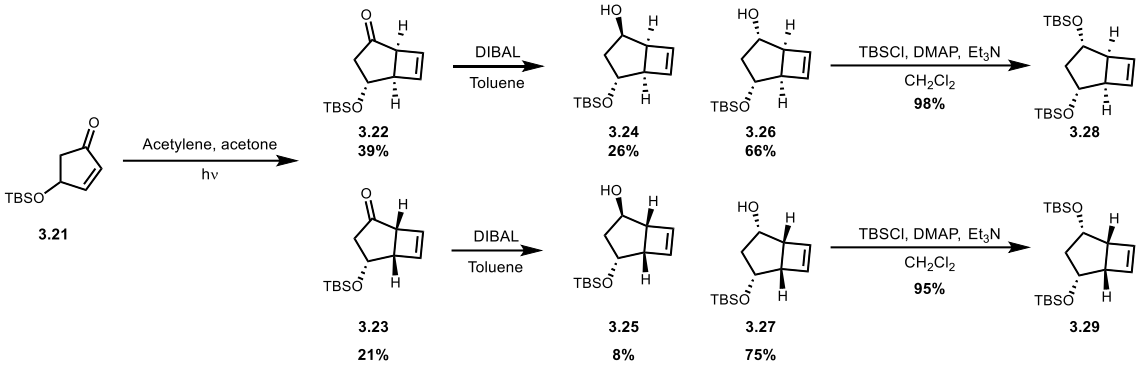

Figure 3.3. Snappers' synthesis of cyclopentanes **3.28** and **3.29** *via* a [2+2] cycloaddition.

With the cyclopentane substitution pattern established, attention was turned toward the omega sidechain installation by a ring opening metathesis with Grubb's second-generation catalyst and allylic alcohol **3.30** to de-symmetrize compounds **3.28** and **3.29** to compounds **3.31** in a 67% yield (1.4:1 E:Z ratio) and **3.33** in a 76% yield (1.2:1 E:Z ratio) (**Scheme 3.4**). Next, the compounds were oxidized to the corresponding enone *via* PCC oxidation, and subsequently treated with catalytic iodine to isomerize the to enone from a mixture of E and Z isomers to the single E isomer of compounds **3.32** and **3.34** in good yields.

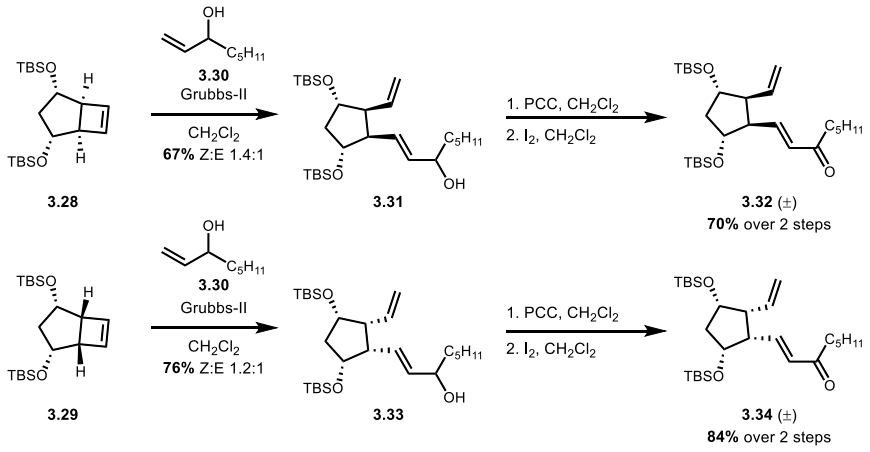

Scheme 3.4. Conversion of compound **3.28** to compound **3.32** and compound **3.29** to compound **3.34** through a ring opening metathesis and olefin isomerization.

.

Attention was turned toward resolution of enantiomers (**Scheme 3.5**) using Corey's CBS reduction. Treatment of enone **3.32** with (S)-CBS catalyst reduced the enone to the

enantiomerically enriched allylic alcohol. This provided two diastereomers which were separable by flash chromatography to give compounds **3.35** (85% ee) and **3.36** (91% ee) in excellent yields. Then, to improve enantiomeric excess, and access all possible stereoisomers, the corresponding compounds were oxidized with PCC to the enone and then followed by (R/S)-CBS reduction which set the C15 stereocenter at >98% ee for all compounds. Finally, a hydroboration, oxidation sequence afforded compounds **3.39**, **3.40**, **3.41** and **3.42** in good yield over 3 steps.

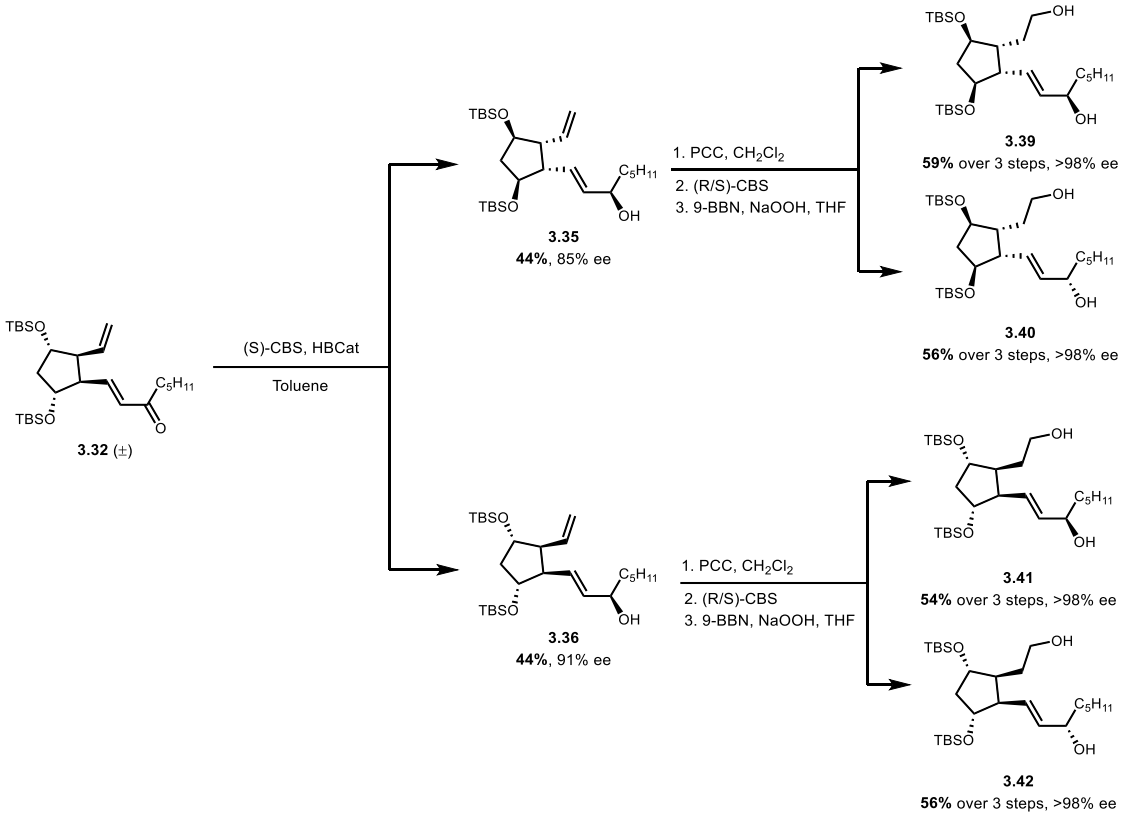

Scheme 3.5. Separation of racemic compound **3.32** allowing access to compounds **3.39**, **3.40**, **3.41** and **3.42**.

Compound **3.34** was resolved by first reducing the enone to a mixture of allylic alcohols, and the diastereomers were separated by flash chromatography to afford racemic diastereomers **3.44** and **3.45** (**Scheme 3.6**) in an 80% yield. The resulting enantiomers were separated by esterification with (*R*)-O-acetylmandelic chloride and, the diastereomers were separated by flash chromatography. The mandelic ester was removed by treatment with DIBAL followed by a

hydroboration, oxidation sequence to afford compounds **3.46**, **3.47**, **3.48**, and **3.49** in >98% ee in yields varying from 34-68%.

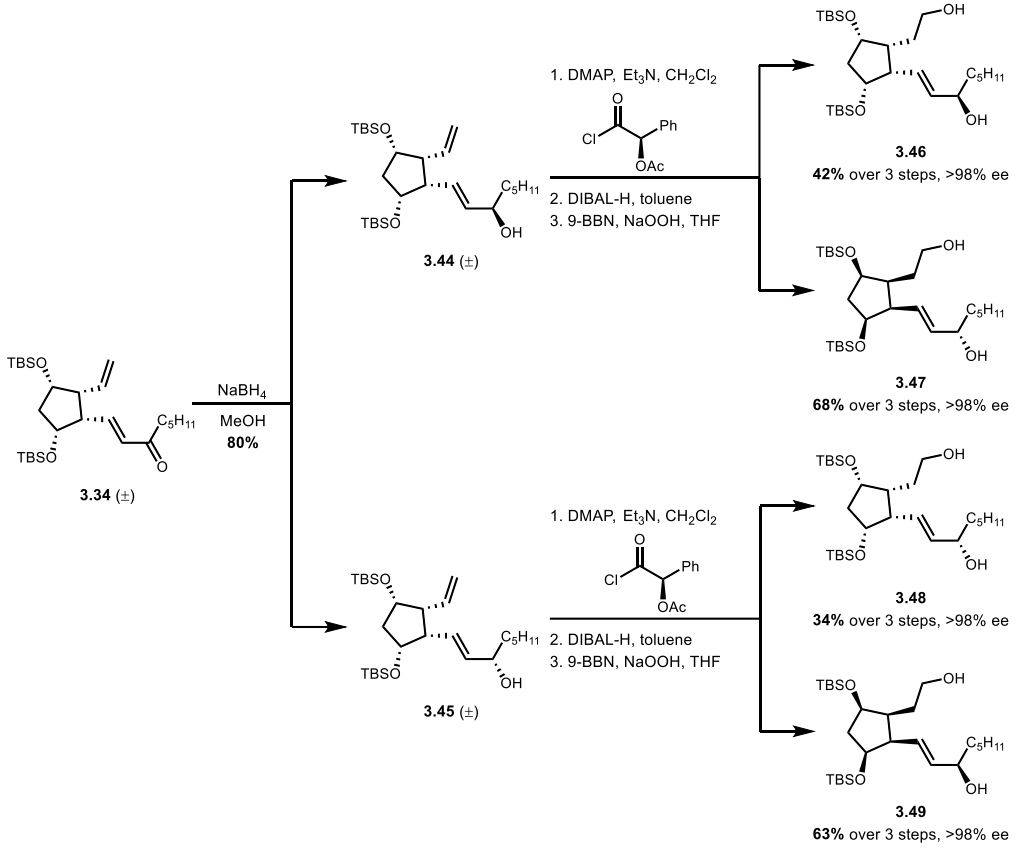

Scheme 3.6. Separation of racemic compound **3.34** allowing access to compounds **3.46**, **3.47**, **3.48** and **3.49**.

The next step for all eight compounds was oxidation of the primary alcohol to the aldehyde by TEMPO oxidation using NCS as a co-oxidant. A subsequent Wittig olefination with phosphorous ylide **3.58** and, followed by tetrabutylammonium fluoride deprotection afforded all eight of the F-2 isoprostanes **3.59-3.66** in yields varying from 31-85% over three steps (**Scheme 3.7**). This synthesis shows the power of an astute stereodivergent synthesis which allowed access to multiple diastereomers from one common building block.

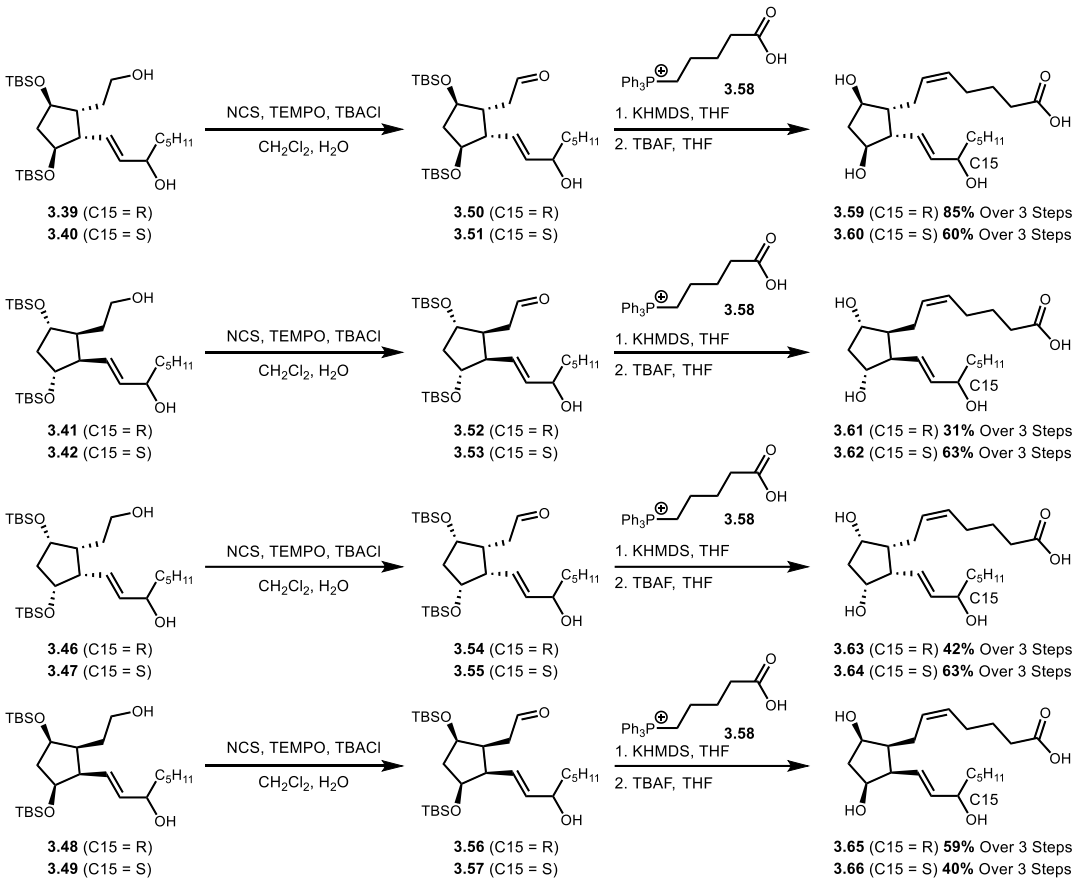

Scheme 3.7. Conversion of compound **3.39**-**3.49** to isoprostanes **3.58**-**3.66**.

Stereodivergent Approaches to Isofuran Synthesis

After the discovery of the isofurans by the Roberts group, Professor Douglas Tabor at the University of Delaware began developing synthetic routes to access the isofurans. The first disclosed route of the Δ^{13}-9-isofurans was published by the Taber group in 2002. The Δ^{13}-9 isofurans were chosen because they had the same alpha and omega side chains as PGH_2 so it was hypothesized that this class of isofurans would be the most likely to have some biological activity. They used a stereodivergent approach to generate multiple enantiomerically pure diastereomers of the isofurans where the stereocenters are set through reagent control.

Their synthesis began with generation of a silyl enol ether from diene-al **3.67** using TMSCl and triethylamine. Subsequent treatment with bromine and diol **3.68** afforded allylic bromide **3.69**

in a 41% yield. Then treatment with propargyl alcohol **3.70**, copper iodide, sodium iodide and potassium carbonate afforded an S_N2-like reaction affording propargyl alcohol **3.71** in good yield. Next, treatment of propargyl alcohol 3.71 with LAH lead to *trans* allylic alcohol **3.72** in a 61% yield. The next step was a Sharpless Asymmetric Epoxidation (SAE) to afford epoxy alcohol **3.73** in excellent yield (**Scheme 3.8**). Unfortunately, the ee of the reaction was not reported.

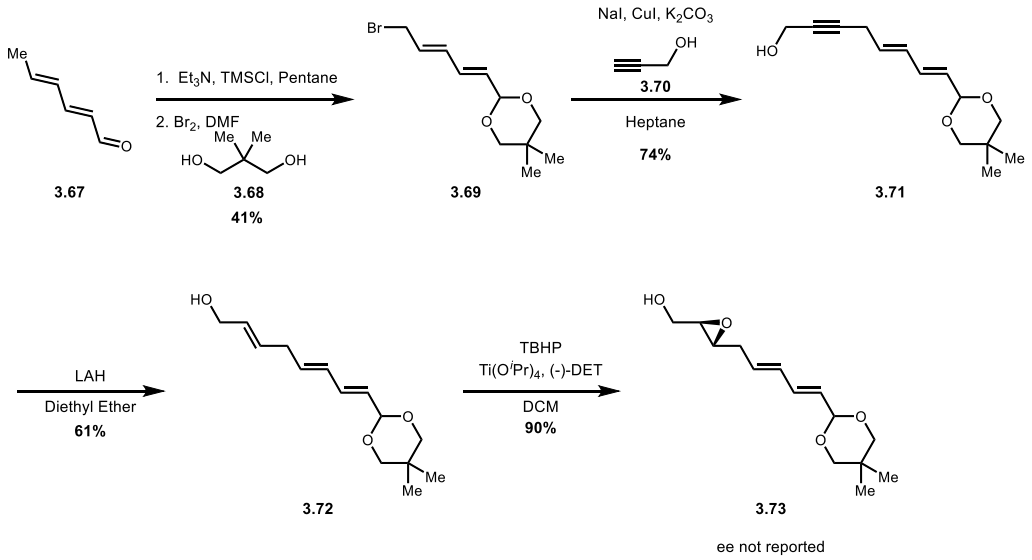

Scheme 3.8. Conversion of diene-al **3.67** to epoxy alcohol **3.73**.

After the first two stereocenters were introduced through a reagent-controlled epoxidation, the goal of the Taber group was to install two more stereocenters and set the furan core of the isofurans. This was achieved through brosylation of compound **3.73** with brosyl chloride to afford epoxide **3.74** in 96% yield. The next set of stereocenters were introduced through a Sharpless Asymmetric Dihydroxylation (SAD) with AD-mix-alpha to afford a mixture of the desired dihydroxylated product **3.76** in 47% yield and the undesired regioisomer **3.75** in 37% yield. The selectivity of the reaction is poor with a ratio of 4:3 of the desired **3.76** to the undesired compound **3.75**. Fortunately, the undesired compound **3.76** could be recycled by treating it with PTSA and trimethyl orthoformate followed by potassium carbonate in methanol to give rise to compound **3.73** in 47 % yield which is a synthetically viable precursor in the synthetic sequence. Treatment

of epoxide **3.76** with potassium carbonate in methanol forged the furan ring through a 5-*exo-tet* cyclization to give rise to furan **3.77**. Then, Mitsonobu inversion followed by ester methanolysis afforded compound **3.78**, however; they did not carry this stereoisomer forward into the synthetic sequence (**Scheme 3.9**).[38]

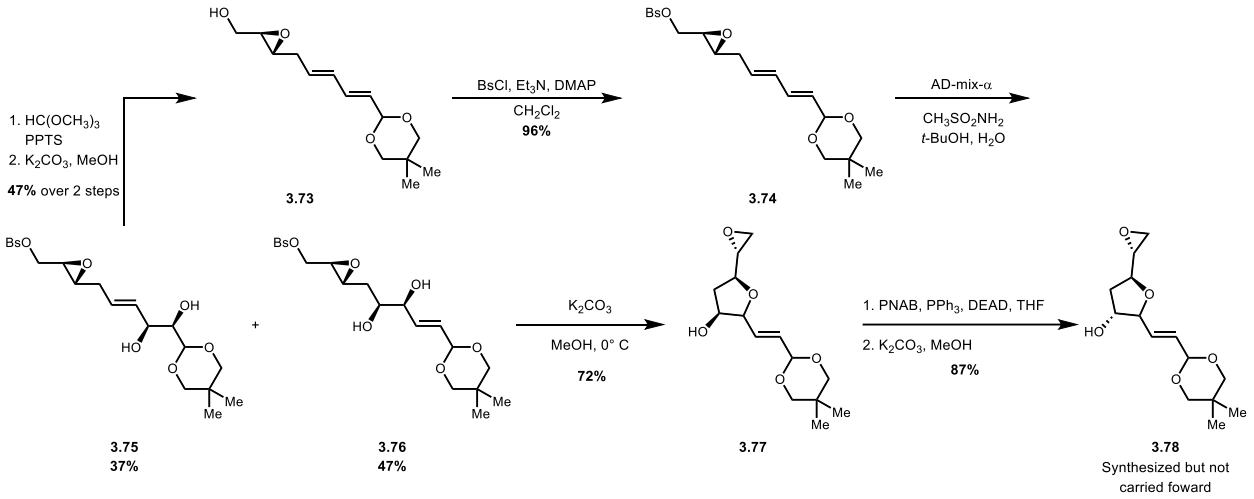

Scheme 3.9. Conversion of epoxy alcohol **3.73** to furan **3.77**.

With the furan core of compound **3.77** in hand the next step was protection of the secondary alcohol with TBSCl followed by a nucleophilic epoxide opening with lithium acetylide **3.80** to afford compound **3.81**, thereby installing the alpha sidechain in 87% yield (**Scheme 3.10**). Then, the alkyne was reduced to the *cis* alkene with P-2 nickel, followed by hydrolysis of the acetonide with acetone and hydrochloric acid to access aldehyde **3.82** in good yields. Treatment with TBSCl provided a protected alcohol, which was then treated with *n*-pentyl magnesium bromide to install the omega sidechain and give a 1:1 mixture of diastereomers at the C15 position which were subsequently separated by flash chromatography to afford compound **3.83** as the S diastereomer and **3.84** as the R diastereomer. The final synthetic sequence was deprotection of the TBS groups using tetrabutylammonium fluoride, followed by hydrolysis of the nitrile to the carboxylic acid. When NMRs of the isofurans were recorded as the carboxylic acids, the NMR's were inconclusive

due to significant broadening of signals. To resolve this issue, the isofurans were treated with TMS diazomethane to make compounds **3.86** and **3.87** in excellent yields; these compounds gave a much clearer NMR signals and their structural assignment was confirmed.

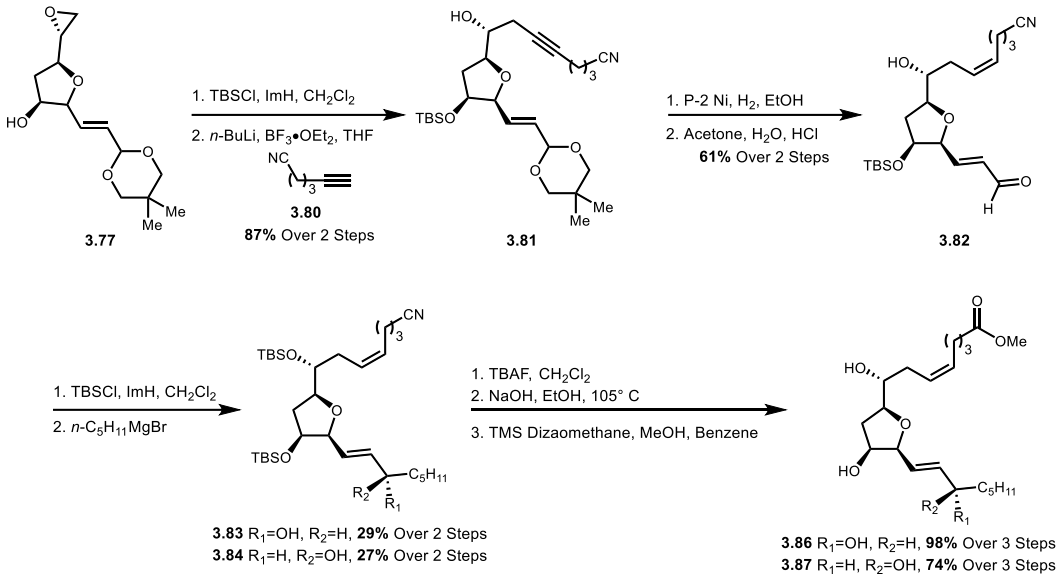

Scheme 3.10. Conversion of **3.78** to isofuran methyl esters **3.86** and **3.87**.

After achieving the first synthesis of the Δ^{13}-9 isofurans, the Taber group published a synthesis of Δ^{13}-8 isofurans. This synthesis began from commercially available alkynol alcohol **3.88** which was protected with benzyl bromide to afford benzyl ether **3.89** in 99% yield. Next, a copper-mediated coupling with allylic chloride **3.90** afforded skipped enyne **3.91** in 65% yield. A second copper-mediated coupling with THP protected propargyl alcohol **3.92** afforded skipped enyne **3.93** in good yield. Then a THP deprotection with PPTS followed by reduction with LAH established the *trans* allylic alcohol **3.94** in 55% yield over 2 steps. The first two stereocenters are introduced through a SAE to afford epoxide **3.95** in 72% yield, and then brosylation gave rise to epoxide **3.96** is excellent yields. The second set of diastereomers was introduced *via* a SAD which afforded diol **3.97** in 92% yield as an enantioenriched compound, but the ee is not reported (**Scheme 3.11**).

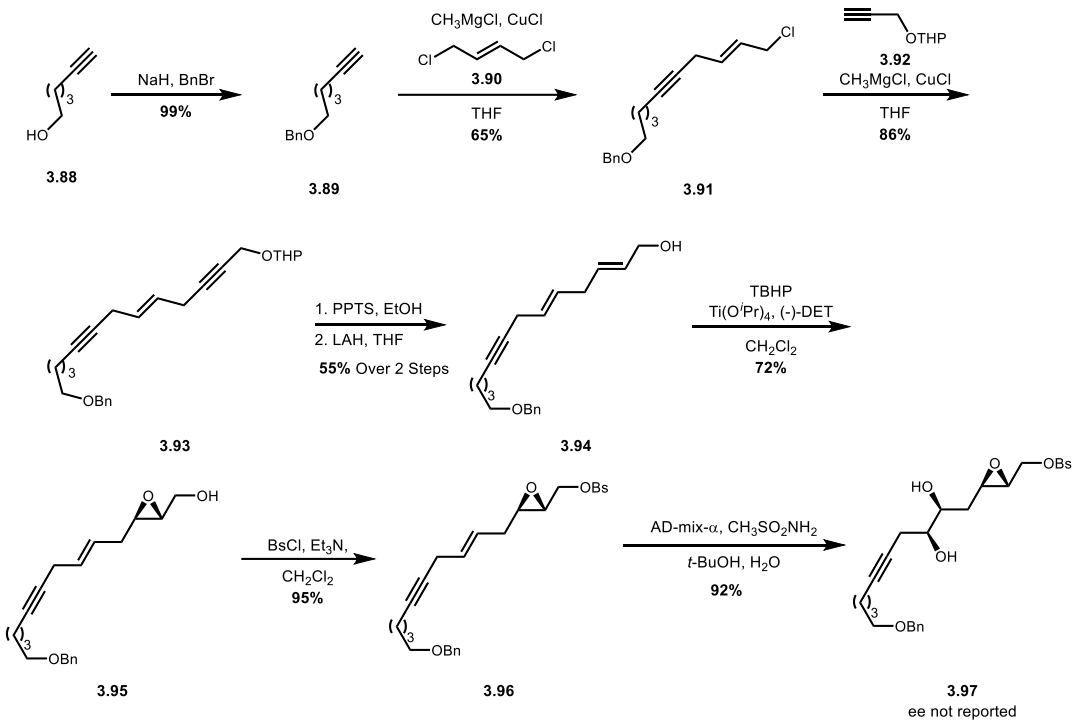

Scheme 3.11. Synthesis of chiral diol **3.97** from alkynol **3.88.**

The next goal was to install the furan core which was achieved by treating diol **3.97** with potassium carbonate in methanol to promote a 5-*exo*-*tet* cyclization which accessed furan **3.98** in a fair yield (**Scheme 3.12**). Then, treatment with methyl sulfonium ylide installed allylic alcohol **3.99** in a 70% yield. Subsequent TBS protection resulted in **3.100** in a near quantitative yield; then SAD, followed by oxidative cleavage with sodium periodate afforded aldehyde **3.101** in a 70% yield over 2 steps. Next, Horner-Wadsworth-Emmons olefination with keto phosphonate **3.102** installed the omega sidechain as enone **3.103** in a 90% yield.

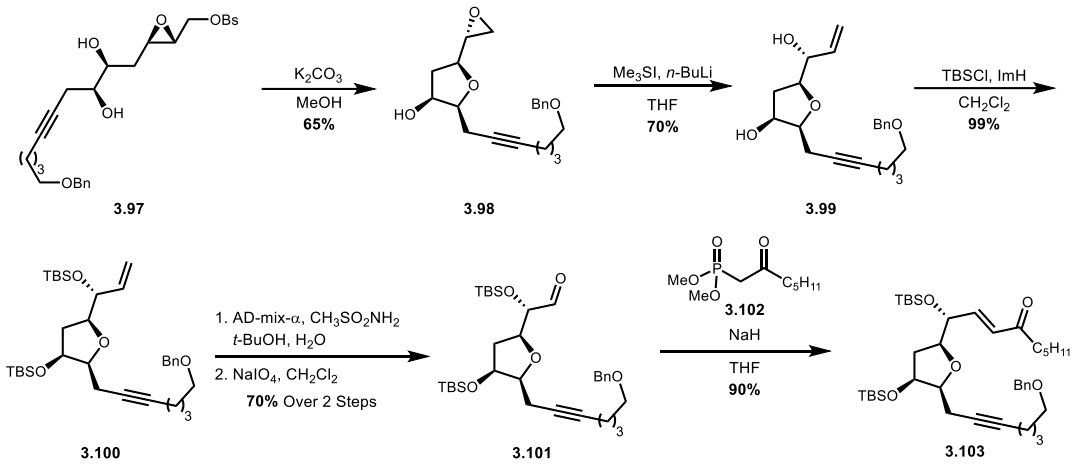

Scheme 3.12. Conversion of **3.97** to furan **3.103** through a 5-*exo-tet* cyclization and installation of the omega side-chain through a HWE reaction**.**

Luche reduction of **3.103** afforded allylic alcohols **3.104** and **3.105** which were separable by flash chromatography. They also were able to diastereoselectively reduce **3.103** to either **3.104** or **3.105** as single diastereomers with either (+) or (-) DIP-Cl in good yields (**Scheme 3.13**).

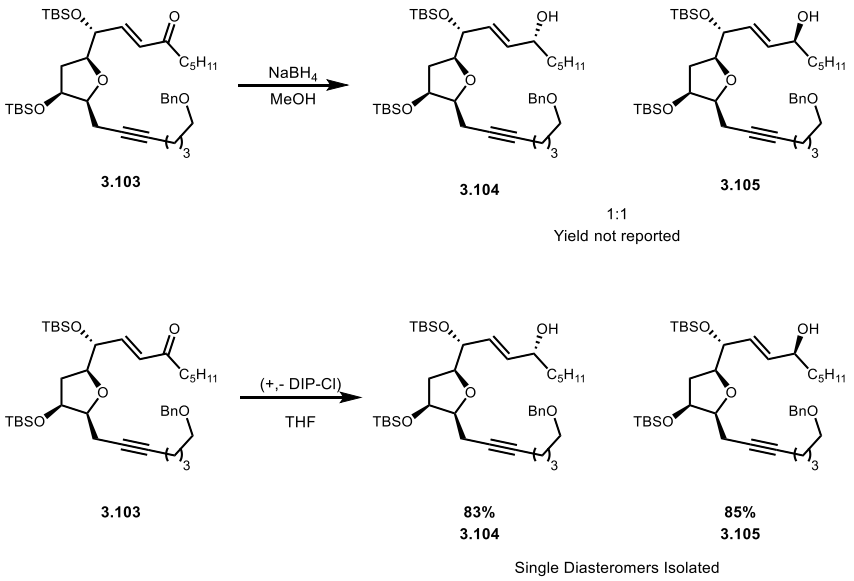

Scheme 3.13. Reduction of enone **3.103** to alcohols **3.104** and **3.105** via DIP-Cl or $NaBH_4$**.**

Secondary alcohol **3.105** was then protected with TBSCl to afford compound **3.106** in 91% yield. With the omega sidechain installed and the C15 stereocenter set, their goal was to bring the alpha side chain to the correct oxidation state (**Scheme 3.14**). This was achieved by first

semireducing compound **3.106** with P-2 nickel under an atmosphere of hydrogen to afford *cis* olefin **3.107** in 83-89% yields. The benzyl group was subsequently removed with lithium napthalide to provide alcohol **3.108** in excellent yields. Finally, the synthesis was completed with oxidation of the alcohol to the aldehyde with Dess-Martin Periodinane (DMP), followed by Pinnick oxidation and tetrabutylammonium fluoride deprotection to allow access to compound **3.109** in a 57% yield over 3 steps. Using this synthetic sequence, the Taber group was able synthesize two of the Δ^{13}-8 isofurans (*epi*-ent-SC-Δ^{13}-8 Isof and ent-SC-Δ^{13}-8 Isof).

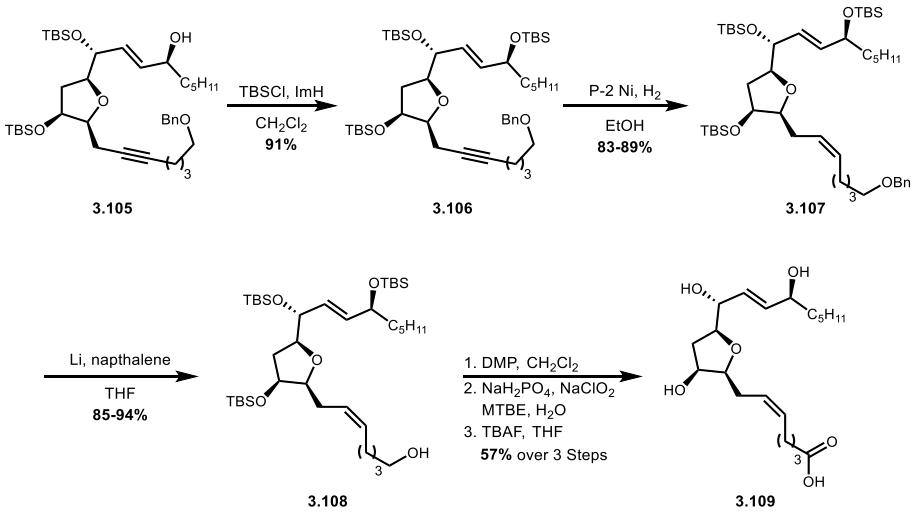

Scheme 3.14. Conversion of furan **3.105** to Δ^{8}-13 isofuran **3.109**.

The two previous synthetic routes toward the isofurans only accessed a few isofurans and the ee's were not reported. When testing some of the Δ^{13}-9 isofurans, the Taber group announced the biological results were not consistent between batches. This suggests their products were not enantiomerically pure, they believe the SAD was not consistently diastereoselective which resulted in contamination of undesired stereoisomers. To address this issue the Taber group set out to make a synthetic route to access all 32 isomers of the Δ^{13}-9 isofurans and as single enantiomers. Their chosen starting material, bromo crotyl ester **3.110**, was reduced with aluminum hydride to the alcohol; then copper-mediated coupling with propargyl alcohol gave a 1:0.5 ratio of **3.112** (desired

S_N2 product) to **3.113** (undesired S_N2' product) as a mixture of isomers in a good yield over 2 steps. Next, and LAH reduction reduced the propargyl alcohols to the *trans* allylic alcohols **3.114** and **3.115** in a 76% yield. Desired **3.114** compound is symmetrical and can be desymmetrized by treatment with trityl chloride afford mono-tritylated compound **3.116** in fair yield. SAE is the first point of stereodivergence where **3.116** is stereoselectively oxidized to epoxide **3.117** or **3.118** depending on the use of either (+) or (-) diethyl tartrate (**Scheme 3.15**).

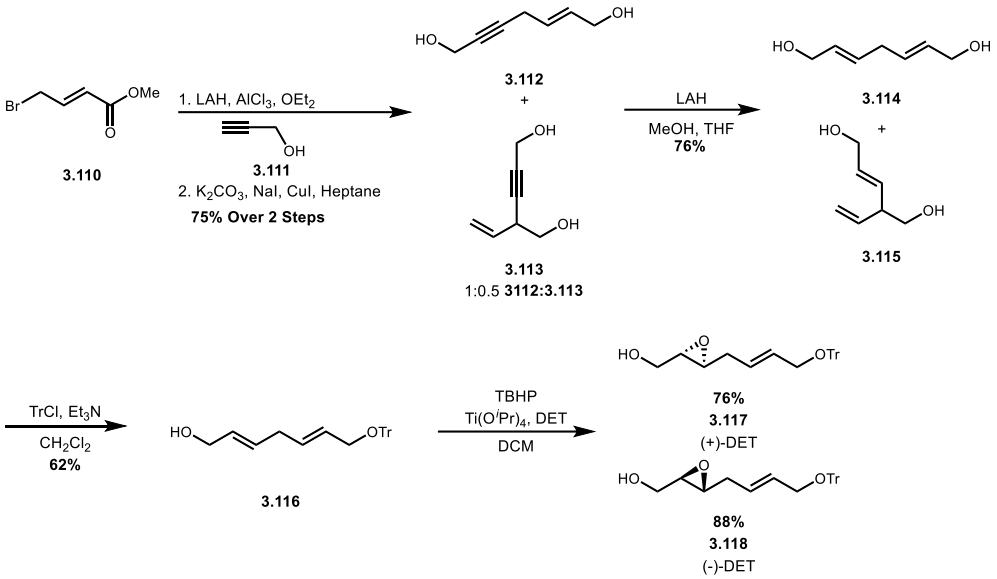

Scheme 3.15. Conversion of bromo crotyl ester **3.110** to epoxides **3.117** and **3.118**.

Both epoxides were carried forward separately in the synthetic sequence to a brosylation with brosyl chloride which yielded compounds **3.119** and **3.120**. Both compounds were asymmetrically dihydroxylated with either AD mix alpha or beta, and then treatment with potassium carbonate induced a 5-*exo*-*tet* cyclization which set the furan core of the molecules. TBS protection then gave rise to furans **3.121**-**3.124** in good yields over 3 steps. The specific reagents for the SAE and SAD furnished the furan core (four of eight possible stereoisomers) which is outlined in **Scheme 3.16**. The other four stereoisomers of the furan core can be accessed through a through a three-step sequence involving a tetrabutylammonium fluoride deprotection,

followed by a Mitsonobu inversion, and then ester methanolosis to afford furans **3.125**-**3.128** in excellent yields (**Scheme 3.16**). The use of the SAE, SAD, and Mitsonobu inversion allowed for access of all 8 stereoisomers of the isofuran core.

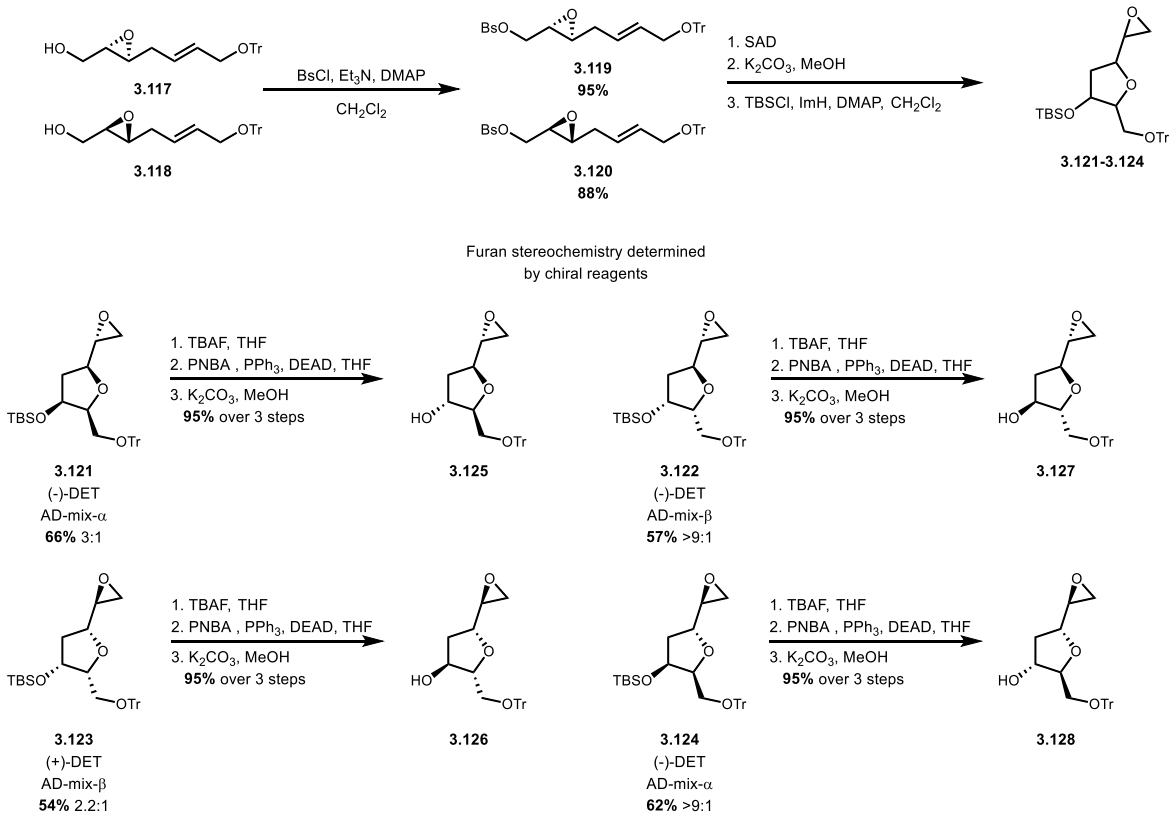

Scheme 3.16. Conversion of epoxides **3.117** and **3.118** to furans **3.121**-**3.124** where the stereochemistry is determined by a SAE and SAD.

All eight isomers were carried forward in the sequence, however; only **3.121** will be shown for clarity (**Scheme 3.17**). The alpha side chain was introduced through a nucleophilic epoxide opening with alkyne **3.80** in the presence of $BF_3 \bullet OEt_2$ to afford alkyne **3.128** in high yields. Then the alkyne was semi-reduced to the *cis* olefin with P-2 nickel under an atmosphere of hydrogen to access olefin **3.129** in 95% yield. The secondary alcohol was protected with TBSCl which afforded **3.130** 84% yield. With the alpha side chain successfully installed, efforts towards the installation of the omega sidechain began. The sequence began with removing the trityl group with diethyl aluminum chloride to afford alcohol **3.131** in 84% yield. Alcohol **3.129** can be

inverted through an oxidation with Dess-Martin Periodinane, followed by a reduction with L-selectride to provide alcohol **3.132** in 77% yield over 2 steps, allowing access to 16 total stereoisomers of the Δ^{13}-9 isofurans (**Scheme 3.18)**.

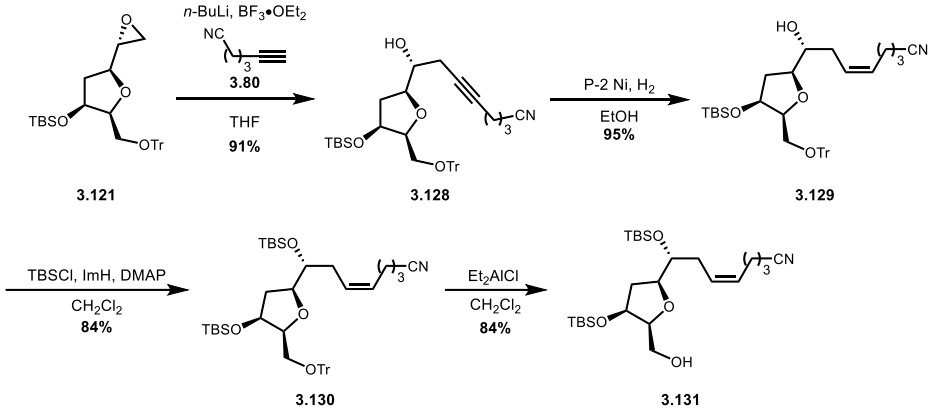

Scheme 3.17. Conversion of epoxide **3.121** to furan **3.131.**

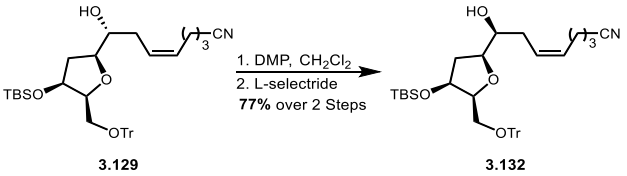

Scheme 3.18. Inversion of the C8 alcohol through an oxidation and reduction sequence.

Then, oxidation with Dess-Martin Periodinane oxidation of alcohol **3.131**, followed by Horner-Wadsworth-Emmons olefination with keto phosphonate **3.102** afforded enone **3.132** which finished the synthesis of the carbon framework in 84% yield over 2 steps. Enone **3.132** was then reduced with sodium borohydride resulting in a 1:1 mixture of separable diastereomers **3.133** and **3.134** which were separated by flash chromatography in good yields. This final point of divergence allows access to all 32 stereoisomers of the Δ^{13}-9 isofurans. The synthesis was finished with desilylation with tetrabutylammonium fluoride, followed by nitrile hydrolysis to the carboxylic acid with sodium hydroxide which gave rise to isofurans **3.135** and **3.136** in excellent yields over 2 steps. To confirm the structure of isofuran **3.135** it was treated with TMS diazomethane to afford methyl ester **3.137** which was easier to analyze by NMR. The Taber group

employed this synthesis to access all 32 stereoisomers of the Δ^{13}-9 isofurans which is an impressive feat (**Scheme 3.19**).

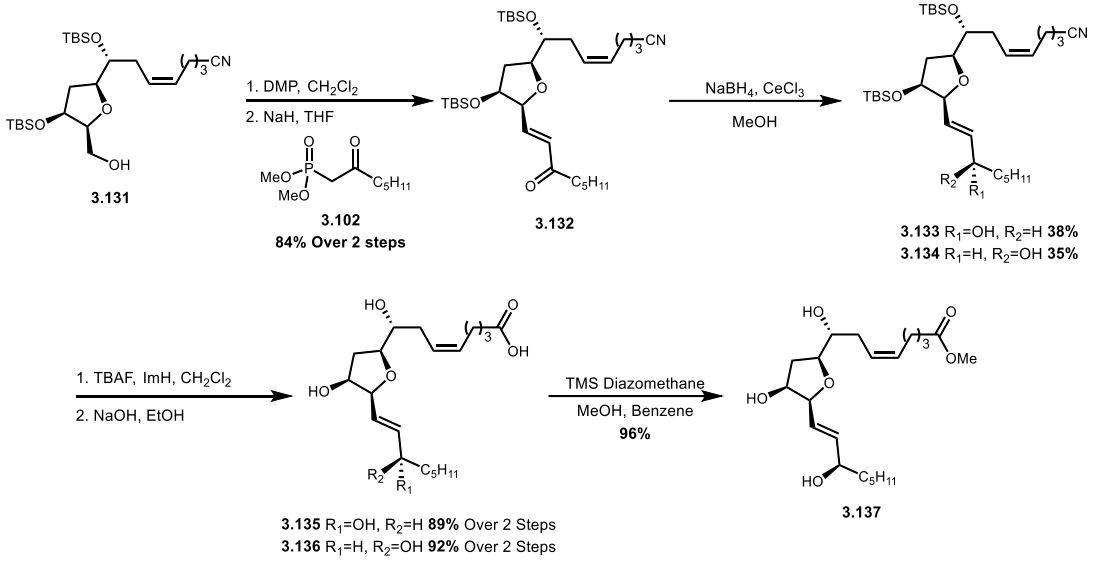

Scheme 3.19. Conversion of furan **3.131** to isofurans **3.135** and **3.136**. Esterification of **3.135** to **3.137** allows for NMR confirmation of the structure.

Stereodivergent Synthesis of Linoleic Triol Methyl Esters

Oxidative metabolites of fatty acids have been a synthetic target of the Sulikowski lab in recent years. The group has employed a stereodivergent approach to four triols which are derived from linoleic acid. In this synthesis two of the stereocenters are accessed from the chiral pool which allows for high enantiopurity of the starting material which allows for high enantiopurity in the final product compared to previous syntheses which use achiral or racemic starting material and introduce stereocenters through asymmetric means which do not afford single diastereomers.

2-deoxy-L-ribose and D-tartaric acid are used as the enantiomerically pure starting materials (**Scheme 3.20**). Both compounds were transformed into alkynols which are diastereomers. This was achieved with 2-deoxy-L-ribose **3.138** by first protecting the diol as the acetonide with PTSA in acetone followed by the Colvin reaction with LDA and TMS diazomethane which yielded alkynol **3.139** in 53% yield over 2 steps. D-tartaric acid **3.140** is first

treated with PTSA, methanol and 2,2-dimethoxypropane to install a methyl ester and acetonide; then, LAH reduction revealed a diol which was followed by desymmetrization of the molecule with TBDPSCl and NaH, then triflation of the remaining alcohol, displacement with TMS acetylide, and removal of the TMS group with potassium carbonate and methanol furnished alkynol **3.141** in a 22% yield over 5 steps.

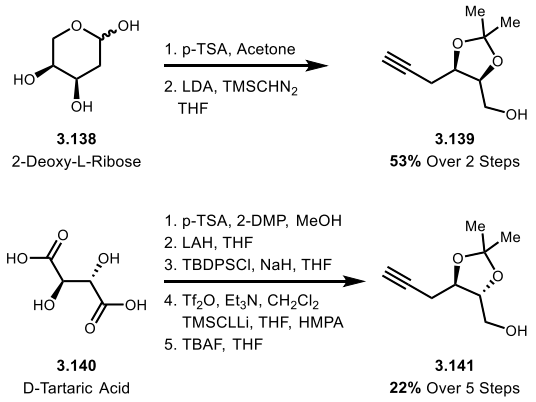

Scheme 3.20. Synthesis of enantiomerically pure diols **3.139** and **3.141** which are accessed from enantiomerically pure compounds **3.138** and **3.140**.

Using compounds **3.139** and **3.141** allowed access to diols with a syn relationship (**3.139**) or an anti relationship (**3.141**). Both compounds were taken forward but only **3.139** will be shown for simplicity (**Scheme 3.21**). The carbon framework of **3.139** was extended by a Sonogashira reaction with vinyl iodide **3.142** to afford enyne **3.143** in 82% yield. Then the enyne was reduced with P-1 nickel to the aliphatic compound **3.144** in near quantitative yields. The final side chain was introduced through oxidation of **3.144** Dess-Martin Periodinane which afforded aldehyde **3.145** in 82% yield. Subsequent treatment with keto phosphonate **3.102** afforded enone **3.146** in 82% yield. Next treatment with sodium borohydride afforded a mixture of diastereomers **3.147** and **3.148** which were separable by flash chromatography, and both were isolated in 37% yield. Then, both compounds were separately treated with aqueous HCl to cleave the acetonide and reveal diols **3.149** and **3.150** in good yields. Using this synthetic route, four linoleic triol methyl

esters were synthesized (**3.149-152**). This approach significantly inspired the future synthesis of the Δ^{13}-9 isofurans through a stereodivergent approach using optically pure starting material and substrate-controlled reactions to access multiple stereoisomers of natural products (**Scheme 3.22**).

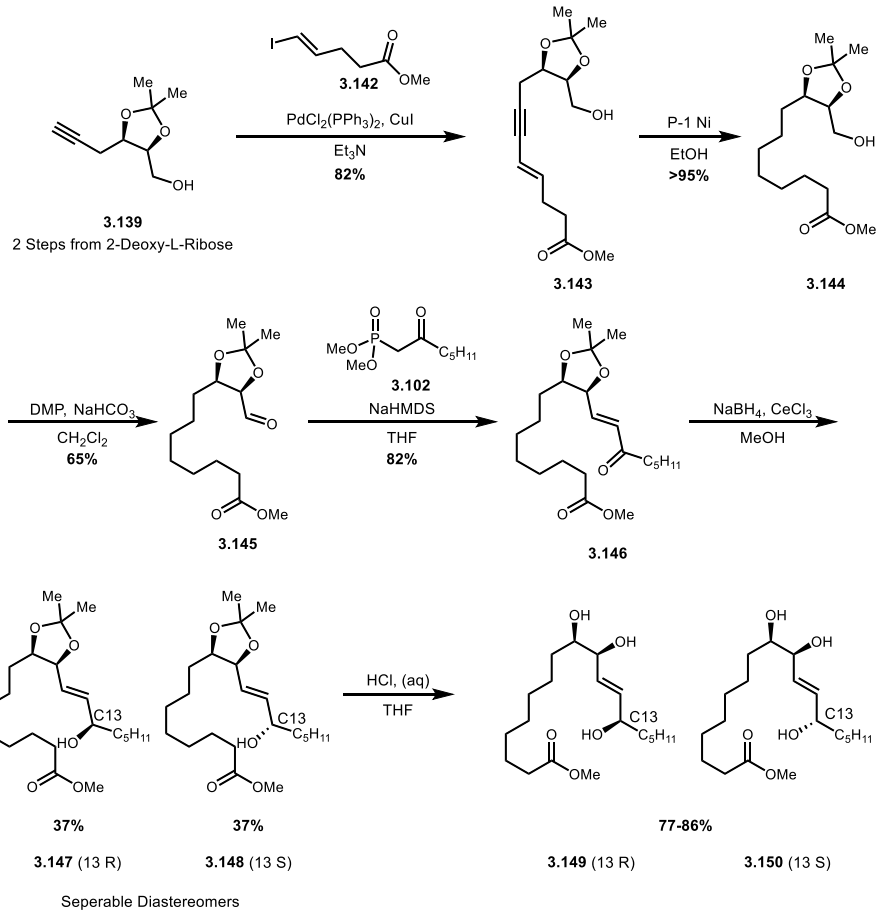

Scheme 3.21. Stereodivergent synthesis of linoleic triols **3.147** and **3.148** from cis acetonide **3.139**.

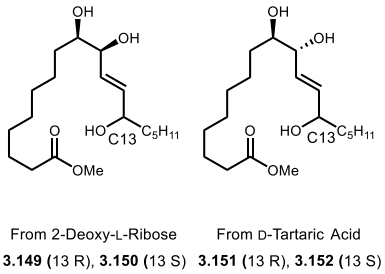

Scheme 3.22. Four linoleic triol methyl esters which are accessed from compounds 2-Deoxy-L-Ribose and D-Tartaric Acid.

References

30) Corey, E. J.; Shih, C.; Shih, N. Y.; Shimoji, K. Preferential Formation of 8-Epi-Prostaglandin F2α via the Corresponding Endoperoxide by a Biomimetic Cyclization. *Tetrahedron Letters*. 1984, pp 5013–5016. https://doi.org/10.1016/S0040-4039(01)91105-

0.

(31) Vanrheenen, V.; Kelly, R. C.; Cha, D. Y. An Improved Catalytic OSO4 Oxidation of Olefins to Cis-1,2 Glycols Using Tertiary Amine Oxides as the Oxidant. *Tetrahedron Lett.* **1976**, *17* (23), 1973–1976.

(32) Lindlar, H.; Dubuis, R. Palladium Catalyst for Partial Reduction of Acetylenes. *Org. Synth.* **1966**, *46* (5), 880. https://doi.org/10.15227/orgsyn.046.0089.

(33) Durand, T.; Guy, A.; Vidal, J.-P.; Rossi, J.-C. Total Synthesis of (15R) and (15S) F2t Isoprostanes by a Biomimetic Process Using Hte Cyclization of Acyclic Dihydroxylated Octa 5,7 Dienyl Radicals. *J. Or* **2002**, *67*, 3615–3624.

(34) Just, G.; Luthe, C. Oxidation Products of Arachidonic Acid I. The Synthesis of Methyl 8R, 11R, 15-Trihydroxy-9S, 12-Oxyeicosa-5Z, 13E-Dienoate (19). *Can. J. Chem* **1980**, *58*, 1799. https://doi.org/10.1016/S0040-4039(00)78823-X.

(35) Schiesser, C.; Beckwith, A. Regio- and Stereo-Selectivity of Alkenyl Radical Ring Closure: A Theoredical Study. *Tetrahedron* **1985**, *41* (19), 3925–3941.

(36) Spellmeyer, D. .; Houk, K. A Force-Field Model for Intromolecular Radical Additions. *J. Org. Chem.* **1987**, *52* (6), 959–974.

(37) Brown, C. A.; Ahuja, V. K. "P-2 Nickel" Catalyst with Ethylenediamine, a Novel System for Highly Stereospecific Reduction of Alkynes to Cis-Olefins. *Journal of the Chemical Society, Chemical Communications*. 1973, pp 553–554. https://doi.org/10.1039/C39730000553.

(38) Mitsunobu, O.; Yamada, M. Preparation of Esters of Carboxylic and Phosphoric Acid via Quaternary Phosphonium Salts . *Bull. Chem. Soc. Jpn.* **1967**, *40* (10), 2380–2382. https://doi.org/10.1246/bcsj.40.2380.

(39) Baldwin, J. E. Rules for Ring Closure. *J.C.S. Chem. Comm.* **1976**, No. 734, 734–736.

(40) Shankar, M.; Mohan, H. R.; Prasad, U. V.; Krishna, M. H.; Rao, P. M.; Lakshmikumar, T.; Subbaraju, G. V. A Facile Route for Synthesis of (±)-Dinoprost, (±)-Carboprost and Its Analogs. *Asian J. Chem.* **2013**, *25* (2), 913–920. https://doi.org/10.14233/ajchem.2013.13139.

(41) Davis, R. W.; Allweil, A.; Tian, J.; Brash, A. R.; Sulikowski, G. A. Stereocontrolled Synthesis of Four Isomeric Linoleate Triols of Relevance to Skin Barrier Formation and Function. *Tetrahedron Lett.* **2018**, *59* (52), 4571–4573. https://doi.org/10.1016/j.tetlet.2018.11.033.

Chapter 4: Stereodivergent Synthesis of Δ^{13}-9-Isofurans

Introduction and Analysis

Previous work by the Taber, Snapper and Sulikowski groups demonstrated stereodivergent approaches to access Δ^{13}-9-isofurans, F2-isoprostanes, and isomeric linoleic triols. In part, based on our group's work on linoleic acids, we chose to employ a stereodivergent strategy to the Δ^{13}-9-isofurans starting from the same set of four isomeric diols (*vide infra*).

In contrast to employing optically active starting materials combined with stereospecific transformations, the Taber group synthesized the Δ^{13}-9-isofurans using a strategy dependent on reagent-controlled selectivity starting from prochiral substrates. In the Taber approach, stereocenters were introduced through a combination of Sharpless asymmetric epoxidations and dihydroxylations to produce common stereoisomeric furans. The isolated side-chain C15 secondary alcohol was introduced by a non-selective reduction of the corresponding keto group. Our route to isomeric furans establishes stereodivergency by starting from one of four acetonide-protected optically pure diols (**4.1** to **4.4**, **Figure 4.1**). The remaining ring and neighboring secondary alcohol stereocenters were introduced by two sequential stereospecific reactions, an alkene epoxidation and epoxy-alcohol cyclization (**Figure 4.2**). As described in the linoleic acid synthesis, optically pure 1,2-diols **4.1** to **4.4** were derived from tartaric acid or 2-deoxy ribose, respectively (**Figure 4.1**).

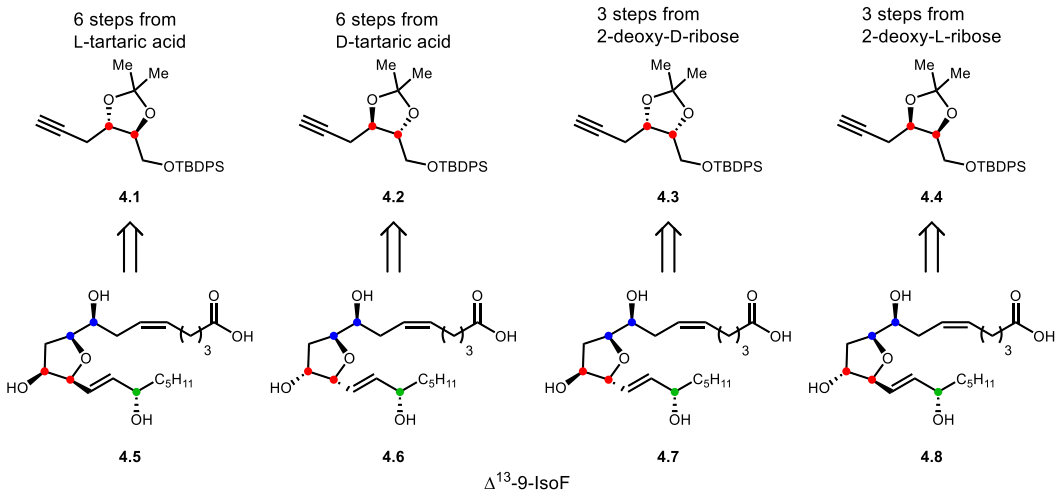

Figure 4.1. Known optically pure 1,2-diols (**4.1-4.4**) can be used to introduce two stereocenters (shown in red) in the isofuran synthesis.

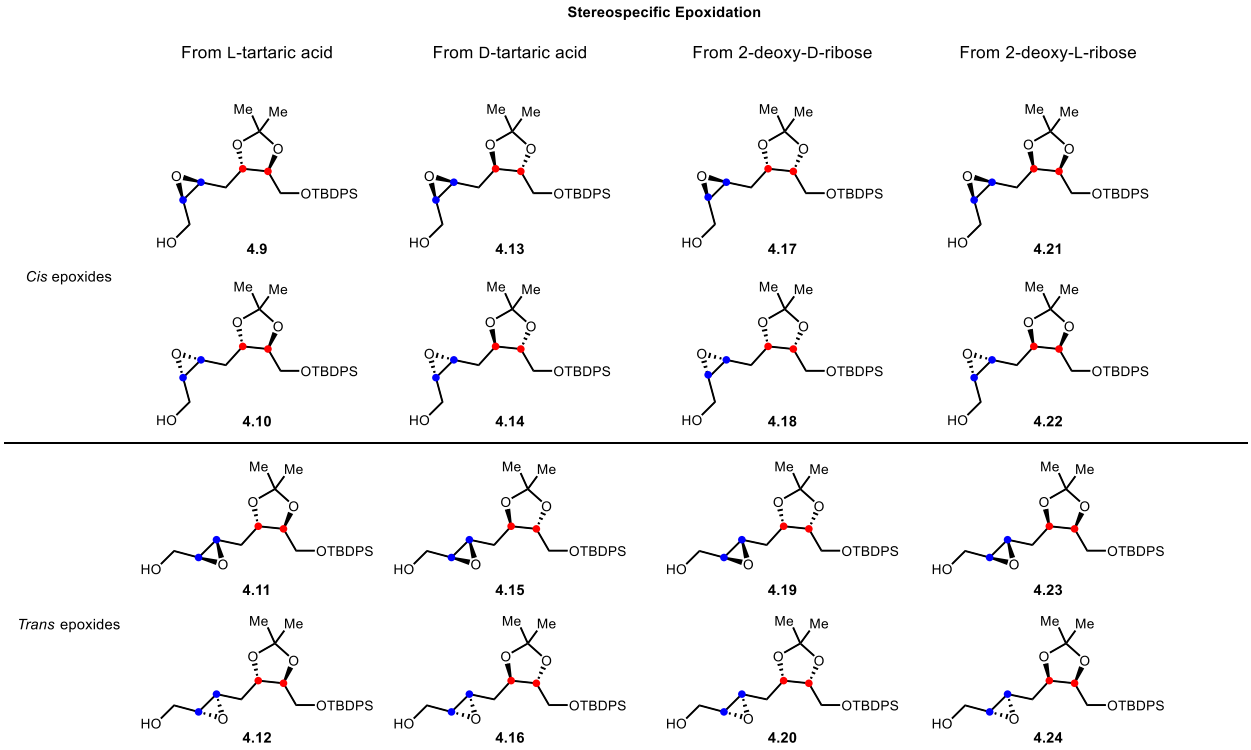

Figure 4.2. All cis/trans epoxides (stereocenters in blue) which are accessed from L/D Tartaric Acid and 2-deoxy-L/D-ribose.

As discussed above, the second set of stereocenters (highlighted in blue **Figure 4.1** were to be introduced from a stereospecific, non-stereoselective, epoxidation of a geometrically defined olefins leading to a mixture of two epoxide isomers (**4.9/4.10**; **4.11/4.12**; **4.13/4.14**, etc, **Figure 4.2)**. Removal of the acetonide protecting group reveals a 4-hydroxy epoxide poised for a 5-*exo*-

tet cyclization leading to all furan stereoisomers (cf. **Figures 4.3** and **4.5**).[39] In order to obtain single isomer furans, we anticipated either the epoxide or furan product isomers could be separated by chromatography. We planned to assign structure (stereochemistry) following cyclization as this produces a secondary alcohol (C8) which would be subjected to a Mosher ester analysis. From the C8 absolute stereochemistry we would assign the C8-C9 relative stereochemistry by extension of the stereospecificity of the cis or trans epoxide ring closure (for an analysis of the stereospecific ring closure, see Figure 4.5). This stereodivergent strategy would allow access to all stereoisomers of the furan ring (All possible furan rings shown in **Figure 4.3**).

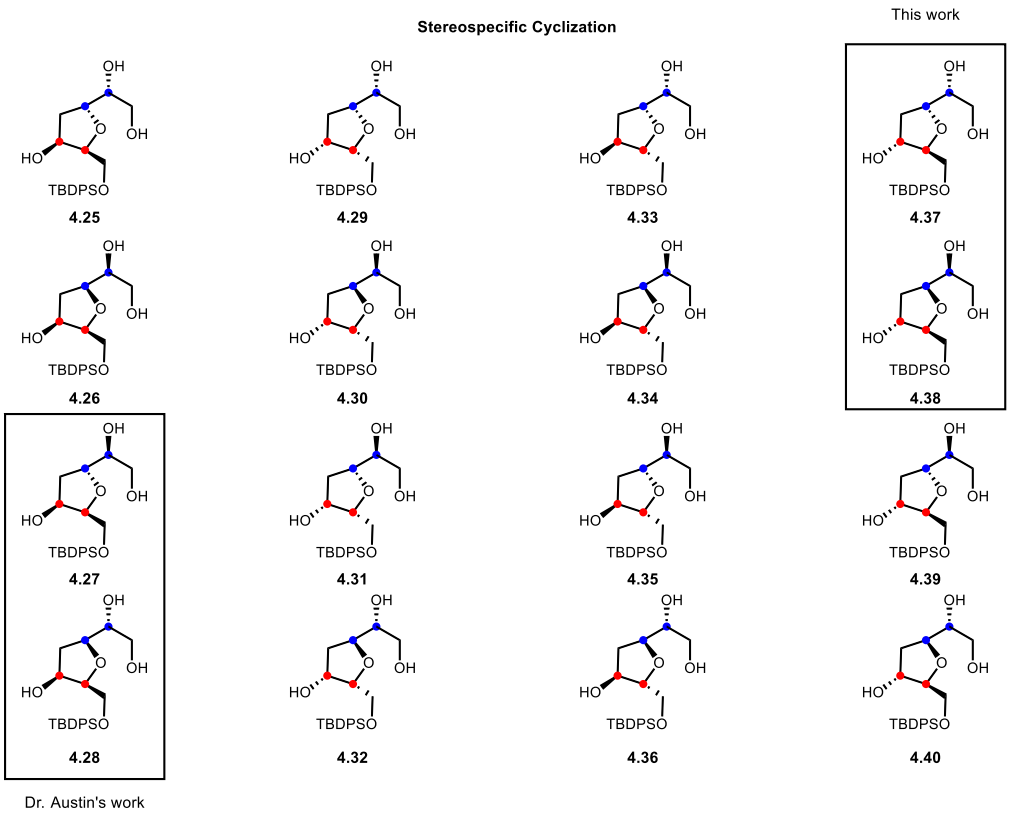

Figure 4.3. All possible isomers of the furan core which can be accesses by a stereospecific 5-*exo*-*tet* cyclization.

Several variations of reaction sequence were projected to install the remaining side-chains to complete the small library of isofurans. The omega side-chain, terminating in an n-pentyl group would be installed by a Horner-Wadsworth-Emmons (HWE) olefination reaction by conversion

of the silyl-protected primary alcohol to an aldehyde. The latter aldehyde would be condensed with a β-keto phosphonate **4.42** (cf. **Figure 4.4**).[40] The remaining C15 stereocenter was anticipated to be installed *via* a non-stereoselective reduction of the enone produced from the HWE reaction. Once again, we considered the possibility of chromatographic separation of diastereomers (as in the case of Taber synthesis of Δ^{13}-9-isofurans. For the side-chain terminating in a carboxylic acid, PMB protected alkyne **4.41**[39] **(Figure 4.4)** would serve as a precursor with the terminal alkyne serving as a site of carbon-carbon bond formation.

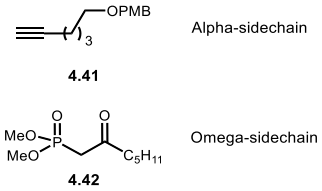

Figure 4.4. The alpha sidechain can be introduced through PMB protected alkyne **4.41**. The sidechain can be installed using keto phosphonate **4.42**.

Discussion and Results The synthetic strategy described in the previous section is capable of leading to all 32 isomers of Δ^{13}–9-isofurans or stated differently, 16 of each enantiomeric series. Based on the synthetic strategy, the 16 Δ^{13}–9-isofuran stereoisomers were conveniently divided into four sets of isomers, each consisting of four sub-sets. Stated differently, trans (from tartaric acid) or cis (from 2-deoxy ribose) acetonides each diverge to either cis or trans alkenes, then to mixtures of epoxides and subsequently furans (cf. Figures **4.2** and **4.3**). By the described route, an single isomer of epoxide would diverge to four isomeric furans (cf. Figure **4.3**) and following introduction of the C18 secondary alcohol would further diverge from four isomers to eight Δ^{13}-9-isofurans. Ultimately, the synthetic plans were divided into two, between myself and my colleague Dr. Zach Austin. This synthesis began with *trans* acetonides (**4.1** or **4.2**, Figure **4.1**) from L-tartaric acid. Dr. Austin fashioned L-tartaric acid to furans **4.27** and **4.28** (**Figure 4.3**) via *trans* epoxides. Each of these two furans diverged to two Δ^{13}–9-isofurans following non-selective reductio of a

C15 keto group leading epi-15- Δ^{13}–9-isofurans and the corresponding 15S-isomers. My thesis work will focus on using 2-deoxy-L-ribose as a starting material leading to cis acetonides (**4.3** or **4.4**, Figure **4.1**) and installing a *cis* epoxide to access furan cores (**4.37** and **4.38**, **Figure 4.3**).

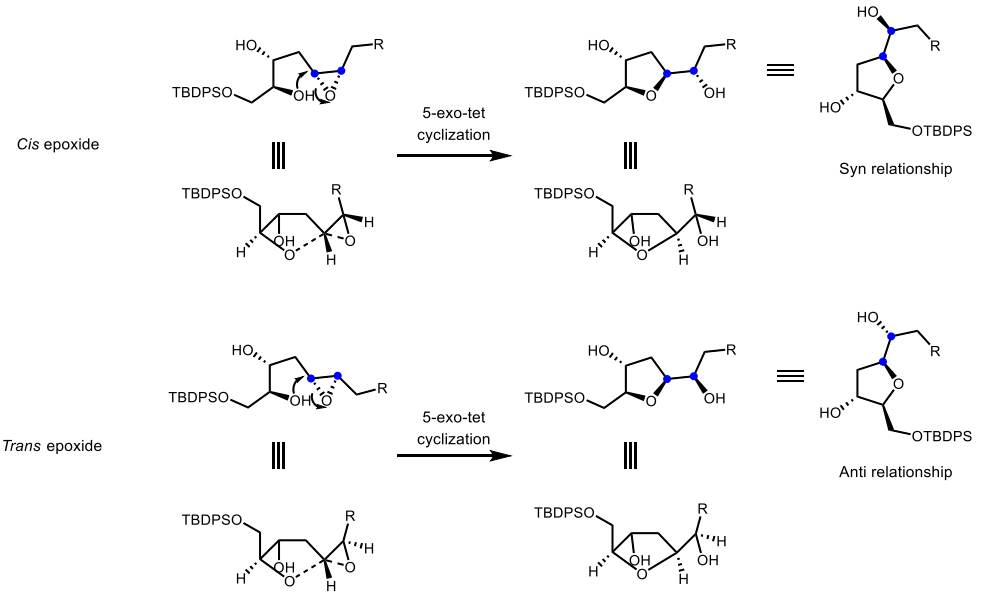

Figure 4.5. 2D and 3D representation of the stereospecific 5-*exo-tet*, cyclization and how the stereochemistry of the epoxide determines the stereochemistry of the furan product. The cis epoxide will afford a syn relationship between the two oxygens (shown in blue dots). The trans epoxides will afford an anti-relationship between the two oxygens (shown in blue dots).

As mentioned earlier, inspiration for the described stereodivergent synthetic strategy originated from a synthesis of four linoleic triols previously described by the Sulikowski group.[41] L- and D-tartaric acids are ideal starting materials because they are commercially available and inexpensive, 12 cents per gram for L-tartaric acid and 1 dollar per gram for D-tartaric acid. This allowed the synthetic sequence to start on a 100-gram scale or an even higher scale. However, a drawback is conversion to alkynes **4.1** and **4.2** required six steps and proceeded in 7-10 % overall yield.[41] By comparison 2-deoxy- ribose costs $7.20 per gram ($4.00 per gram at the time of purchase in 2019) for the L-isomer and $0.80 per a gram for the D-isomer. While these materials are more expensive than tartaric acid, they only require a 3-step reaction sequence to advance to

alkynes **4.3** and **4.4 (Figure 4.1).** The short reaction sequence proceeds in 37 % yield over 3 steps. This route allowed material to be accessed quicker and in quantity.

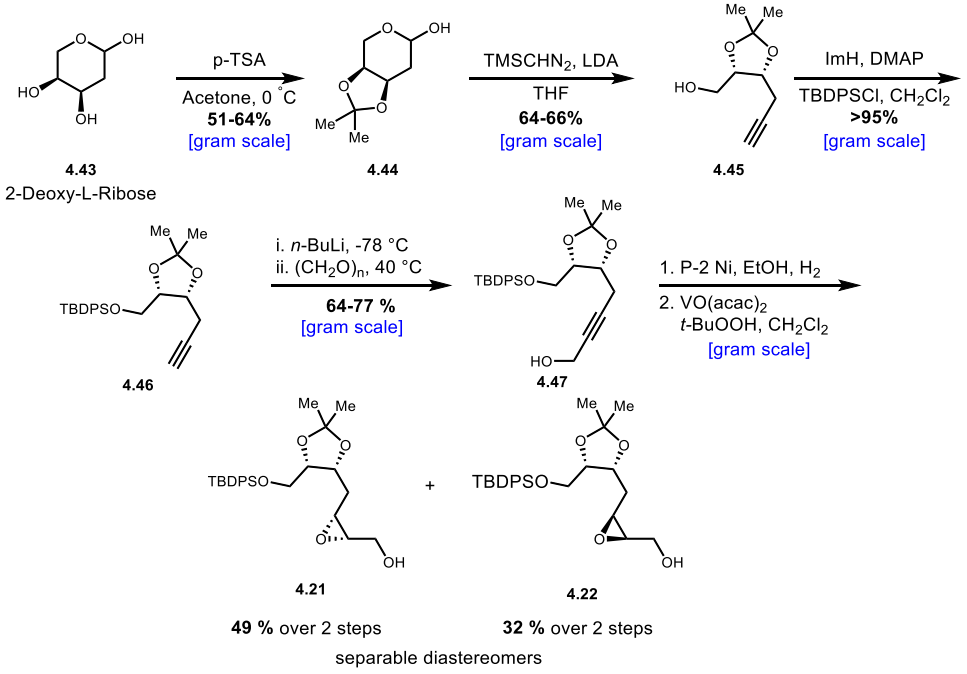

Scheme 4.1. Synthesis of epoxides **4.21** and **4.22** from 2-deoxy-L-ribose as the first point of stereodivergence.

The synthesis of epoxides **4.21** and **4.22** as shown in **Scheme 4.1** began with 2-deoxy-L-ribose in acetone and a catalytic amount of p-TSA. This afforded acetonide **4.44** in yields ranging from 51 to 64% on multi-gram scale. Early in our studies, yields were often irreproducible and low, subsequently we determined careful maintaining of reaction temperature 0 °C was critical for reproducibility. If there was any increase to the temperature, the yield of the reaction would often decrease. Lactol **4.44** was then subjected to a Colvin alkynylation starting with trimetylsilyldiazomethane, deprotonation with LDA in THF at -78 °C followed by addition of **4.44**. This reaction was previously reported, but in our hands the yield was significantly lower.[42]

Eventually, it was discovered the product, alkynol **4.45,** was slightly volatile and if left on the vacuum pump overnight, the product was lost resulting in a lower yield. Lowering time under vacuum resulted in increased yields similar to that reported in the literature.[42] Silylation of alcohol

4.45 proceeded smoothly to afford TBDPS ether **4.46** in >95% yield. Deprotonation of the alkyne followed by quenching with paraformaldehyde at 40 °C generated propargyl alcohol **4.47** in 64-77% yield. This represents a key point in the synthesis because the propargyl alcohol can be semi-reduced to afford either the *cis* olefin or the *trans* olefin leading to either *cis* or *trans* epoxide (**Figure 4.2**) serving as a key divergent point of stereochemistry. My work focused on generating the *cis* olefin, which was accessed by semireduction of **4.47** with P-2 nickel, and when followed by $VO(acac)_2$ epoxidation gave rise to epoxides **4.21** and **4.22** in 49 and 32% yield respectivley.[43,44] Gratifyingly, these diastereomers are separable by flash chromatography, allowing the first key point of divergence in the synthetic route. With the diastereomers separated, **4.21** and **4.22** were subjected to parallel reaction sequences (**Scheme 4.2**).

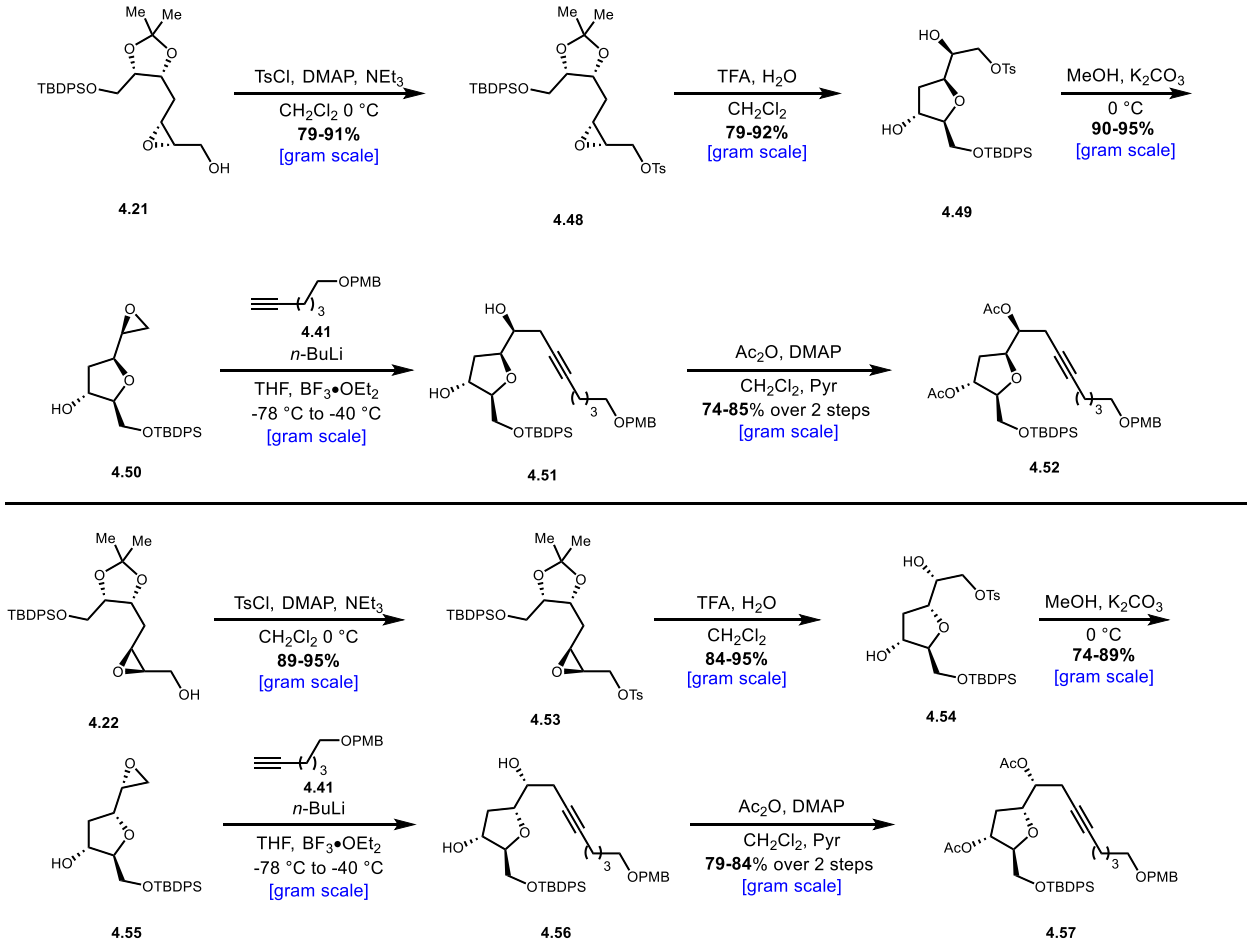

Scheme 4.2. Conversion of compounds **4.21** and **4.22** to **4.52** and **4.57** respectively *via* a stereospecific cyclization to install the furan core and installation of the alpha sidechain.

Epoxy alcohol **4.21** was treated with p-toluensulfonyl chloride, DMAP, and triethylamine as a solution in dichloromethane at 0 °C to afford tosylate **4.48** in high yield. Subjection of **4.48** to a solution of TFA and trace water in dichloromethane resulted in acetonide removal followed by 5-*exo-tet* cyclization to give furan **4.49** as a single isomer (**Figure 4.5**). In preparation for introduction of the alpha-side-chain, **4.49** was treated with K_2CO_3 in methanol at 0 °C to give epoxide **4.50** in 90-95% yield. The latter was added to a lithium anion of alkyne **4.41** in the presence of $BF_3 \bullet OEt_2$ to afford furan **4.51**, upon peracetylation diactetate **4.52** was obtained in high yield. Following an identical reaction sequence, epoxy alcohol **4.22** was converted to isomeric diacetate **4.57** (**Scheme 4.2**). The stereochemistry of epoxides **4.50** and **4.55** were assigned by Mosher ester analysis (*vide infra* **Figure 4.8** and **4.9**).

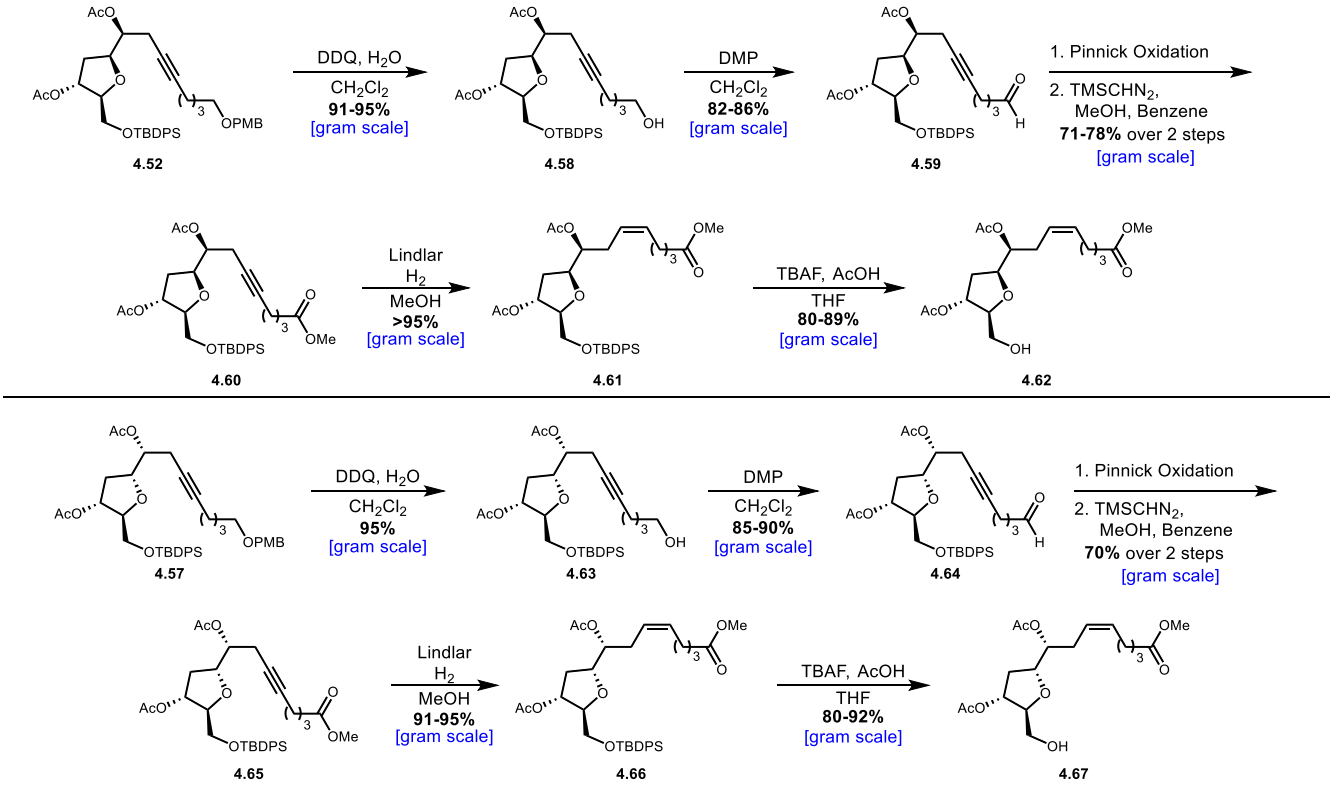

Scheme 4.3. Elaboration of the alpha side chain to the correct oxidation state of the isofurans, resulting in alcohols **4.62** and **4.67**.

With furans **4.52** and **4.57** in hand, we turned our attention to functionalization of the alpha-side chain starting with oxidation state adjustment of the primary alcohol. To this end the PMB protecting group of **4.52** was removed using DDQ and trace water in dichloromethane to afford alcohol **4.58** (**Scheme 4.3)** in excellent yield. Next, a standard two-step oxidation was employed starting with Dess-Martin periodinane oxidation to afford aldehyde **4.59**.[45] Further oxidation under Pinnick conditions provided the corresponding carboxylic acid and immediate reaction with TMS diazomethane gave methyl ester **4.60** with yields ranging from 10-78% over 2 steps.[46,47] Semi-hydrogenation of the isolated alkyne with Lindlar's catalyst provided *cis*-alkene **4.61** in near quantitative yield and completed the alpha-side-chain. Installation of the omega-sidechain began with removal of the silyl ether protecting group using acetic acid buffered-TBAF to give **4.62** in 80-89% yield. If acetic acid buffer was not used, acyl migration of the secondary acetate to the primary alcohol was observed. A parallel sequence advanced furan **4.57** to **4.67**.

With the alpha-sidechain installed in the correct oxidation state the synthetic focus moves to installing the omega-sidechain (**Scheme 4.4**). The sequence begins with Moffat oxidation of alcohol **4.62** followed by immediate olefination of the crude aldehyde under Horner-Wadsworth-Emmons condition with ketophosphonate **4.42** to give enone **4.68** in a 33-46% yield.[48,49] Luche reduction afforded an insperable mixture of epimeric C15 alcohols. Separation was conveniently achieved using lipase Amano AK to selectively acetylate one stereoisomer. Three enzymes were used in the initial screen, Novozyme 435. Amano AK and Amano SD. Novozyme 435 failed to give any reasonable conversion, however, Amano AK and Amano SD gave promising conversion and eventually the Amano AK conditions were optimized to fully convert **4.69** to triacetylated compound **4.71** in 45-50% yield as a single diastereomer and provided the enriched, bis-acetate compound **4.70** in 45-50 % yield as a single diastereomer.

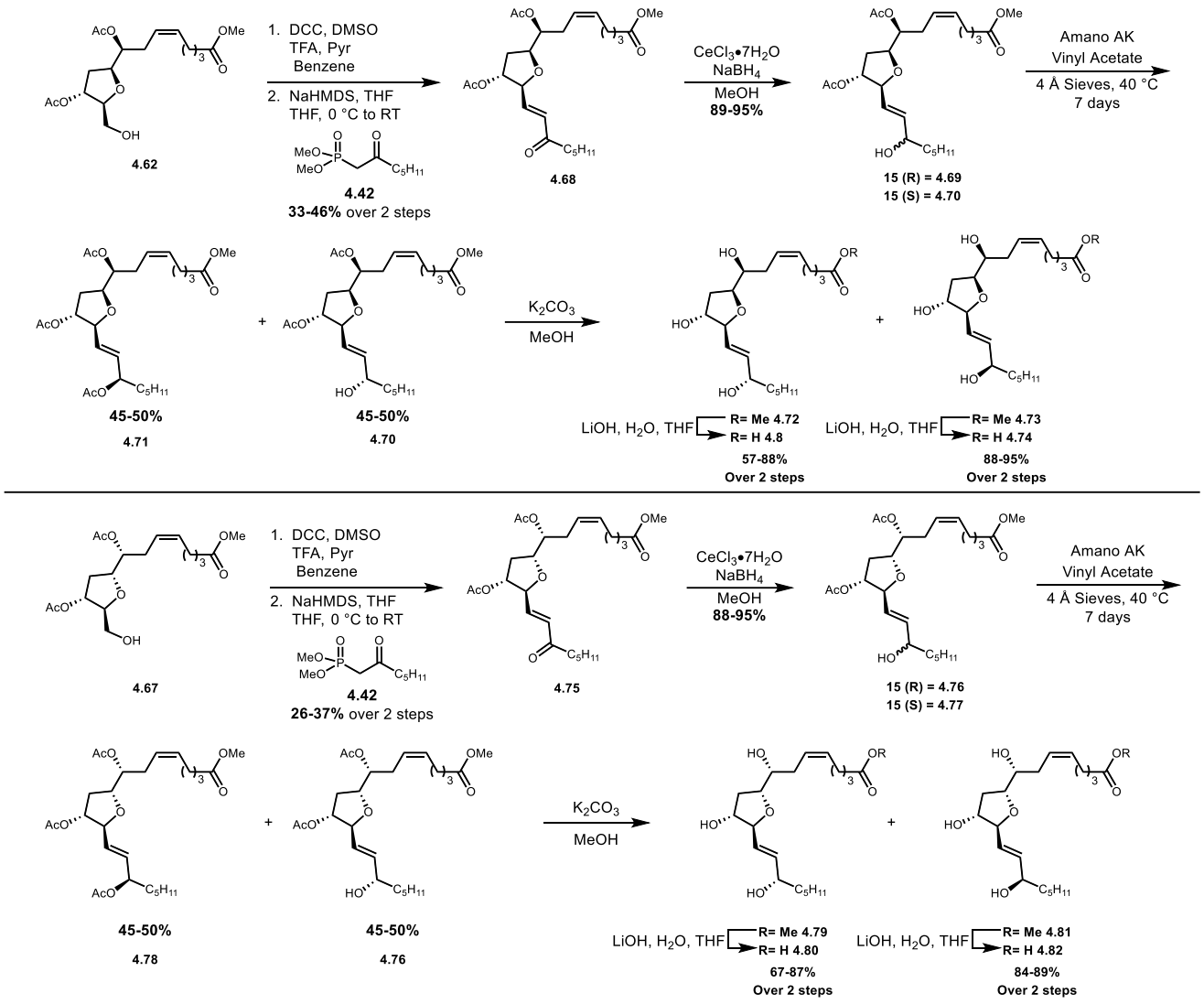

Scheme 4.4. Synthesis of final isofurans **4.8**, **4.74**, **4.80**, and **4.82** through a stereodivergent approach.

Through Mosher ester analysis it was discovered that the (R) stereoisomer was selectively acetylated leaving the (S) isomer as the allylic alcohol (*vide infra* **figure 4.10**). After the stereoisomers had been resolved and separated by flash chromatography compounds **4.71** and **4.70** were separately treated with K_2CO_3 in methanol to afford triol's **4.72** and **4.73**. Then treatment with LiOH in aqueous THF gave rise to isofurans **4.8** and **4.74** in a good yield over 2 steps. The deprotection procedure could likely be done in one step by treating compounds **4.71** and **4.70** with excess LiOH (**Scheme 4.4**). However, storage of the methyl ester isofuran was preferred, so a

two-step deprotection sequence where most of the compounds would be stored as the isofuran methyl ester and hydrolyzed to the carboxylic acid so they can be tested as needed.

Mosher Ester Analysis

A challenge of employing a stereodivergent strategy to synthesize isofurans is the stereochemical assignment of the stereocenters (**Figure 4.6**). When using a chiral reagent such as CBS reduction, BINAL reduction, Sharpless epoxidation or Sharpless dihydroxylation, there is typically a model to predict which stereoisomer will be generated in the chemical reaction, although not always correct. By using reactions which give equal distributions of diastereomers, these models cannot be used.

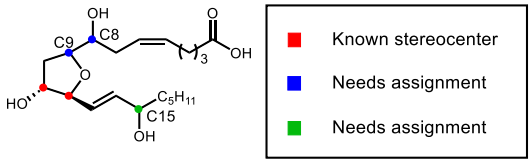

Figure 4.6. Stereocenters shown in red C(11, 12) are known because of the starting material. Stereocenters in blue C(8, 9) are introduced via stereoselective epoxidation. The stereocenter in green C(15) is introduced via non-selective Luche reduction.

However, the use of Mosher ester analysis can assign the stereochemistry of secondary alcohols.[50,51] After installing epoxides **4.21** and **4.22** the stereochemistry of these epoxides were not known. To discover the stereochemistry of the epoxides we needed to ensure only the C8 alcohol can react with the Mosher acid.

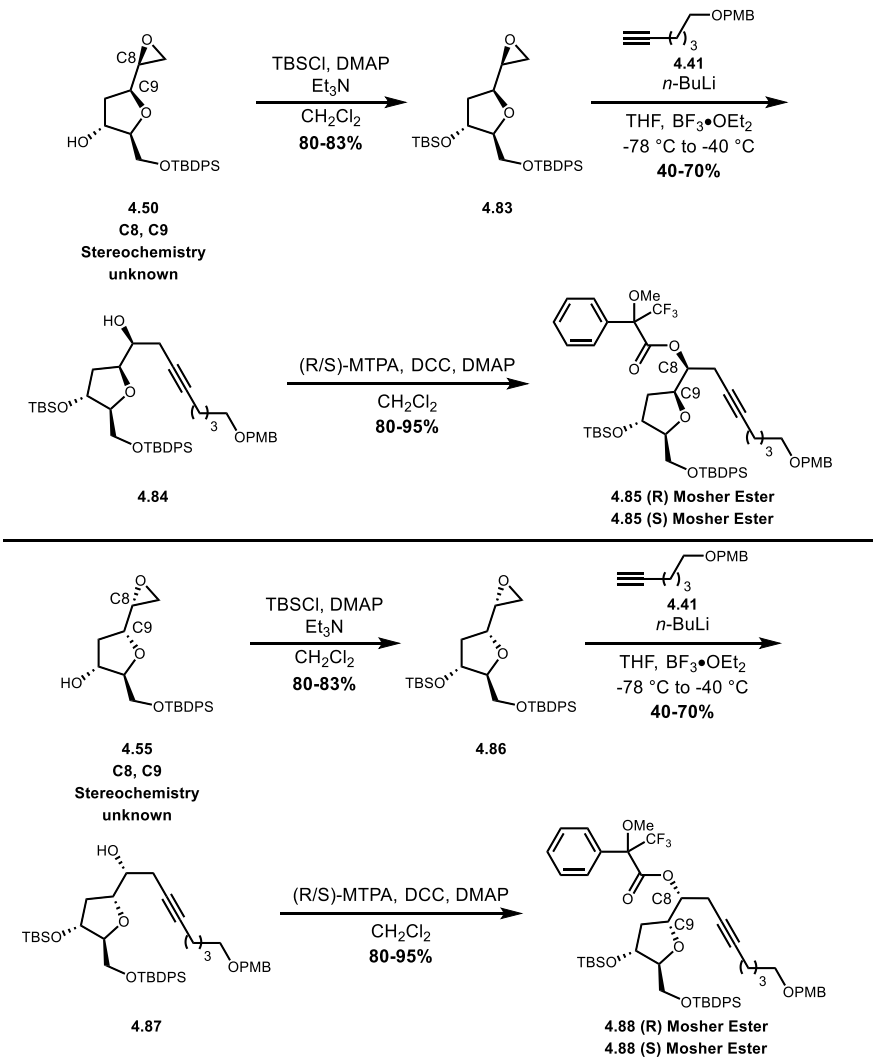

Scheme 4.5. Conversion of epoxide **4.50** to Mosher esters **4.85 (R)** and **4.85 (S)**, and conversion of epoxide **4.55** to Mosher ester **4.88 (R)** and **4.88 (S)**.

The Mosher ester analysis began by treating epoxides **4.50** and **4.55** (whose stereochemistry was unknown at the time) with TBSCl to install TBS ether **4.83**. Then treatment of with lithiated alkyne **4.41** in the presence of BF_3•EtO_2 afforded **4.84** which had the appropriate C8 alcohol which was exposed to DCC for a Steglitch esterification of the corresponding R/S Mosher acid.[52] This allowed access to Mosher esters (R)-**4.85** and (S)-**4.85** which enables the assignment of the C8 stereocenter. The lowest energy conformation of the Mosher ester is in the s-*trans* conformation allowing the methine of unknown stereochemistry, and trifluoromethyl

group to eclipses the carbonyl (C=O) bond. This allows for a predicted confirmation of the Mosher ester (**Figure 4.7**). Furthermore, the phenyl ring shields the protons through anisotropy. This means the R_1 protons on the (S) Mosher ester will be shielded, while in the (R) Mosher ester the R_2 protons will be shielded. The difference between the two ^1H NMR shifts (listed as ppm) can be listed as the $\Delta\delta^{SR}=\delta_S-\delta_R$. In this case the R_1 protons will have a $\Delta\delta^{SR} < 0$ and the R_2 protons will have a $\Delta\delta^{SR} > 0$. If the R groups are of the other diastereomer then the $\Delta\delta^{SR}$ values will be inverted.

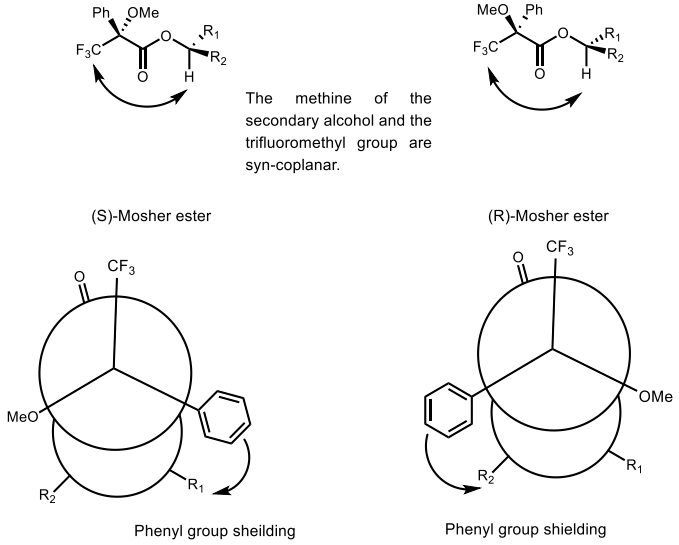

Figure 4.7. The model for Mosher ester analysis presented by the Hoye group which allows for stereochemical assignment of secondary alcohols.

NMR analysis of chemical shift of protons at the C7 and C9 position showed the C8 stereocenter of compounds **4.85 (S)** and **4.85 (R)** (**Figure 4.8, Table 4.1**) was in the **S configuration**. Since the cyclization of *cis* epoxide **4.48** to **4.49** is stereospecific the stereochemistry of C9 can be extrapolated to be the **S configuration** (See **Figure 4.5**).

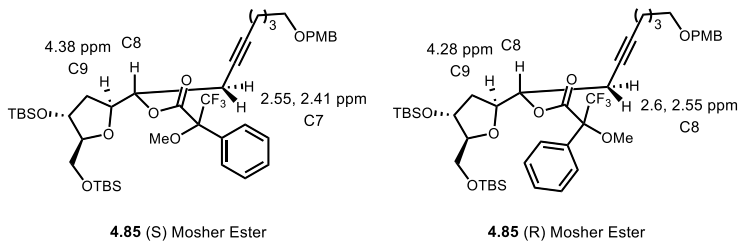

4.85 (S) Mosher Ester **4.85** (R) Mosher Ester

Figure 4.8. Chemical shift of C7 and C9 protons allowing for stereochemical assignment of the C8 position (S) of compound **4.85** based on the $\Delta\delta_H$ value.

Proton Identification	$\Delta\delta_H$ **4.85(S)-4.85(R)**
H7	- 0.095
H9	+ 0.10

Table 4.1. Based off the $\Delta\delta_H^{SR}$ values in **figure 4.8** of H7 and H9 the stereochemistry of **4.85** (R) and **4.85** (S) C8 is determined as S.

The stereochemistry of compounds **4.87 (S)** and **4.87 (R)** was determined by the same NMR analysis resulting in stereochemical assignment of the C8 stereocenter as the **R configuration (Figure 4.9, Table 4.2)** and the C9 stereocenter was assigned as the **R configuration**. Similarly, in compound **4.48** the stereochemistry of the C9 stereocenter is set by a stereospecific cyclization, so it can be extrapolated from the C8 stereocenter. With stereochemistry of compounds **4.48** and **4.53** assigned, the stereochemistry of epoxides **4.21** and **4.22** were assigned, allowing for continuation of the synthesis of the isofurans.

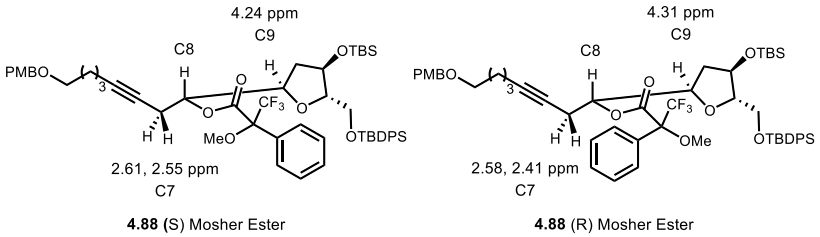

Figure 4.9. Chemical shift of C7 and C9 protons allowing for stereochemical assignment of the C8 position (R) of compound **4.88** based on the $\Delta\delta_H$ value.

Proton Identification	$\Delta\delta_H$ **4.88(S)-4.88(R)**
H7	+ 0.085
H9	- 0.07

Table 4.2. Based off the $\Delta\delta_H^{SR}$ values in **Figure 4.9** of H7 and H9 the stereochemistry of **4.88** (R) and **4.88** (S) C8 is determined as R.

After the enzymatic resolution of allylic alcohols **4.70** and **4.76** the stereochemistry of the C15 carbon was unknown for both the triacetylated compound and the bis-acetylated compound. To solve this task the recovered enriched allylic alcohol **4.76** with unknown stereochemistry was esterified with R/S MPTA to give rise to Mosher esters **4.89 (S)** and **4.89 (R)** (**Scheme 4.6**). Then NMR analysis of the chemical shift of proton on carbons C13, 14, and 16 was used to determine the stereochemistry of the C15 position. Based off the chemical shifts of protons H13, H14 and H16 in both the R and S Mosher ester the absolute stereochemistry of the 15 carbon is the **S configuration** (**Figure 4.10** and **Table 4.3)**. This implies the enzymatic resolution of compounds **4.76** to tri acetylated compound **4.78** acylated the **(R)** stereoisomer while the **(S)** stereocenter is recovered. Due to the lack of material so far into the synthetic sequence (21 steps) the (ST) series could not be tested to confirm the stereochemistry of the C15 stereocenter.

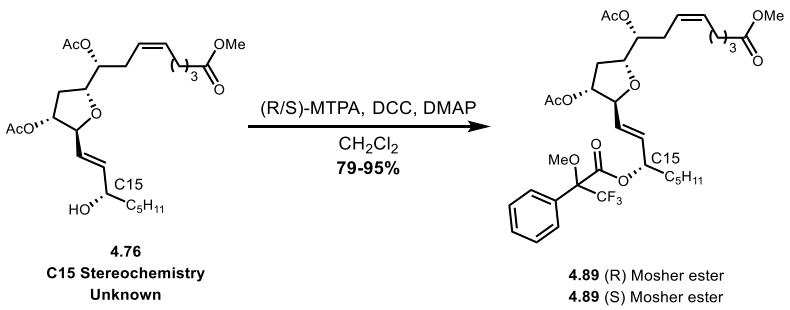

4.76
C15 Stereochemistry
Unknown

4.89 (R) Mosher ester
4.89 (S) Mosher ester

Scheme 4.6. Conversion of allylic alcohol to Mosher esters **4.89 (R)** and **4.89 (S)**.

However, given the structural similarities between the AT and ST series the stereochemistry of the AT series can be presumed to acetylate the R stereoisomer. Also, Dr. Zach Austin performed a similar Mosher ester analysis using on the SC series and had the same result of acetylating the R stereoisomer giving further confidence to our assumption that Amano AK is acetylating to R stereoisomer and not acetylating the S stereoisomer.

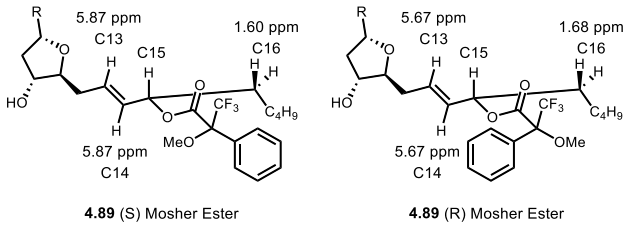

4.89 (S) Mosher Ester **4.89** (R) Mosher Ester

Figure 4.10. Chemical shift of C13, C14 and C16 protons allowing for stereochemical assignment of the C15 position (S) based on the $\Delta\delta_H$ value.

Proton Identification	$\Delta\delta_H$ **4.89(S)-4.89(R)**
H13	+ 0.20
H14	+0.20
H16	-0.08

Table 4.3. Based off the $\Delta\delta_H^{SR}$ values in **Figure 4.10** of H13, H14, and H16 the stereochemistry of C15 is determined to be S.

Conclusion

In conclusion four of the Δ^{13}-9-Isofurans from the ST and AT series have been synthesized from 2-deoxy-L-ribose with a LLS of 23 steps. In conjunction with Zach Austin who has accesses four other diastereomers of the Δ^{13}-9-Isofurans from the AC and SC series we have developed a route to install the furan core of the Δ^{13}-9-Isofurans, install the alpha and omega-sidechain and separate the diastereomers through flash chromatography or enzymatic resolution. This shows we have a robust route to access all the Δ^{13}-9-Isofurans which will enable our collaborators in the West lab to probe their function in the pathogenesis of PAH.

References

(42) Yuen, T.-Y.; Brimble, M. A. Total Sythesis of 7', 8'-Dihydroaigialospirol. *Org. Lett.* **2012**, *14* (9), 5154–5157.

(43) Brown, C. A.; Ahuja, V. K. "P-2 Nickel" Catalyst with Ethylenediamine, a Novel System for Highly Stereospecific Reduction of Alkynes to Cis-Olefins. *J. Chem. Soc. Chem.*

Commun. **1973**, No. 15, 553–554. https://doi.org/10.1039/C39730000553.

(44) Rossiter, B. E.; Verhoeven, T. R.; Sharpless, K. B. Stereoselective Epoxidation of Acyclic Allylic Alcohols. A Correction of Our Previous Work. *Tetrahedron Lett.* **1979**, No. 49, 4733–4736.

(45) Dess, D. B.; Martin, J. C. Readily Accessible 12-I-5 Oxidant for the Conversion of Primary and Secondary Alcohols to Aldehydes and Ketones. *J. Org. Chem.* **1983**, *48* (22), 4155–4156. https://doi.org/10.1177/002205740706502225.

(46) Bal, B. S.; Childers, W. E.; Pinnick, H. W. Oxidation of α,β-Unsaturated Aldehydes. *Tetrahedron* **1981**, *37* (11), 2091–2096. https://doi.org/10.1016/S0040-4020(01)97963-3.

(47) Hashimoto, H.; Aoyama, T.; Shioiri, T. New Methods and Reagents in Organic Synthesis 14. A Simple Efficient Preparation of Methyl Esters with Trimethylsilyldiazomethane and Its Application to Gas Chromatographic Analysis of Faccy Acids. *Chem. Pharm. Bull.* **1981**, *29*, 1475–1478.

(48) Danishefsky, S. J.; DeNinno, S. L.; Chen, S. hui; Boisvert, L.; Barbachyn, M. Fully Synthetic Stereoselective Routes to the Differentially Protected Subunits of the Tunicamycins. *J. Am. Chem. Soc.* **1989**, *111* (15), 5810–5818. https://doi.org/10.1021/ja00197a047.

(49) Wadsworth, W. S.; Emmons, W. D. The Utility of Phosphonate Carbanions in Olefin Synthesis. *J. Am. Chem. Soc.* **1961**, *83* (7), 1733–1738. https://doi.org/10.1021/ja01468a042.

(50) Hoye, T. R.; Jeffrey, C. S.; Shao, F. Mosher Ester Analysis for the Determination of Absolute Configuration of Stereogenic (Chiral) Carbinol Carbons. *Nat. Protoc.* **2007**, *2* (10), 2451–2458. https://doi.org/10.1038/nprot.2007.354.

(51) Dale, J. A.; Masher, H. S. Nuclear Magnetic Resonance Enantiomer Reagents. Configurational Correlations. *J. Am. Chem. Soc.* **1973**, *95* (2), 512–519.

(52) Neises, B.; Steglitch, W. Simple Method for the Esterification of Carboxylic Acids. *Angew. Chemie - Int. Ed.* **1978**, *17*, 552–524.

1. General Procedure: All non-aqueous reactions were performed in flame-dried or oven dried round-bottomed flasks under an atmosphere of argon. Stainless steel syringes or cannula were used to transfer air- and moisture-sensitive liquids. Reaction temperatures were controlled using a thermocouple thermometer and analog hotplate stirrer and monitored using liquid-in-glass thermometers. Reactions were conducted at room temperature (approximately 21-23 °C) unless otherwise noted. Flash column chromatography was conducted using silica gel 230-400 mesh or Silica RediSep Rf flash columns on a CombiFlash Rf automated flash chromatography system. Reactions were monitored by analytical thin-layer chromatography, using Analtech silica gel GF 250 micron glass-backed pre-coated silica gel plates. The plates were visualized with UV light (254 nm) and stained with potassium permanganate or *p*- anisaldehyde-sulfuric acid followed by charring. Yields were reported as isolated, spectroscopically pure compounds.

2. Materials: Solvents and chemicals were purchased from Sigma-Aldrich, Acros Organics, TCI and/or Alfa Aesar and used without further purification. Solvents were purchased from Fisher Scientific. Dry dichloromethane (CH_2Cl_2) was collected from an MBraun MB-SPS solvent system. Triethylamine, N,N-dimethylformamide (DMF) and dimethyl sulfoxide (DMSO) were used as received in a bottle with a Sure/Seal. Tetrahydrofuran (THF) was distilled for a sodium/benzophenone still. Deuterated solvents were purchased from Cambridge Isotope Laboratories.

3. Instrumentation: Infrared spectra were obtained as thin films on NaCl plates using a Thermo Electron IR100 series instrument and are reported in terms of frequency of absorbance (cm^{-1}). ^1H NMR spectra were recorded on Bruker 400 or 600 MHz spectrometers and are reported relative to internal chloroform (^1H, δ 7.26). Data for ^1H NMR spectra are reported as follows: chemical shift (δ ppm), multiplicity (s = singlet, d = doublet, t = triplet, dd = doublet of doublet, ddd = doublet of

doublet of doublet, m = multiplet, br=broad), coupling constants (Hz), and integration. ^{13}C NMR were recorded on Bruker 100 or 150 MHz spectrometers and are reported relative to internal chloroform (^{13}C, δ 77.1). Low-resolution mass spectra were acquired on an Agilent Technologies Series 1200 series 6130 using electrospray ionization (ESI) in positive mode.

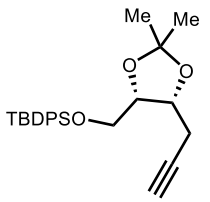

4.46

4.46: To a solution of alcohol **4.45**[42] (3.8 g, 22 mmol) in CH_2Cl_2 (28 ml) was added imidazole (3.3 g, 49 mmol) and DMAP (270 mg, 2.2 mmol). The resulting solution was then cooled to 0 °C, and TBDPSCl (6.4 ml, 25 mmol) was added dropwise over 10 min. The reaction mixture was allowed to warm to room temperature and maintained for 16 h. The reaction was quenched with satd. aq. $NaHCO_3$ (20 mL). The aqueous layer was extracted with CH_2Cl_2 (3 x 25 ml) and the combined organics were dried ($MgSO_4$), then filtered, and conc. *in vacuo*. The residue was purified by flash chromatography (gradient: hexanes to 19:1 to 9:1 hexanes/EtOAc) to afford 9.1 g (>95%) **4.46** as a clear oil: R_f 0.8 (4:1 hexanes: EtOAc); $[a]^{23}_D$ +2.0 (*c* 1.0, $CHCl_3$); ^1H NMR (400 MHz, $CDCl_3$) δ 7.70-7.67 (m, 4H), 7.45-7.37 (m, 6H), 4.38, (m, 1H), 4.26, (m, 1H), 3.79 (ddd, *J* = 6.8, 10.8, 20.9 Hz, 2H), 2.68 (ddd, *J* = 2.6, 5.3, 16.7 Hz, 1H), 2.54 (ddd, *J* = 2.7, 7.8, 16.8 Hz, 1H), 2.00 (t, *J* = 2.7 Hz, 1H), 1.44 (s, 3H), 1.37 (s, 3H), 1.07 (s, 9H); ^{13}C NMR (100 MHz, $CDCl_3$) δ 135.7, 133.3, 129.9, 127.9, 108.7, 81.2, 77.7, 75.8, 69.9, 62.3, 28.2, 27.3, 25.8, 20.6; LRMS calculated for $C_{25}H_{32}O_3Si$ $[M+Na]^+$ m/z 431.2; measured LC/MS (ESI) R_t 1.3 min, m/z 431.0 $[M+Na]^+$.

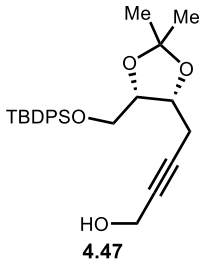

4.47

4.47: To a cooled stirred solution of **4.46** (9.10 g, 22.3 mmol) in THF (55 mL), at -78 °C, was added *n*-BuLi (11 ml, 26.7 mmol) in a 2.5 M solution in hexanes dropwise over 10 min. Then the reaction mixture was maintained at -78 °C for 15 min, and allowed to warm to 0 °C for 45 min. The mixture was then cooled to -78 °C and $(CH_2O)_n$ (1.7 g, 55 mmol) was added by solid addition funnel in one portion. The

reaction mixture was stirred at -78 °C for 15 min, allowed to warm to 0 °C for 15 min, then brought to room temperature for 15 min. Then the reaction mixture was heated to 40 °C for 24 h. After 24 h the reaction was quenched at 0 °C with saturated ammonium chloride (30 mL). Then the reaction mixture was partitioned with EtOAc (40 mL). The aqueous layer was extracted with EtOAc (3 x 40 mL). The combined organics were washed with brine (40 mL), dried ($MgSO_4$), filtered and concentrated *in vacuo*. The crude residue was purified by flash chromatography (gradient: 9:1 to 4:1 Hexanes/EtOAc) to afford 6.90 g (70 %) of propargyl alcohol **S5** as an amber oil: R_f 0.2 (4:1 hexanes: EtOAc); $[a]^{23}_D$ -4.1 (*c* 0.4, $CHCl_3$); ^{1}H NMR (400 MHz, $CDCl_3$) δ 7.69-7.66 (m, 4H), 7.45-7.26 (m, 6H), 4.33 (m, 1H), 4.23 (m, 1H), 4.19 (s, 2H), 3.70 (ddd, *J* = 7, 10.9, 24.6 Hz, 2H), 2.63 (dt, *J* = 1.9, 16.7 Hz, 1H), 2.48 (dt, *J* = 2.1, 16.9 Hz, 1H), 1.43 (s, 3H), 1.35, (s, 3H), 1.09, (s, 9H); ^{13}C NMR (100 MHz, $CDCl_3$) δ 135.7, 133.3, 129.9, 127.89, 108.7, 83.0, 80.0, 77.3, 75.9, 62.4, 54.5, 30.0, 27.0, 25.5, 20.6, 19.3; LRMS calculated for $C_{26}H_{34}O_4Si$ $[M+Na]^+$ m/z 461.2; measured LC/MS (ESI) R_t 1.1 min, m/z 461.0 $[M+Na]^+$.

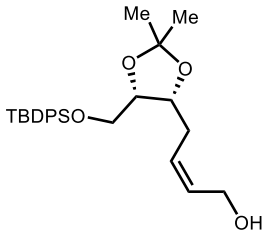

(Z)-4.47

(Z)-4.47: To a suspension of $Ni(OAc)_2 \cdot 4H_2O$ (724 mg, 2.55 mmol) in thoroughly degassed EtOH (19 mL) was added $NaBH_4$ (90.4 mg, 2.42 mmol) in a solution of EtOH (2.4 mL). The suspension turned black accompanied by evolution of gas. Ethylene diamine (156 µL, 2.3 mmol) was added followed by a solution of propargyl alcohol **4.47** (5.6 g, 12.8 mmol) in EtOH (130 mL). The final solution was then evacuated and refilled with hydrogen gas three times and allowed to stir for 2 h. The mixture was diluted with ether (150 mL) and filtered through a plug of silica washed with Et_2O (ca. 100 mL). The filtrate was concentrated *in vacuo* to afford 5.3 g (95 %) of crude **(Z)-4.47** as a yellow oil: R_f 0.2 (4:1 Hexanes: EtOAc); $[a]^{23}_D$ +8.6 (*c* 1.0, $CHCl_3$); ^{1}H NMR (400 MHz, $CDCl_3$) δ 7.68-7.65 (m, 4H), 7.46-7.37 (m, 6H), 5.83 (m, 1H), 5.67 (m, 1H), 4.20 (m,

3H), 4.02 (dd, *J* = 6.6, 12.4 Hz, 1H), 3.78-3.67 (m, 2H), 2.54-2.41 (m, 2H), 1.39 (s, 3H), 1.32 (s, 3H), 1.07 (s, 9 H); ^{13}C NMR (100 MHz, $CDCl_3$) δ 135.73, 135.71, 133.4, 133.3, 131.1, 130.0, 129.5, 127.91, 127.90, 108.2, 77.7, 76.6, 62.7, 58.0, 27.9, 27.8, 25.4, 19.3; LRMS calculated for $C_{26}H_{36}O_4Si$ $[M+Na]^+$ m/z 463.2; measured LC/MS (ESI) R_t 1.1 min, m/z 463.0 $[M+Na]^+$.

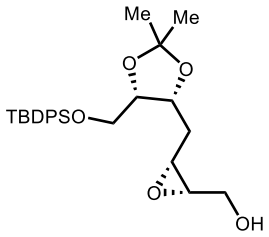

4.21

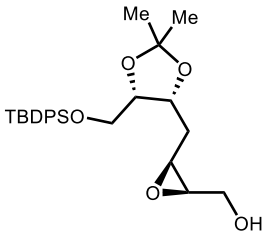

4.22

To a solution of crude allylic alcohol **(Z)-4.47** (5.3 g, 12 mmol) in CH_2Cl_2 (120 mL) at 0 °C was added $VO(acac)_2$ (127 mg, 0.48 mmol) and *t*-BuOOH (3.3 mL of 5.5 M nonane solution, 18 mmol). The reaction was allowed to warm to room temperature and maintained for 24 h. The reaction was quenched with aq. Satd. sodium thiosulfate (50 mL). The aqueous layer was extracted with CH_2Cl_2 (3 x 50 mL), combined organic extracts were washed with brine (20 mL), dried ($MgSO_4$), filtered and concentrated *in vacuo*. The residue was purified by flash chromatography (gradient: 4:1 to 2:1 Hexanes/EtOAc) to afford 2.54 g (46% yield) of **4.21** and 2.22 g (38 %) of **4.22** as clear oils. **4.21:** R_f 0.55 (1:1 Hexanes: EtOAc); $[a]^{23}_D$ +2.0 (*c* 1.0, $CHCl_3$); ^{1}H NMR (400 MHz, $CDCl_3$) δ 7.62-7.67 (m, 4H), 7.36-7.47 (m, 6H), 4.40 (ddd, *J* = 1.6, 6.5, 10.9 Hz, 1H), 4.23 (m, 1H), 3.68 (ddd, *J* = 4.9, 10.1, 12.0 Hz, 1H), 3.66 (m, 2H), 3.46 (ddd, *J* = 3.6, 8.2, 12 Hz, 1H), 3.20 (m, 1H), 3.13 (m, 1H), 2.93, (dd, *J* = 3.6, 10.1 Hz, 1H), 2.34 (ddd, *J* = 1.6, 4.5, 14.4 Hz, 1H), 1.66 (ddd, *J* = 9.0, 11.3, 14.4 Hz, 1H), 1.39 (s, 3H), 1.35 (s, 3H), 1.05 (s, 9H); ^{13}C NMR (100 MHz, $CDCl_3$) δ 135.7, 133.1, 130.0, 128.0, 108.7, 77.4, 74.4, 62.3, 60.1, 55.6, 55.1, 27.9, 27.6, 25.3, 19.3; LRMS calculated for $C_{26}H_{36}O_5Si$ $[M+Na]^+$ m/z 479.2; measured LC/MS (ESI) R_t 1.0 min, m/z 479.0 $[M+Na]^+$. **4.22:** R_f 0.5 (1:1 Hexanes: EtOAc); $[a]^{23}_D$ +2.0 (*c* 1.0, $CHCl_3$); ^{1}H NMR (400 MHz, $CDCl_3$) δ 7.59-7.67 (m, 4H), 7.34-7.46 (m, 6H), 4.36 (dt, *J* = 5.6, 7.9 Hz, 1H), 4.24, (dt, *J* = 5.4, 7.9 Hz, 1H), 3.79 (m, 1H), 3.75-3.64 (m, 3H), 3.24 (dt, *J* = 4.4, 6.2 Hz, 1H), 3.16

(dt, *J* = 4.5, 6.3 Hz, 1H), 1.98 (m, 2H), 1.76 (t, *J* = 6.7 Hz, 1H), 1.39 (s, 3H), 1.34 (s, 3H), 1.05 (s, 9H); ^{13}C NMR (100 MHz, $CDCl_3$) δ 135.7 (2), 133.2, 133.1, 128.0, 127.9, 108.6, 77.3, 75.6, 62.5, 60.9, 56.2, 54.9, 28.4, 28.0, 27.0, 25.1, 19.3; LRMS calculated for $C_{26}H_{36}O_5Si$ $[M+Na]^+$ m/z 479.2; measured LC/MS (ESI) R_t 1.0 min, m/z 479.0 $[M+Na]^+$.

General procedure for synthesis of tosylates 4.48 and 4.53

To a solution of alcohol **4.21** (1.36 g, 2.98 mmol) in CH_2Cl_2 (30 mL) at 0 °C was added triethylamine (1.0 mL, 7.5 mmol), DMAP (37 mg, 0.30 mmol) and p-toluenesulfonyl chloride (680 mg, 3.57 mmol). The subsequent solution was stirred to 0 °C for 3 h and quenched with water (10 mL). The aqueous layer was extracted with CH_2Cl_2 (3 x 15 mL). The combined organic extracts were washed with brine (20 mL), dried ($MgSO_4$), filtered and concentrated *in vacuo*. The residue was purified by flash chromatography (gradient: 9:1 to 4:1 hexanes/EtOAc) to afford 1.74 g (95 %) of tosylate **4.48** as clear oil.

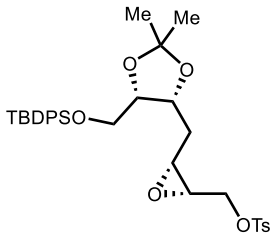

4.48

4.48: R_f 0.3 (4:1 Hexanes: EtOAc); $[a]^{23}_D$ -4.0 (*c* 1.0, $CHCl_3$); ^{1}H NMR (400 MHz, $CDCl_3$) δ 7.79 (d, *J* = 8.3 Hz, 2H), 7.64-7.61 (m, 4H), 7.46-7.35 (m, 6H), 7.31 (d, *J* = 8.1 Hz, 2H), 4.35 (m, 1H), 4.32 (m, 1H), 4.18 (m, 1H), 3.93 (dd, *J* = 7.1, 11.5 Hz, 1H), 3.66-3.58 (m, 2H), 2.42 (s, 3H), 1.90 (ddd, *J* = 2.3, 6.8, 14.2 Hz, 1H), 1.67 (m, 1H), 1.33 (s, 3H), 1.31 (s, 3H), 1.01 (s, 9H); ^{13}C NMR (100 MHz, $CDCl_3$) δ 145.1, 135.7, 133.1, 133.1, 130.0, 128.1, 128.0, 127.9, 108.5, 74.4, 69.1, 62.4, 54.5, 53.9, 28.9, 28.0, 26.9, 25.4, 21.8, 19.3; LRMS calculated for $C_{33}H_{42}O_7SSi^+$ $[M+NH_4]^+$ m/z 628.2, measured LC/MS (ESI) R_t 2.6 min, m/z 628.1 $[M+NH_4]^+$.

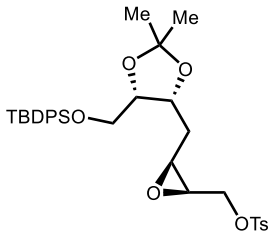

4.53

4.53: R_f 0.3 (4:1 Hexanes: EtOAc); $[a]^{23}_D$ +8.6 (*c* 1.0, $CHCl_3$); ^1H NMR (400 MHz, $CDCl_3$) δ 7.79 (d, *J* = 8.3 Hz, 2H), 7.67-7.60 (m, 4H), 7.48-7.35 (m, 6H), 7.32 (d, *J* = 7.9 Hz, 2H), 4.29 (dt, *J* = 5.4, 8.5 Hz, 1H), 4.23-4.14 (m, 2H), 4.08, (dd, *J* = 6.2, 11.3 Hz, 1H), 3.66 (m, 2H), 3.22 (m, 1H), 3.17 (m, 1H), 2.43 (s, 3H), 1.85 (m, 2H), 1.35 (s, 3H), 1.31 (s, 1H), 1.02 (s, 9H); ^{13}C NMR (100 MHz, $CDCl_3$) δ 145.3, 135.7, 133.1, 133.0, 132.9, 130.1, 130.0, 128.1, 128.0, 127.9, 108.5, 77.3, 75.3, 68.0, 62.4, 54.5, 52.9, 28.4, 28.1, 27.0, 25.6, 21.8, 19.3; LRMS calculated for $C_{33}H_{42}O_7SSi^+$ $[M+NH_4]^+$ m/z 628.2, measured LC/MS (ESI) R_t 2.6 min, m/z 628.2 $[M+NH_4]^+$.

General procedure for synthesis of furans 4.49 and 4.54

To a solution of epoxide **4.48** (4.05 g, 6.60 mmol) in CH_2Cl_2 (66 mL) was added water (4.2 mL) dropwise, the mixture was stirred vigorously for 5 min, TFA (0.75 mL, 10 mmol) was added and stirring continued for 2 h. Additional TFA (0.75 mL, 10 mmol) was added, and stirring continued for 2 h. The reaction mixture was then concentrated *in vacuo* and the residue purified by flash chromatography (gradient: 2:1 to 1:1 hexanes: EtOAc) to afford 3.5 g (93 %) of furan **4.49** as clear oil.

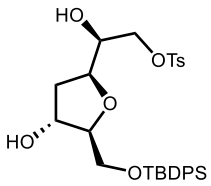

4.49

4.49: R_f 0.35 (2:1 hexanes/EtOAc); $[a]^{23}_D$ -6.5 (*c* 0.75, $CHCl_3$); ^1H NMR (400 MHz, $CDCl_3$) δ 7.80 (d, *J* = 8.3 Hz, 2H), 7.65-7.92 (m, 4H), 7.46-7.36 (m, 6H), 7.32 (d, *J* = 8.0 Hz, 2H), 4.44 (dt, *J* = 3.4, 6.8 Hz, 1H), 4.25 (m, 1 H), 4.05 (m, 2H), 3.80 (m, 1H), 3.73-3.65 (m, 3H), 2.73 (br s, 1H), 2.42 (s, 3H), 2.17 (ddd, *J* = 6.5, 8.1, 13.8 Hz, 1H), 1.92 (ddd, *J* = 3.6, 6.7, 13.0 Hz, 1H), 1.80 (br s, 1H), 1.04 (s, 9H); ^{13}C NMR (100 MHz, $CDCl_3$) δ 145.0, 135.7, 135.6, 133.0, 132.9, 132.8, 130.1 (2), 130.0, 128.1, 128.0, 86.6, 77.3, 73.3, 70.9, 70.8, 64.2, 37.1, 27.0, 21.8, 19.3; LRMS calculated for $C_{30}H_{38}O_7SSi$ $[M+Na]^+$ m/z 593.2; measured LC/MS (ESI) R_t 1.1 min, m/z 592.9 $[M+Na]^+$.

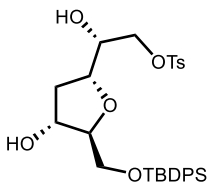

4.54

4.54: R_f 0.35 (2:1 hexanes/EtOAc); $[a]^{23}_D$ -15 (*c* 0.2, $CHCl_3$); ^1H NMR (400 MHz, $CDCl_3$) δ 7.80 (d, *J* = 8.2 Hz, 2H), 7.66-7.59 (m, 4H), 7.46-7.31 (m, 8H), 4.35 (m, 1H), 4.20-4.09 (m, 3H), 4.02 (m, 1H), 3.18 (ddd, *J* = 2.2, 4.6, 7.3 Hz, 1H), 3.62 (dd, *J* = 3.9, 10.8 Hz, 1H), 3.52 (dd, *J* = 5.5, 10.8 Hz, 1H), 2.50-2.40 (m, 4H), 1.91 (m, 1H), 1.04 (s, 9H); ^{13}C NMR (100 MHz, $CDCl_3$) δ 145.3, 135.7 (2), 133.3, 132.7, 130.1, 130.0, 129.9, 128.2, 127.9, 88.4, 78.3, 73.6, 71.9, 71.8, 64.9, 37.2, 27.0, 21.8, 19.3; LRMS calculated for $C_{30}H_{38}O_7SSi$ $[M+Na]^+$ m/z 593.2; measured LC/MS (ESI) R_t 2.1 min, m/z 592.9 $[M+Na]^+$.

General procedure for synthesis of epoxides 4.50 and 4.55

To a solution of tosylate **4.49** (3.4 g, 6.0 mmol) in MeOH (60 mL) at 0 °C was added K_2CO_3 (2.5 g, 18 mmol). The resulting slurry was allowed to stir at 0 °C for 2.5 h and water (30 mL) was added to the reaction followed by EtOAc (45 mL). The aqueous layer was extracted with EtOAc (3 x 45 mL), the combined organic extracts were washed with brine, dried ($MgSO_4$), filtered and concentrated *in vacuo*. The residue was purified by flash chromatography (gradient 2:1 to 1:1 hexanes/EtOAc) to afford 2.4 g (89 %) of epoxide **4.50** as a clear oil.

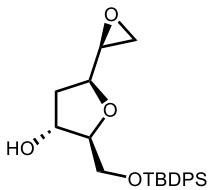

4.50

4.50: R_f 0.3 (2:1 hexanes/EtOAc); $[a]^{23}_D$ -6.8 (*c* 1.0, $CHCl_3$); ^1H NMR (400 MHz, $CDCl_3$) δ 7.71-7.63 (m, 4H), 7.74 (m, 6H), 4.46 (m, 1H), 4.00 (dt, *J* = 5.9, 9.0 Hz, 1H), 3.89 (m, 1H), 3.77 (dd, *J* = 4.2, 10.6 Hz, 1 1H), 3.61 (dd, *J* = 6.5, 10.6 Hz, 1H), 2.96 (m, 1H), 2.74 (t, *J* = 4.7 Hz, 1H), 2.65 (dd, *J* = 2.6, 5.2 Hz, 1H), 2.08 (ddd, *J* = 6.0, 9.0, 13.0 Hz, 1H), 1.99 (ddd, *J* = 3.0, 6.4, 13.0 Hz, 1H), 1.79 (br s, 1 H), 1.06 (s, 9H); ^{13}C NMR (100 MHz, $CDCl_3$) δ 135.7 (2), 133.3, 133.2, 130.0, 129.9, 127.9, 87.0, 78.6, 74.3, 64.8, 53.7, 44.3, 37.4, 27.0, 19.4; LRMS calculated for $C_{23}H_{30}O_4Si$ $[M+Na]^+$ m/z 421.5; measured LC/MS (ESI) R_t 0.9 min, m/z 421.0 $[M+Na]^+$.

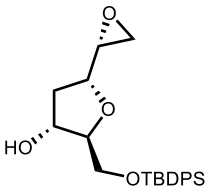

4.55

4.55: R_f 0.3 (2:1 hexanes/EtOAc); $[a]^{23}_D$ -11.4 (*c* 0.65, $CHCl_3$); ^1H NMR (400 MHz, $CDCl_3$) δ 7.68-7.62 (m, 4H), 7.46-7.35 (m, 6H), 4.42 (dt, *J* = 2.2, 9.4 Hz, 1H), 4.30 (m, 1H), 3.95 (t, *J* = 4.3 Hz, 1H), 3.63 (m, 2H), 3.51 (dd, *J* = 5.4, 10.8 Hz, 1H), 3.10 (m, 2H), 2.88 (t, *J* = 4.7 Hz, 1H), 2.54 (ddd, *J* = 6.0, 9.4, 13.6 Hz, 1H), 1.99 (m, 1H), 1.05 (s, 1H); ^{13}C NMR (100 MHz, $CDCl_3$) δ 135.7, 135.68, 133.3, 133.2, 129.93, 129.89, 127.89, 127.88, 88.6, 75.4, 73.2, 65.1, 55.2, 46.8, 37.8, 27.0, 19.3; LRMS calculated for $C_{23}H_{30}O_4Si$ $[M+Na]^+$ m/z 421.2, measured LC/MS (ESI) R_t 1.40 min, m/z 421.0 $[M+Na]^+$.

General procedure of synthesis of alcohols 4.51 and 4.56

To a solution of **4.41** (5.0 g, 23 mmol) in THF (21 mL) at -78 °C was added *n*-BuLi (7.6 mL, 18 mmol) as a solution in hexanes (2.5 M). The solution was allowed to stir at -78 °C for 15 min, then warmed to 0 °C for 15 min. The solution was cooled to -78 °C and epoxide **4.50** (1.5 g, 3.7 mmol) was added to the reaction in a solution of THF (28 mL). $BF_3 \bullet OEt_2$ (1.6 mL, 13 mmol) was added to the reaction in a solution of THF (5.6 mL). The reaction mixture was maintained at -78 °C for 2 h, then -40 °C for 2 h. The reaction was quenched at 0 °C with saturated ammonium chloride (30 mL). The aqueous layer was extracted with EtOAc (3 x 30 mL). The combined organic extracts were washed with brine (30 mL), dried ($MgSO_4$), filtered and concentrated *in vacuo*. The residue was purified by flash chromatography (4:1 to 2:1 Hexanes: EtOAc) to afford 2.1 g (90 %) of diol **S9** as a yellow oil. Stereochemical assignments of diols **(8*R*, 9*R*,) 4.56** and **(8*S*, 9*S*) 4.51** were based on NMR analysis of Mosher esters derived from secondary alcohols at C8.

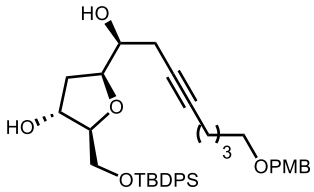

4.51

4.51: R_f 0.3 (2:1 hexanes/EtOAc); $[a]^{23}_D$ +15.6 (*c* 1.0, $CHCl_3$); ^1H NMR (400 MHz, $CDCl_3$) δ 7.70-7.63 (m, 4H), 7.48-7.35 (m, 6H), 7.25 (d, *J* = 8.3 Hz, 2H), 6.87 (d, *J* = 8.6 Hz, 2H), 4.45 (m, 1H), 4.43 (s, 2H), 4.33 (ddd, *J* = 4.1, 6.6, 8.4 Hz, 1H), 3.86 (m, 1H), 3.80 (s, 3H), 3.73-3.70 (m, 2H), 3.56 (m, 1H), 3.45 (t, *J* = 6.4 Hz, 2H), 2.60 (d, *J* = 7.3 Hz, 1H), 2.41 (dt, *J* = 2.4, 6.5 Hz, 1H), 2.16 (tt, *J* = 2.3, 10.3 Hz, 2H), 2.10 (ddd, *J* = 6.4, 8.3, 13.0 Hz, 1H), 1.94 (ddd, *J* = 3.5, 6.5, 12.9 Hz, 1H), 1.88 (d, *J* = 4.1 Hz, 1H), 1.69 (m, 2H), 1.56 (m, 2H), 1.06 (s, 9H); ^{13}C NMR (100 MHz, $CDCl_3$) δ 159.3, 135.8, 135.7, 133.1 (2), 130.8, 130.0 (2), 129.4, 128.0, 113.9, 86.5, 82.3, 79.7, 76.4, 73.7, 72.7, 72.6, 69.7, 64.4, 55.4, 37.4, 29.0, 27.0, 25.8, 24.7, 19.3, 18.7; LRMS calculated for $C_{37}H_{48}O_6Si$ $[M+Na]^+$ m/z 639.3; measured LC/MS (ESI) R_t 2.4 min, m/z 639.0 $[M+Na]^+$.

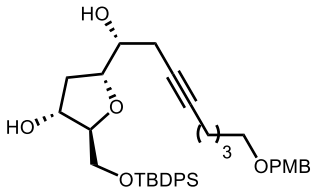

4.56

4.56: R_f 0.3 $[a]^{23}_D$ -14.1 (*c* 1.0, $CHCl_3$); (2:1 hexanes/EtOAc); ^1H NMR (400 MHz, $CDCl_3$) δ 7.69-7.64 (m, 4H), 7.44-7.37 (m, 6H), 7.25 (d, *J* = 8.3 Hz, 2H), 6.89 (dd, *J* = 8.5 Hz, 2H), 4.42 (s, 3H), 3.56 (br, 1H), 4.20 (dt, *J* = 2.9, 9.2 Hz, 1H), 4.05 (m, 1H), 3.83 (br, 1H), 3.90 (s, 3H), 3.68 (dd, *J* = 3.8, 10.7 Hz, 1H), 3.64-3.55 (m, 2H), 3.44 (t, *J* = 6.3 Hz, 2H, 3.02 (br, 1H), 2.55 (ddt, *J* = 2.3, 7.8, 16.7 Hz, 1H), 2.50-2.38 (m, 2H), 2.17 (t, *J* = 6.9 Hz, 2H), 1.88 (m, 1H), 1.68 (m, 2H), 1.56 (m, 2H), 1.06 (s, 9H); ^{13}C NMR (100 MHz, $CDCl_3$) δ 159.2, 135.7 (2), 133.3 (2), 130.7, 129.9, 129.8, 129.4, 127.8 (2), 113.9, 88.0, 82.7, 80.0, 76.6, 72.8. 72.6, 69.6, 65.1, 55.4, 37.5, 29.0, 26.9, 25.7, 24.6, 19.3, 18.7; LRMS calculated for $C_{37}H_{48}O_6Si$ $[M+Na]^+$ m/z 639.3; measured LC/MS (ESI) R_t 2.4 min, m/z 639.0 $[M+Na]^+$.

General procedure for synthesis of biacetylated compounds 4.52 and 4.57

To a solution of diol **4.51** (2.0 g, 3.3 mmol) in CH_2Cl_2 (66 mL) was added pyridine (2.7 mL, 33.2 mmol), DMAP (40 mg, 0.33 mmol) and acetic anhydride (1.25 mL, 13.3 mmol, 1.4 g). The reaction mixture was maintained at room temperature for 20 h. Then the reaction was concentrated *in vacuo*. The residue was purified by flash chromatography (gradient: 4:1 Hexanes: EtOAc) to afford 2.4 g (91 % over 2 steps) of biacetylated compound **4.52** as a pale-yellow oil.

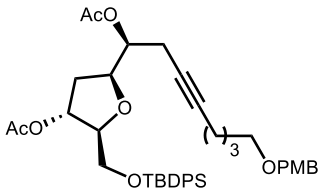

4.52

4.52: R_f 0.3 (2:1 Hexanes: EtOAc); $[a]^{23}_D$ -11.0 (*c* 1.0, $CHCl_3$); ^1H NMR (400 MHz, $CDCl_3$) δ 7.71-7.68 (m, 4H), 7.44-7.34 (m, 6H), 7.25 (m, 2H), 6.78 (d, *J* = 8.6 Hz, 2H), 5.36 (m, 1H), 4.92 (m, 1H), 4.42 (s, 2H), 4.36 (q, *J* = 5.2, 1H), 4.02 (m, 1H), 3.81-3.77 (m, 4H), 3.63 (dd, *J* = 5.0, 10.9 Hz, 1H), 3.44 (t, *J* = 6.3 Hz, 2H), 2.57 (ddt, *J* = 2.3, 6.6, 16.6 Hz, 1H), 2.46 (m, 1H), 2.15 (tt, *J* = 2.3, 10.5 Hz, 2H), 2.05 (s, 3H), 2.01-1.93 (m, 2H), 1.91 (s, 3H), 1.67 (m, 2H), 1.56 (m, 2H), 1.04 (s, 9H); ^{13}C NMR (100 MHz, $CDCl_3$) δ 170.6, 170.5, 159.3, 135.8, 133.4, 133.3, 130.8, 129.9, 129.8, 129.3, 127.9, 127.8, 113.9, 84.8, 82.4, 78.3, 76.3, 75.1, 72.9, 72.7, 69.7, 64.2, 55.4, 34.4, 29.0, 26.9, 25.7, 21.7, 21.3, 21.0, 19.4, 18.7; LRMS calculated for $C_{41}H_{52}O_8Si$ $[M+H]^+$ m/z 701.3; measured LC/MS (ESI) R_t 1.4 min, m/z 701.0 $[M+H]^+$.

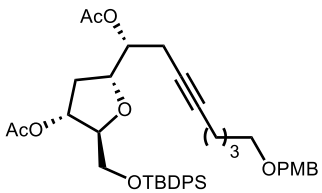

4.57

4.57: R_f 0.3 (4:1 hexanes/EtOAc); $[a]^{23}_D$ -26.0 (*c* 1.0, $CHCl_3$); ^1H NMR (400 MHz, $CDCl_3$) δ 7.70-7.66 (m, 4H), 7.44-7.36 (m, 6H), 7.25 (d, *J* = 8.7 Hz, 2H), 6.87 (d, *J* = 8.6 Hz, 2H), 5.35 (m, 1H), 5.00 (dd, *J* = 6.1, 11.6 Hz, 1H), 4.43 (m, 1H), 4.41 (s, 2H), 4.08 (m, 1H), 3.80 (s, 3H), 3.76 (m, 2H), 3.41 (t, *J* = 6.4 Hz, 2H), 2.62-2.42 (m, 3H), 2.11 (s, 3H), 2.10 (m, 2H), 2.05 (s, 3H), 1.83 (ddd, *J* = 4.1, 6.2, 13.7, 1H), 1.64 (m, 2H), 1.51 (m, 2H), 1.04 (s, 9H); ^{13}C NMR (100 MHz, $CDCl_3$) δ 170.7 (2), 159.2, 135.8, 135.7, 133.3, 130.8, 129.9, 129.8, 129.3, 127.9, 127.8, 113.9,

84.2, 82.4, 79.0, 76.0, 75.1, 73.3, 72.7, 69.6, 64.8, 55.4, 34.8, 29.0, 26.9, 25.7, 21.7, 21.3 (2), 19.3, 18.6; LRMS calculated for $C_{41}H_{52}O_8Si$ $[M+H]^+$ m/z 701.3; measured LC/MS (ESI) R_t 1.4 min, m/z 701.0 $[M+H]^+$.

General procedure for synthesis of compounds 4.58 and 4.63 *via* PMB deprotection

To a solution of the PMB ether **4.52** (3.46 g, 4.90 mmol) in CH_2Cl_2 (40 mL) was added water (2 mL). The heterogenous solution was stirred vigorously for 5 min, then DDQ (1.68 g, 7.4 mmol) was added and the solution was stirred vigorously for 1 h. The solution was filtered through a plug of celite and rinsed with CH_2Cl_2 (2 x 15 mL). The mixture was concentrated *in vacuo*, the residue was purified by flash chromatography (gradient: 2:1 to 1:1 Hexanes: EtOAc) to afford 2.8 0 g (>95 %) of primary alcohol **4.58** as a red oil.

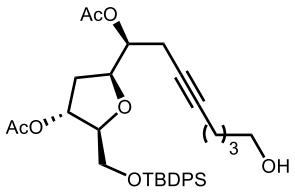

4.58

4.58: R_f 0.3 (2:1 Hexanes: EtOAc); $[a]^{23}_D$ -16.4 (*c* 1.0, $CHCl_3$); ^{1}H NMR (400 MHz, $CDCl_3$) δ 7.63-7.24 (m, 4H), 7.34-7.44 (m, 6H), 5.36 (m, 1H), 4.95 (q, *J* = 6.2 Hz, 1H), 4.34 (m, 1H), 4.02 (m, 1H), 3.79 (dd, *J* = 3.9, 10.9 Hz, 1H), 3.59-3.69 (m, 3H), 2.55 (ddt, *J* = 2.3, 6.6, 16.6 Hz, 1H), 2.48 (ddt, *J*= 2.7, 6.2, 16.7 Hz, 1H), 2.18 (t, *J* = 6.8 Hz, 2H), 2.08 (s, 3H), 1.94-2.02 (m, 2H), 1.93 (s, 3H), 1.65 (m, 2H), 1.55 (m, 2H), 1.05 (s, 9H); ^{13}C NMR (100 MHz, $CDCl_3$) δ 170.7, 170.6, 135.8, 133.4, 133.3, 129.9, 129.8, 127.9, 127.8, 84.8, 82.3, 78.4, 76.4, 75.4, 73.0, 64.2, 62.6, 34.5, 31.9, 27.0, 25.1, 21.7, 21.3, 21.0, 19.4, 18.6; LRMS calculated for $C_{33}H_{44}O_7Si$ $[M+Na]^+$ m/z 603.3; measured LC/MS (ESI) $_{Rt}$ 1.2 min, m/z 603.0 $[M+Na]^+$.

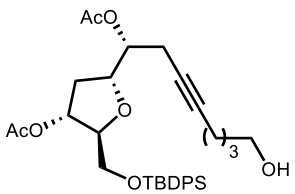

4.63

4.63: R_f 0.3 (2:1 hexanes/EtOAc); $[a]^{23}_D$ -28.2 (*c* 1.0, $CHCl_3$); ^{1}H NMR (400 MHz, $CDCl_3$) δ 7.71-7.65 (m, 4H), 7.44-7.36 (m, 6H), 5.32 (m, 1H), 5.02 (m, 1H), 4.42 (m, 1H), 4.08 (m, 1H), 3.76 (m, 2H), 3.61 (t, *J* = 6.3 Hz, 2H), 2.59-2.53 (m, 2H), 2.47 (m, 1H), 2.16-2.10 (m, 5H), 2.05 (s,

3H), 1.83 (m, 1H), 1.61 (m, 2H), 1.51 (m, 2H), 1.05 (s, 9H); ^{13}C NMR (100 MHz, $CDCl_3$) δ 170.8 (2), 135.7 (2), 133.2 (2), 129.9, 129.8, 127.8 (2), 84.2, 82,3, 79.1, 76.0, 75.3, 73.3, 64.7, 62.4, 34.7, 31.9, 26.9, 25.1, 21.7, 21.3, 21.2, 19.3, 18.6; LRMS calculated for $C_{33}H_{44}O_7Si$ $[M+Na]^+$ m/z 603.3; measured LC/MS (ESI) R_t 1.4 min, m/z 602.9 $[M+Na]^+$

General procedure for synthesis of aldehydes 4.59 and 4.64

To a solution of primary alcohol **4.58** (2.8 g, 4.8 mmol) in CH_2Cl_2 (64 mL) was added DMP (4.1 g, 9.6 mmol). The solution was stirred for 1.5 h, then was quenched with a 1:1 mixture of sodium thiosulfate and sodium bicarbonate (70 mL) and stirred vigorously for 15 min. The aqueous layer was extracted with Et_2O (3 x 75 mL). The combined organic extracts were washed with brine (75 mL), dried ($MgSO_4$), filtered and concentrated *in vacuo*. The residue was purified by flash chromatography (gradient 4:1 to 2:1 Hexanes: EtOAc) to afford 2.3 g (83 %) of aldehyde **4.59** as a clear oil.

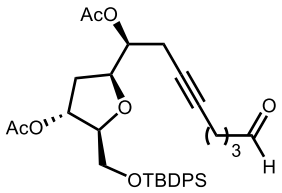

4.59

4.59: R_f 0.4 (2:1 hexanes/EtOAc); $[a]^{23}_D$ -16.0 (*c* 1.0, $CHCl_3$); ^{1}H NMR (400 MHz, $CDCl_3$) δ 9.79 (s, 1H), 7.64-7.21 (m, 4H), 7.33-7.45 (m, 6H), 5.36 (m, 1H), 4.93 (m, 1H), 4.34 (q, *J* = 5.1, 1H), 4.02 (m, 1H), 3.79 (dd, *J* = 3.4, 10.9 Hz, 1H), 3.63 (dd, *J* = 5, 10.9 Hz, 1H), 2.56 (m, 3H), 2.47 (ddt, *J* = 2.3, 5.8, 16.7 Hz, 1H), 2.22 (m, 2H), 2.08 (s, 3H), 1.96 (m, 2H), 1.92 (s, 3H), 1.80 (q, *J* = 7.0 Hz, 2H), 1.05 (s, 9H); ^{13}C NMR (100 MHz, $CDCl_3$) δ 202.0, 170.6, 170.4, 135.8, 133.4, 133.3, 129.9, 129.8, 127.9, 127.8, 84.9, 81.3, 78.3, 76.3, 76.2, 72.7, 64.2, 42.9, 34.4, 27.0, 21.6, 21.4, 21.4, 21.3, 21.0, 19.4, 18.3; LRMS calculated for $C_{33}H_{42}O_7Si$ $[M+H]^+$ m/z 579.3; measured LC/MS (ESI) $_{Rt}$ 1.2 min, m/z 579.0 $[M+H]^+$.

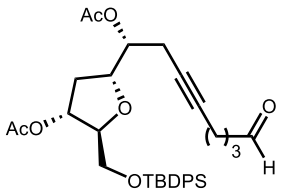

4.64

4.64: R_f 0.4 (2:1 hexanes/EtOAc); $[a]^{23}_D$ -29.8 (*c* 1.0, $CHCl_3$); ^{1}H NMR (400 MHz, $CDCl_3$) δ 9.74 (t, *J* = 1.3 Hz, 1H), 7.70-7.66 (m, 4H), 7.42-7.36

(m, 6H), 5.63 (m, 1H), 5.00 (dd, *J* = 6.1, 11.5 Hz, 1H), 4.43 (m, 1H), 4.08 (dd, *J* = 3.4, 6.8 Hz, 1H), 3.67 (m, 2H), 2.61-2.44 (m, 5H), 2.15 (m, 2H), 2.13 (s, 3H), 2.05 (s, 3H), 1.82 (m, 1H), 1.74 (m, 2H), 1.05 (s, 9H); ^{13}C NMR (100 MHz, $CDCl_3$) δ 202.0, 170.8, 170.7, 135.7, 133.3, 133.2, 129.9, 129.8, 127.9, 127.8, 84.3, 81.3, 79.0, 76.2, 76.0, 73.1, 64.8, 42.8, 34.8, 26.9, 21.6, 21.3 (3), 19.3, 18.2; LRMS calculated for $C_{33}H_{42}O_7Si$ $[M+H]^+$ m/z 579.3; measured LC/MS (ESI) R_t 1.2 min, m/z 579.8.

General procedure for synthesis of methyl esters 4.60 and 4.65

To a solution of aldehyde **4.59** (2.3 g, 4.4 mmol) in *t*-BuOH (20 ml) and 2-methyl-2-butene (13 mL, 120 mmol) was added $NaClO_2$ (840 mg, 9.3 mmol) and NaH_2PO_4 (970 mg, 8.1 mmol) in a solution of water (3.1 mL). The mixture was stirred for 2 hours then quenched with saturated sodium thiosulfate (10 mL). The aqueous layer was extracted with EtOAc (3 x 10 mL), the combined organic extracts were washed with brine (25 mL), dried ($MgSO_4$), filtered and concentrated to afford 2.50 g (>95 %) of crude carboxylic as a clear oil which was carried forward without further purification. To a solution of crude carboxylic acid (2.50 g, 4.0 mmol) in benzene (32 mL) and MeOH (8 mL) was added $TMSCHN_2$ (10 mL, 20 mmol) in a solution in Et_2O (2.0 M). The solution was stirred for 2 h, then concentrated. The residue was purified by flash chromatography (gradient: 4:1 Hexanes: EtOAc) to afford 1.7 g (71 % over 2 steps) of methyl ester **4.60** as a clear oil.

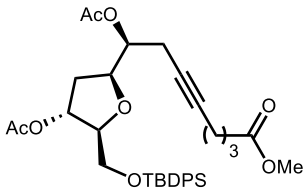

4.60

4.60: R_f 0.3 (4:1 hexane/EtOAc); $[a]^{23}_D$ -13.6 (*c* 1.0, $CHCl_3$); ^{1}H NMR (400 MHz, $CDCl_3$) δ 7.70-7.67 (m, 4H), 7.42-7.35 (m, 6H), 5.37 (m, 1H), 4.92 (m, 1H), 4.35 (q, *J* = 5.1 Hz, 1H), 4.02 (m, 1H), 3.79 (dd, *J* = 3.9, 10.9 Hz, 1H), 3.67 (s, 3H), 3.63 (dd, *J* = 5.0, 10.9 Hz, 1H), 2.58 (ddt, *J* = 2.3, 6.9, 16.6 Hz, 1H), 2.47 (m, 1H), 2.41 (t, *J* = 7.4 Hz, 1H), 2.21 (m, 2H), 2.07 (s, 3H), 2.01-

1.93 (m, 2H), 1.91 (s, 3H), 1.79 (q, *J* = 7.2 Hz, 2H), 1.05 (s, 9H); ^{13}C NMR (100 MHz, $CDCl_3$) δ 173.8, 170.6, 170.5, 135.8, 133.4, 133.3, 129.9, 129.8, 127.9, 127.8, 84.9, 81.3, 78.3, 76.3, 75.9, 72.3, 64.2, 51.7, 34.4, 32.9, 26.9, 24.1, 21.6, 21.3, 21.0, 19.4, 18.3; LRMS calculated for $C_{34}H_{44}O_8Si$ $[M+Na]^+$ m/z 631.3; measured LC/MS (ESI) R_t 1.3 min, m/z 631.60 $[M+Na]^+$.

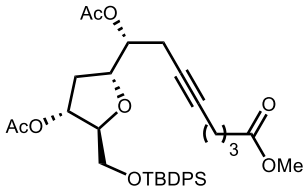

4.65

4.65: R_f 0.3 (4:1 hexane/EtOAc); $[a]^{23}_D$ -35.4 (*c* 1.0, $CHCl_3$); ^{1}H NMR (400 MHz, $CDCl_3$) δ 7.70-7.61 (m, 4H), 7.46-7.32 (m, 6H), 5.36 (m, 1H), 5.00 (p, *J* = 5.89, 1H), 4.43 (m, 1H), 4.08 (m, 1H), 3.77 (dd, *J* = 3.5, 11 Hz, 1H), 3.73 (dd, *J* = 3.9, 10.9 Hz, 1H), 3.66 (s, 3H), 2.62-2.51 (m, 2H), 2.46 (m, 1H), 2.38 (t, *J* = 2.4 Hz, 1H), 2.15 (m, 2H), 2.12 (s, 3H), 2.02 (s, 3H), 1.82 (ddd, *J* = 4.0, 6.3, 13.7 Hz, 1H), 1.75 (q, *J* = 7.2 Hz, 2H), 1.05 (s, 9H); ^{13}C NMR (100 MHz, $CDCl_3$) δ 173.7, 170.8, 170.7, 135.7 (2C), 133.28, 129.9, 129.8, 127.9, 127.8, 84.3, 81.4, 79.0, 76.0, 75.9, 73.2, 64.8, 51.7, 34.8, 32.9, 26.9, 24.1, 21.7, 21.3, 21.27, 19.3, 18.3; LRMS calculated for $C_{34}H_{44}O_8Si$ $[M+Na]^+$ m/z 631.3; measured LC/MS (ESI) R_t 1.2 min, m/z 631.6.

General procedure for synthesis of semireduced alkenes 4.61 and 4.66

To a solution of alkyne **4.60** (1.7 g, 2.7 mmol) in MeOH (91 mL) was added Lindlar's catalyst (420 mg). The flash was evacuated and refilled with H_2 gas three times then stirred vigorously for 15 h, filtered through celite and concentrated to afford 1.7 g (>95 %) of olefin **4.61** as a clear oil.

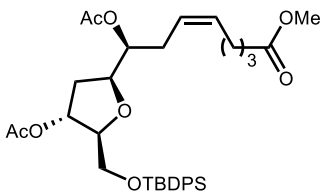

4.61

4.61: R_f 0.3 (4:1 Hexane: EtOAc); $[a]^{23}_D$ -10.4 (*c* 1.0, $CHCl_3$); ^{1}H NMR (400 MHz, $CDCl_3$) δ 7.72-7.66 (m, 4H), 7.46-7.34 (m, 6H), 5.46 (dt, *J* = 7.0, 11 Hz, 1H), 5.41 (m, 1H), 5.35 (m, 1H), 4.91, (m, 1H), 4.18 (m, 1H), 3.99 (m, 1H), 3.80 (dd, *J* = 3.9, 10.7 Hz, 1H), 3.65 (m, 4H), 2.39 (m, 2H), 2.29 (t, *J* = 7.6 Hz, 2H), 2.07 (m, 5H), 1.90 (m, 5H), 1.68 (q, *J* = 7.5 Hz, 2H), 1.05 (s, 9H); ^{13}C NMR (100 MHz, $CDCl_3$) δ 173.9, 170.4 (2), 135.6, 133.2, 133.1, 131.8, 129.7, 129.6,

127.7, 127.6, 124.7, 84.6, 78.6, 73.7, 64.0, 51.4, 34.3, 33.3, 29.1, 26.7, 26.5, 24.6, 21.1, 20.8, 19.1; LRMS calculated for $C_{34}H_{46}O_8Si$ $[M+Na]^+$ m/z 633.3; measured LC/MS (ESI) R_t 1.3 min, m/z 633.7 $[M+Na]^+$.

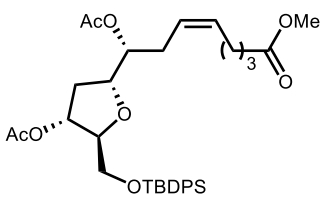

4.66

4.66: R_f 0.3 (4:1 hexane/EtOAc); $[a]^{23}_D$ +0.2 (*c* 0.65, $CHCl_3$); ^1H NMR (400 MHz, $CDCl_3$) δ 7.70-7.65 (m, 4H), 7.44-7.35 (m, 6H), 5.46 (m, 1H), 5.40 (m, 1H), 5.34 (m, 1H), 4.98 (m, 1H), 4.25 (m, 1H), 4.09 (m, 1H), 3.76 (m, 2H), 3.65 (s, 3H), 2.48 (dt, *J* = 7.5, 13.9 Hz, 1H), 2.37 (m, 2H), 2.30 (t, *J* = 7.5 Hz, 2H), 2.09 (m, 4H), 2.05 (m, 4H), 1.77 (ddd, *J* = 4.2, 6.4, 13.6 Hz, 1H), 1.69 (q, *J* = 7.5 Hz, 2H), 1.05 (s, 9H);); ^{13}C NMR (100 MHz, $CDCl_3$) δ 174.1, 170.9, 170.8, 135.8, 133.34, 133.29, 131.9, 129.9, 129.8, 127.9, 127.8, 125.1, 84.1, 79.6, 76.0, 74.4, 64.8, 51.6, 34.9, 33.6, 29.2, 26.9, 26.8, 24.8, 21.33, 21.26, 19.3; LRMS calculated for $C_{34}H_{46}O_8Si$ $[M+Na]^+$ m/z 633.3; measured LC/MS (ESI) R_t 1.3 min, m/z 632.6.

General procedure for synthesis of compounds 4.62 and 4.67

To a solution of silyl ether **4.61** (1.7 g, 2.7 mmol) in THF (27 mL) was added acetic acid (0.78 mL, 14 mmol), followed by a TBAF (14 mmol) in a solution of 1.0 M THF (14 mL). The reaction mixture was maintained for 3 h, then quenched with saturated ammonium chloride (25 mL). The aqueous layer was extracted with EtOAc (3 x 25 mL). The combined organic extracts were washed with brine, dried ($MgSO_4$), filtered and concentrated *in vacuo*. The crude residue was purified by flash chromatography (1:1 to 1:2 hexanes: EtOAc) to afford 900 mg (90 %) of the desired primary alcohol **4.62** as a clear oil.

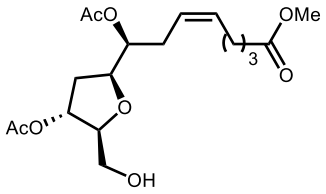

4.62

4.62: R_f 0.3 (1:2 Hexane: EtOAc); $[a]^{23}_D$ +85.7 (*c* 0.3, $CHCl_3$); ^1H NMR (400 MHz, $CDCl_3$) δ 5.50 (dt, *J* = 7.3, 10.0 Hz, 1H), 5.39 (dt, *J* = 7.3, 10.8 Hz, 1H), 5.16 (m, 1H), 4.90 (dt, *J* = 5.6, 7.4 Hz, 1H), 4.23 (dt, *J* = 5.2, 7.9 Hz, 1H), 4.00 (m, 1H), 3.73 (m, 1H), 3.67 (s, 3H), 3.63 (m, 1H), 2.56 (dd, *J* = 4.8, 8.8 Hz, 1H), 2.38 (m, 2H), 2.31 (t, *J* = 7.5 Hz, 1H), 2.10 (m, 2H), 2.09 (s, 3H), 2.06 (s, 3H), 1.99 (m, 2H), 1.70 (q, *J* = 7.4 Hz, 2H); ^{13}C NMR (100 MHz, $CDCl_3$) δ 173.9, 171.0, 170.6, 132.1, 124.5, 85.1, 79.2, 77.1, 74.5, 63.0, 51.4, 34.9, 33.3, 29.1, 26.5, 24.5, 21.0(2); LRMS calculated for $C_{18}H_{29}O_8$ $[M+H]^+$ m/z 373.2; measured LC/MS (ESI) R_t 1.3 min, m/z 372.8 $[M+H]^+$.

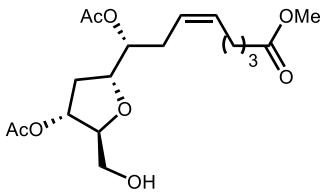

4.67

4.67: R_f 0.3 (1:2 hexane/EtOAc); $[a]^{23}_D$ -15.0 (*c* 1.0, $CHCl_3$); ^1H NMR (400 MHz, $CDCl_3$) δ 5.46 (m, 1H), 5.37 (m, 1H), 5.12 (dt, *J* = 4.7, 7.8 Hz, 1H), 4.96 (m, 1H), 4.16 (dt, *J* = 5.8, 7.5 Hz, 1H), 4.02 (q, *J* = 4.25 Hz, 1H), 3.73 (dt, *J* = 4.4, 11.7 Hz, 1H), 3.65 (s, 3H), 3.62 (m, 1H), 2.49-2.27 (m, 5H), 2.21 (t, *J* = 6.2 Hz, 1H), 2.13-2.07 (m, 4H), 2.07-2.01 (m, 4H), 1.80 (m, 1H), 1.68 (q, *J* = 7.4 Hz, 2H); ^{13}C NMR (100 MHz, $CDCl_3$) δ 174.1, 171.0, 170.8, 132.0, 124.9, 83.8, 78.8, 75.0, 74.2, 62.5, 51.7, 34.4, 33.5, 29.0, 26.7, 24.7, 21.3, 21.1; LRMS calculated for $C_{18}H_{29}O_8$ $[M+H]^+$ m/z 373.4; measured LC/MS (ESI) R_t 0.9 min, m/z 373.0.

General procedure for synthesis of compounds 4.68 and 4.75

To a solution of alcohol **4.62** (200 mg, 0.54 mmol) in benzene (2.1 mL) was added DMSO (360 µL) followed by pyridine trifloroacetate (52 mg, 0.27 mmol) and DCC (350 mg, 1.7 mmol). The reaction was maintained for 1.5 h then filtered through a plug of cotton and saturated sodium bicarbonate (2 mL) was added. The aqueous layer was extracted with diethyl ether (3 x 5 mL). The combined organic extracts were washed with brine (1 x 5 mL), dried ($MgSO_4$), filtered and

concentrated. The residue was purified by flash chromatography with pH 7 buffered silica (gradient: 4:1 to 3:2 hexanes: EtOAc) to afford 160 mg of crude aldehyde which was immediately carried forward to the next step.

To a solution of phosphonate **4.42** (110 mg, 0.5 mmol) in THF (2.5 mL) at 0 °C was added NaHMDS dropwise (0.44 ml, 0.44 mmol) in a 1.0 M solution of THF. The reaction was allowed to stir at 0 °C for 5 min then warmed to room temperature and maintained for 30 min. Then cooled to 0 °C and crude aldehyde from the previous step was added to the reaction (150 mg, 0.4 mmol) in a solution of THF (2.5 mL). The reaction was allowed to warm to room temperature and stir for 14 h. The reaction was quenched with water (5 mL) and partitioned with EtOAc (5 mL). The aqueous layer was extracted with EtOAc (3 x 5 mL). The combined organic extracts were washed with brine (5 mL), dried ($MgSO_4$), filtered and concentrated *in vacuo*. The residue was purified by flash chromatography (gradient: 4:1 hexanes: EtOAc) to afford 62 mg (24 % over 2 steps) of enone **4.68** as a clear oil.

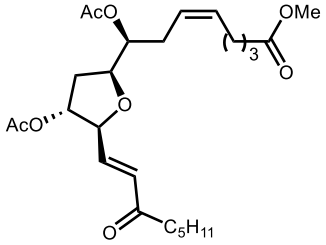

4.68

4.68: R_f 0.4 (2:1 hexane/EtOAc); $[a]^{23}_D$ -12.2 (*c* 0.7, $CHCl_3$); ^{1}H NMR (400 MHz, $CDCl_3$) δ 6.80 (dd, *J* = 4.4, 15.7 Hz, 1H), 6.50 (dd, *J* = 1.8, 15.8 Hz, 1H), 5.49 (m, 1H), 5.40 (m, 1H), 5.03 (m, 1H), 4.94 (dt, *J* = 4.4, 6.7 Hz, 1H), 4.56 (m, 1H), 4.30 (m, 1H), 3.66 (s, 3H), 2.56 (t, *J* = 7.4 Hz, 2H), 2.43 (t, *J* = 7.0 Hz, 1H), 2.31 (t, *J* = 7.5 Hz, 1H), 2.09 (m, 9H), 1.95 (ddd, *J* = 1.4, 5.5, 13.4 Hz, 1H), 1.82 (ddd, *J* = 5.5, 10.5, 13.6 Hz, 1H), 1.69 (q, *J* = 9.9 Hz, 2H), 1.61 (m, 2H), 1.29 (m, 6H), 0.89 (t, *J* = 6.9 Hz, 3H); ^{13}C NMR (100 MHz, $CDCl_3$) δ 200.6, 174.1, 170.7, 170.6, 142.2, 132.3, 130.1, 124.7, 83.2, 79.5, 78.2, 73.6, 51.6, 41.0, 33.6, 33.0, 31.6, 29.5, 26.8, 24.8,

23.8, 22.6, 21.2, 21.1, 14.1; LRMS calculated for $C_{25}H_{38}O_8$ $[M+H]^+$ m/z 467.3; measured LC/MS (ESI) $_{Rt}$ 1.4 min, m/z 466.7 $[M+H]^+$.

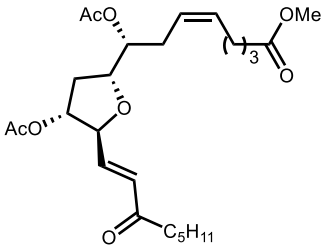

4.75

4.75: R_f 0.3 (4:1 hexane/EtOAc); $[a]^{23}_D$ -23.2 (*c* 0.6, $CHCl_3$); ^{1}H NMR (400 MHz, $CDCl_3$) δ 6.74 (dd, *J* = 4.5, 15.9 Hz, 1H), 6.31 (dd, *J* = 1.8, 15.9 Hz, 1H), 5.49 (m, 1H), 5.40 (m, 1H), 5.04-4.99 (m, 2H), 4.62 (td, *J* = 1.7, 4.1 Hz, 1H), 3.66 (s, 3H), 2.55 (t, *J* = 7.4 Hz, 2H), 2.38 (m, 3H), 2.32 (t, *J* = 7.5 Hz, 2H), 2.13-2.04 (m, 9H), 1.82 (ddd, *J* = 4.2, 6.3, 13.9 Hz, 1H), 1.70 (m, 2H), 1.60 (m, 2H), 1.35-1.24 (m, 6H), 0.89 (t, *J* = 7.0 Hz, 3H); ^{13}C NMR (100 MHz, $CDCl_3$) δ 200.4, 174.0, 170.8 (2), 141.8, 132.2, 129.9, 124.8, 82.4, 78.9, 77.7, 74.1, 51.6, 40.7, 33.5 (2), 31.6, 29.1, 26.8, 24.8, 23.8, 22.6, 21.3, 21.1, 14.1; LRMS calculated for $C_{25}H_{38}O_8$ $[M+H]^+$ m/z 467.26; measured LC/MS (ESI) R_t 1.3 min, m/z 467.0.

General procedure for synthesis of 4.69/4.70 and 4.76/4.77

To a solution of enone **4.68** (60 mg, 0.13 mmol) in MeOH (3 mL) was added $Ce(Cl_3)\bullet 7H_2O$ (58 mg, 0.15 mmol). The reaction was allowed to stir for 5 min, then $NaBH_4$ (5 mg, 0.13 mmol) was added accompanied by evolution of gas. The reaction was allowed to stir for 50 min, then the reaction was concentrated *in vacuo* and the residue purified by flash chromatography (3:2 to 1:1 hexanes: EtOAc) to afford 60 mg (>95 %) of allylic alcohols **4.69** and **4.70** as an inseperable 1:1 mixture of isomers as a colorless oil.

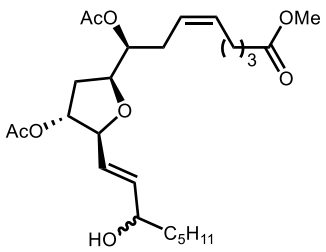

4.69/4.70

4.69/4.70: R_f 0.4 (2:1 Hexane: EA); ^{1}H NMR (400 MHz, $CDCl_3$) δ 5.88 (m, 1H), 5.68 (m, 1H), 5.47 (m, 1H), 5.40 (m, 1H), 4.97 (m, 1H), 4.93 (m, 1H), 4.38 (m, 1H), 4.23 (m, 1H), 4.11 (q, *J* = 6.4 Hz, 1H), 3.66 (s, 1H), 2.40 (m, 2H), 2.31 (t, *J*= 7.5 Hz, 2H), 2.12-2.06 (m, 8H), 1.89 (m, 2H), 1.68 (q, *J* = 7.4 Hz, 2H), 1.51 (m, 2H), 1.29 (m, 6H), 0.88 (t, *J* =

6.7 Hz, 3H); ^{13}C NMR (100 MHz, $CDCl_3$) δ 174.2, 170.7, 170.68 (isomers); 170.6, 135.8, 135.6 (isomers); 132.1, 128.2, 128.1 (isomers); 124.9, 83.9, 83.8 (isomers); 78.9, 78.8, 74.2, 74.1 (isomers); 72.3, 72.2 (isomers); 51.7, 37.3, 33.6, 33.3, 33.27 (isomers) 31.8, 29.3, 26.7, 25.22, 25.2 (isomers); 24.8, 22.7, 21.2, 14.1; LRMS calculated for $C_{25}H_{40}O_8$ $[M+Na]^+$ m/z 491.3, measured LC/MS (ESI) R_t 1.2 min, m/z 491.0 $[M+Na]^+$.

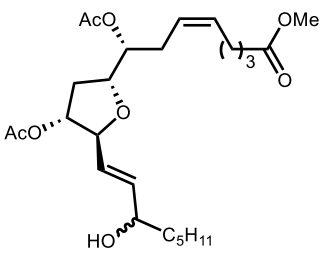

4.76/4.77

4.76/4.77: R_f 0.3 (2:1 hexane/EtOAc); ^{1}H NMR (400 MHz, $CDCl_3$) δ 5.79 (m, 1H), 5.63 (dt, *J* = 6.15, 15.2 Hz, 1H), 5.47 (m, 1H), 5.38 (m, 1H), 5.00-4.94 (m, 2H), 4.45 (m, 1H), 4.17 (m, 1H), 4.11 (m, 1H), 3.66 (s, 3H), 2.44-2.34 (m, 3H), 2.31 (t, *J* = 7.6 Hz, 2H), 2.13-2.04 (m, 8H), 1.75 (m, 1H), 1.68 (m, 3H), 1.50 (m, 2H), 1.34-1.25 (m, 6H), 0.87 (t, *J* = 6.7 Hz, 3H); ^{13}C NMR (100 MHz, $CDCl_3$) δ 173.9; 170.6, 170.5 (isomers); 135.8, 135.7 (isomers); 131.8; 127.2, 127.1 (isomers); 124.7; 82.7; 77.9, 77.8 (isomers); 77.7; 74.0; 72.1, 71.9 (isomers); 51.4, 37.0 (isomers); 33.4; 33.3; 31.6; 28.9; 26.5; 25.0, 24.9 (isomers); 24.6; 22.5; 21.1, 21.0 (2 isomers); 13.9; LRMS calculated for $C_{25}H_{38}O_8$ $[M+Na]^+$ m/z 491.3; measured LC/MS (ESI) R_t 0.8 min, m/z 491.0.

General procedure for the enzymatic resolution of alcohols 4.69/4.70 and 4.76/4.77

To a solution of allylic alcohols **4.69**/**4.70** (56 mg, 0.12 mmol) in vinyl acetate (1.2 mL) in a microwave vial was added powered sieves (56 mg). Then Lipase Amano AK (390 mg) was added, the microwave vial was sealed and heated to 40 °C for 8 days. The mixture was cooled to room temperature and filtered through a plug of celite and washed with EtOAc (3 x 10 mL). The mixture was concentrated *in vacuo* and the residue purified by flash chromatography (gradient: 4:1 to 2:1 Hexanes: EtOAc) to afford 26 mg (43 %) of diastereomerically pure acetate **4.71** as a yellow oil and 24 mg (43 %) of the diastereomerically pure allylic alcohol **4.70** as a yellow oil.

Stereochemical assignment of was based on NMR analysis of Mosher esters derived from secondary alcohols at C15.

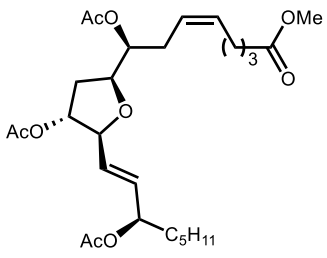

4.71

4.71: R_f 0.4 (4:1 Hexane: EtOAc); $[a]^{23}_D$ +2.0 (*c* 0.9, $CHCl_3$); ^1H NMR (400 MHz, $CDCl_3$) δ 5.83 (ddd, *J* = 1.4, 6.4, 15.5 Hz, 1H), 5.70 (m, 1H), 5.48 (m, 1H), 5.40 (m, 1H), 5.26 (m, 1H), 4.96 (m, 1H), 4.92 (m, 1H), 4.38 (m, 1H), 4.23 (m, 1H), 3.66 (s, 3H), 2.40 (t, *J* = 6.9 Hz, 2 H), 2.31 (t, *J* = 7.5 Hz, 2H), 2.11-2.03 (m, 13H), 1.88-1.83 (m, 2H), 1.96 (q, *J* = 7.5 Hz, 2H), 1.27 (m, 6H), 0.87 (t, *J* = 6.6 Hz, 3H); ^{13}C NMR (100 MHz, $CDCl_3$) δ 174.1, 170.7, 170.4, 132.1, 130.7, 130.1, 124.9, 83.6, 79.0, 78.8, 74.0, 73.9, 51.3, 34.5, 33.6, 33.1, 31.7, 29.4, 26.8, 24.9, 24.8, 22.7, 21.4, 21.2, 21.19, 14.1; LRMS calculated for $C_{27}H_{42}O_9^+$ $[M+Na]^+$ m/z 533.3, measured LC/MS (ESI) R_t 1.4 min, m/z 533.0 $[M+Na]^+$.

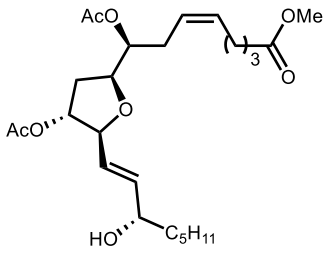

4.70

4.70: R_f 0.4 (2:1 Hexane: EtOAc); $[a]^{23}_D$ -15.2 (*c* 0.2, $CHCl_3$); ^1H NMR (400 MHz, $CDCl_3$) δ 5.90 (ddd, *J* = 1.5, 6.2, 15.8 Hz, 1H), 5.70 (m, 1H), 5.48 (m, 1H), 5.40 (m, 1H), 4.98 (m, 1H), 4.93 (m, 1H), 4.39 (m, 1H), 4.23 (m, 1H), 4.12 (m, 1H), 3.66 (s, 3H), 2.46-2.36 (m, 2H), 2.31 (t, *J* = 5.0 Hz, 2H), 2.13-2.04 (m, 8H), 1.89 (m, 2H), 1.69 (q, *J* = 7.4 Hz, 2H), 1.51 (m, 2H), 1.29 (m, 6H), 0.88 (t, *J* = 6.7 Hz, 3H); ^{13}C NMR (100 MHz, $CDCl_3$) δ 174.2, 170.7, 170.6, 135.6, 132.1, 128.1, 124.9, 83.8, 78.9, 78.8, 74.1, 72.4, 51.2, 37.3, 33.6, 33.3, 31.9, 29.4, 26.7, 25.2, 24.8, 22.7, 21.2, 14.2; LRMS calculated for $C_{25}H_{40}O_8$ $[M+Na]^+$ m/z 491.3, measured LC/MS (ESI) R_t 1.2 min, m/z 491.0 $[M+Na]^+$.

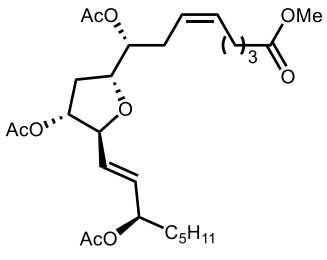

4.78

4.78: R_f 0.3 (4:1 hexane/EtOAc); $[a]^{23}_D$ +15.0 (*c* 0.4, $CHCl_3$); ^1H NMR (400 MHz, $CDCl_3$) δ 5.71 (dd, *J* = 5.8, 15.7 Hz, 1H), 5.63 (dd, *J* = 4.6, 15.7 Hz, 1H), 5.46 (m, 1H), 5.39 (m, 1H), 5.24 (m, 1H), 5.01-4.94 (m, 2H), 4.45 (t, *J* = 3.9 Hz, 1H), 4.16 (m, 1H), 3.66 (s, 3H), 2.42-2.34 (m, 3H), 2.31 (t, *J* = 7.5 Hz, 2H), 2.12-2.03 (m, 11 H), 1.75 (m, 1H), 1.69 (m, 2H), 1.62-1.55 (m, 2H), 1.31-1.23 (m, 6H), 0.87 (t, *J* = 6.4, 3H); ^{13}C NMR (100 MHz, $CDCl_3$) δ 174.1, 170.9, 170.7, 170.4, 132.0, 131.0, 129.4, 125.0, 82.8, 78.2, 78.0, 74.3, 73.8, 51.6, 34.4, 33.6, 33.5, 31.6, 29.1, 26.8, 24.9, 24.8, 22.6, 21.4, 21.3, 21.2, 14.1; LRMS calculated for $C_{27}H_{42}O_9$ $[M+Na]^+$ m/z 533.3; measured LC/MS (ESI) R_t 1.9 min, m/z 533.0.

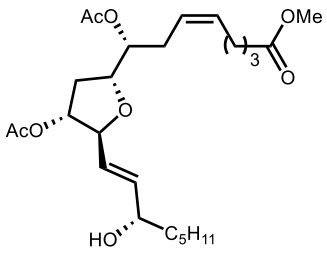

4.76

4.76: R_f 0.3 (2:1 Hexane: EtOAc); $[a]^{23}_D$ +23.0 (*c* 0.3, $CHCl_3$); ^1H NMR (400 MHz, $CDCl_3$) δ 5.80 (dd, *J* = 5.7, 15.6 Hz, 1H), 5.65 (dd, *J* = 5.6, 15.6 Hz, 1H), 5.48 (m, 1H), 5.39 (m, 1H), 4.99 (m, 2H), 4.46 (m, 1H), 4.17 (m, 1H), 4.12 (m, 1H), 3.66 (s, 3H), 2.45-2.34 (m, 3H), 2.31 (t, *J* = 7.6Hz, 2H), 2.13-2.05 (m, 8 H), 1.77 (m, 1H), 1.69 (m, 3H), 1.54-1.48 (m, 2H), 1.35-1.26 (m, 6H), 0.88 (t, *J* = 6.5 Hz, 3H); ^{13}C NMR (100 MHz, $CDCl_3$) δ 174.2, 170.9, 170.8, 136.0, 132.0, 127.4, 124.9, 83.0, 78.1, 78.0, 74.2, 72.1, 51.7, 37.2, 33.6, 33.5, 31.9, 29.1, 26.8, 25.2, 24.8, 22.7, 21.3, 21.2, 14.2; LRMS calculated for $C_{25}H_{38}O_8$ $[M+Na]^+$ m/z 491.3; measured LC/MS (ESI) R_t 0.8 min, m/z 491.0.

General procedure synthesis of isofuran methyl esters 4.72, 4.73, 4.79, and 4.81

To a solution of triacetate **4.71** (16 mg, 0.03 mmol) in MeOH (1 mL) was added K_2CO_3 (22 mg, 0.16 mmol). The reaction mixture was maintained for 2 h and quenched with 1 M HCl until pH 2 was reached (ca 0.2 mL). The mixture was diluted with water (1 mL), and EtOAc (1 mL). The aqueous layer was extracted with EtOAc (3 x 2 mL). The combined organic extacts were

washed with brine (1 mL), and dried (Na_2SO_4), filtered and concentrated *in vacuo*. The crude mixture was purified by flash chromatography (gradient: 1:3 hexanes: EtOAc to EtOAc) to afford 11 mg (>95 %) of methyl ester **4.72** as a colorless oil.

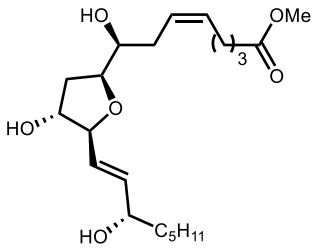

4.72

4.72: R_f 0.3 (EtOAc); $[a]^{23}_D$ -13.0 (*c* 0.2, $CHCl_3$); ^{1}H NMR (400 MHz, $CDCl_3$) δ 5.82 (ddd, *J* = 1.0, 5.9, 15.4 Hz, 1H), 5.66 (ddd, *J* = 1.2, 6.7, 15.5 Hz, 1H), 5.54-5.47 (m, 2H), 4.25 (m, 1H), 4.18-4.09 (m, 3H), 3.67 (s, 3H), 3.53-3.48 (m, 2H), 2.32 (t, *J* = 7.4 Hz, 2H), 2.29-2.26 (m, 2 H), 2.21 (d, *J* = 5.7 Hz, 1H), 2.13-2.08 (m, 2H), 2.02-1.97 (m, 1H), 1.89 (ddd, *J* = 3.1, 6.4, 13.0 Hz, 1H), 1.82 (d, *J* = 4.4 Hz, 1H), 1.71 (q, *J* = 7.4 Hz, 2H), 1.35-1.27 (m, 6H), 0.89 (t, *J* = 6.8 Hz, 3H); ^{13}C NMR (125 MHz, $CDCl_3$) δ 174.4, 136.2, 131.4, 128.8, 126.2, 86.8, 80.8, 77.0, 73.7, 72.2, 51.7, 37.4, 36.8, 33.6, 32.1, 31.8, 26.8, 25.2, 24.8, 22.7, 14.2.; LRMS calculated for $C_{21}H_{36}O_6$ $[M+Na]^+$ m/z 407.3, measured LC/MS (ESI) R_t 0.9 min, m/z 407.5 $[M+Na]^+$.

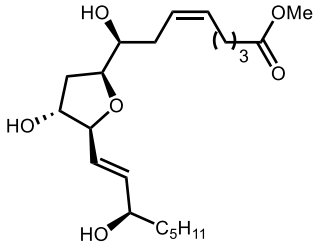

4.73

4.73: R_f 0.3 (EtOAc); $[a]^{23}_D$ -6.9 (*c* 0.7, $CHCl_3$); ^{1}H NMR (400 MHz, $CDCl_3$) δ 5.81 (m, 1H), 5.64 (m, 1H), 5.54-5.47 (m, 2H), 4.25 (m, 1H), 4.16 (m, 1H), 4.12 (m, 2H), 3.67 (s, 3H), 3.51 (m, 1H), 2.33 (t, *J* = 7.4 Hz, 2H), 2.29-2.23 (m, 3H), 2.10 (m, 2H), 2.00 (m, 1H), 1.93 (br s, 1H), 1.89 (ddd, *J* = 2.9, 6.3, 13.0 Hz, 1H), 1.70 (q, *J* = 7.4 Hz, 2H), 1.53 (m, 2H), 1.39 (m, 1H), 1.30 (m, 6H), 0.89 (t, *J* = 6.9 Hz, 3H); ^{13}C NMR (100 MHz, $CDCl_3$) δ 174.4, 136.2, 131.4, 128.9, 126.3, 86.8, 80.8, 77.1, 73.7, 72.3, 51.7, 37.3, 36.8, 33.6, 32.1, 31.8, 26.8, 25.3, 25.2, 24.8, 22.7, 14.2; LRMS calculated for $C_{21}H_{36}O_6$ $[M+Na]^+$ m/z 407.3, measured LC/MS (ESI) R_t 0.9 min, m/z 407.4 $[M+Na]^+$.

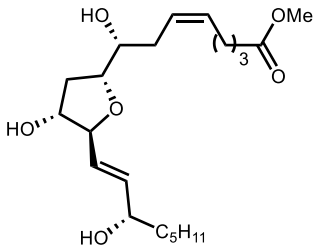

4.79

4.79: R_f 0.3 (EtOAc); $[a]^{23}_D$ -15.3 (*c* 0.6, $CHCl_3$); ^1H NMR (400 MHz, $CDCl_3$) δ 5.74 (ddd, *J* = 1.0, 6.3, 15.5 Hz, 1H), 5.58-5.44 (m, 3H), 4.47 (d, 5.3 Hz, 1H), 4.15 (dt, *J* = 2.9, 9.5 Hz, 1H), 4.12-4.04 (m, 2H), 3.67 (s, 3H), 3.56 (ddd, *J* = 2.2, 5.3, 7.8 Hz, 1H), 2.47 (m, 1H), 2.39-2.31 (m, 4H), 2.13 (m, 2H), 1.85 (m, 1H), 1.71 (m, 3H), 1.54-1.45 (m, 2H), 1.34-1.26 (m, 6H), 0.88 (t, *J* = 6.7 Hz, 3H); ^{13}C NMR (100 MHz, $CDCl_3$) δ 174.4, 134.7, 132.3, 129.7, 126.3, 87.6, 79.7, 75.8, 73.6, 72.3, 51.8, 37.3, 36.5, 33.6, 32.4, 26.7, 25.2, 24.9, 22.7, 14.2; LRMS calculated for $C_{21}H_{36}O_6$ $[M+Na]^+$ m/z 407.3, measured LC/MS (ESI) R_t 1.0 min, m/z 407.0 $[M+Na]^+$.

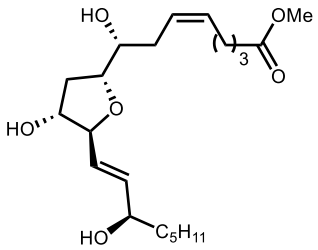

4.81

4.81: R_f 0.3 (EtOAc); $[a]^{23}_D$ -26.1 (*c* 0.7, $CHCl_3$); ^1H NMR (400 MHz, $CDCl_3$) δ 5.71 (ddd, *J* = 1.1, 6.0, 15.5 Hz, 1H), 5.62-5.44 (m, 3H), 4.48 (d, *J* = 5.2 Hz, 1H), 4.16 (dt, *J* = 2.9, 9.6 Hz, 1H), 4.12-4.06 (m, 2H), 3.67 (s, 3H), 3.57 (ddd, *J* = 2.4, 5.4, 7.9 Hz, 1H), 2.44 (m, 1H), 2.39-2.30 (m, 4H), 2.14 (m, 2H), 1.85 (m, 1H), 1.72 (m, 3H), 1.51 (m, 2H), 1.35-1.26 (m, 6H), 0.88 (t, *J* = 6.7 Hz, 3H); ^{13}C NMR (100 MHz, $CDCl_3$) δ 174.4, 134.7, 132.4, 128.7, 126.2, 87.5, 79.7, 75.8, 73.6, 72.2, 51.8, 37.4, 36.4, 33.6, 32.4, 31.9, 26.8, 25.2, 24.9, 22.7, 14.2; LRMS calculated for $C_{21}H_{36}O_6$ $[M+Na]^+$ m/z 407.3, measured LC/MS (ESI) R_t 1.0 min, m/z 407.0 $[M+Na]^+$.

General procedure for synthesis of Isofurans 4.8, 4.74, 4.80, and 4.82

To a solution of **4.79** (10.8 mg, 0.028 mmol) in THF (0.3 mL) was added LiOH (93 µL, 0.093 mmol, 1 M in water). The mixture was maintained for 8 h, then quenched with KH_2PO_4 (0.5 mL, 1 M in water) and HCl (0.3 mL, 1 M in water). The reaction was concentrated *in vacuo* to remove the THF. The aqueous layer was extracted with EtOAc (3 x 2 mL). The combined organic extracts

were washed with brine, dried (Na_2SO_4), filtered, and concentrated *in vacuo* to afford 9.4 mg (91%) of **4.80** as a colorless oil**.**

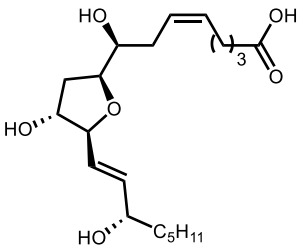

4.8

4.8: R_f 0.3 (EtOAc); ^{1}H NMR (400 MHz, $CDCl_3$) δ 5.83 (dd, *J* = 6.0, 15.5 Hz, 1H), 5.67 (dd, *J* = 5.9, 15.5 Hz, 1H), 5.56-5.44 (m, 2H), 4.24 (m, 1H), 4.17-4.09 (m, 4H), 3.50 (m, 1H), 2.37-2.31 (m, 3H), 2.28-2.19 (m, 2H), 2.17-2.07 (m, 2H), 2.03 (m, 1H), 1.91 (ddd, *J* = 3.5, 6.6, 12.9 Hz, 1H), 1.71 (m, 2H), 1.51 (m, 2H), 1.29 (m, 6H), 0.88 (t, *J* = 6.7 Hz, 3H); ^{13}C NMR (125 MHz, $CDCl_3$) δ 177.4, 135.7, 131.4, 129.1, 126.6, 86.4, 81.0, 76.7, 73.7, 72.3, 37.1, 36.4, 32.9, 32.0, 31.8, 26.4, 25.2, 24.5, 22.7, 14.2; LRMS calculated for $C_{20}H_{34}O_6$ $[M+Na]^+$ m/z 393.2, measured LC/MS (ESI) R_t 0.14 min, m/z 393.4 $[M+Na]^+$.

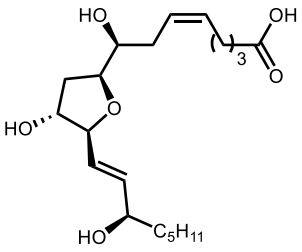

4.74

4.74: R_f 0.3 (EtOAc); ^{1}H NMR (400 MHz, $CDCl_3$) δ 5.81 (dd, *J* = 6.0, 15.7 Hz, 1H), 5.70 (dd, *J* = 6.3, 15.6 Hz, 1H), 5.57-5.44 (m, 2H), 4.26 (m, 1H), 4.18-4.10 (m, 3H), 3.50 (m, 1H), 2.41-2.33 (m, 3H), 2.23-2.16 (m, 2H), 2.12-2.05 (m, 2H), 1.91 (ddd, *J* = 3.4, 6.6, 12.9 Hz, 1H), 1.78-1.67 (m, 2H), 1.60-1.49 (m, 2H), 1.33-1.1.27 (m, 6H), 0.88 (t, *J* = 6.8 Hz, 3H); ^{13}C NMR (100 MHz, $CDCl_3$) δ 177.2, 135.1, 131.5, 129.6, 126.8, 86.1, 81.2, 76.8, 73.5, 72.8, 37.0, 36.5, 32.7, 32.1, 31.8, 26.3, 25.2, 24.4, 22.7, 12.2; LRMS calculated for $C_{20}H_{34}O_6$ $[M+Na]^+$ m/z 393.2, measured LC/MS (ESI) R_t 0.14 min, m/z 393.5 $[M+Na]^+$.

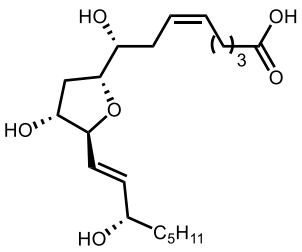

4.80

4.80: R_f 0.3 (EtOAc); ^{1}H NMR (400 MHz, $CDCl_3$) δ 5.73 (dd, *J* = 5.8, 15.5 Hz, 1H), 5.58 (dd, *J* = 5.2, 15.5 Hz, 1H), 5.53-5.46 (m, 2H), 4.46 (d, *J* = 5.0 Hz, 1H), 4.17-4.06 (m, 3H), 3.55 (dt, *J* = 2.3, 6.8 Hz, 1H), 2.40-2.30 (m, 5H), 2.19-2.13 (m, 2H), 1.84 (m, 1H), 1.76-1.70 (m, 2H), 1.53-1.47 (m, 2-3 H), 1.28 (m, 7H), 0.88 (t, J = 6.7 Hz, 3H); ^{13}C NMR

(100 MHz, $CDCl_3$) δ 177.6, 134.5, 132.0, 129.0, 126.4, 87.0, 79.5, 75.6, 73.7, 72.5, 37.2, 36.2, 33.2, 32.2, 31.8, 26.5, 25.2, 24.6, 22.7, 14.2; LRMS calculated for $C_{20}H_{34}O_6$ $[M+Na]^+$ m/z 393.2, measured LC/MS (ESI) R_t 0.16 min, m/z 393.5 $[M+Na]^+$.

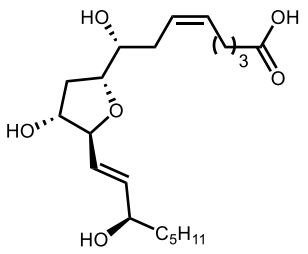

4.82

4.82: R_f 0.3 (EtOAc); ^1H NMR (400 MHz, $CDCl_3$) δ 5.73 (dd, *J* = 5.8, 15.9 Hz, 1H), 5.56 (dd, *J* = 5.7, 15.5 Hz, 1H), 5.52-5.46 (m, 2H), 4.46 (d, *J* = 5.5 Hz, 1H), 5.73 (dt, *J* = 5.8, 16.0 Hz, 1H), 4.11-4.06 (m, 2H), 3.54 (dt, *J* = 2.2, 6.8 Hz, 1H), 2.40-2.31 (m, 5 H), 2.18-2.13 (m, 2H), 1.85 (m, 1H), 1.71 (m, 2H), 1.53-1.42 (m, 2H), 1.28 (m, 6H), 0.88 (t, *J* = 6.7 Hz, 3H); ^{13}C NMR (100 MHz, $CDCl_3$) δ 177.7, 134.7, 132.0, 128.7, 126.4, 87.2, 79.5, 75.7, 73.6, 72.4, 37.1, 36.3, 33.2, 32.2, 31.8, 26.5, 25.2, 24.7, 22.7, 14.2; LRMS calculated for $C_{20}H_{34}O_6$ $[M+Na]^+$ m/z 393.2, measured LC/MS (ESI) R_t 0.16 min, m/z 393.4 $[M+Na]^+$.

Experimentals for Mosher Ester Analysis

General procedure for synthesis of compound 4.83

To a solution of alcohol **4.50** (68 mg, 0.17 mmol) in dichloromethane (1.3 mL) was added imidazole (34 mg, 0.51 mmol), DMAP (2.0 mg, 0.017 mmol) and TBSCl (38 mg, 0.25 mmol). The reaction was maintained for 4 h, then water (1 mL) was added to the reaction. The aqueous layer was extracted with dichloromethane (3 x 2 mL), the combined organic extracts were washed with brine (1 x 4 mL), dried ($MgSO_4$), filtered and concentrated *in vacuo*. The residue was purified by flash chromatography (gradient: 9:1 to 4:1 hexanes: EtOAc) to afford 62 mg (71%) of epoxide **4.83** as a clear oil.

Procedure for synthesis of compound 4.84

To a solution of alkyne **4.41** (43 mg, 0.2 mmol) in THF (0.2 mL) at -78 °C was added *n*-BuLi (0.07 mL, 0.17 mmol) as a solution in hexanes (2.4 M). The solution was allowed to stir at -78 °C for 15 min, then warmed to 0 °C for 15 min. The solution was cooled to -78 °C and epoxide **4.83** (67 mg, 0.13 mmol) was added to the reaction in a solution of THF (1.0 mL). $BF_3 \bullet OEt_2$ (56 µL, 0.45 mmol) was added to the reaction in a solution of THF (0.2 mL). The reaction mixture was maintained at -78 °C for 2 h, then -40 °C for 2 h. The reaction was quenched at 0 °C with saturated ammonium chloride (2 mL). The aqueous layer was extracted with EtOAc (3 x 5 mL). The combined organic extracts were washed with brine (5 mL), dried ($MgSO_4$), filtered and concentrated *in vacuo*. The residue was purified by flash chromatography (4:1 to 2:1 Hexanes: EtOAc) to afford 39 mg (40 %) of the alcohol **4.84** as a clear oil.

General procedure for synthesis of Mosher esters 4.85 (R/S) and 4.85 (R/S)

To a solution of alcohol **4.84** (16 mg, 0.022 mmol) in CH_2Cl_2 (0.5 mL) was added R MTPA (16 mg, 0.069 mmol), DCC (14 mg, 0.069 mmol) and DMAP (4 mg, 0.036 mmol). The reaction mixture was maintained for 14 h. CH_2Cl_2 was added, the solution was filtered and concentrated. The crude mixture was purified by flash chromatography (gradient: 9:1 Hexanes: EtOAc) to afford 17 mg (81%) of desired Mosher ester **4.85 (R)**.

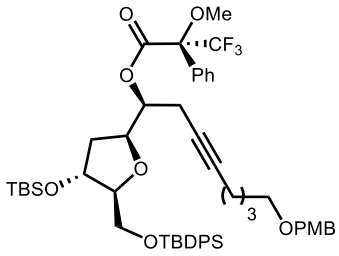

4.85 S

4.85 S: R_f 0.5 (4:1 hexanes/EtOAc); ^{1}H NMR (400 MHz, $CDCl_3$) δ 7.66 (m, 4H), 7.59 (m, 2H), 7.45-7.27 (m, 10H), 7.25 (m, 2H), 6.87 (m, 2H), 5.11 (dd, *J* = 6.1, 11.9 Hz, 1H), 4.41 (s, 2H), 4.40-4.37 (m, 2H), 3.91 (m, 1H), 3.80 (s, 3H), 3.60 (dd, *J* = 4.3, 10.9 Hz, 1H), 3.50-3.46 (m, 4H), 3.41 (t, *J* = 6.3 Hz, 2H), 2.55 (m, 1H), 2.43 (m, 1H), 2.06 (m, 2H), 1.87 (m, 1H), 1.77-1.70 (m, 2H), 1.62 (m, 2H), 1.49 (m, 2H), 1.04 (s, 9H), 0.87 (s, 9H), 0.06 (s, 3H), 0.05 (s, 3H); ^{13}C NMR (100 MHz, $CDCl_3$) δ 166.2, 159.3, 135.7, 133.4, 133.3,

132.3, 130.9, 129.9, 129.5, 129.3, 128.9, 128.4, 127.9, 113.9, 87.9, 82.6, 78.1, 76.5, 74.4, 74.1, 72.7, 69.6, 64.6, 55.5, 55.4, 37.4, 29.0, 27.0, 25.9, 25.6, 21.4, 19.3, 18.6, 18.1, -4.5, -4.6.

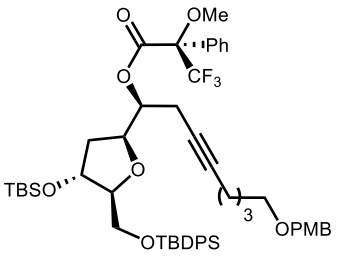

4.85 R

4.85 R: R_f 0.5 (4:1 hexanes/EtOAc); ^{1}H NMR (400 MHz, $CDCl_3$) δ 7.67-7.63 (m, 4H), 7.54 (d, *J* = 7.5 Hz, 2H), 7.45-7.35 (m, 7H), 7.32-7.28 (m, 2H), 6.87 (d, *J* = 8.6 Hz, 2H), 5.16 (dd, *J* = 5.3, 12.1 Hz, 1H), 4.41 (s, 2H), 4.34 (m, 1H), 4.26 (m, 1H), 3.84-3.80 (m, 4H), 3.57-3.53 (m, 4H), 3.42 (t, *J* = 6.3 Hz, 2H), 3.35 (dd, *J* = 6.6, 10.8 Hz, 1H), 2.60 (m, 1H), 2.52 (m, 1H), 2.12 (t, *J* = 6.9 Hz, 2H), 1.69-1.61 (m, 3H), 1.58-1.51 (m, 3H), 1.04 (s, 9 H), 0.86 (s, 9H), 0.2 (s, 6H); ^{13}C NMR (100 MHz, $CDCl_3$) δ 166.0, 159.2, 135.7, 133.5, 133.4, 132.4, 130.9, 129.9, 129.6, 129.3, 128.3, 127.9, 127.8, 127.6, 113.8, 87.6, 82.7, 77.7, 76.0, 75.0, 73.9, 72.7, 69.6, 64.4, 55.7, 55.4, 36.5, 29.0, 27.0, 25.9, 25.6, 21.3, 19.3, 18.6, 18.1, -4.5, -4.6.

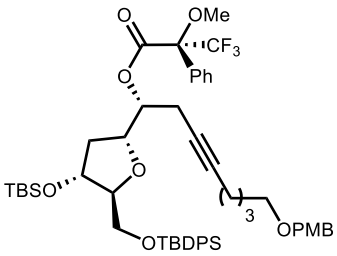

4.88 S

4.88 S: R_f 0.5 (4:1 hexanes/EtOAc); ^{1}H NMR (400 MHz, $CDCl_3$) δ 7.68-7.62 (m, 6H), 7.44-7.30 (m, 11 H), 7.24 (d, *J* = 8.6 Hz, 2H), 6.88 (m, 2H), 5.40 (dt, *J* = 4.8, 6.8 Hz, 1H), 4.44 (dd, *J* = 5.2, 11.0 Hz, 1H), 4.40 (s, 2H), 4.25 (dd, *J* = 6.7, 13.4 Hz, 1H), 3.81-3.77 (m, 4H), 6.65-3.61 (m, 3H), 3.59 (s, 3H), 3.41 (t, *J* = 6.3 Hz, 2H), 2.63 (m, 1H), 2.51 (ddt, *J* = 2.2, 7.1, 16.9 Hz, 1H), 2.17-2.10 (m, 3H), 1.03 (s, 9H), 0.87 (s, 9H), 0.05 (s, 3H), 0.04 (s, 3H); ^{13}C NMR (100 MHz, $CDCl_3$) δ 168.1, 159.3, 135.8, 135.7, 133.7, 133.4, 132.6, 130.9, 129.8 (2), 129.5, 129.3, 128.9, 128.3, 127.8, 127.0, 113.9, 86.1, 82.6, 78.176.0, 75.1, 72.7, 69.6, 63.9, 55.7, 55.4, 37.1, 29.0, 26.9, 25.9, 25.7, 21.2, 19.3, 18.6, 18.0, -4.6, -4.7.

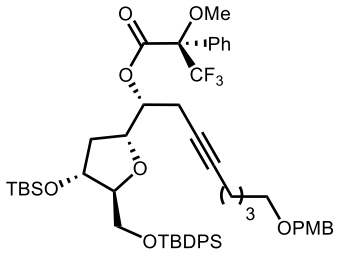

4.88 R

4.88 R: R_f 0.5 (4:1 hexanes/EtOAc); ^{1}H NMR (400 MHz, $CDCl_3$) δ 7.69-7.64 (m, 6H), 7.42-7.30 (m, 10 H), 7.25 (m, 2H), 6.87 (m, 2H), 5.36 (dd, *J* = 6.2, 12.3 Hz, 1H), 4.48 (dd, *J* = 4.9, 10.7 Hz, 1H), 4.41 (s, 2H), 4.32 (dd, *J* = 7.2, 13.5 Hz, 1H), 3.86 (dd, *J*= 3.6, 7.6 Hz, 1H), 3.80 (s, 3H), 3.67 (m, 2H), 3.60 (s, 3H), 3.40 (t, *J* = 6.3 Hz, 2H), 2.57 (m, 1H), 2.41 (m, 1H), 2.25 (m, 1H), 2.06 (m, 2H), 1.77 (dt, *J* = 5.6, 12.6 Hz, 1H), 1.62 (m, 2H), 1.48 (m, 2H), 1.04 (s, 9H), 0.88 (s, 9 H), 0.06 (s, 3H), 0.04 (s, 3H); ^{13}C NMR (100 MHz, $CDCl_3$) δ 166.2, 159.3, 135.8, 135.7, 133.6, 133.3, 132.7, 130.9, 129.8 (2), 129.4, 129.3, 128.9, 128.3, 127.8 (2), 113.9, 86.2, 82.5, 78.4, 76.2, 74.5, 72.8, 72.7, 69.7, 64.0, 55.7, 55.4, 37.6, 29.0, 26.9, 25.9, 25.6, 21.3, 19.3, 18.6, 18.0, -4.6, -4.7.

General procedure for coupling (R/S) Mosher Ester to compound 4.89 (R/S)

To a solution of allylic alcohol **4.78** (2.7 mg, 0.0057 mmol) in CH_2Cl_2 (0.5 mL), was added S-MPTA (4 mg, 0.018 mmol), DCC (3.7 mg, 0.018 mmol) and DMAP (2.2 mg, 0.018 mmol). The reaction mixture was maintained for 14 h. CH_2Cl_2 (1 mL) was added to the reaction mixture, the solution was filtered and concentrated. The crude mixture was purified by flash chromatography (gradient: 9:1 Hexanes: EtOAc) to afford 3.7 mg (95 %) of desired Mosher Ester **4.88 S**.

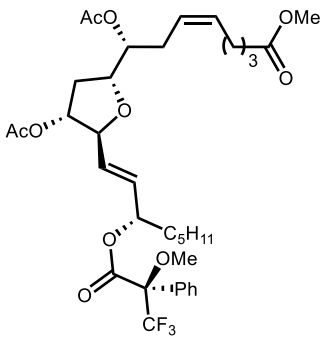

4.89 R

4.89 R: R_f 0.4 (4:1 hexanes/EtOAc); ^{1}H NMR (600 MHz, $CDCl_3$) δ 7.51-7.49 (m, 2H), 7.40-7.39 (m, 3H), 5.70-5.64 (m, 2H), 5.51-5.43 (m, 2H), 5.41-5.36 (m, 2H), 4.98 (dd, *J* = 6.3, 12.2 Hz, 1H), 4.87 (m, 1H), 4.44 (m, 1H), 4.12 (dd, *J* = 6.1, 13.7 Hz, 1H), 3.66 (s, 3H), 3.54 (s, 3H), 2.37-2.34 (m, 3H), 2.31 (t, *J* = 7.5 Hz, 3H), 2.11-2.07 (m, 6H), 2.05 (s, 3H), 1.76-1.68 (m, 5H), 1.66-1.59 (m, 2H), 1.29-1.27 (m, 6H), 0.87 (m, 3H); ^{13}C NMR (125 MHz, $CDCl_3$) δ 174.1, 170.8, 170.3, 165.9, 132.5, 132.1, 131.2, 129.7, 129.4,

128.5, 127.5, 124.9, 82.6, 78.3, 78.0, 76.6, 74.2, 55.6, 51.6, 34.2, 34.1, 33.5 (2), 31.5, 29.8, 29.1, 26.8, 25.8, 25.1, 24.8, 22.9, 22.6, 21.3, 21.2, 14.1.

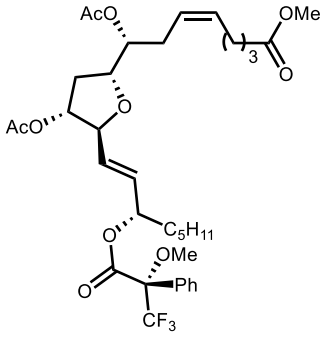

4.89 S

4.89 S: R_f 0.4 (4:1 hexanes/EtOAc); ^{1}H NMR (600 MHz, $CDCl_3$) δ 7.51-7.50 (m, 2H), 7.40-7.38 (m, 3H), 5.81-5.75 (m, 2H), 5.50-5.45 (m, 2H), 5.39 (m, 1H), 4.99 (dd, *J* = 6.2, 12.2 Hz, 1H), 4.46 (t, *J* = 3.6 Hz, 1H), 4.14 (dd, *J* = 6.1, 13.7 Hz, 1H), 3.66 (s, 3H), 2.53 (s, 3H), 2.39-2.53 (m, 3H), 2.31 (t, *J* = 7.5 Hz, 2H), 2.10-2.08 (m, 5H), 2.07-2.06 (m, 4H), 1.76 (ddd, *J* = 4.3, 6.2, 13.8 Hz, 1H), 1.72-1.67 (m, 3H), 1.62-1.56 (m, 2H), 1.22 (m, 6H), 0.84 (m, 3H); ^{13}C NMR (125 MHz, $CDCl_3$) δ 174.1, 170.8, 170.6, 166.0, 132.6, 132.0, 131.8, 129.7, 129.5, 128.5, 127.5, 124.9, 82.7, 78.4, 78.0, 76.6, 74.2, 55.6, 51.6, 34.1, 33.5 (2), 31.4, 29.8, 29.1, 26.8, 24.8, 24.5, 22.5, 21.3, 21.1, 14.0.

Appendix 1

Relevant Spectra for Chapter 4

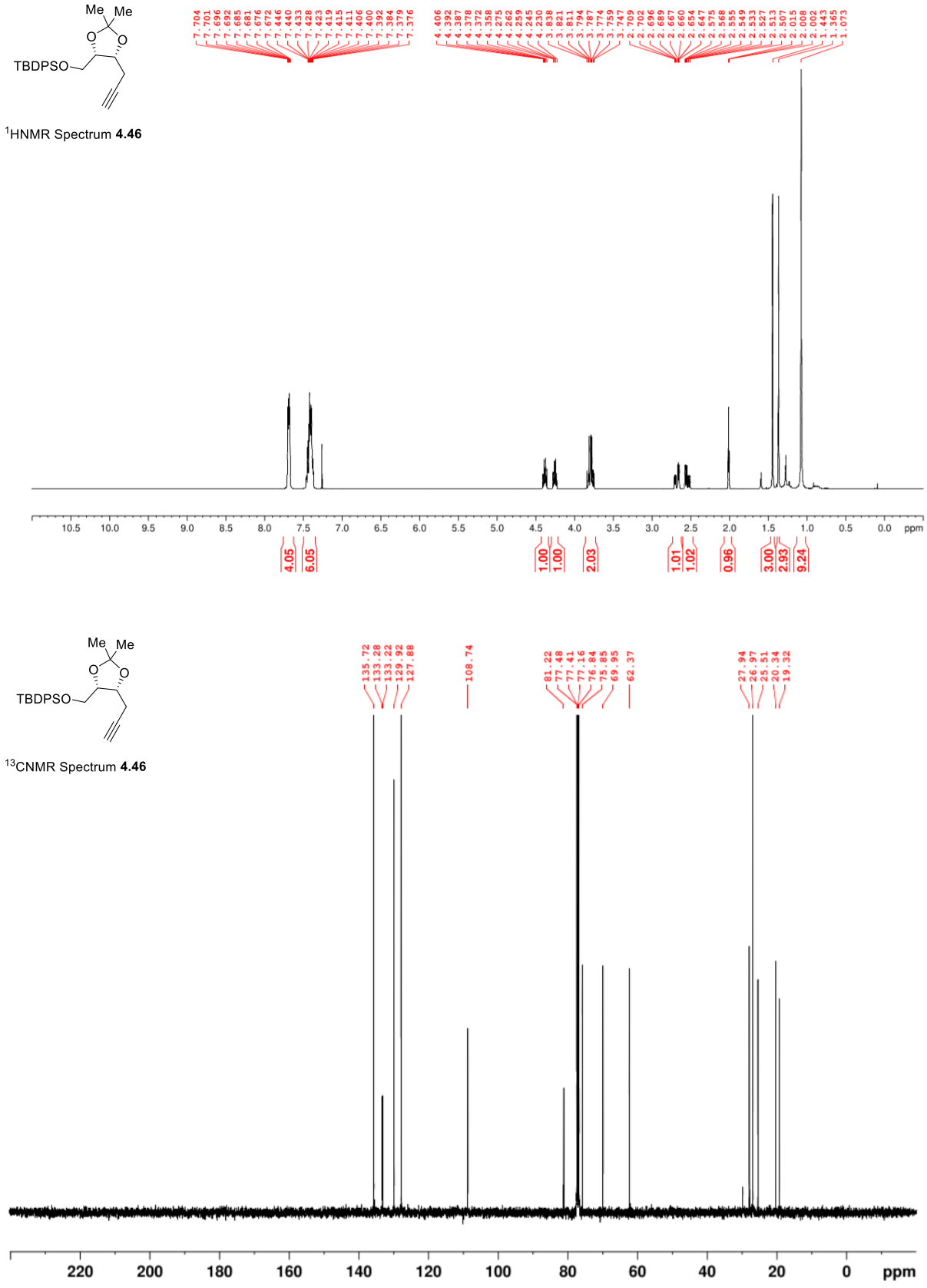

Figure A.1 ^{1}H NMR (400 MHz, $CDCl_3$) and ^{13}C NMR (100 MHz, $CDCl_3$) of **4.46**

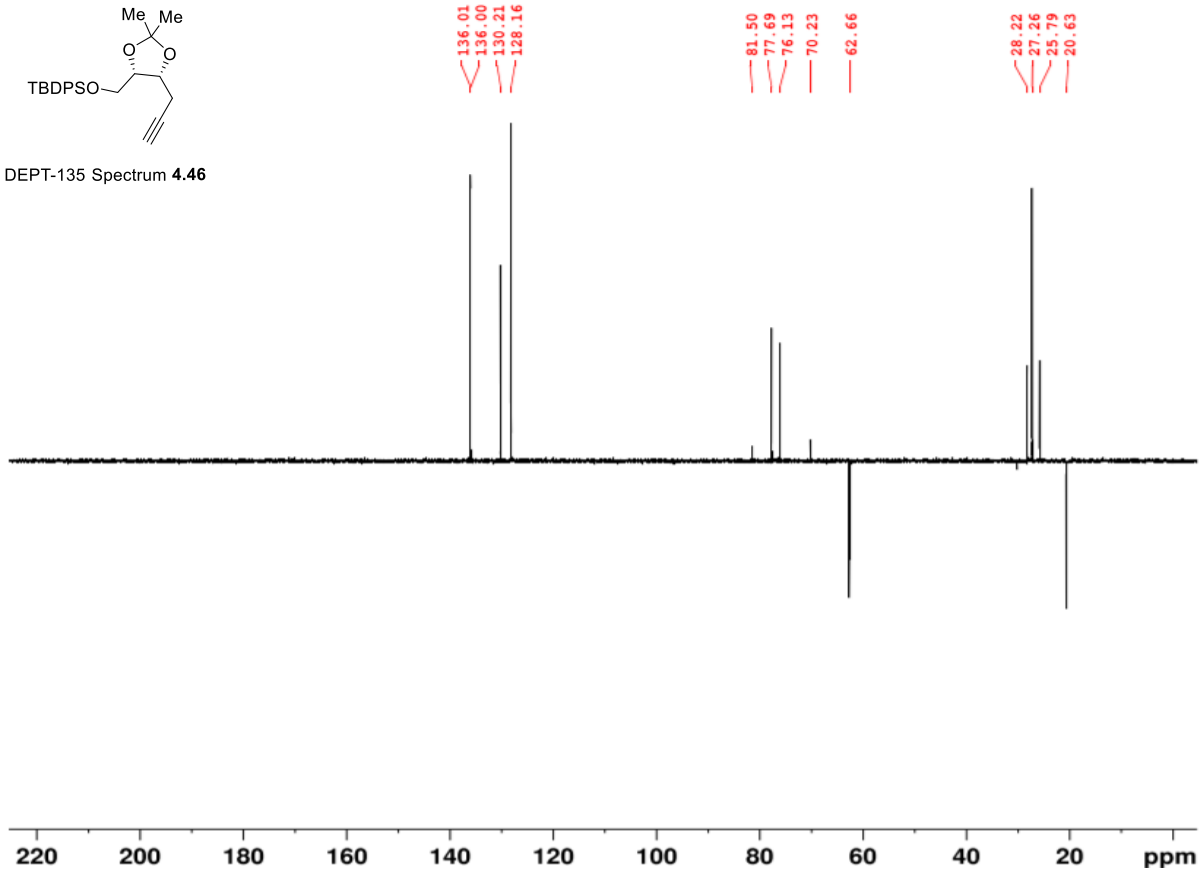

Figure A.2 DEPT-135 (100MHz, $CDCl_3$) of **4.46**

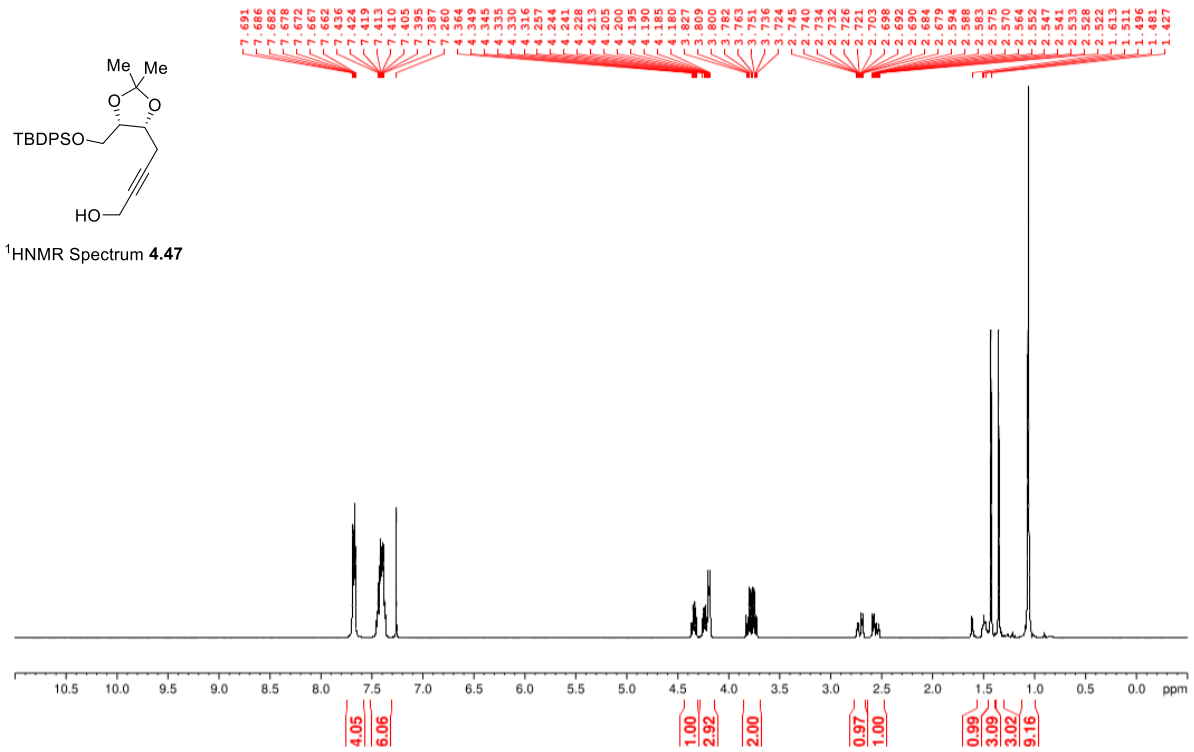

Figure A.3 ^1H NMR (400 MHz, $CDCl_3$) of **4.47**

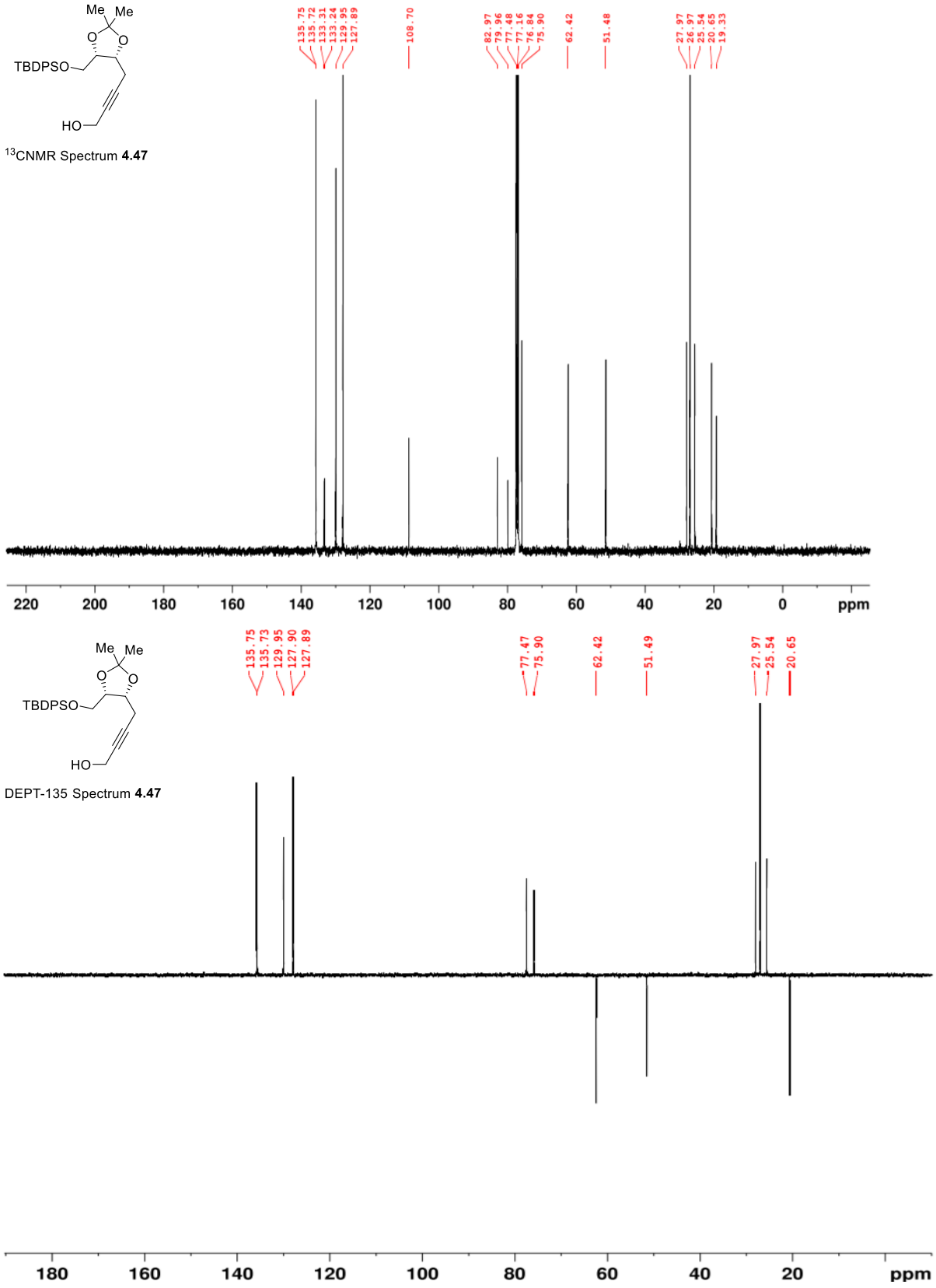

Figure A.4 ^{13}C NMR (100 MHz, $CDCl_3$) and of DEPT-135 (100MHz, $CDCl_3$) of **4.47**.

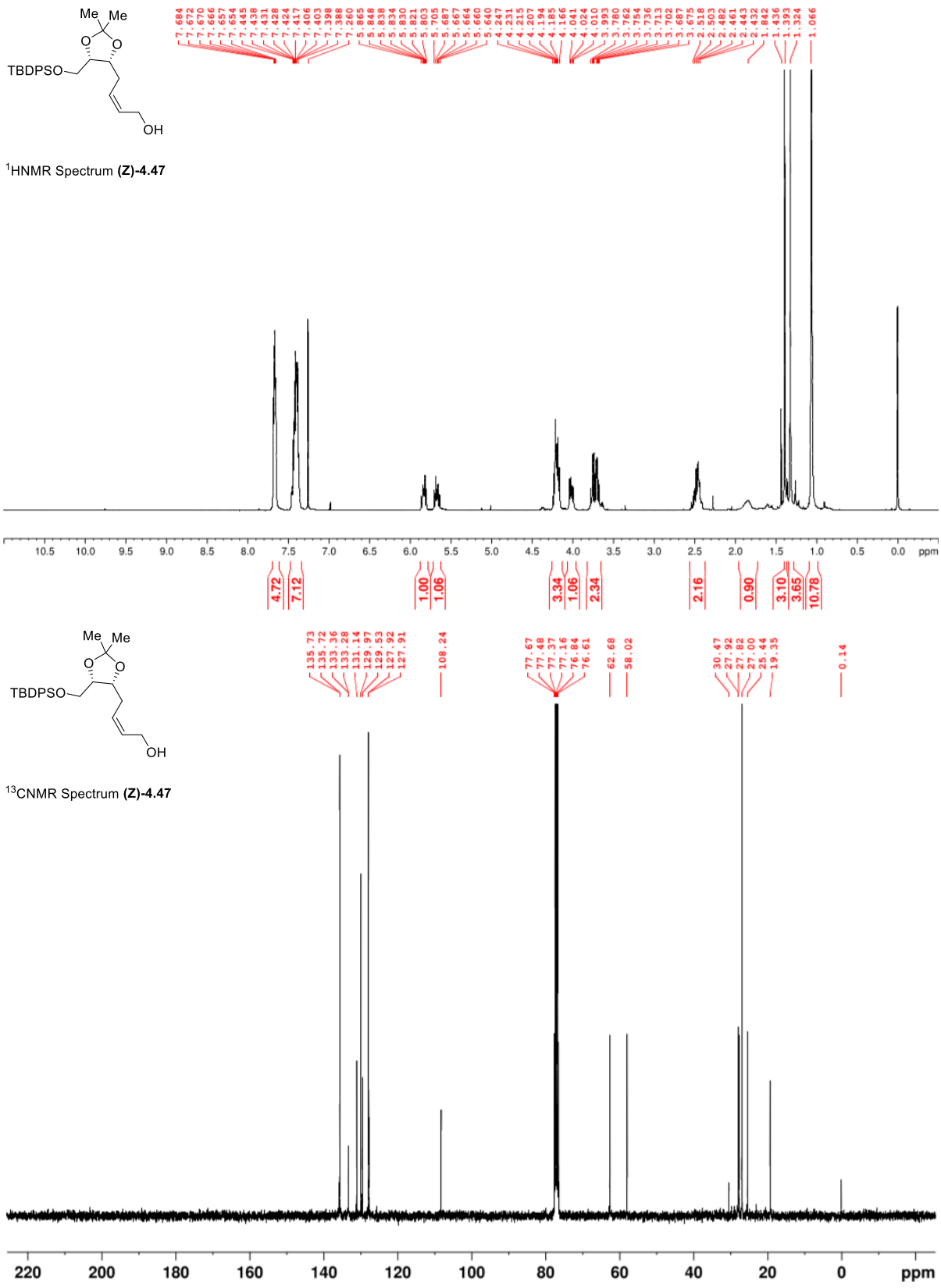

Figure A.5 ^{1}H NMR (400 MHz, $CDCl_3$) and ^{13}C NMR (100 MHz, $CDCl_3$) of **(Z)-4.47**.

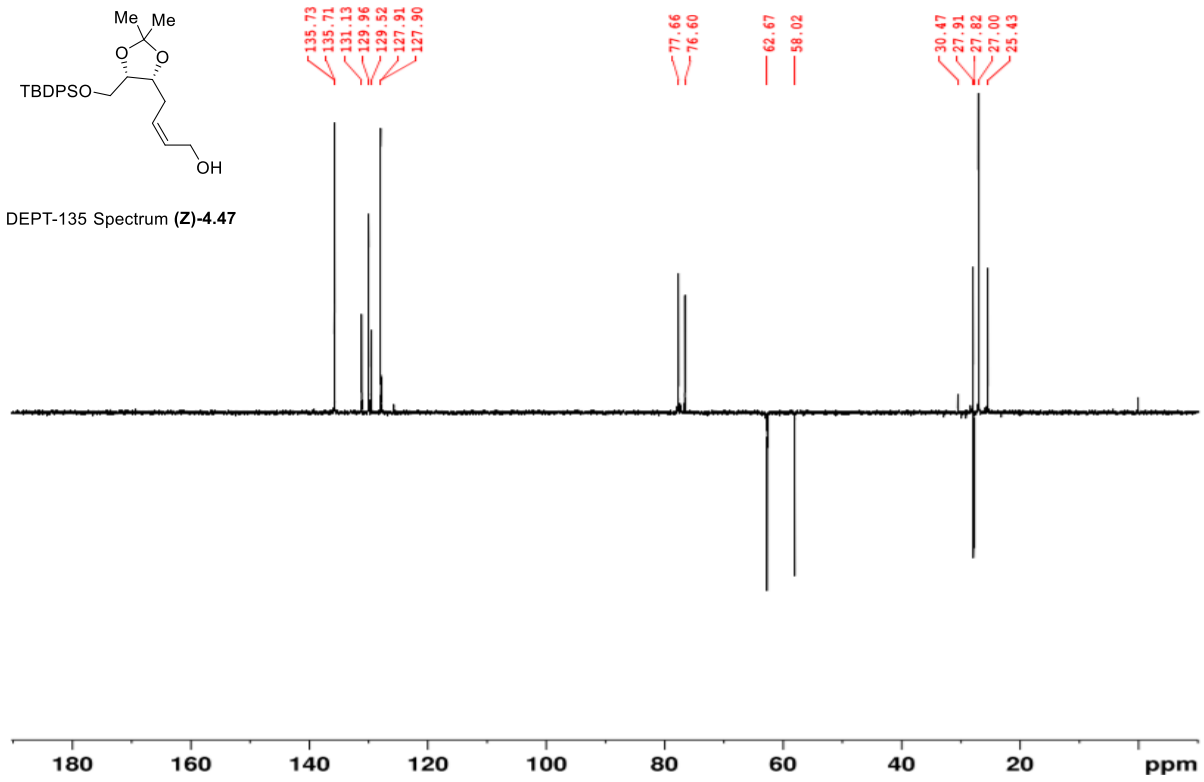

Figure A.6 DEPT-135 (100MHz, $CDCl_3$) of **(Z)-4.47**.

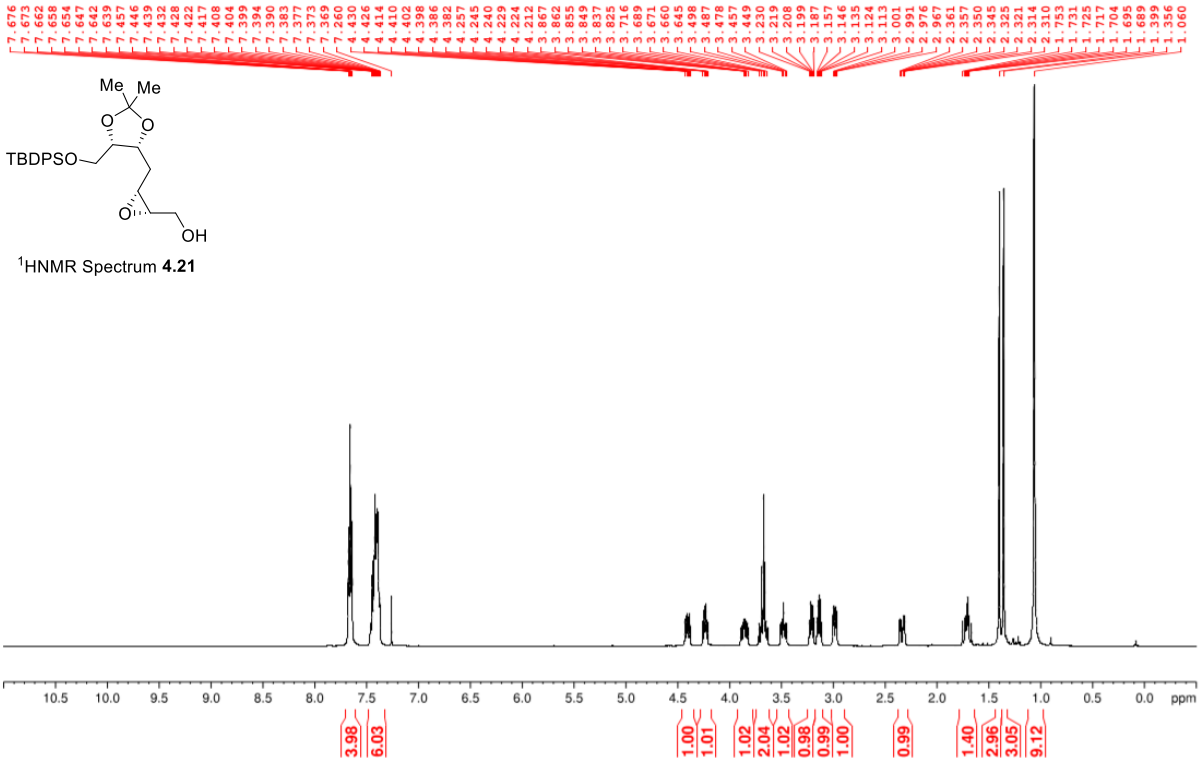

Figure A.7 ^{1}H NMR (400 MHz, $CDCl_3$) of **4.21**.

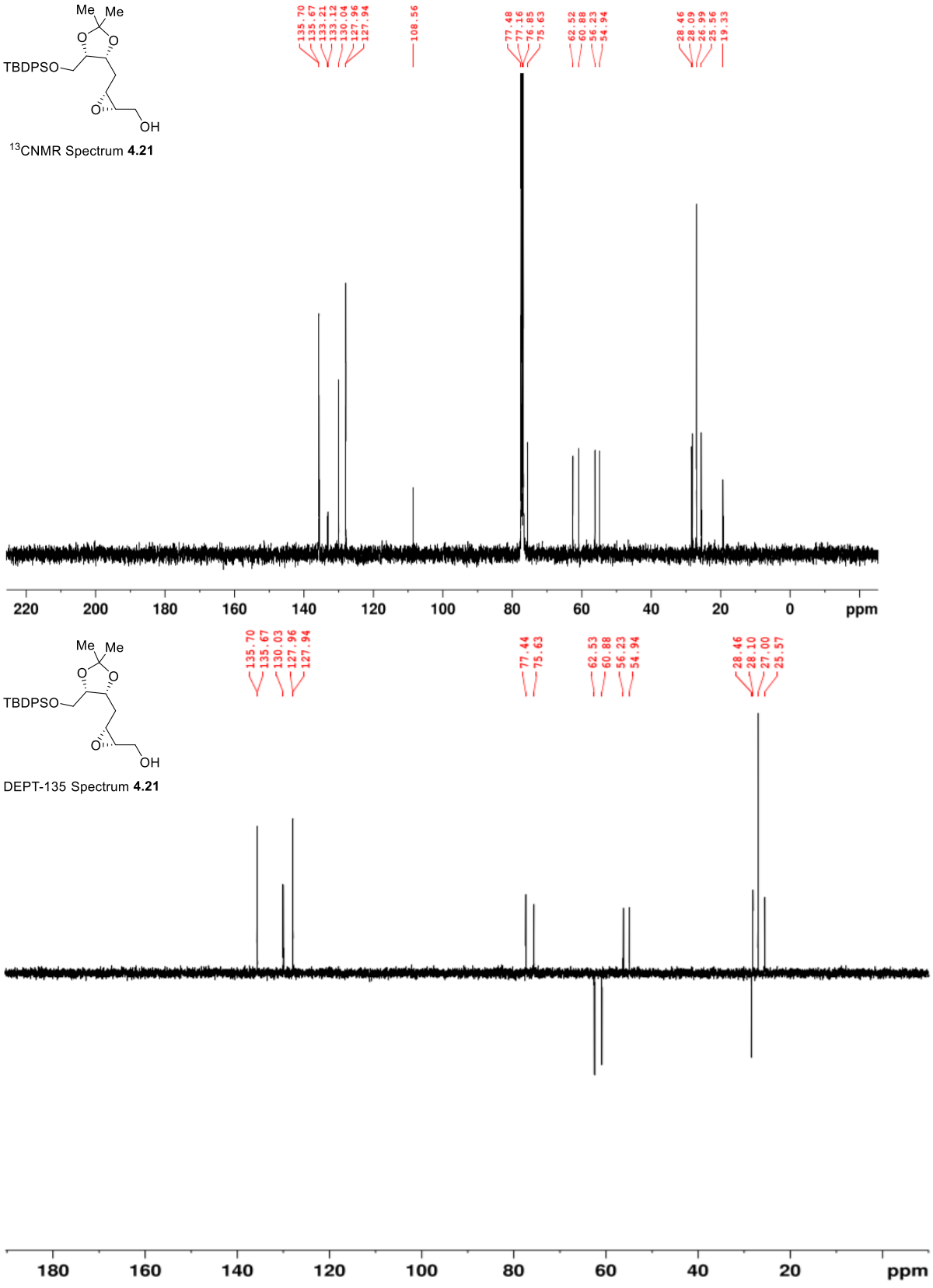

Figure A.8 ^{13}C NMR (100 MHz, $CDCl_3$) and DEPT-135 (100MHz, $CDCl_3$) of **4.21**.

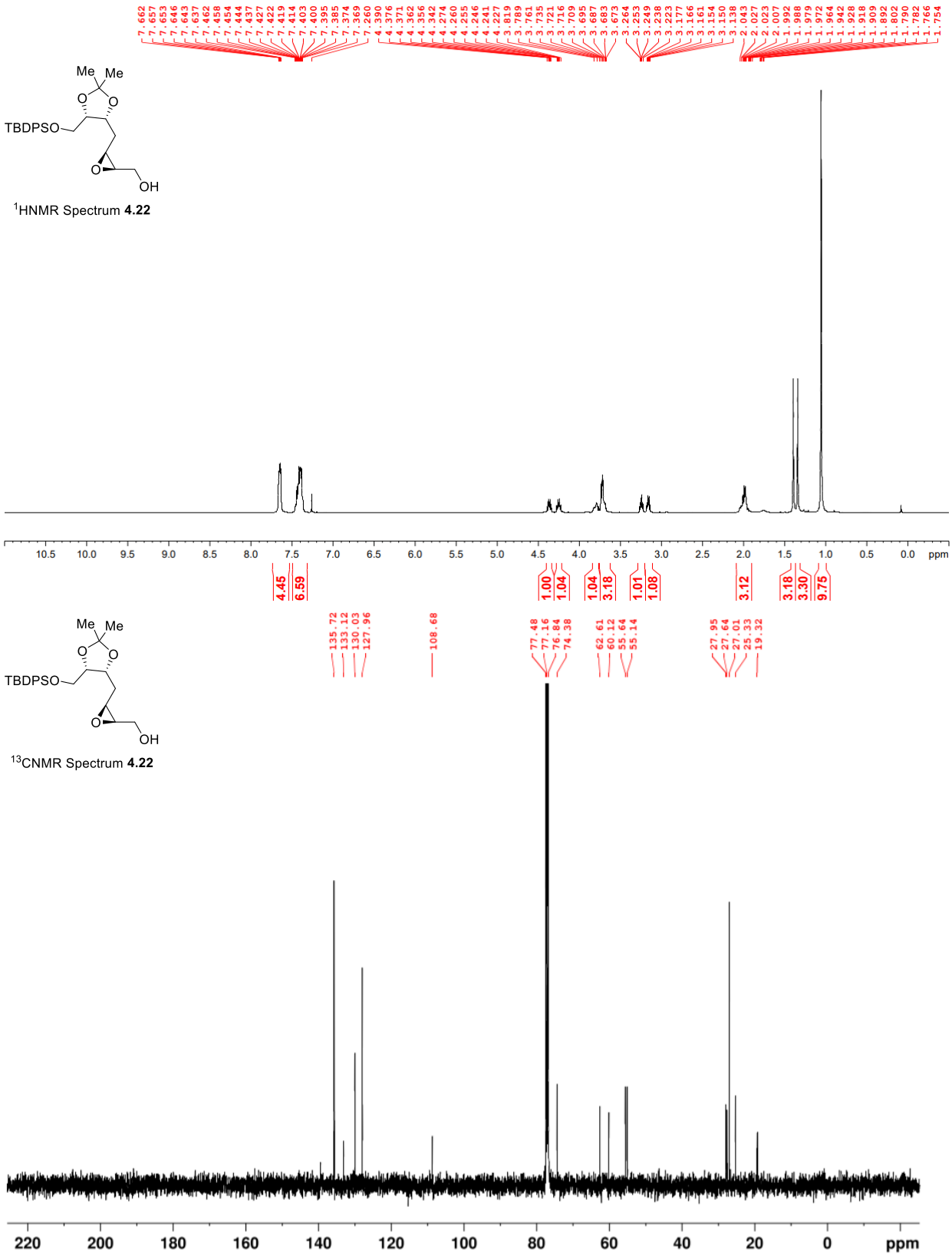

Figure A.9 ^{1}H NMR (400 MHz, $CDCl_3$) and ^{13}C NMR (100 MHz, $CDCl_3$) of **4.22**.

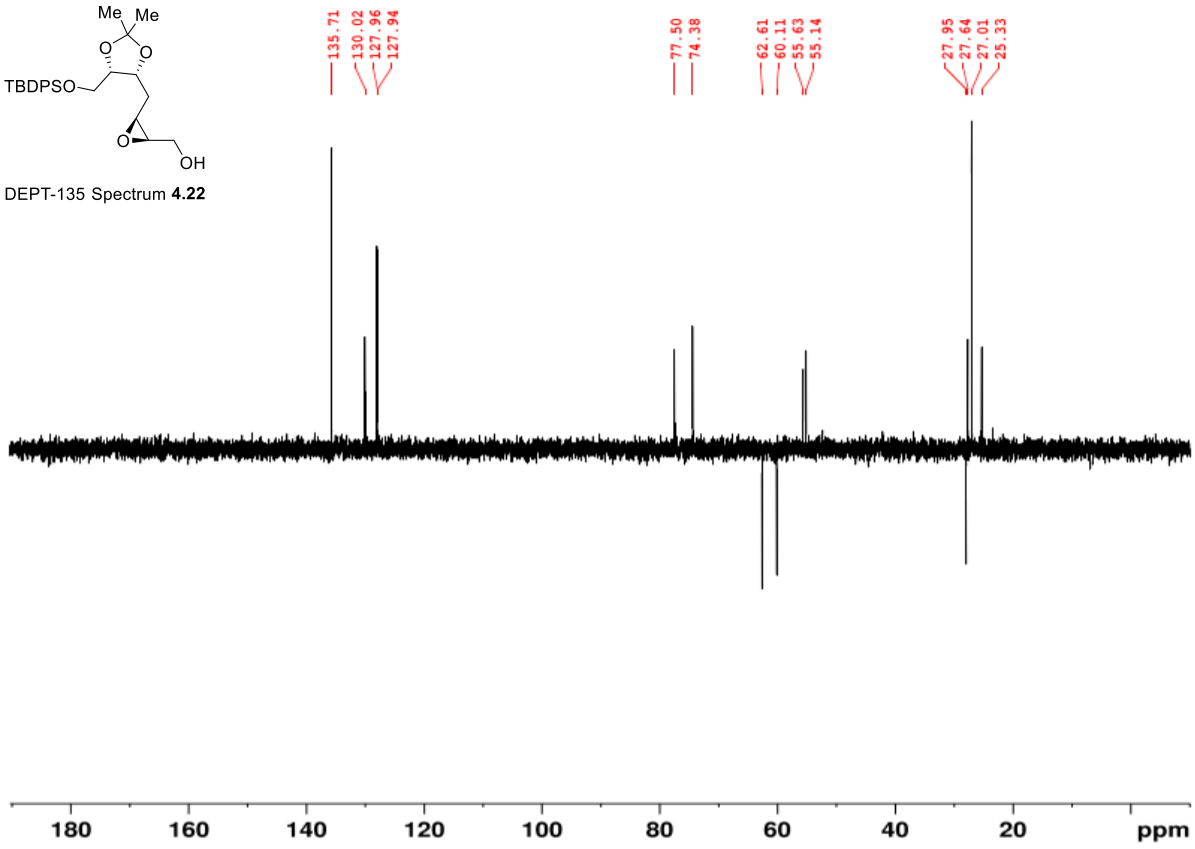

Figure A.10 DEPT-135 (100MHz, $CDCl_3$) of **4.22**.

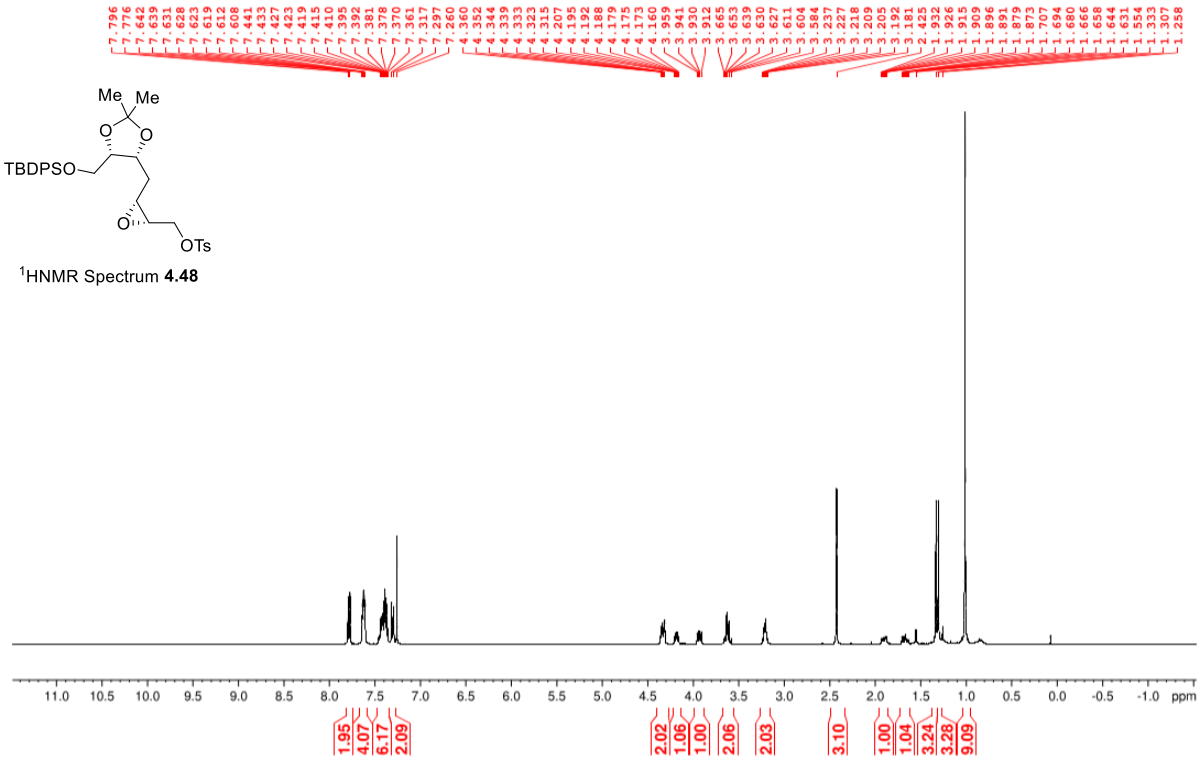

Figure A.11 ^{1}H NMR (400 MHz, $CDCl_3$) of **4.48**.

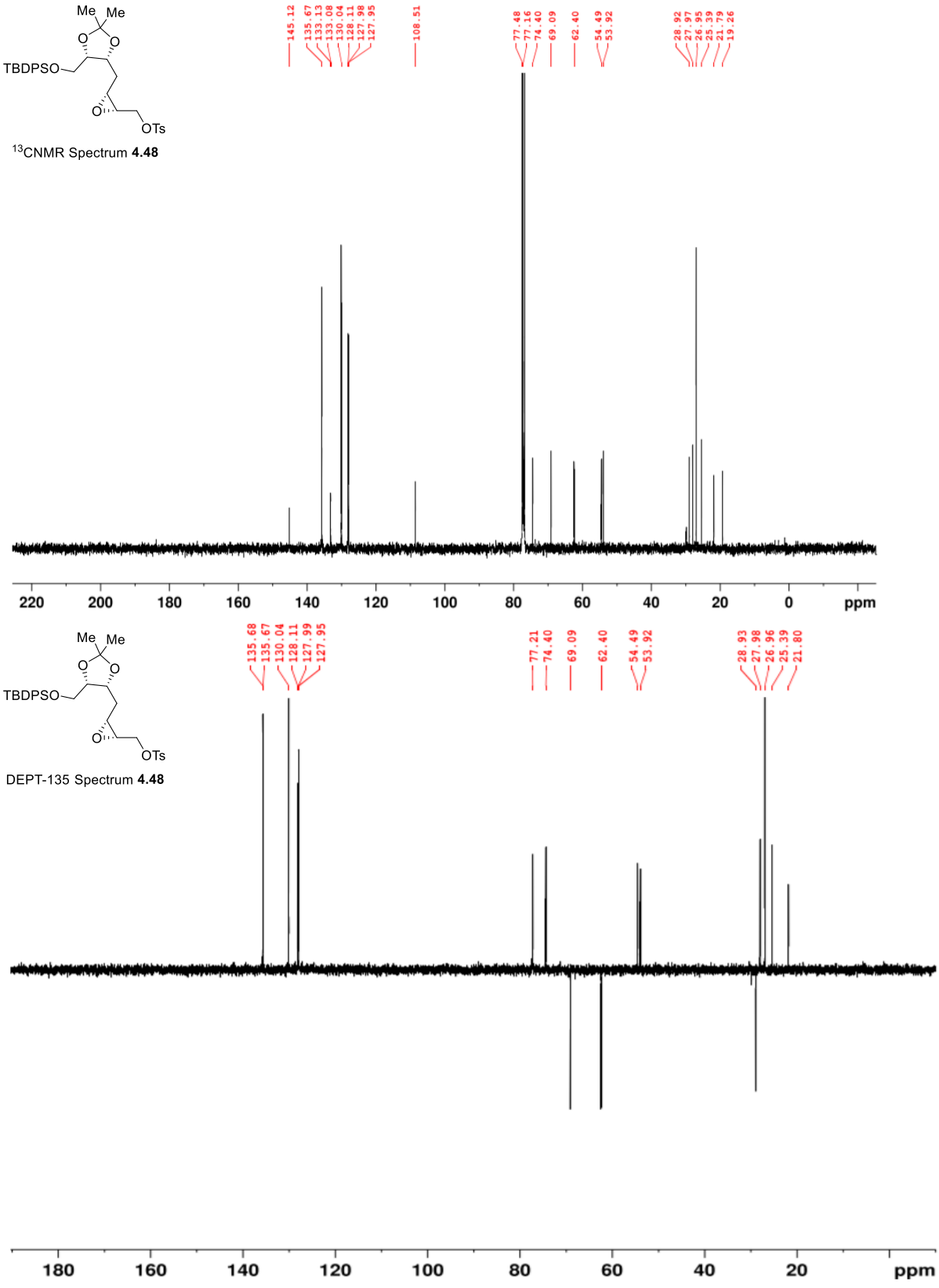

Figure A.12 ^{13}C NMR (100 MHz, $CDCl_3$) and DEPT-135 (100MHz, $CDCl_3$) of **4.48**.

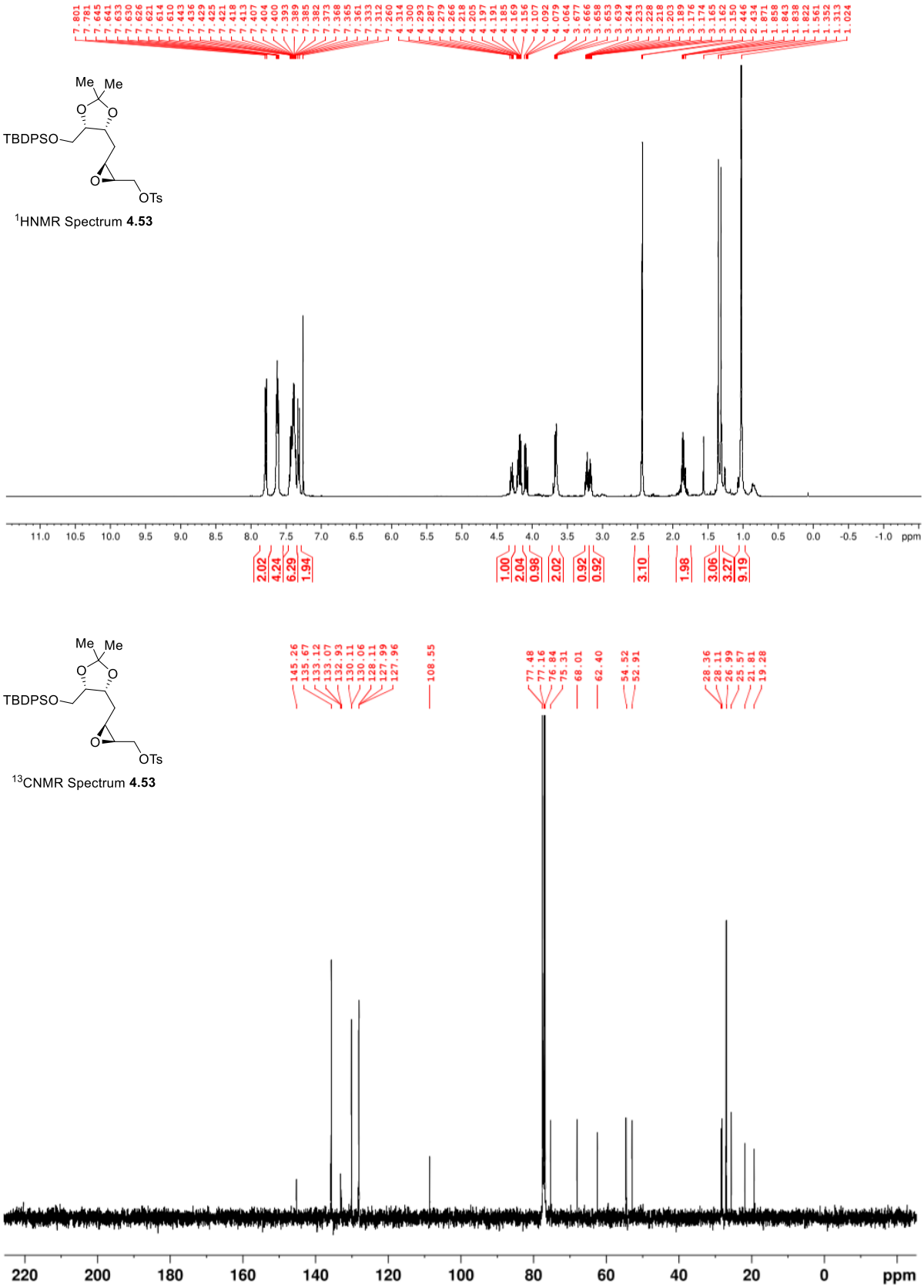

Figure A.13 ^{1}H NMR (400 MHz, $CDCl_3$) and ^{13}C NMR (100 MHz, $CDCl_3$) of **4.53**.

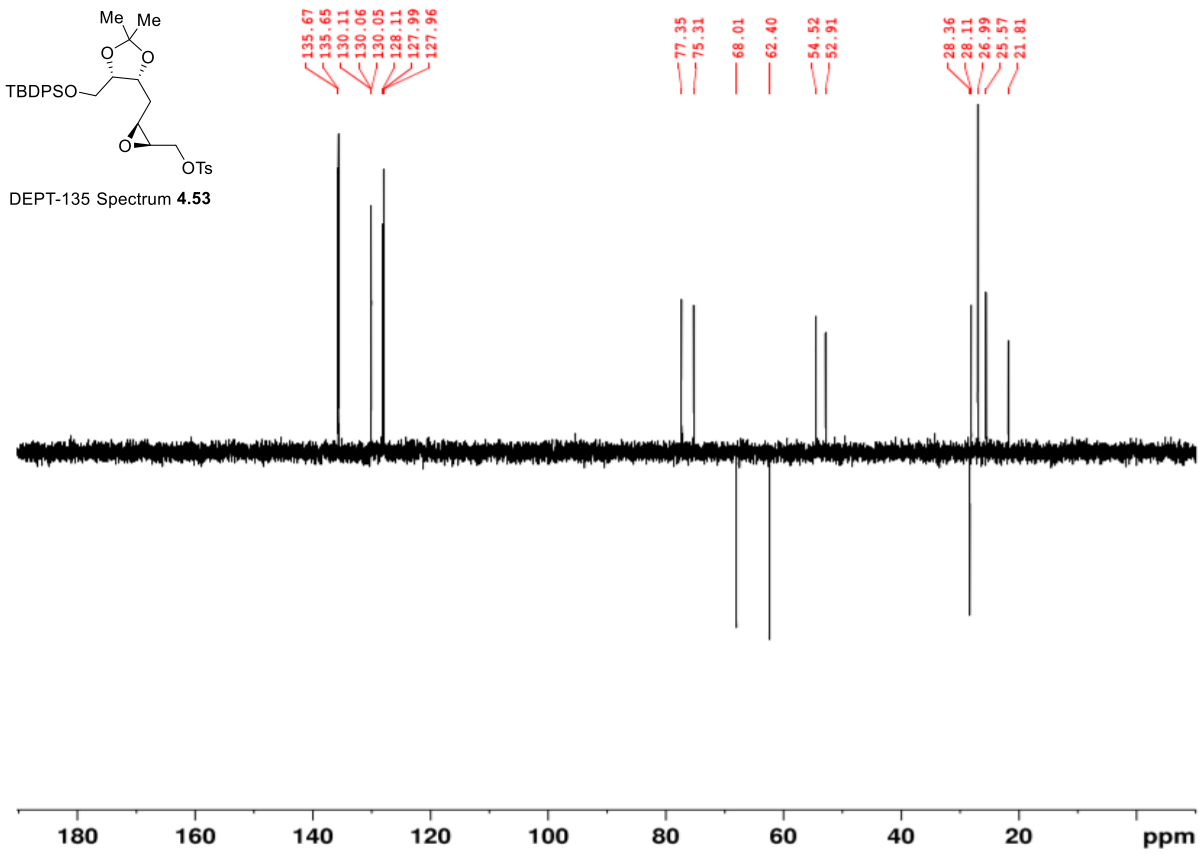

Figure A.14 DEPT-135 (100MHz, $CDCl_3$) of **4.53**.

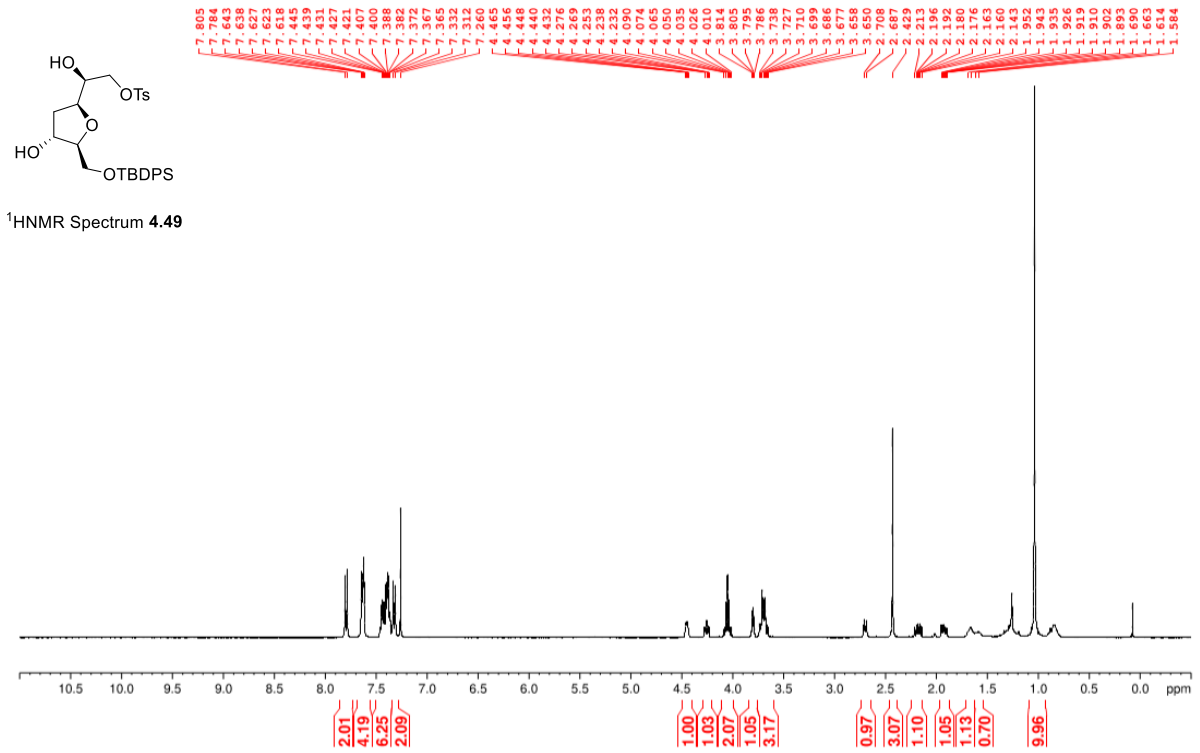

Figure A.15 ^{1}H NMR (400 MHz, $CDCl_3$) of **4.49**.

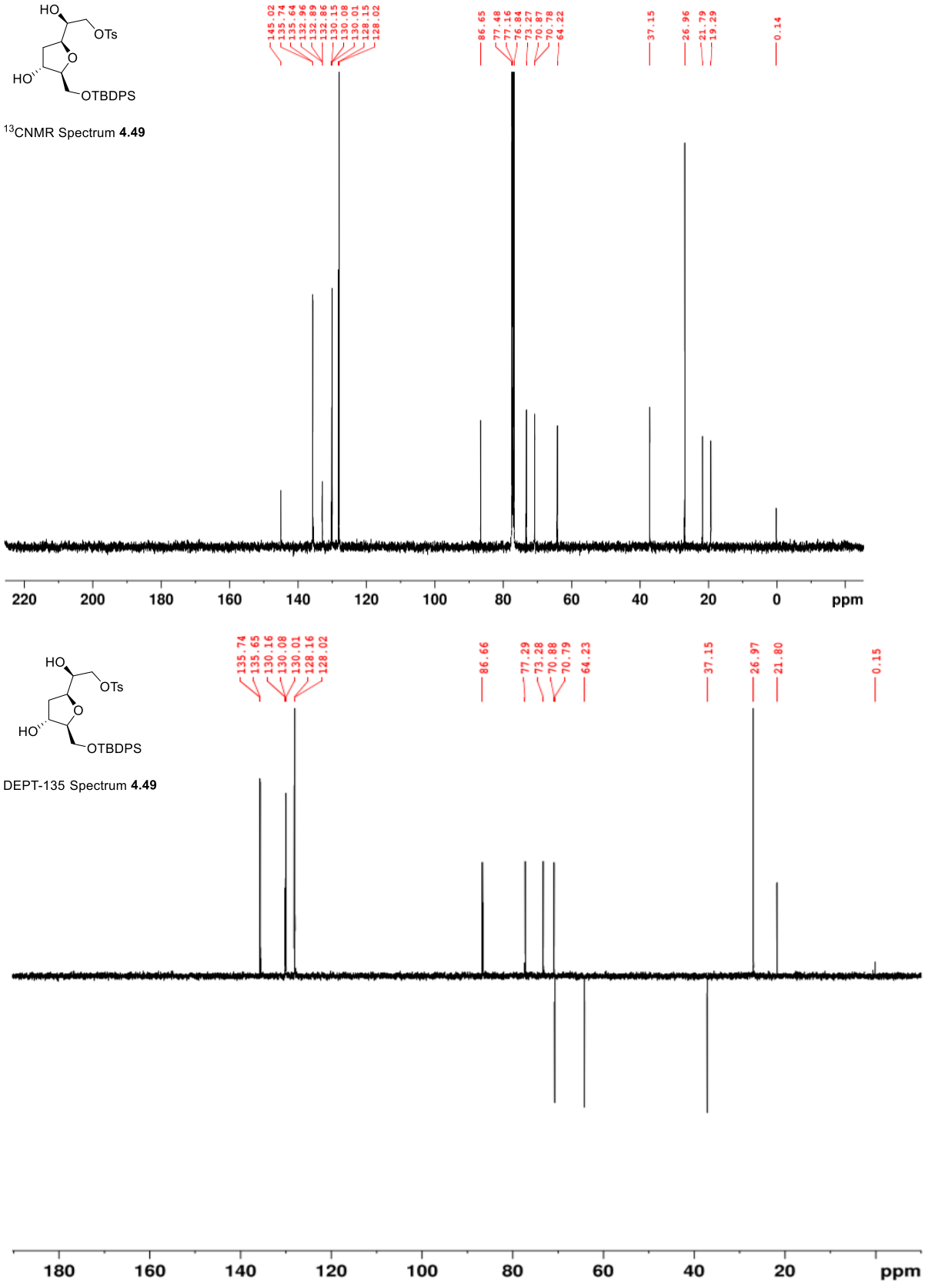

Figure A.16 ^{13}C NMR (100 MHz, $CDCl_3$) and DEPT-135 (100MHz, $CDCl_3$) of **4.49**.

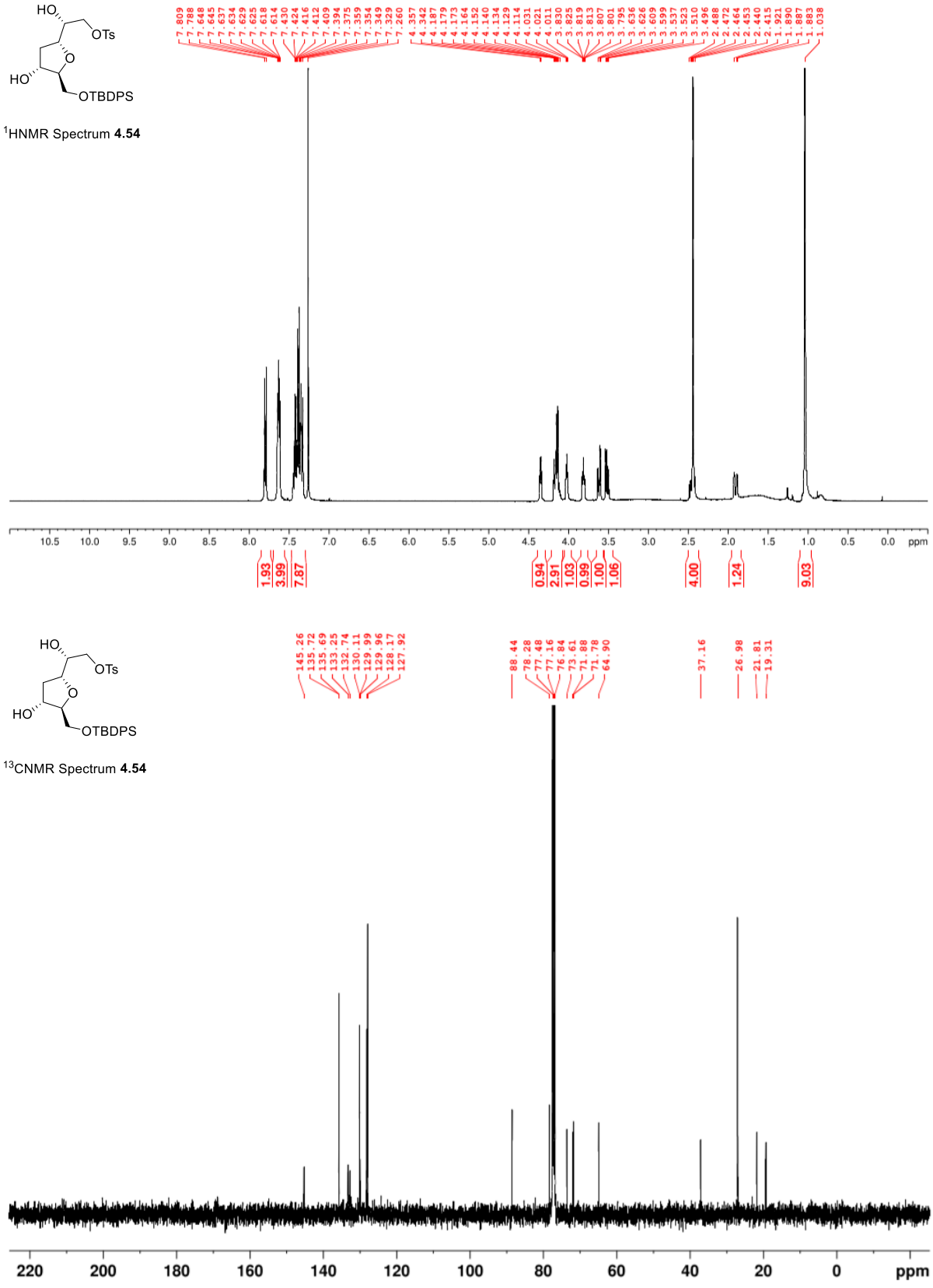

Figure A.17 ^{1}H NMR (400 MHz, $CDCl_3$) and ^{13}C NMR (100 MHz, $CDCl_3$) of **4.54**.

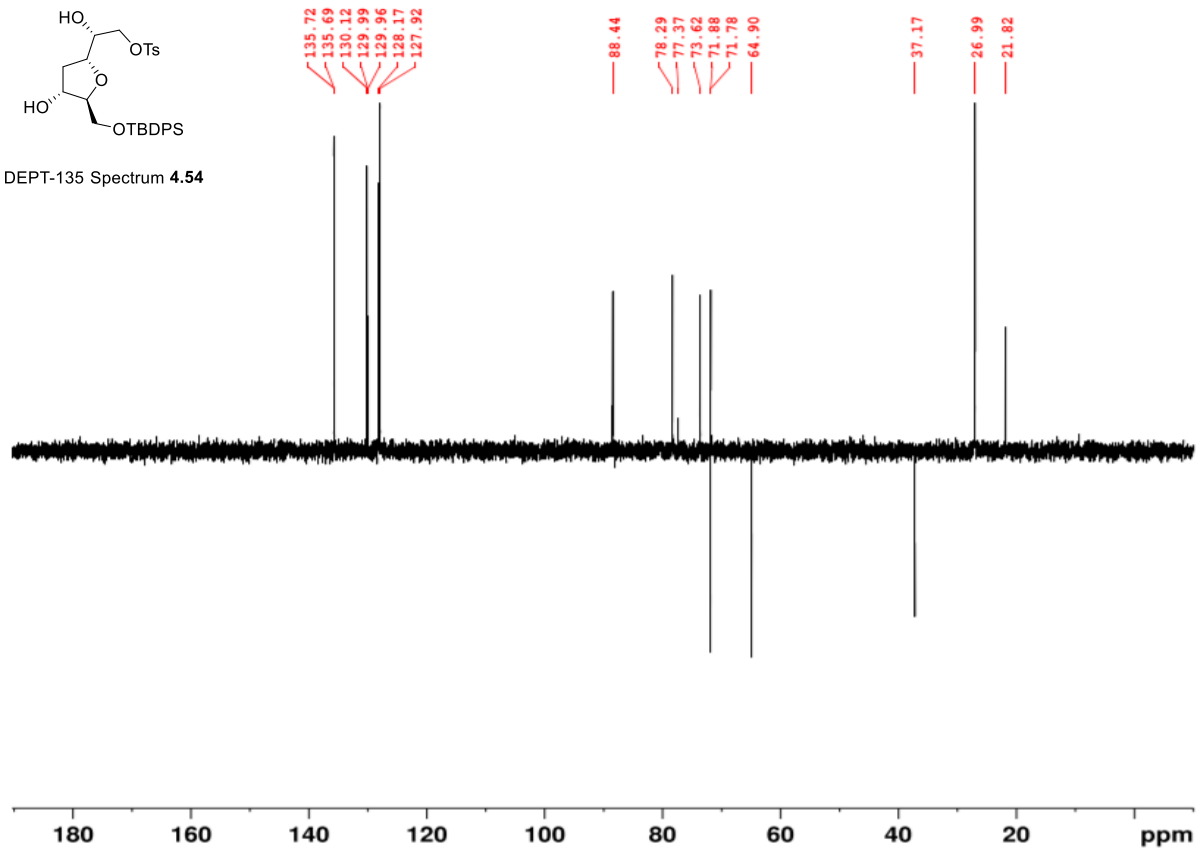

Figure A.18 DEPT-135 (100MHz, $CDCl_3$) of **4.54**.

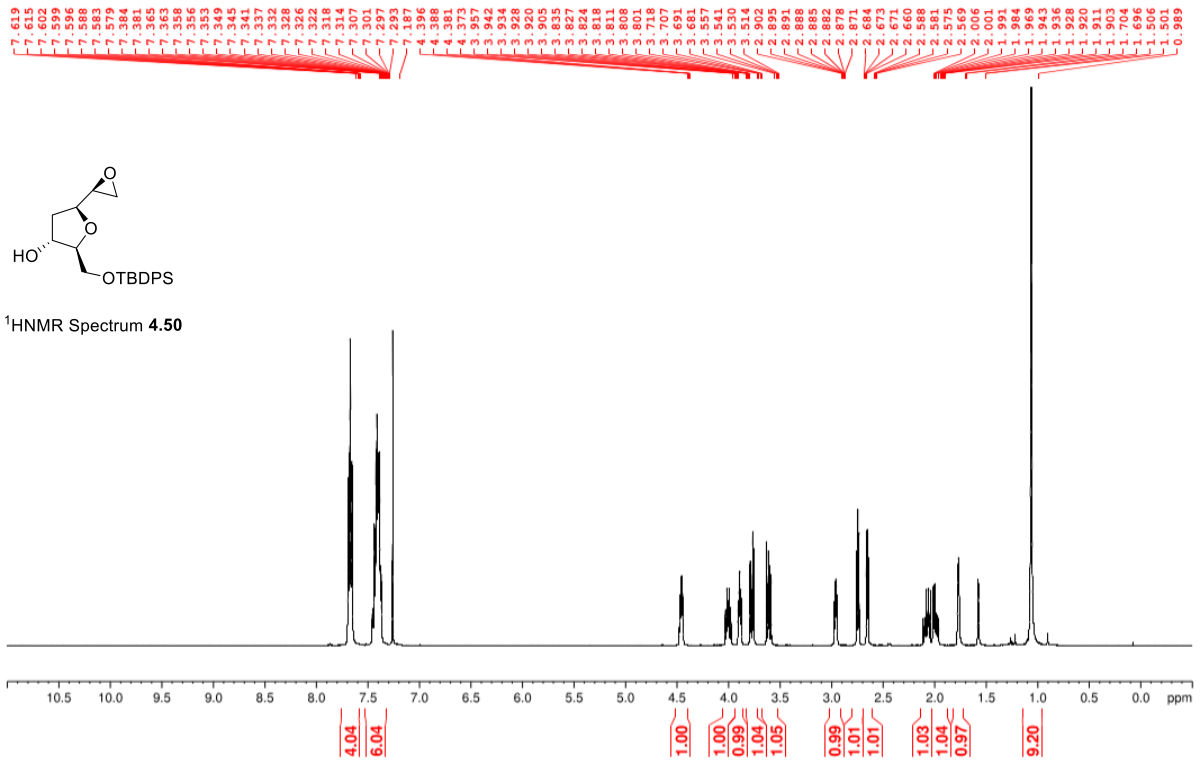

Figure A.19 ^{1}H NMR (400 MHz, $CDCl_3$) of **4.50**.

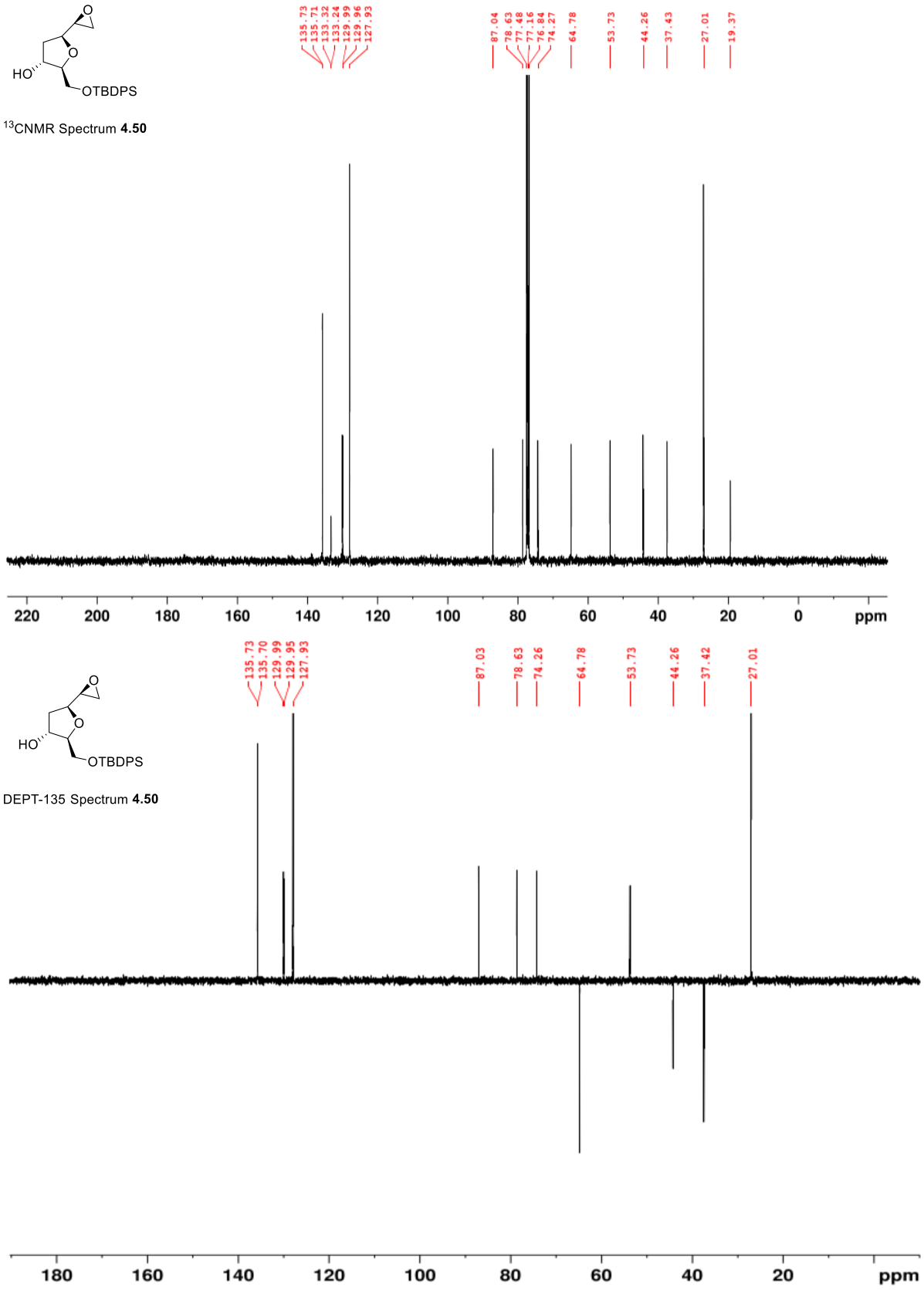

Figure A.20 ^{13}C NMR (100 MHz, $CDCl_3$) and DEPT-135 (100MHz, $CDCl_3$) of **4.50**.

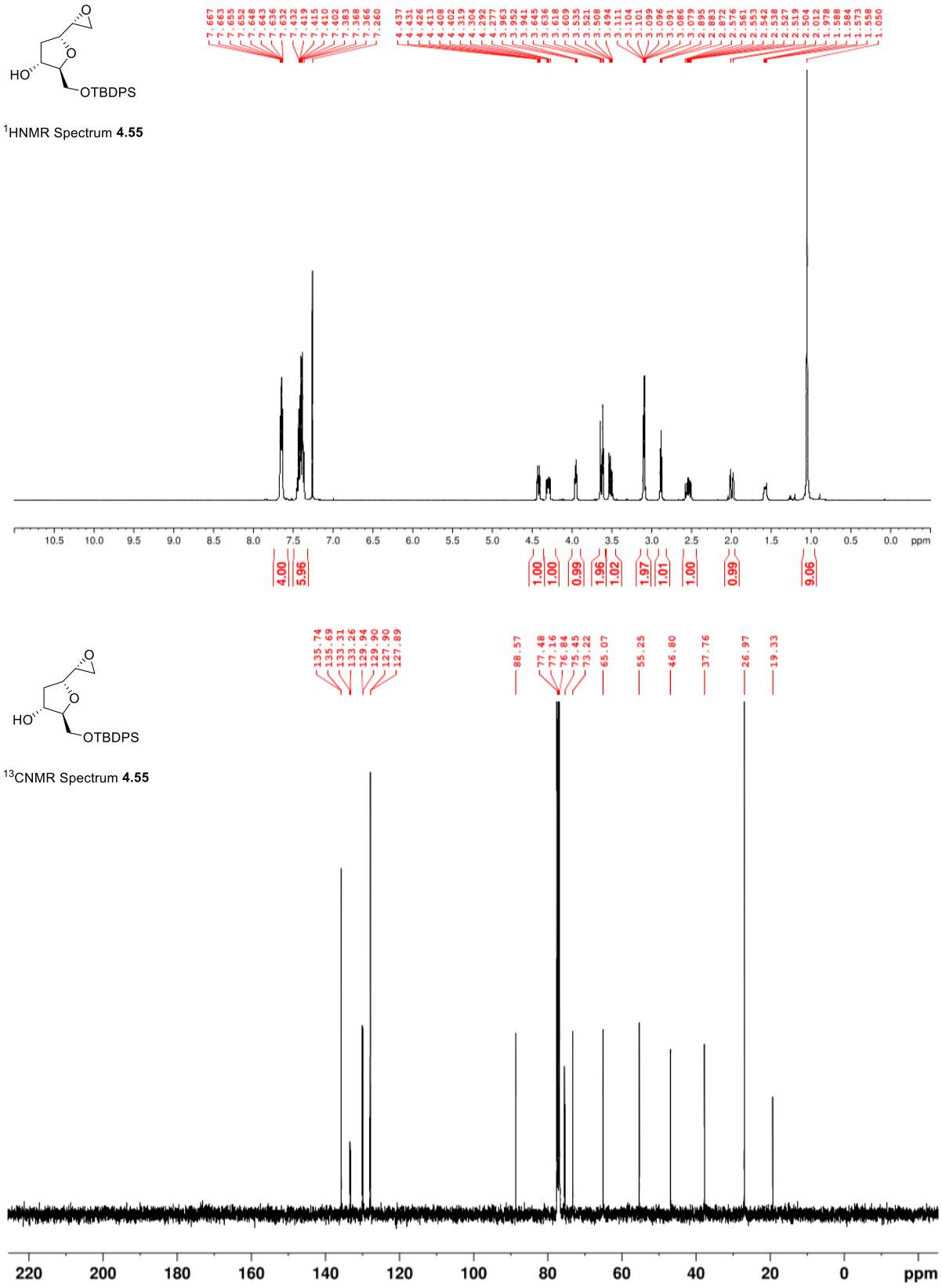

Figure A.21 ^{1}H NMR (400 MHz, $CDCl_3$) and ^{13}C NMR (100 MHz, $CDCl_3$) of **4.55**.

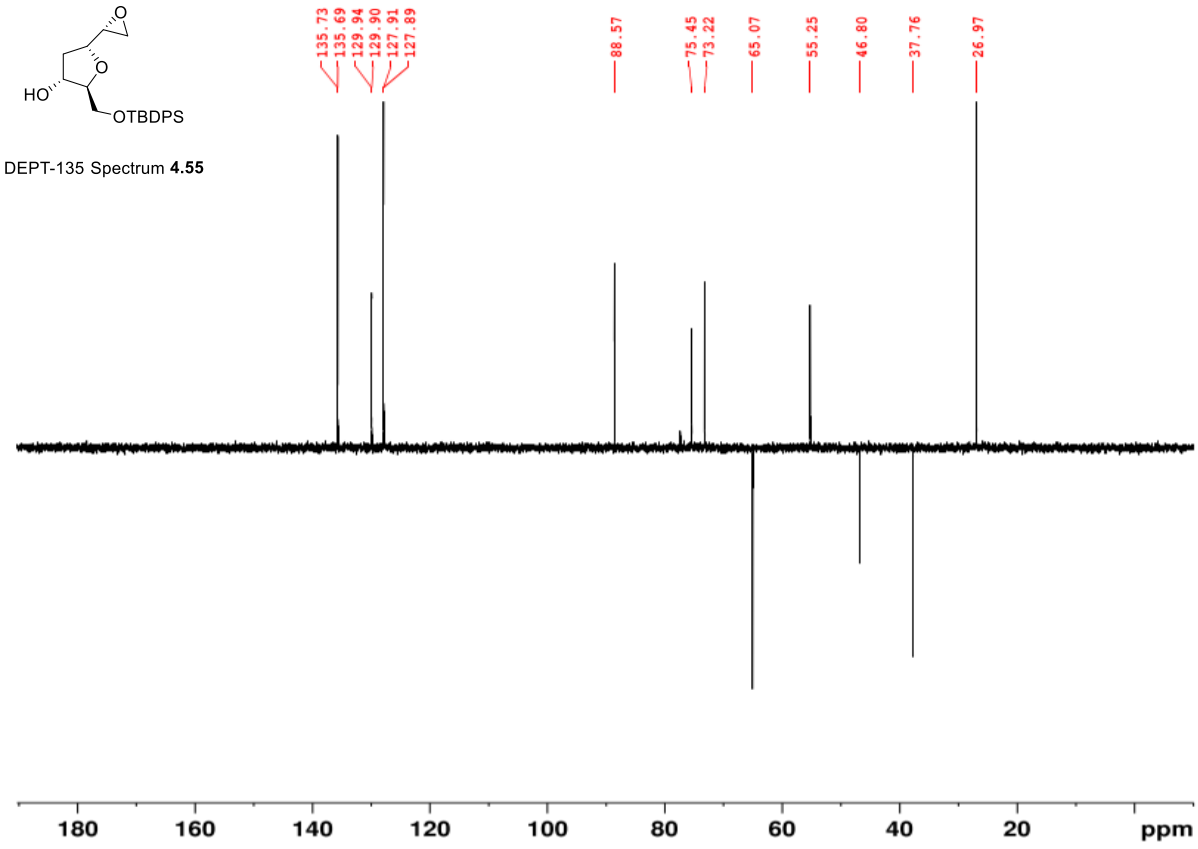

Figure A.22 DEPT-135 (100MHz, $CDCl_3$) of **4.55**.

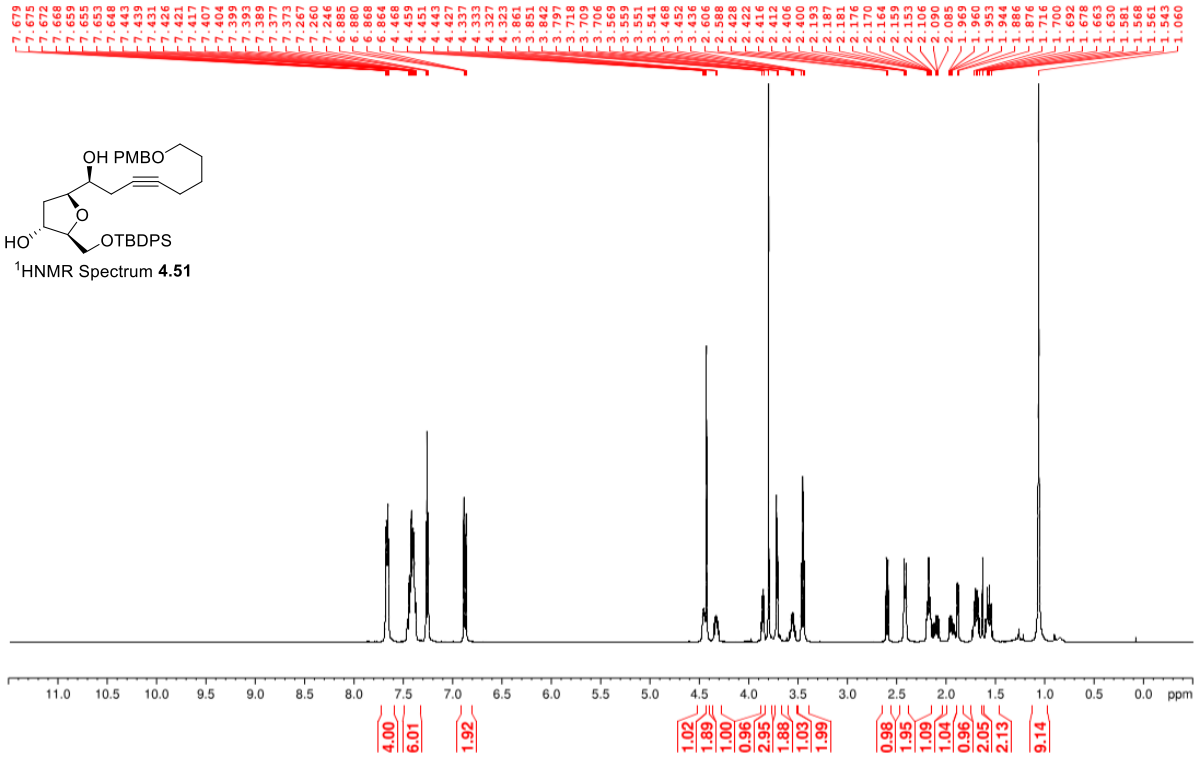

Figure A.23 ^{1}H NMR (400 MHz, $CDCl_3$) **4.51**.

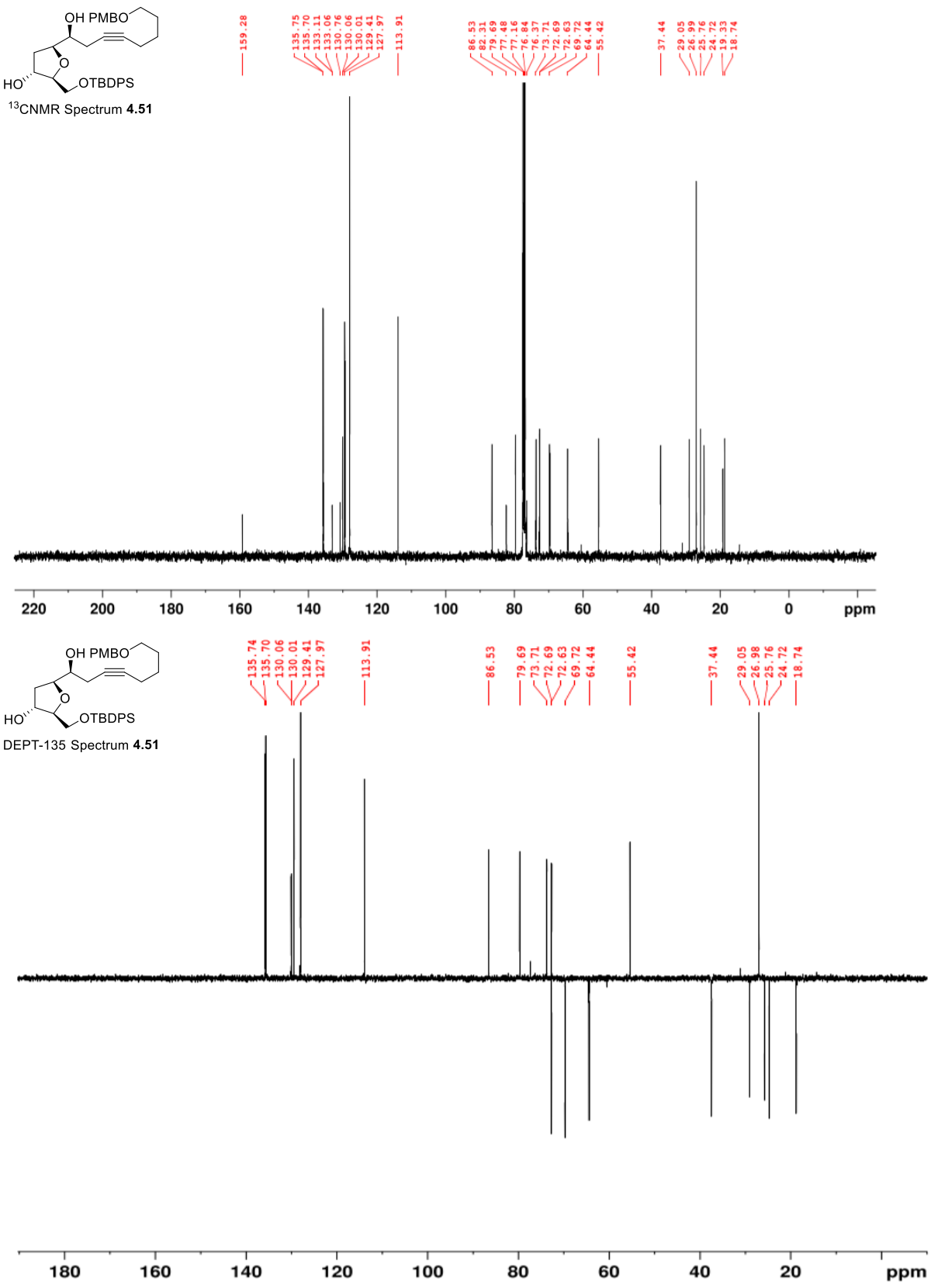

Figure A.24 ^{13}C NMR (100 MHz, $CDCl_3$) and DEPT-135 (100MHz, $CDCl_3$) of **4.51**.

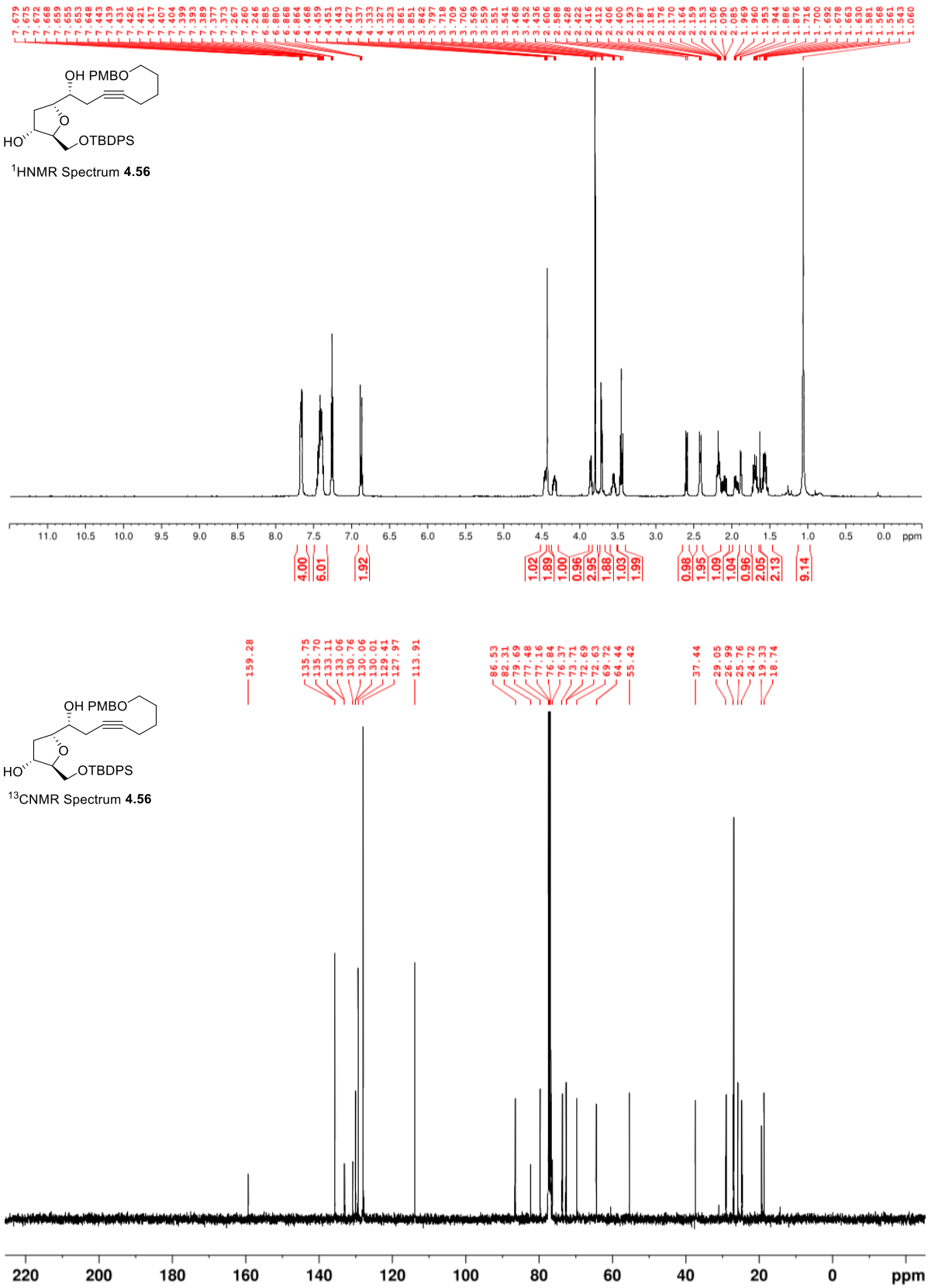

Figure A.25 ^{1}H NMR (400 MHz, $CDCl_3$) and ^{13}C NMR (100 MHz, $CDCl_3$) of **4.56**.

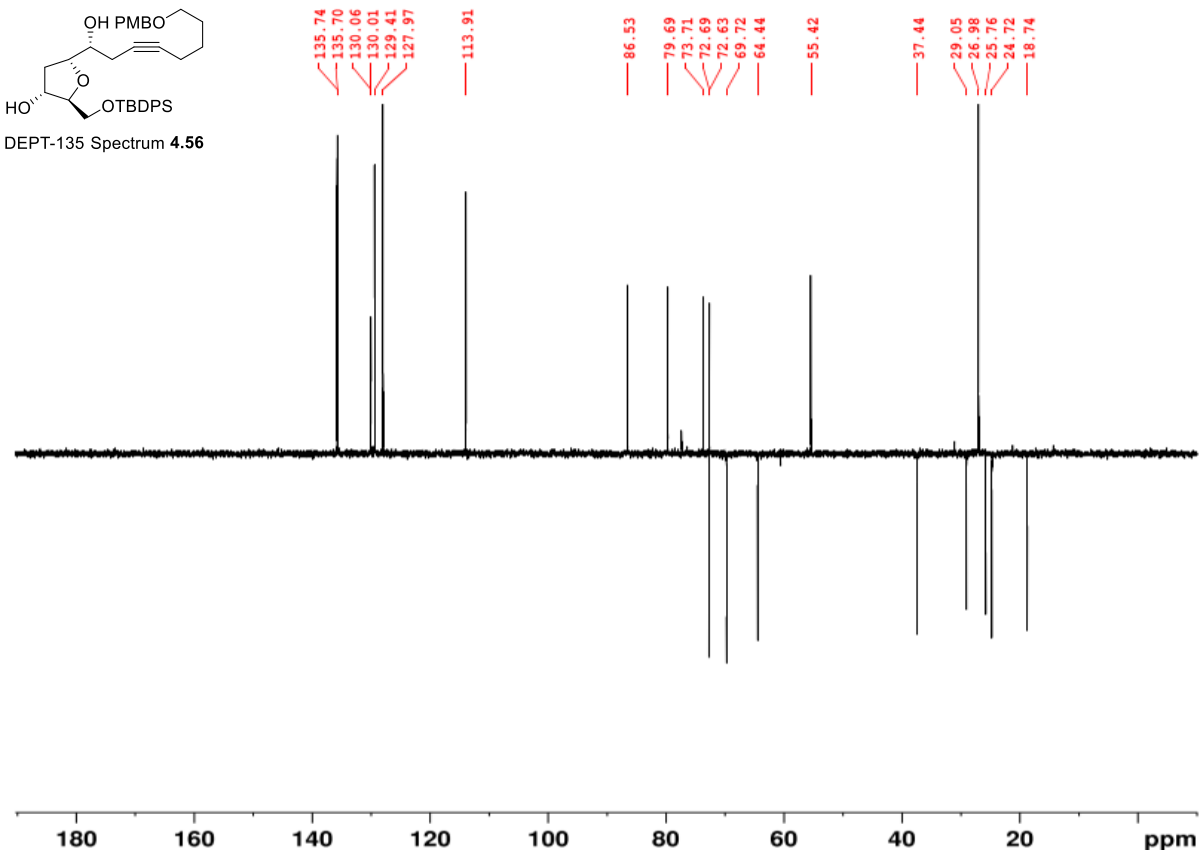

Figure A.26 DEPT-135 (100MHz, $CDCl_3$) of **4.56**.

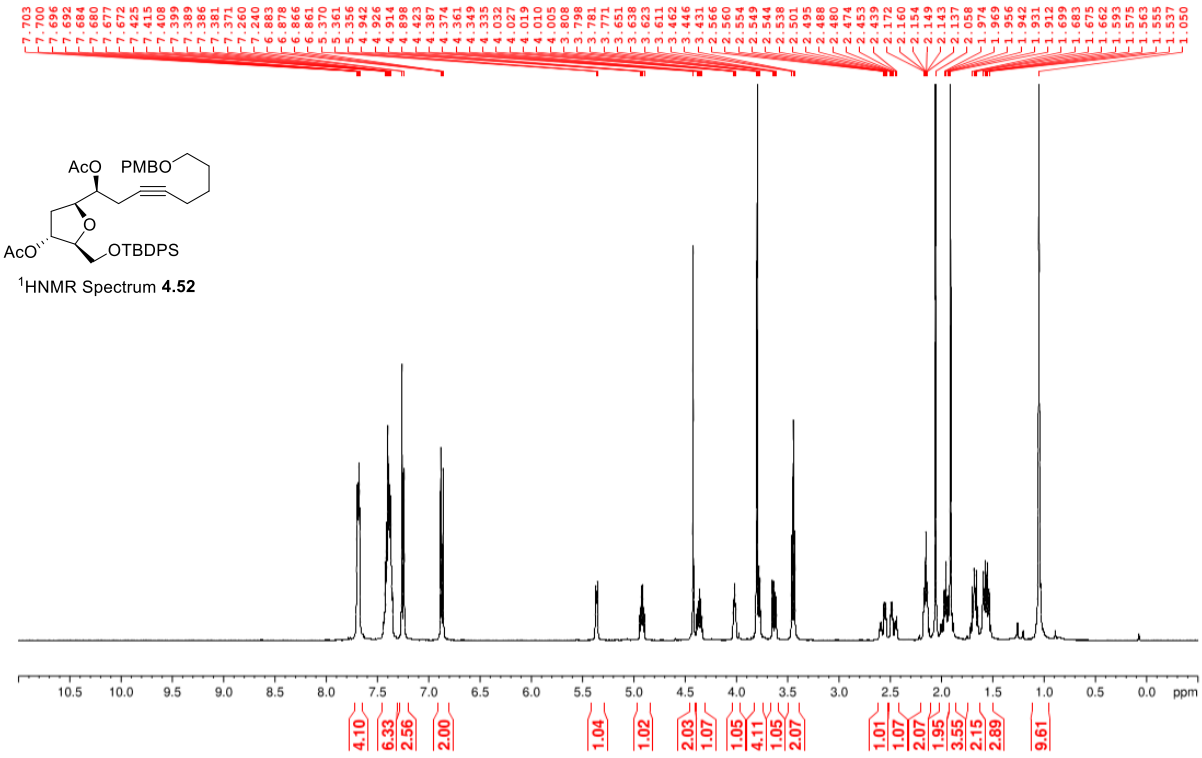

Figure A.27 ^{1}H NMR (400 MHz, $CDCl_3$) of **4.52**.

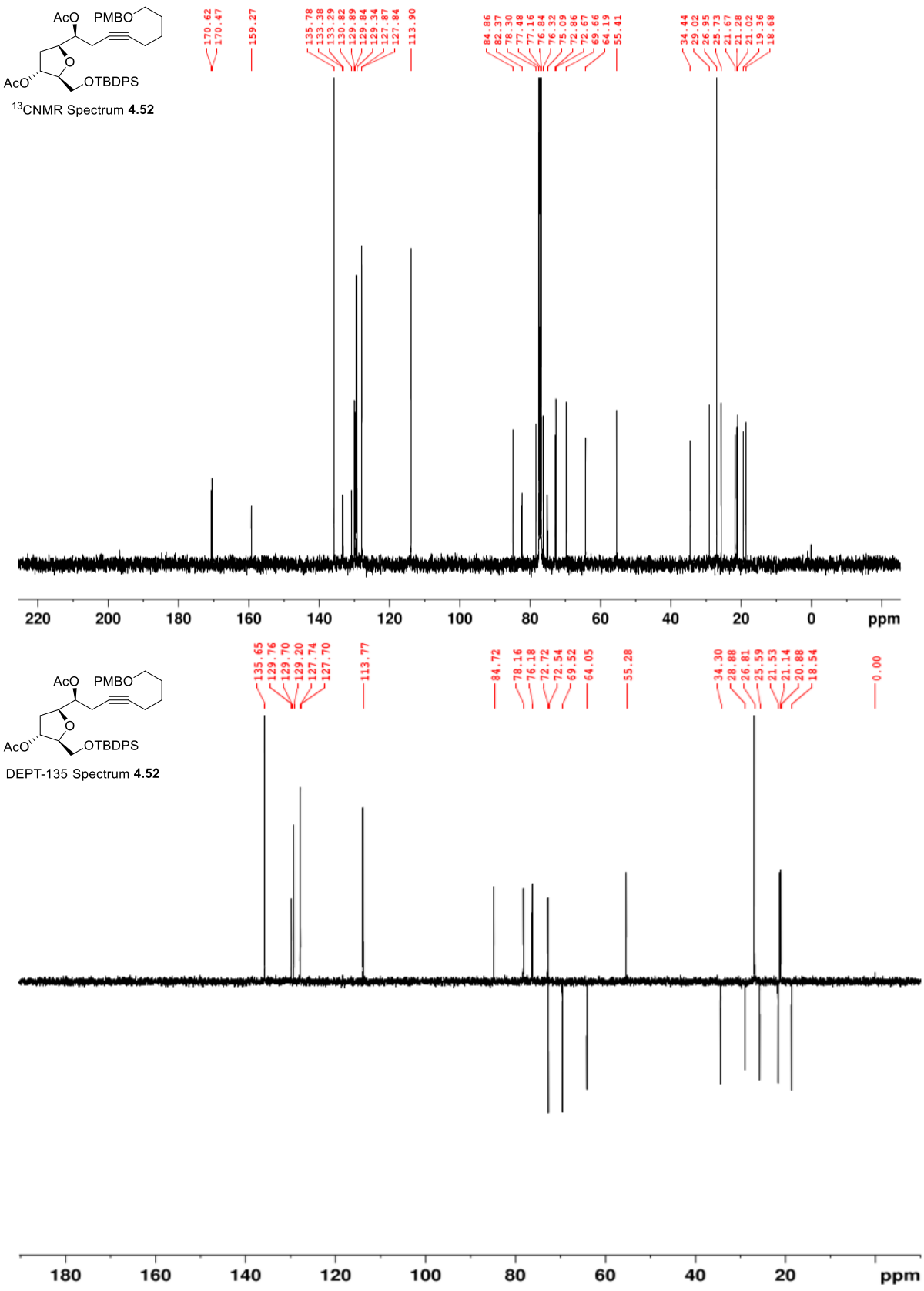

Figure A.28 ^{13}C NMR (100 MHz, $CDCl_3$) and DEPT-135 (100MHz, $CDCl_3$) of **4.52**.

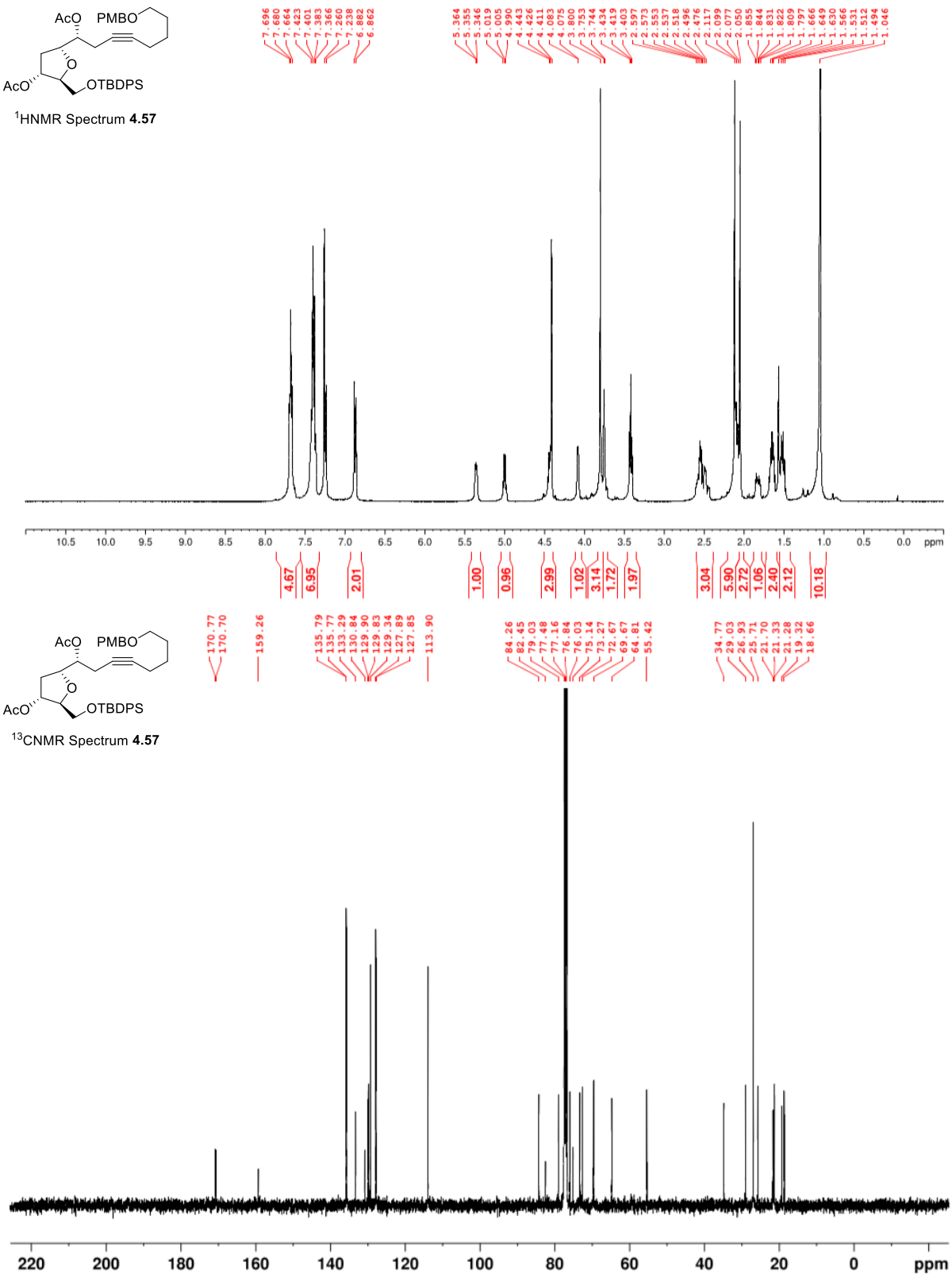

Figure A.29 ^{1}H NMR (400 MHz, $CDCl_3$) and ^{13}C NMR (100 MHz, $CDCl_3$) of **4.57**.

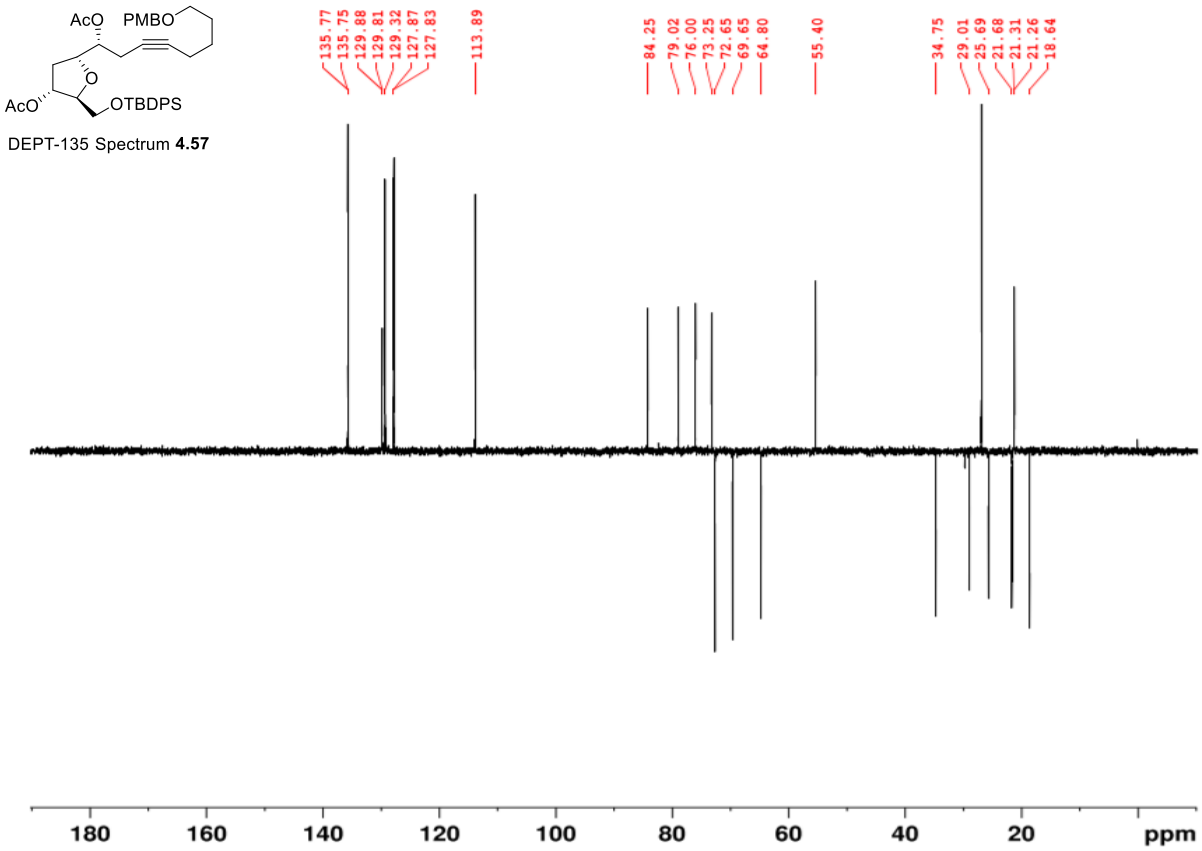

Figure A.30 DEPT-135 (100MHz, $CDCl_3$) of **4.57**.

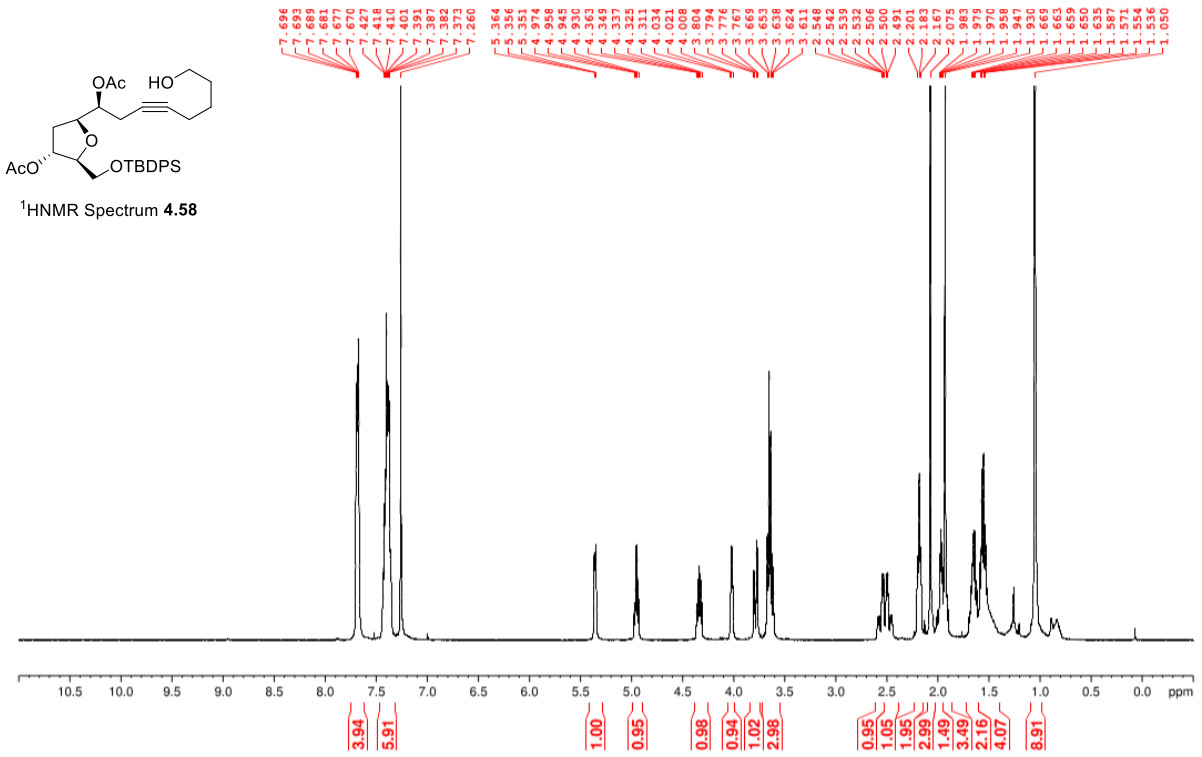

Figure A.31 ^{1}H NMR (400 MHz, $CDCl_3$) of **4.58**.

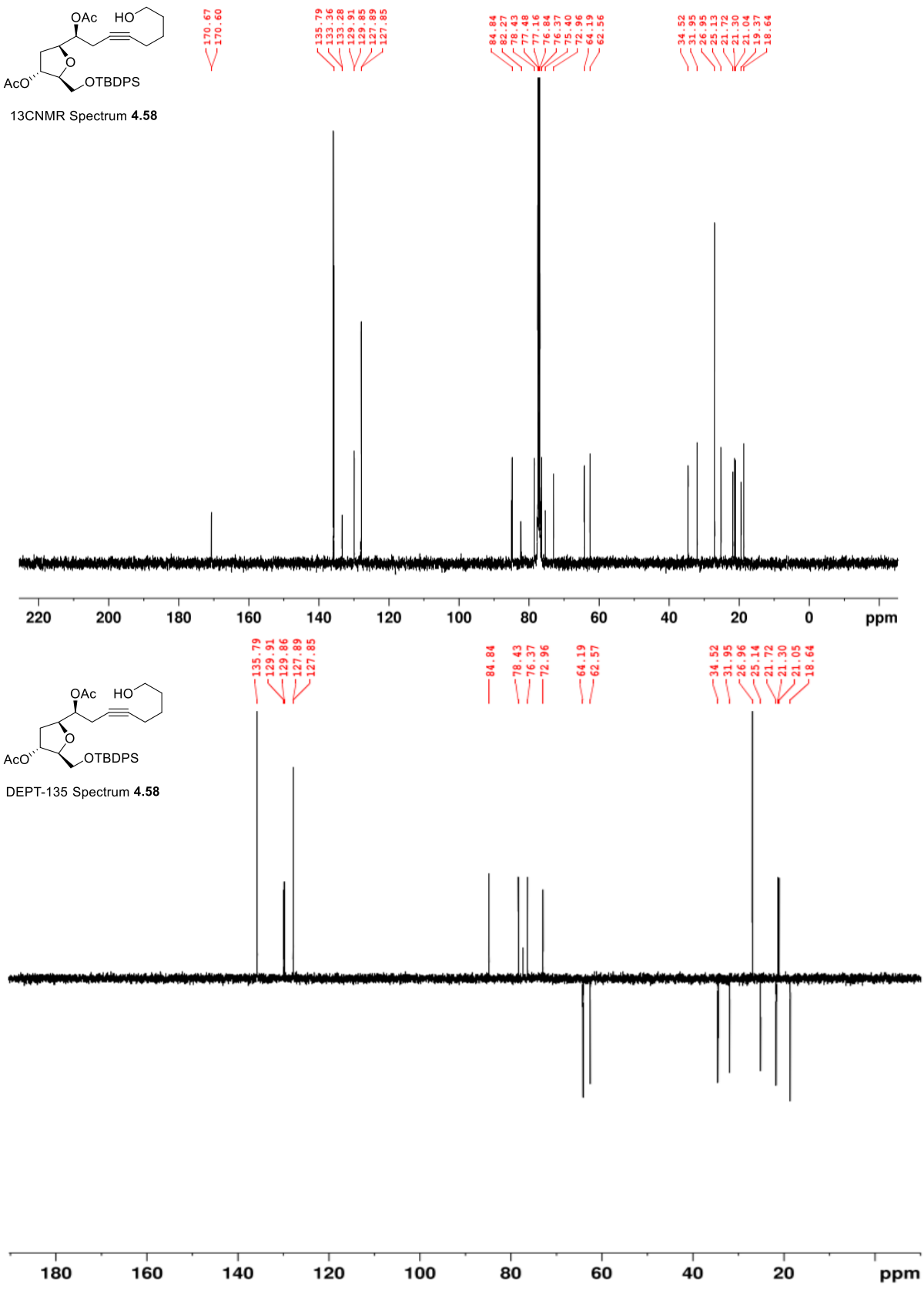

Figure A.32 ^{13}C NMR (100 MHz, $CDCl_3$) and DEPT-135 (100MHz, $CDCl_3$) of **4.58**.

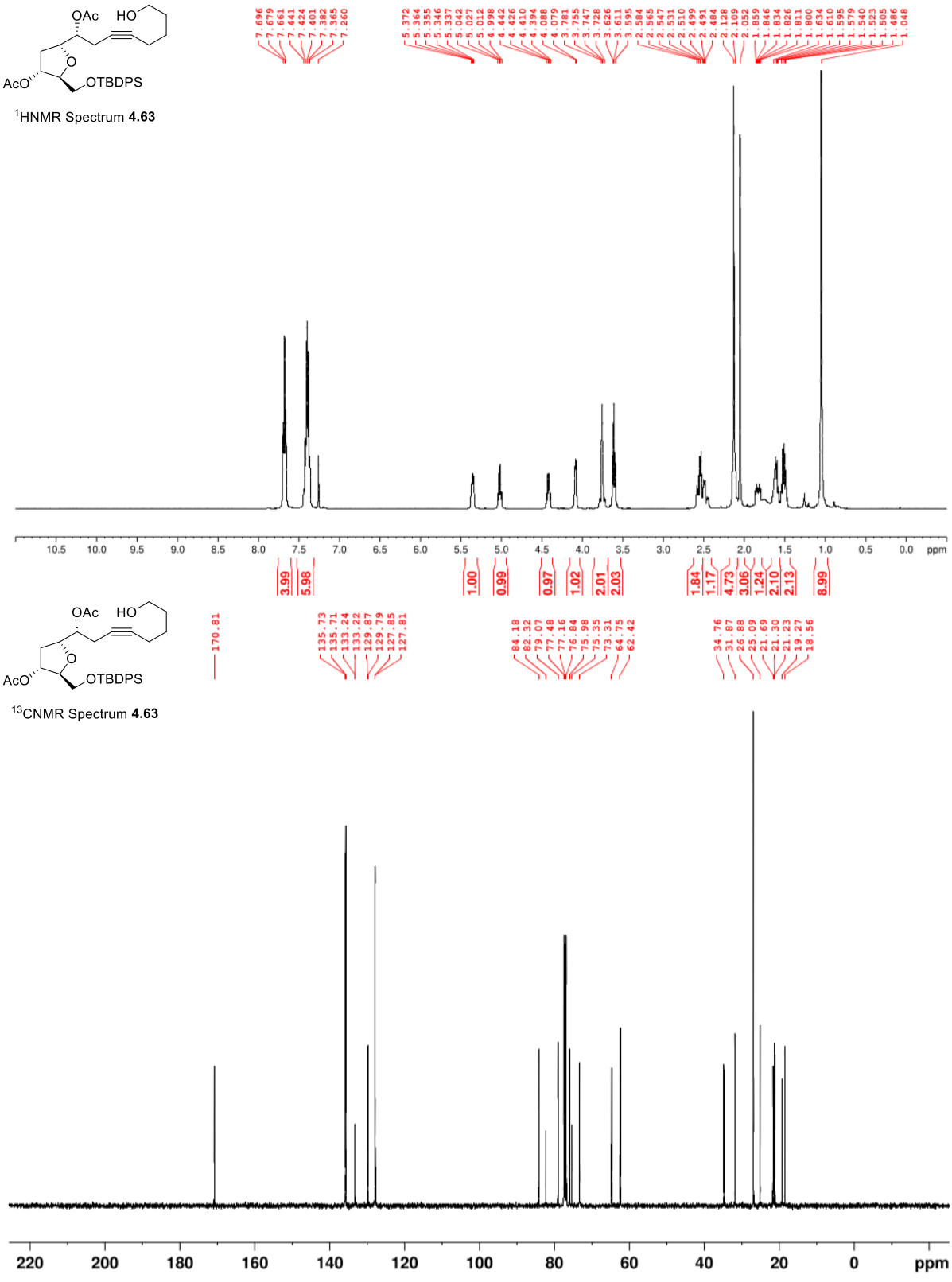

Figure A.33 ^{1}H NMR (400 MHz, $CDCl_3$) and ^{13}C NMR (100 MHz, $CDCl_3$) of **4.63**.

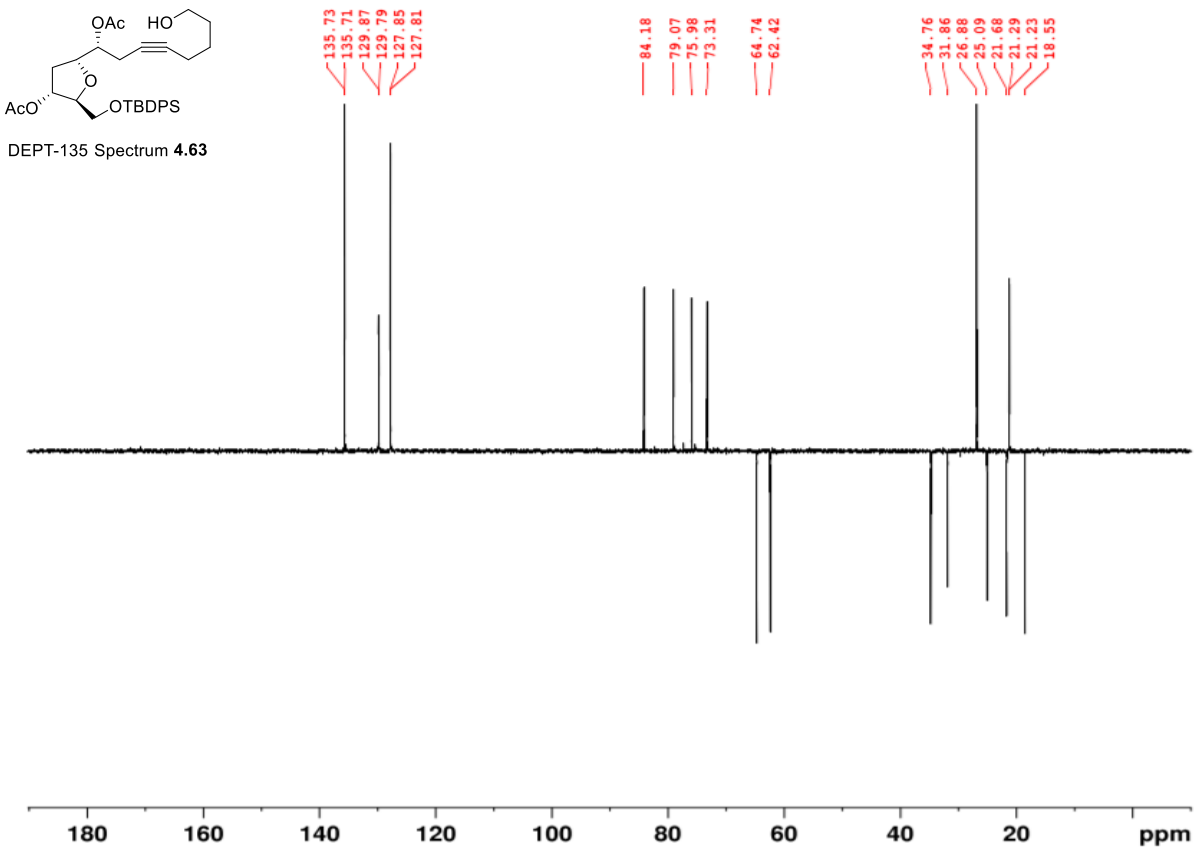

Figure A.34 DEPT-135 (100MHz, $CDCl_3$) of **4.63**.

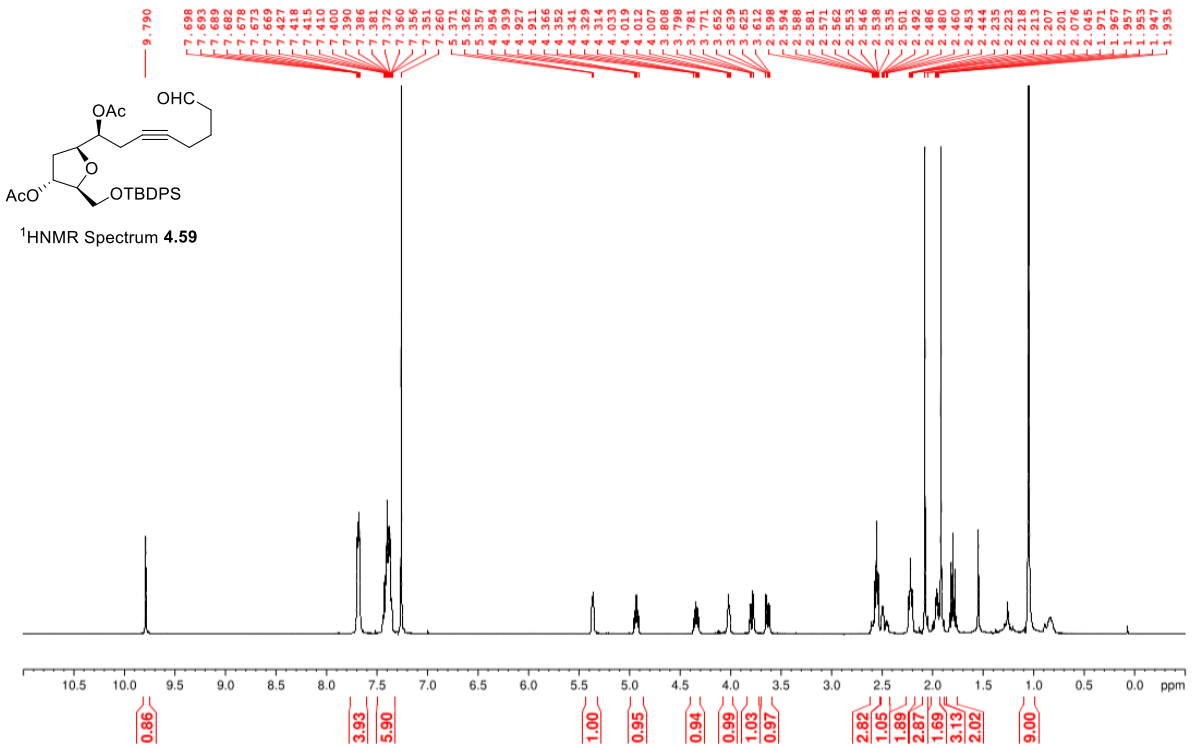

Figure A.35 ^{1}H NMR (400 MHz, $CDCl_3$) of **4.59**.

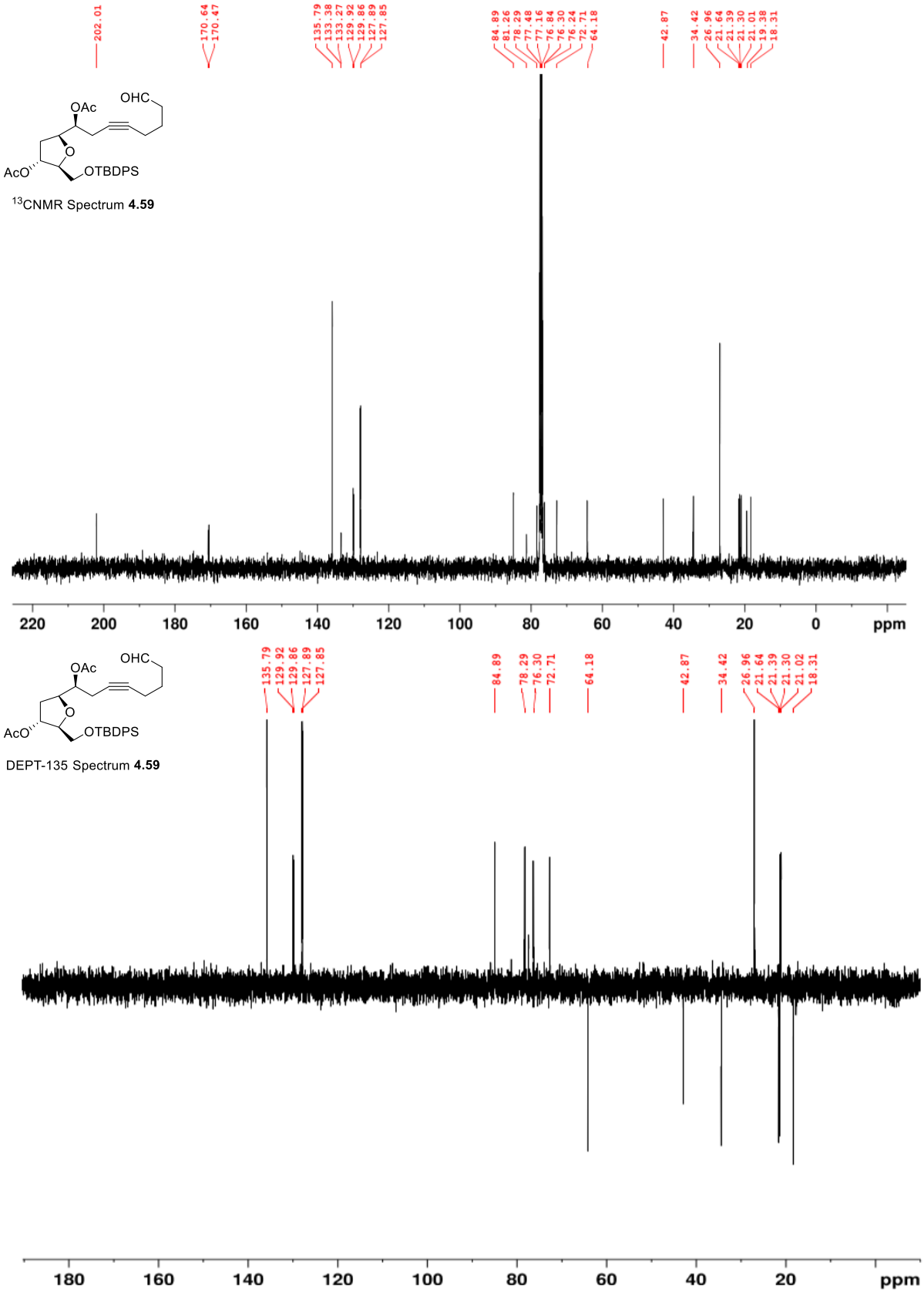

Figure A.36 ^{13}C NMR (100 MHz, $CDCl_3$) and DEPT-135 (100MHz, $CDCl_3$) of **4.59**.

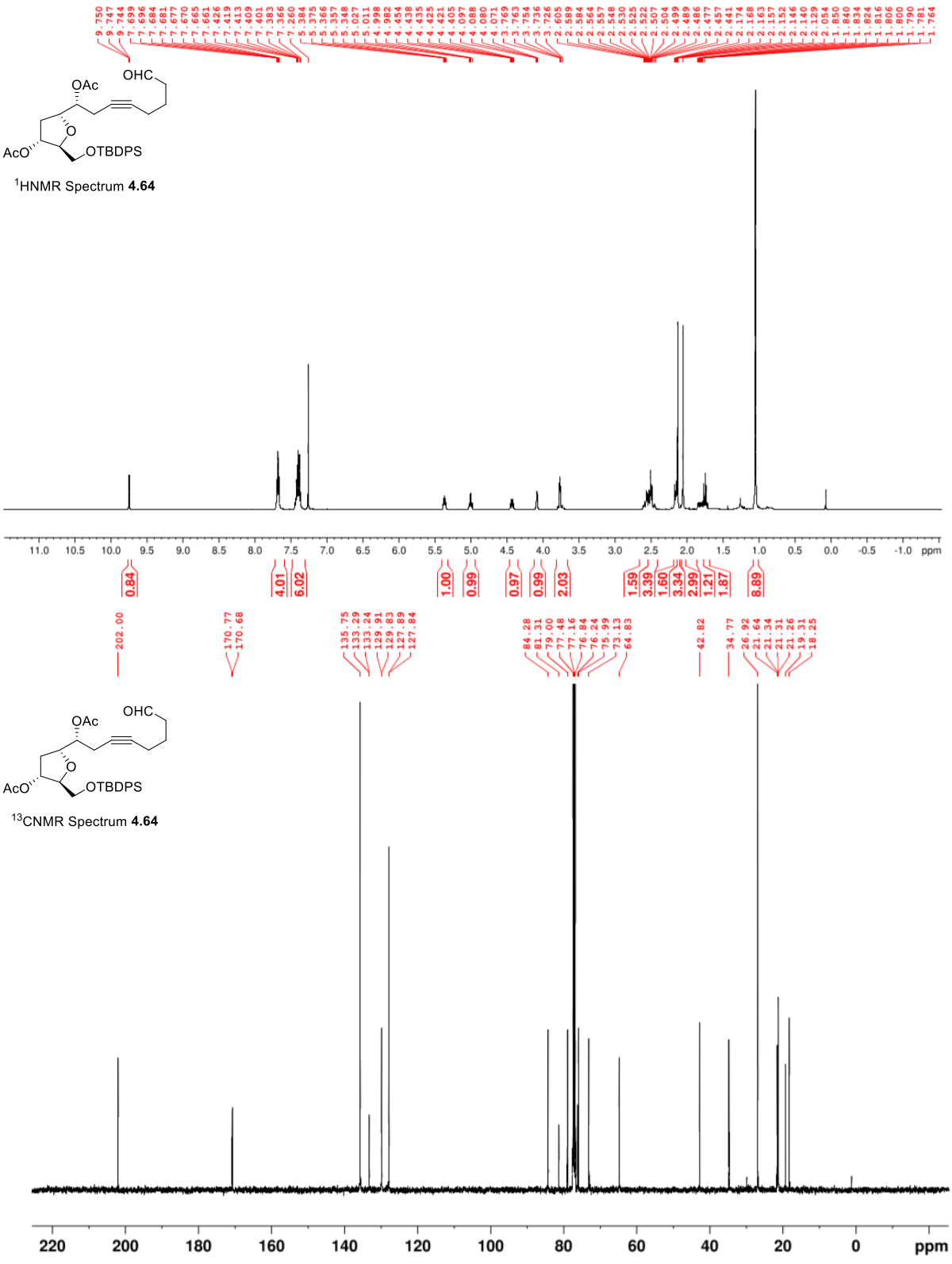

Figure A.37 ^{1}H NMR (400 MHz, $CDCl_3$) and ^{13}C NMR (100 MHz, $CDCl_3$) of **4.64**.

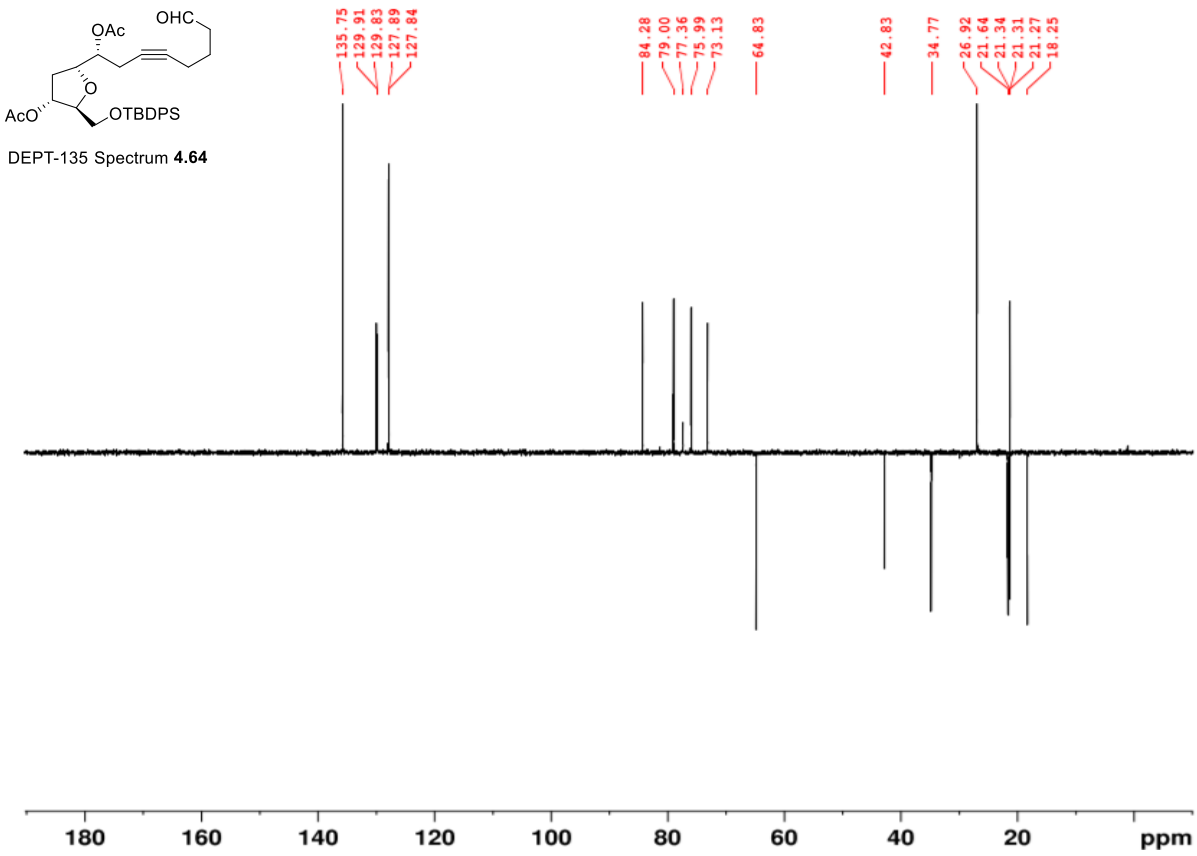

Figure A.38 DEPT-135 (100MHz, $CDCl_3$) of **4.64**.

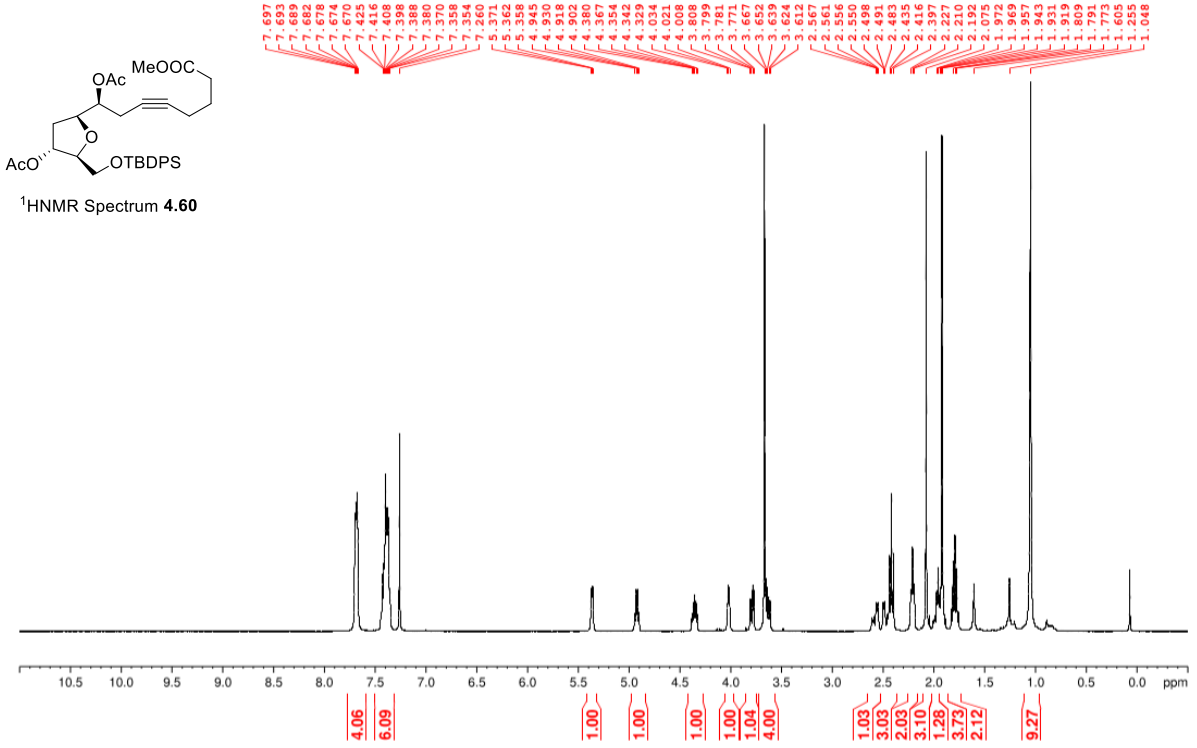

Figure A.39 ^{1}H NMR (400 MHz, $CDCl_3$) of **4.60**.

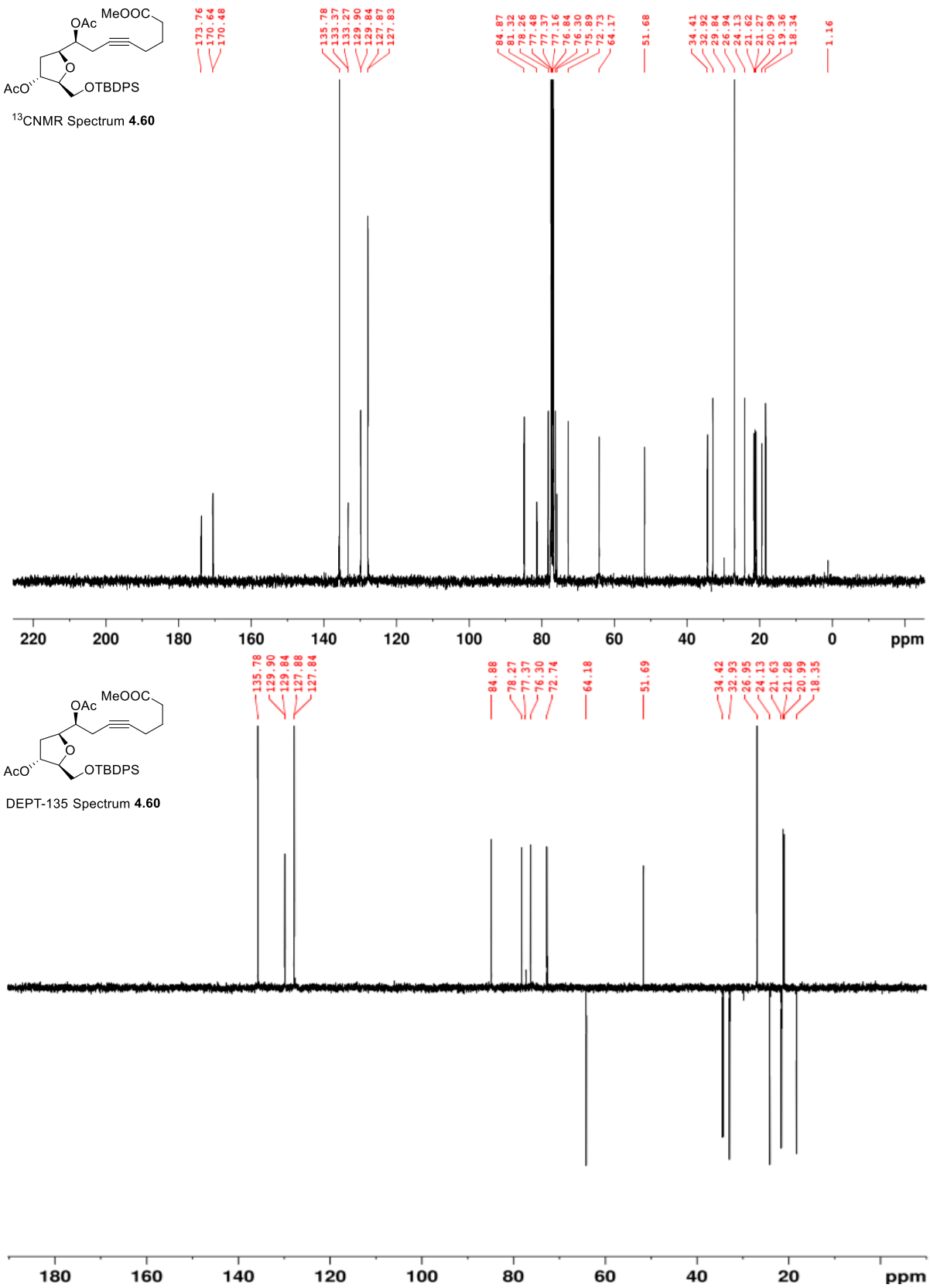

Figure A.40 ^{13}C NMR (100 MHz, $CDCl_3$) and DEPT-135 (100MHz, $CDCl_3$) of **4.60**.

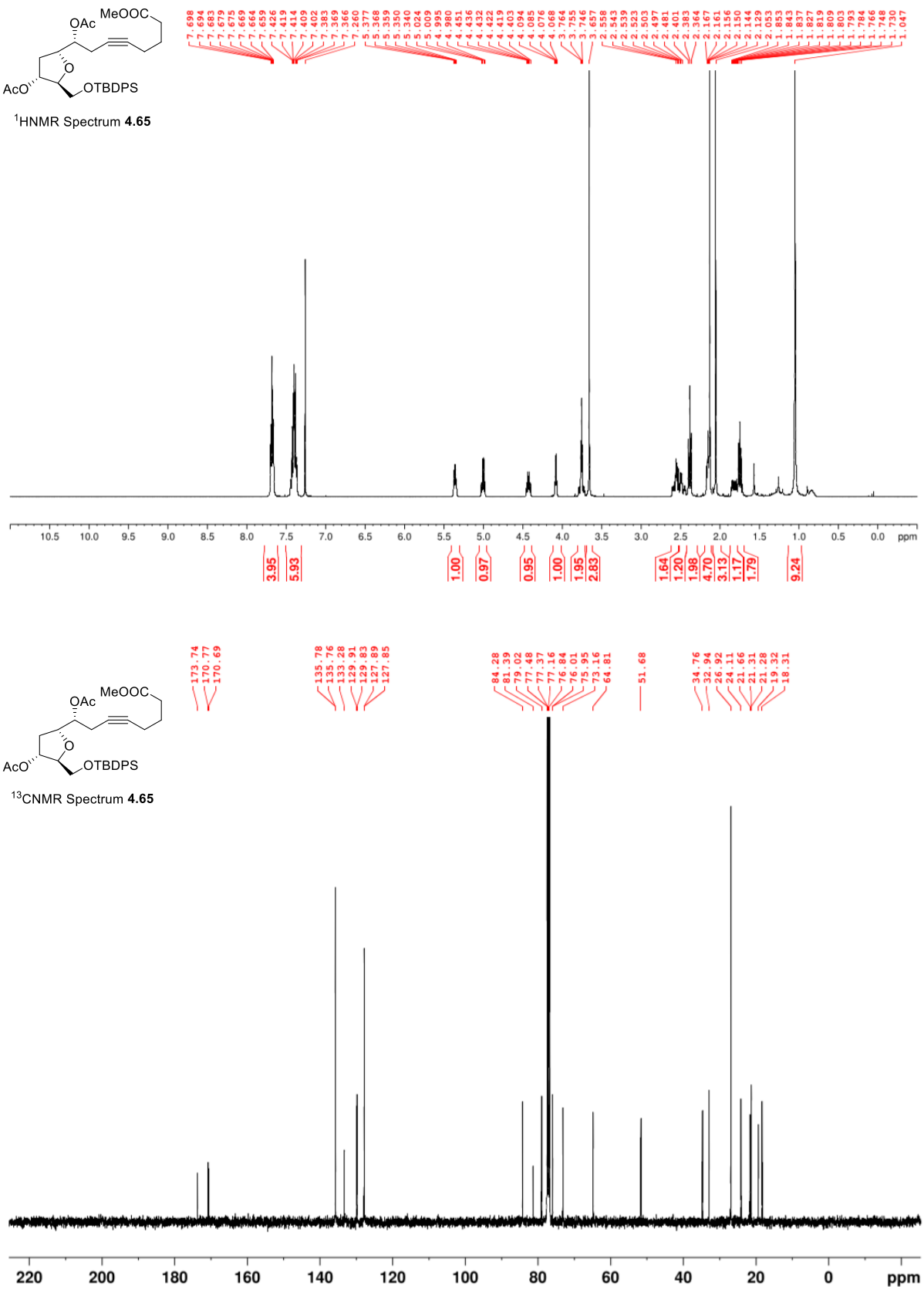

Figure A.41 ^{1}H NMR (400 MHz, $CDCl_3$) and ^{13}C NMR (100 MHz, $CDCl_3$) of **4.65**.

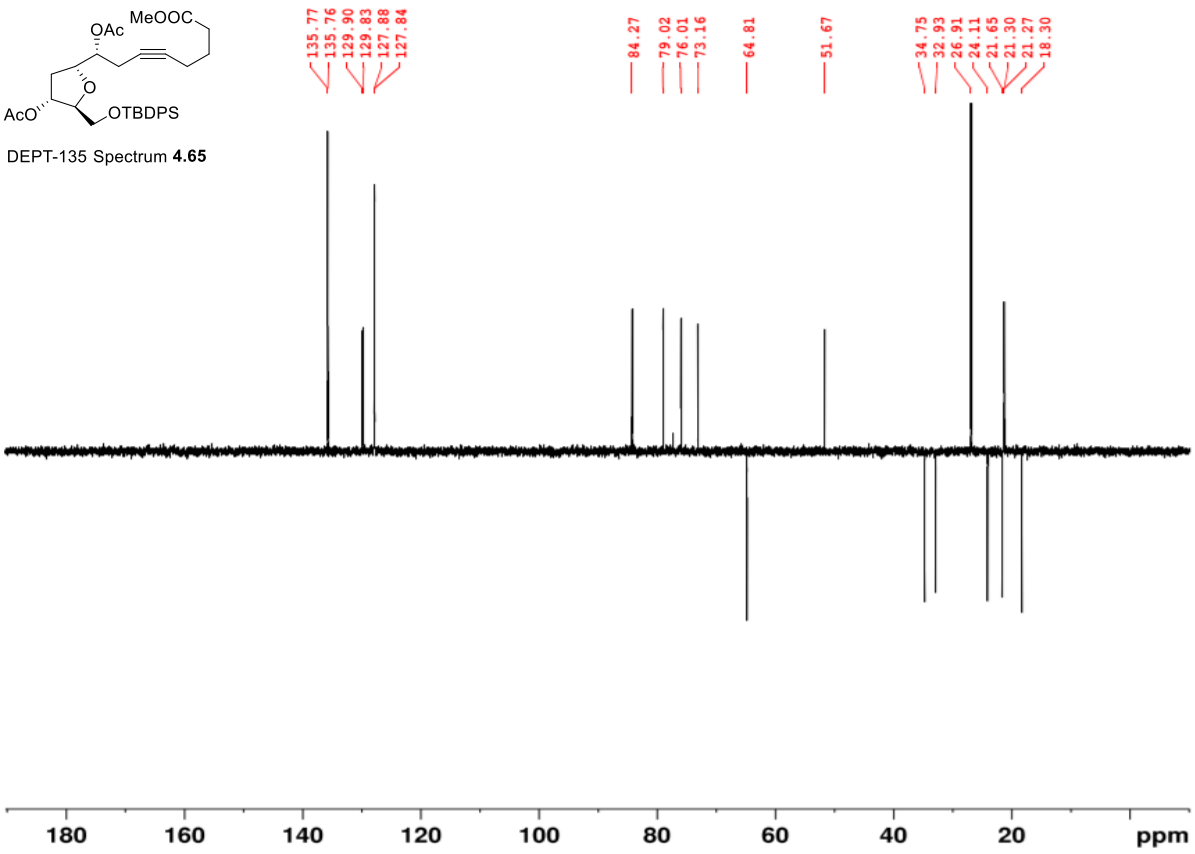

Figure A.42 DEPT-135 (100MHz, $CDCl_3$) of **4.65**.

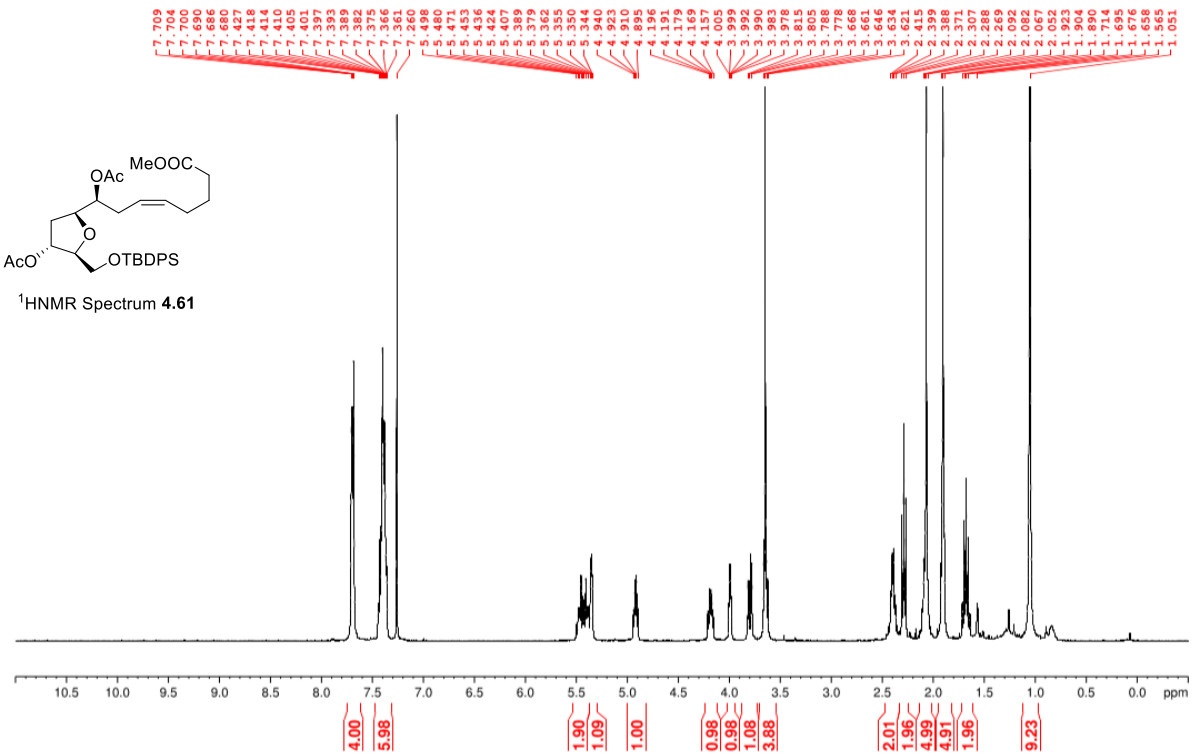

Figure A.43 ^{1}H NMR (400 MHz, $CDCl_3$) of **4.61**.

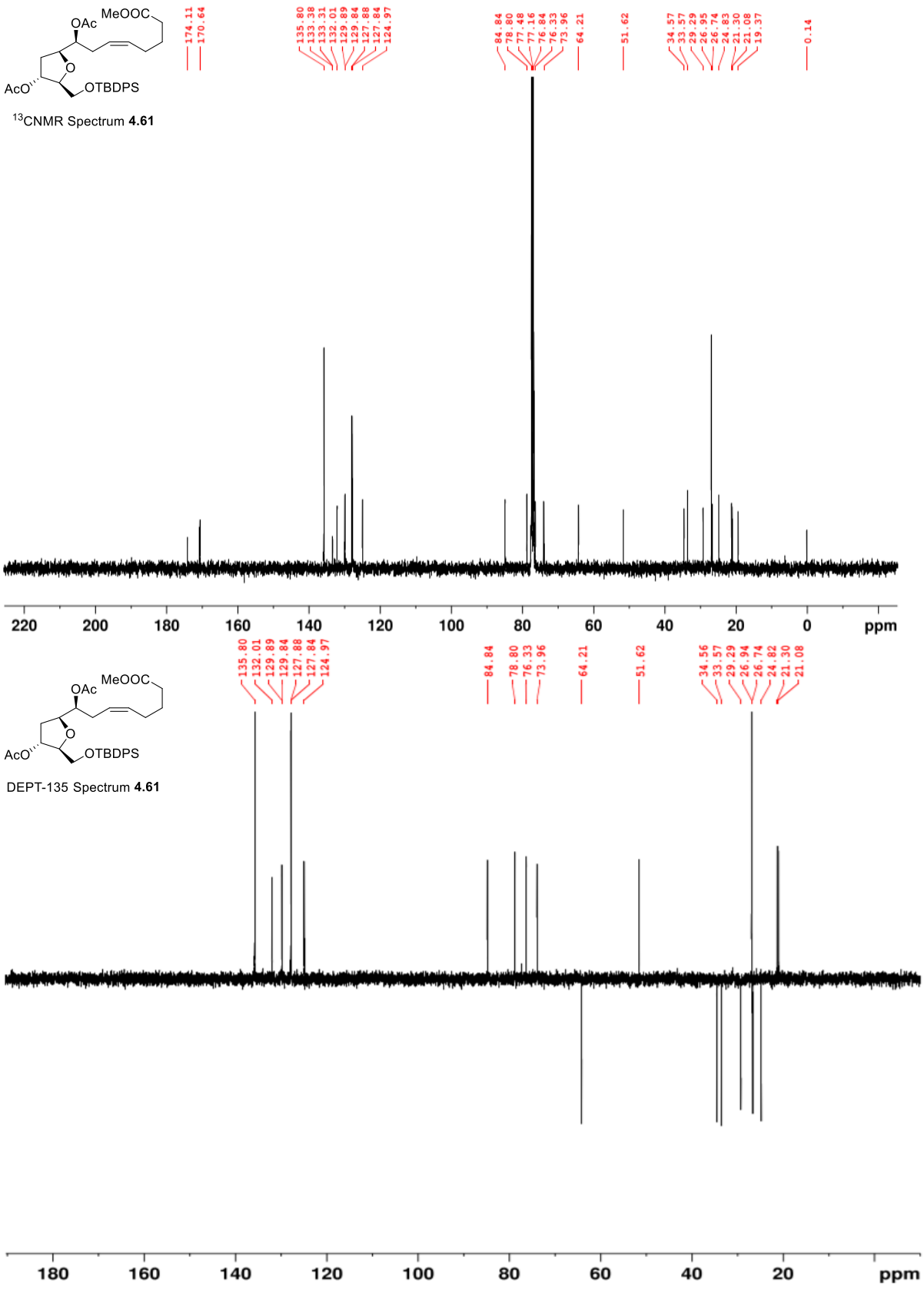

Figure A.44 ^{13}C NMR (100 MHz, $CDCl_3$) and DEPT-135 (100MHz, $CDCl_3$) of **4.61**.

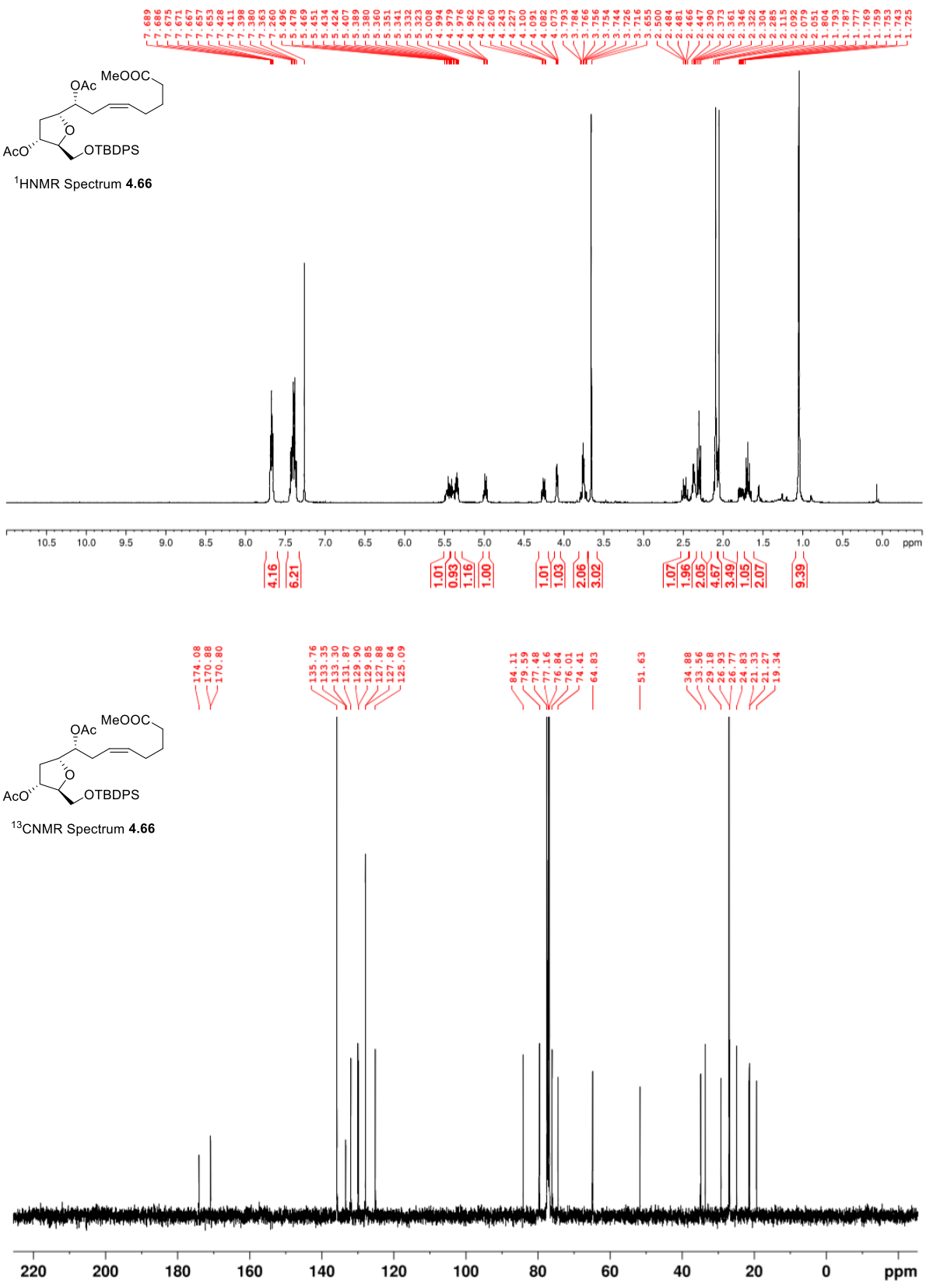

Figure A.45 ^{1}H NMR (400 MHz, $CDCl_3$) and ^{13}C NMR (100 MHz, $CDCl_3$) of **4.66**.

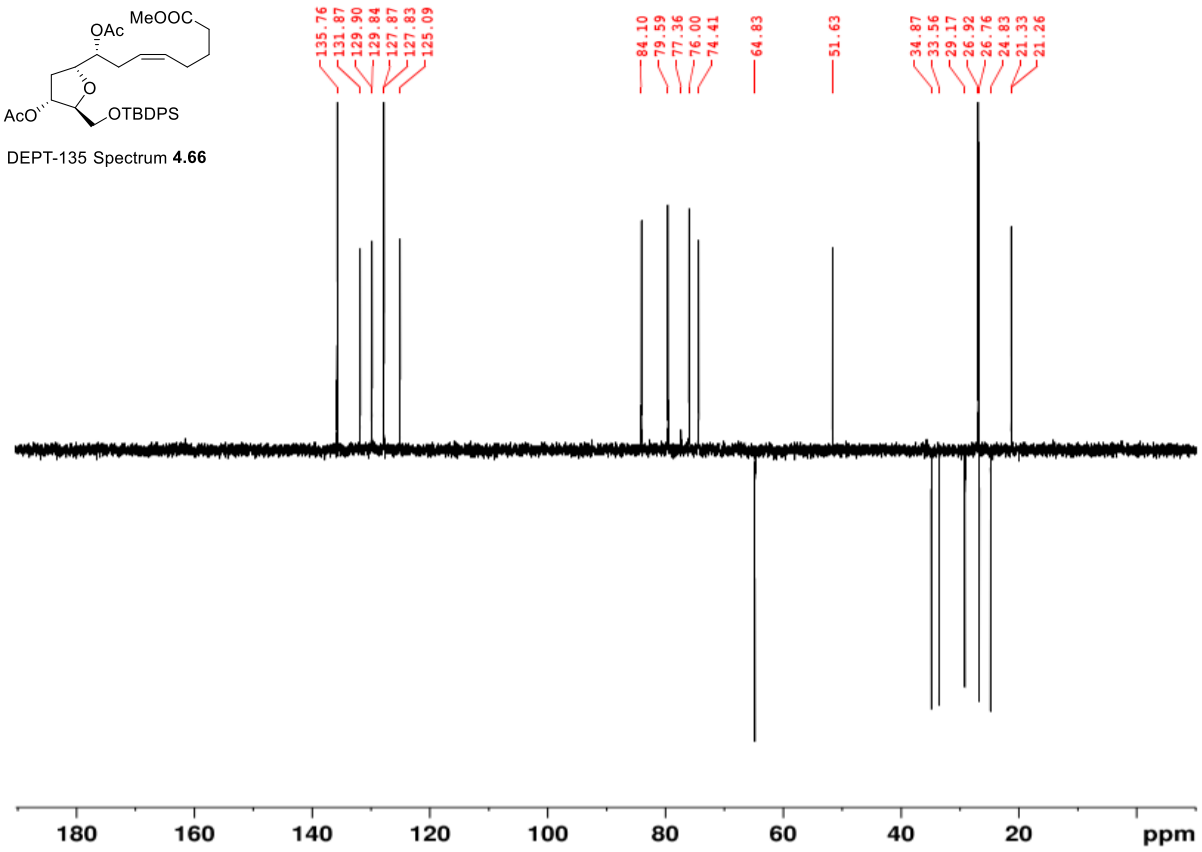

Figure A.46 DEPT-135 (100MHz, $CDCl_3$) of **4.66**.

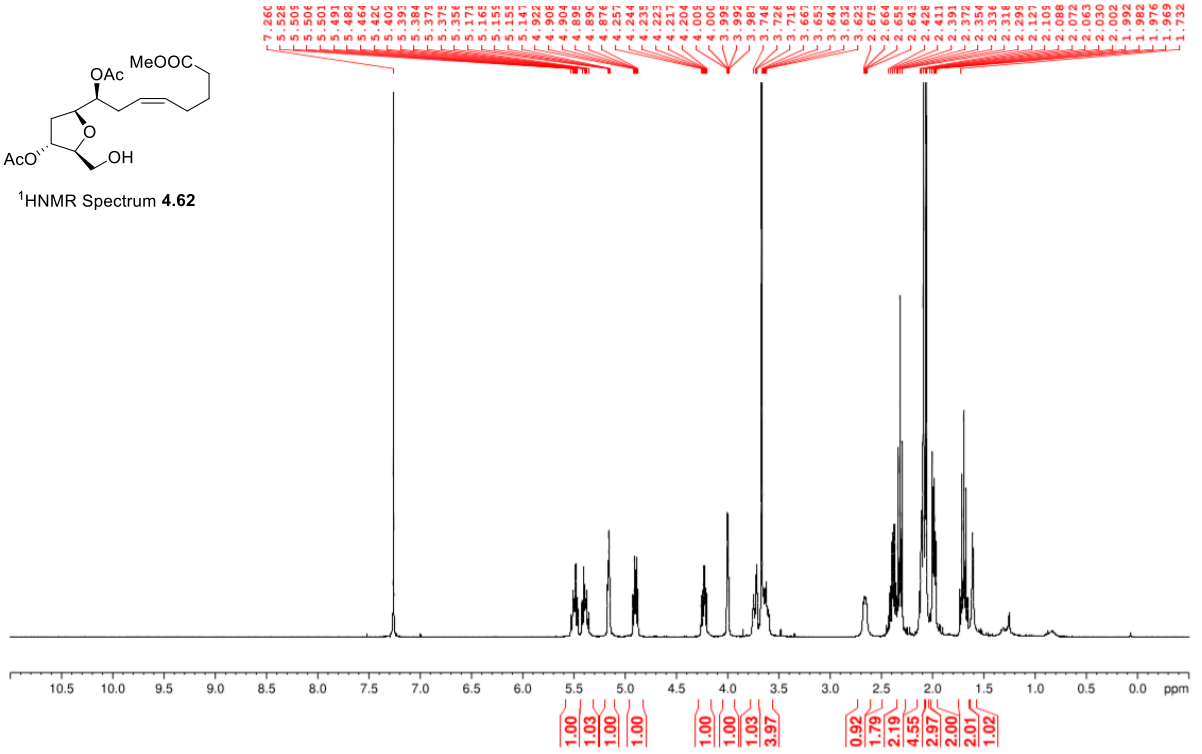

Figure A.47 ^{1}H NMR (400 MHz, $CDCl_3$) of **4.62**.

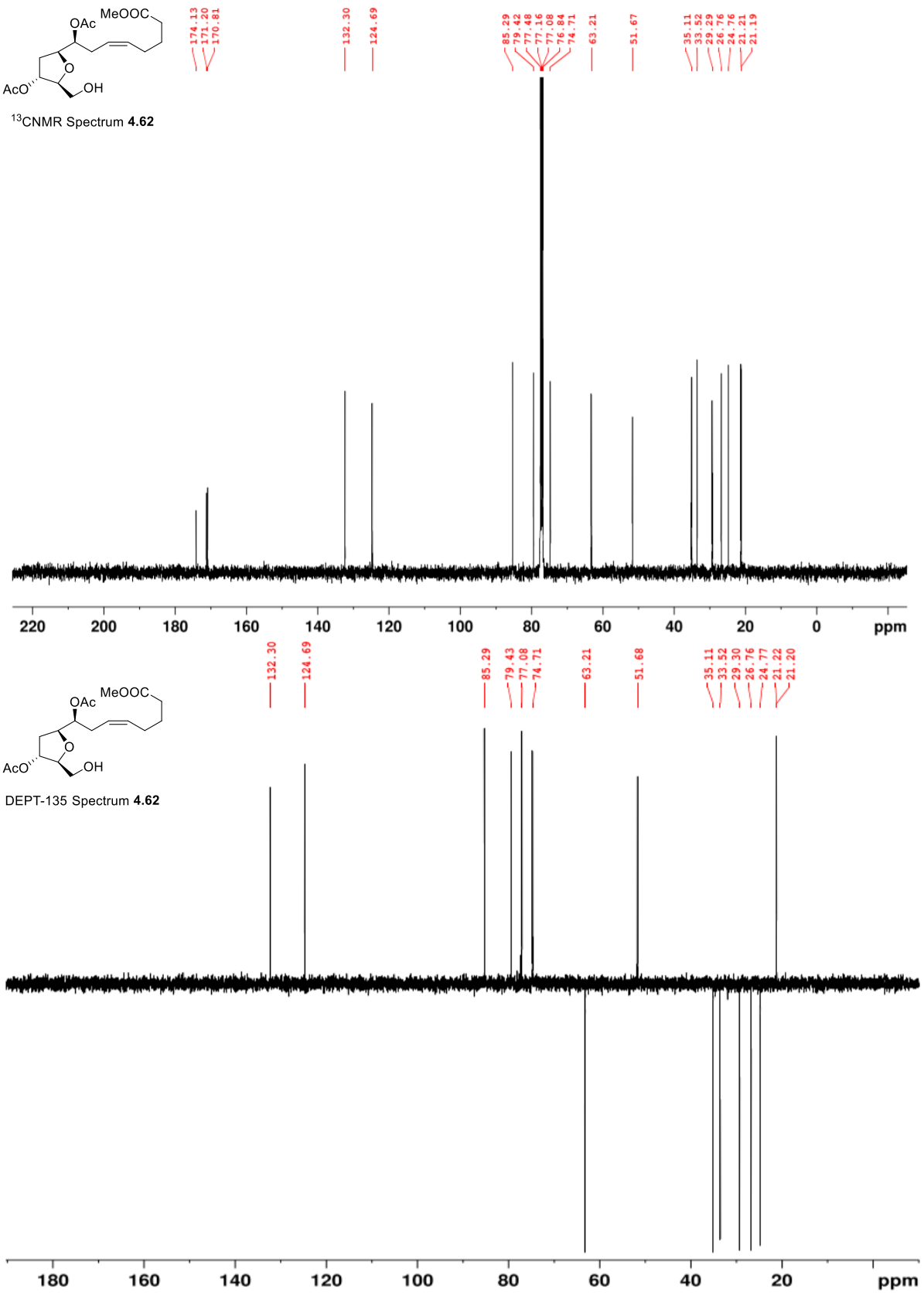

^{13}CNMR Spectrum **4.62**

DEPT-135 Spectrum **4.62**

Figure A.48 ^{13}C NMR (100 MHz, $CDCl_3$) and DEPT-135 (100MHz, $CDCl_3$) of **4.62**.

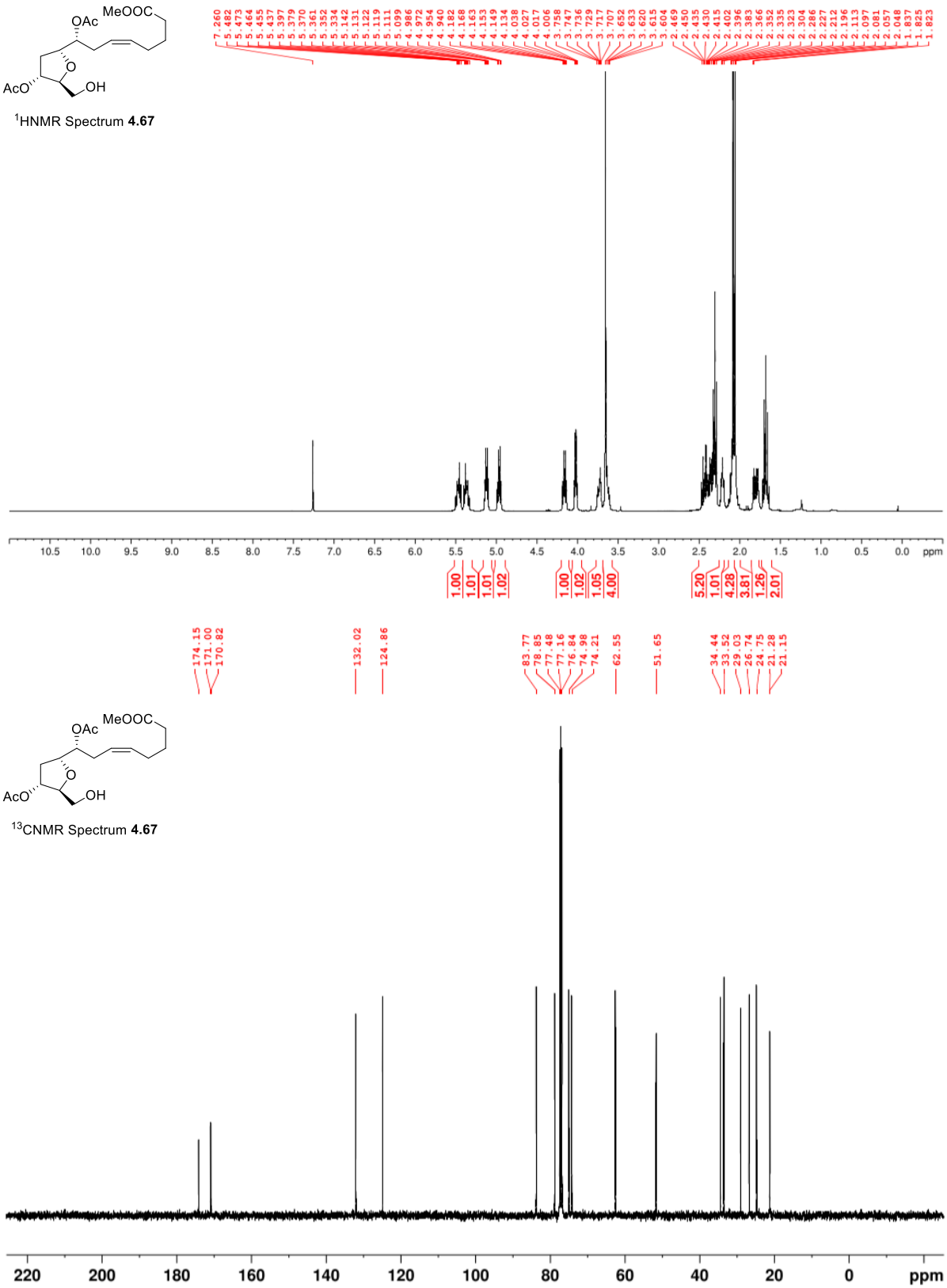

Figure A.49 ^{1}H NMR (400 MHz, $CDCl_3$) and ^{13}C NMR (100 MHz, $CDCl_3$) of **4.67**.

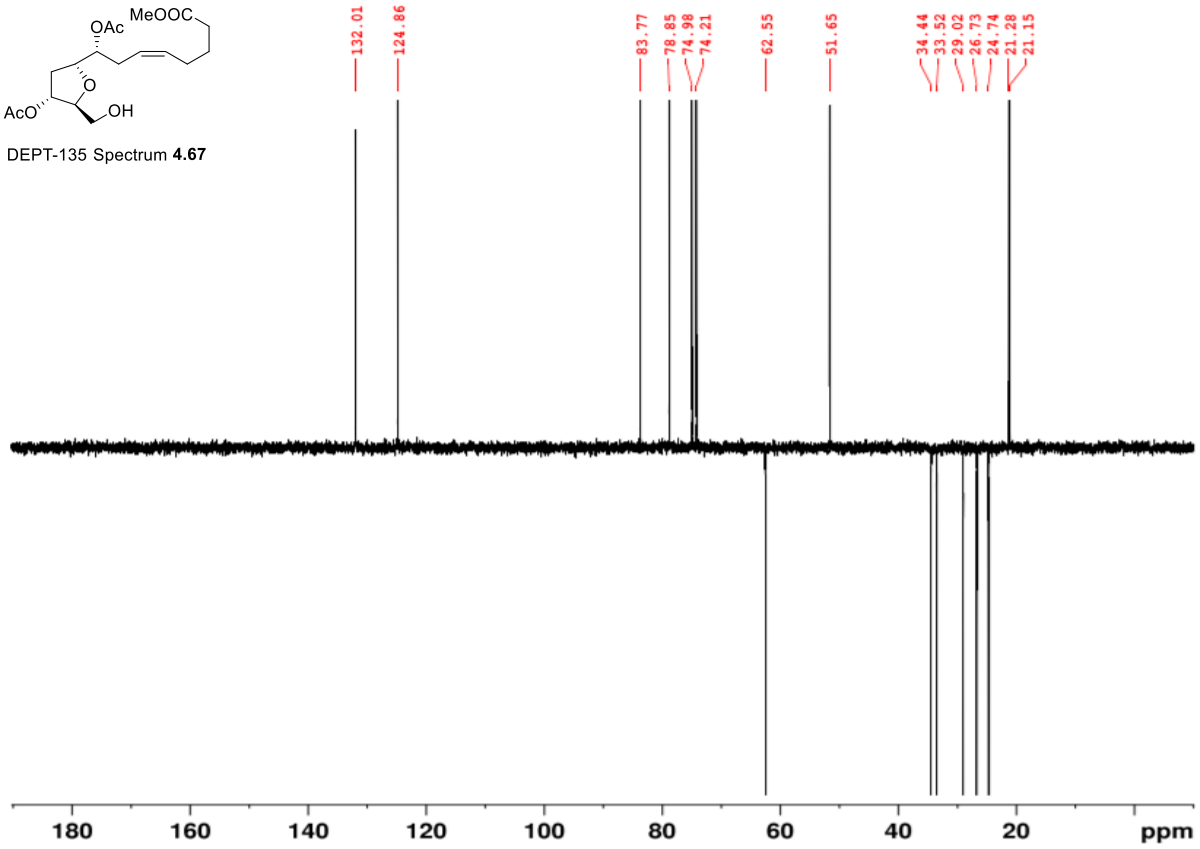

Figure A.50 DEPT-135 (100MHz, $CDCl_3$) of **4.67**.

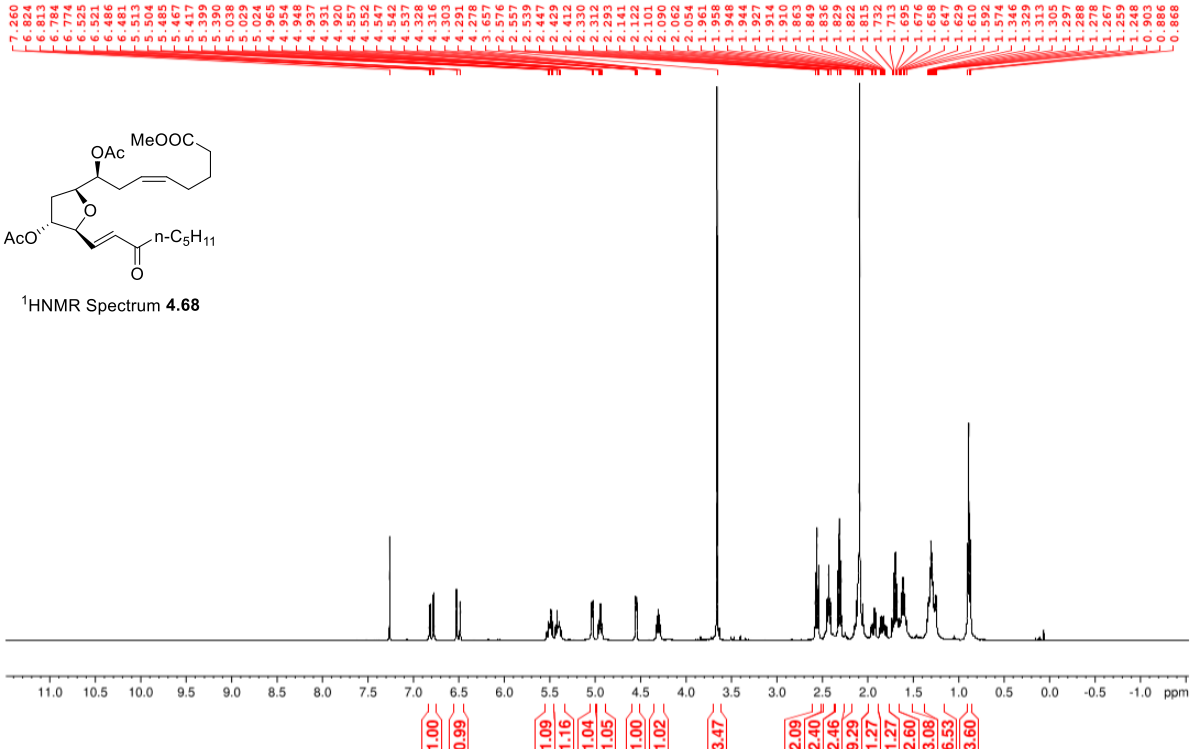

Figure A.51 ^{1}H NMR (400 MHz, $CDCl_3$) of **4.68**.

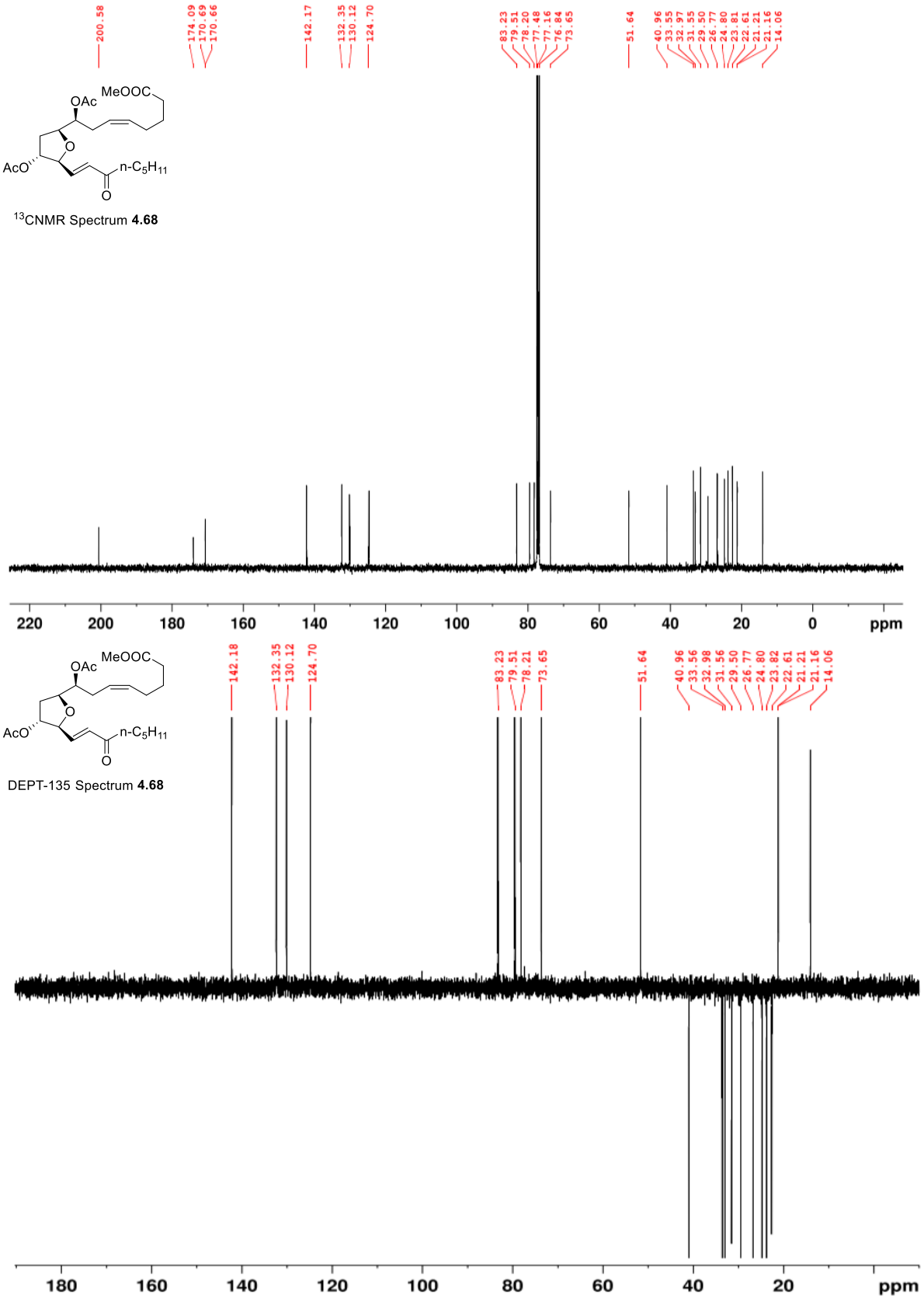

Figure A.52 ^{13}C NMR (100 MHz, $CDCl_3$) and DEPT-135 (100MHz, $CDCl_3$) of **4.68**.

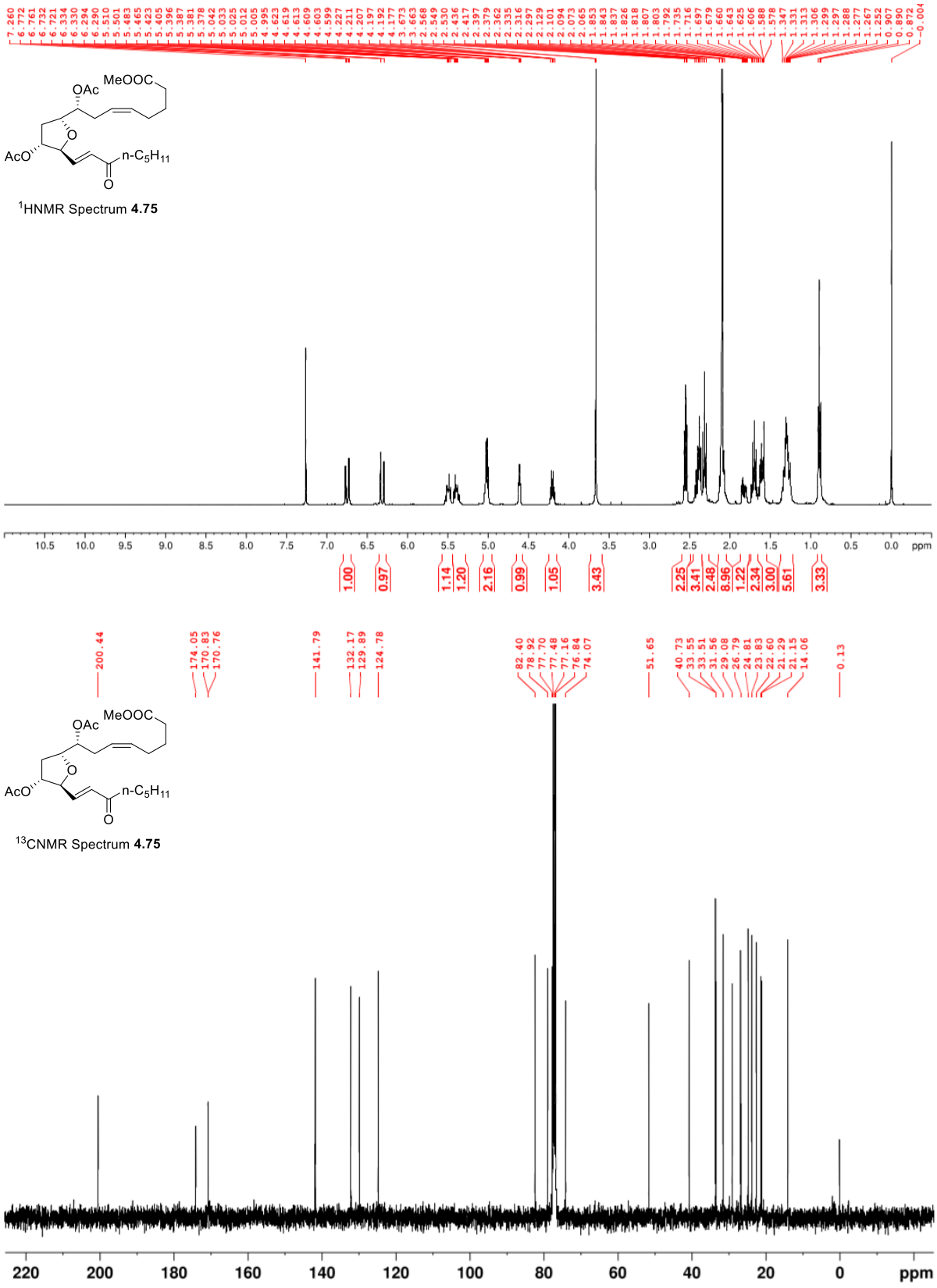

Figure A.53 ^{1}H NMR (400 MHz, $CDCl_3$) and ^{13}C NMR (100 MHz, $CDCl_3$) of **4.75**.

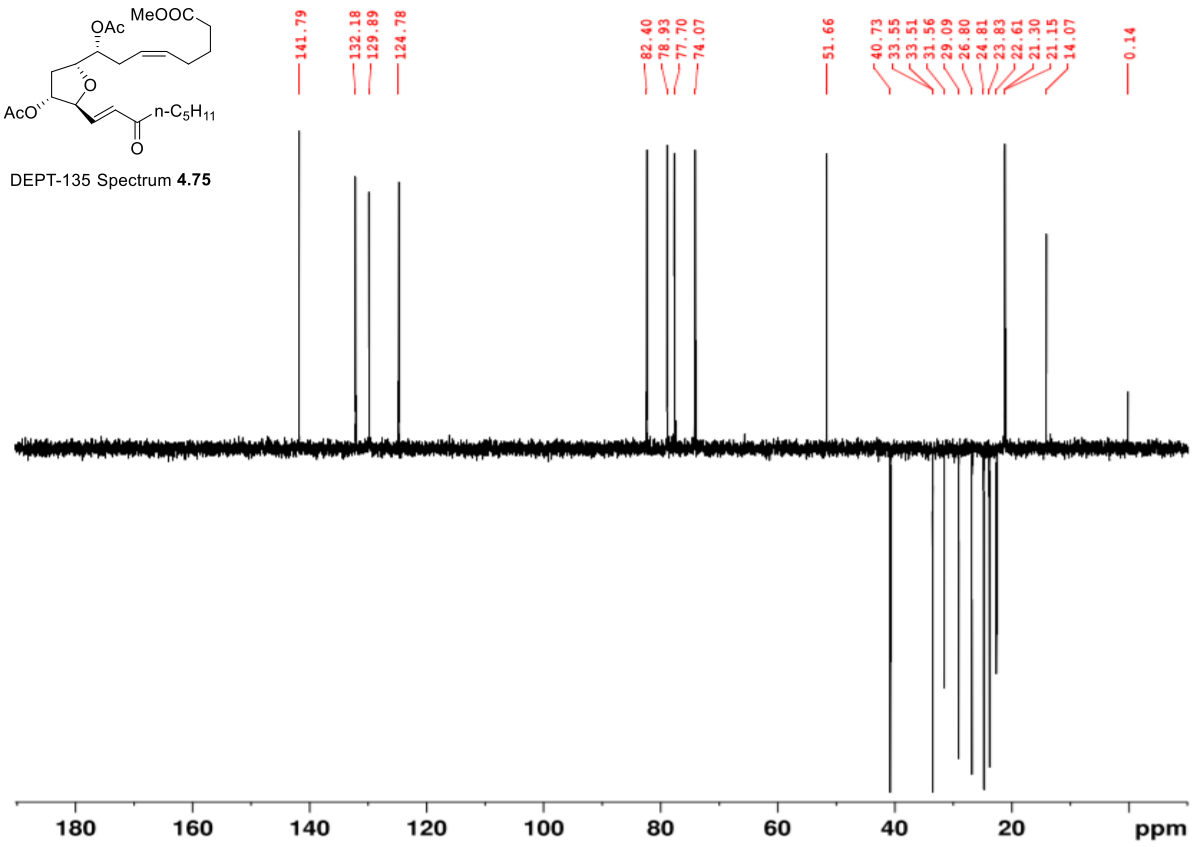

Figure A.54 DEPT-135 (100MHz, $CDCl_3$) of **4.75**.

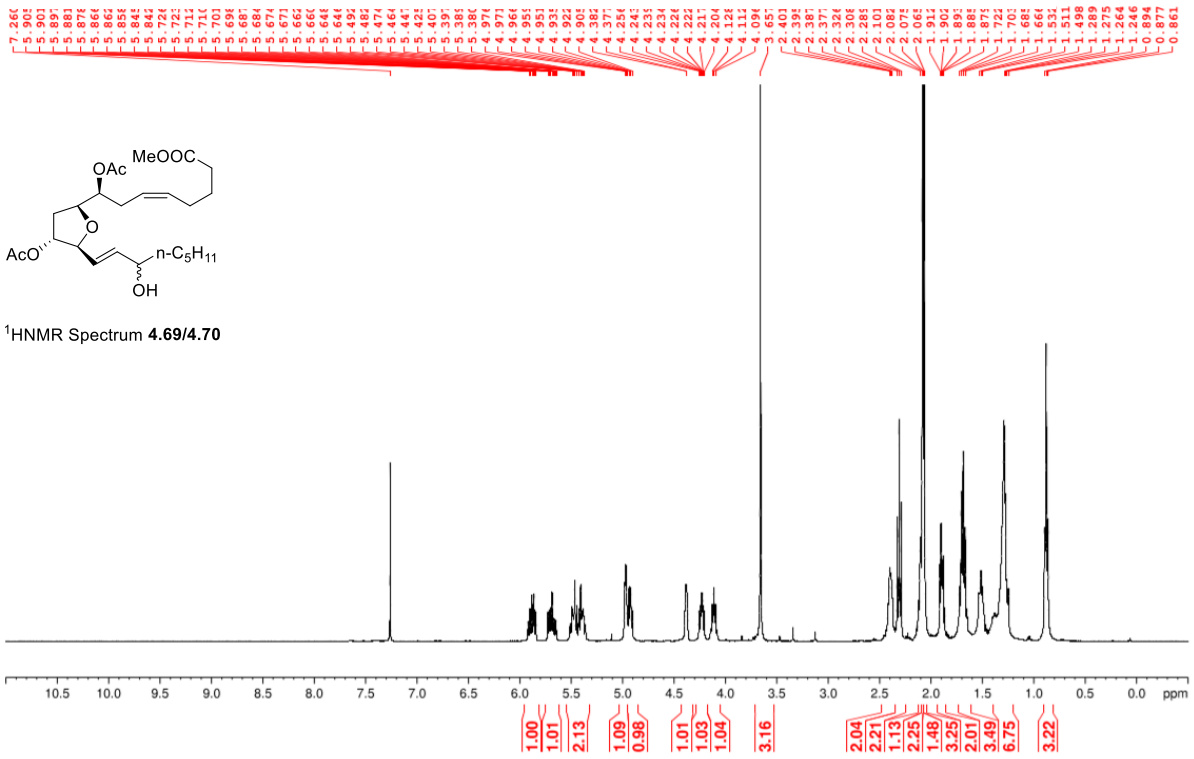

Figure A.55 ^{1}H NMR (400 MHz, $CDCl_3$) of **4.69/70**.

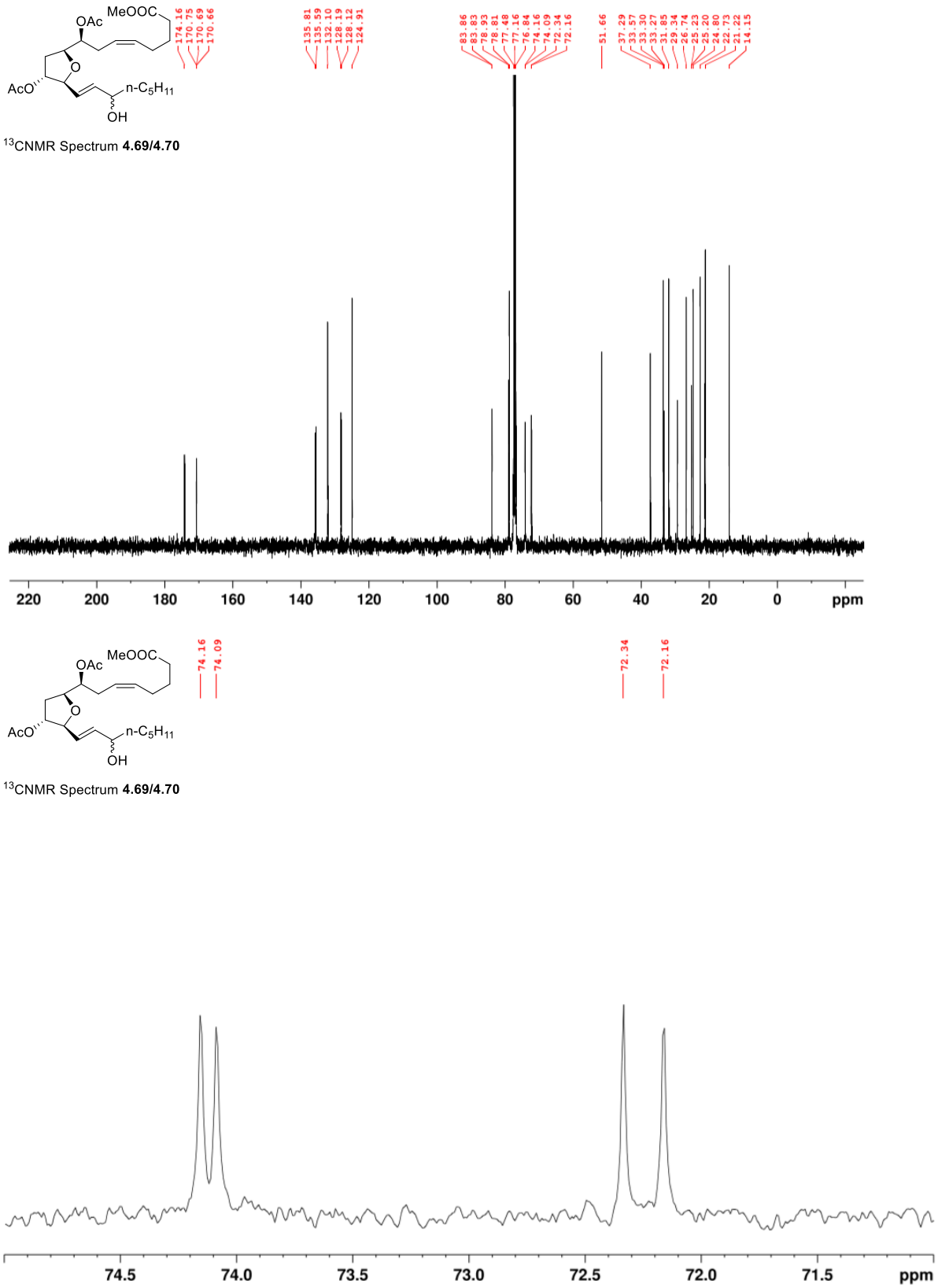

^{13}CNMR Spectrum **4.69/4.70**

^{13}CNMR Spectrum **4.69/4.70**

Figure A.56 ^{13}C NMR (100 MHz, $CDCl_3$) of **4.69**/**70** and ^{13}C NMR (100 MHz, $CDCl_3$) of **4.69**/**70** 71-75 ppm showing two distinct diastereomeric alcohols (74.2, 74.1, 72.3 and 72.1).

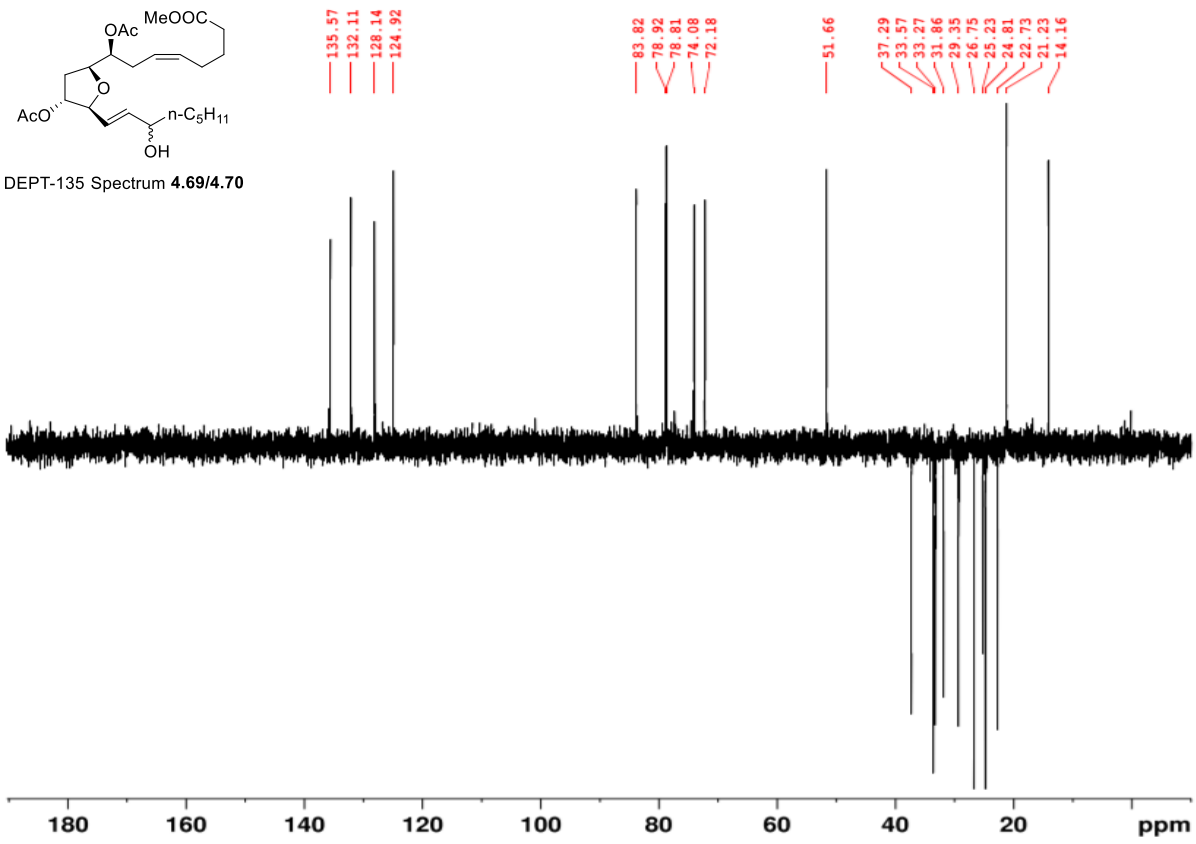

Figure A.57 DEPT-135 (100MHz, $CDCl_3$) of **4.69/70**.

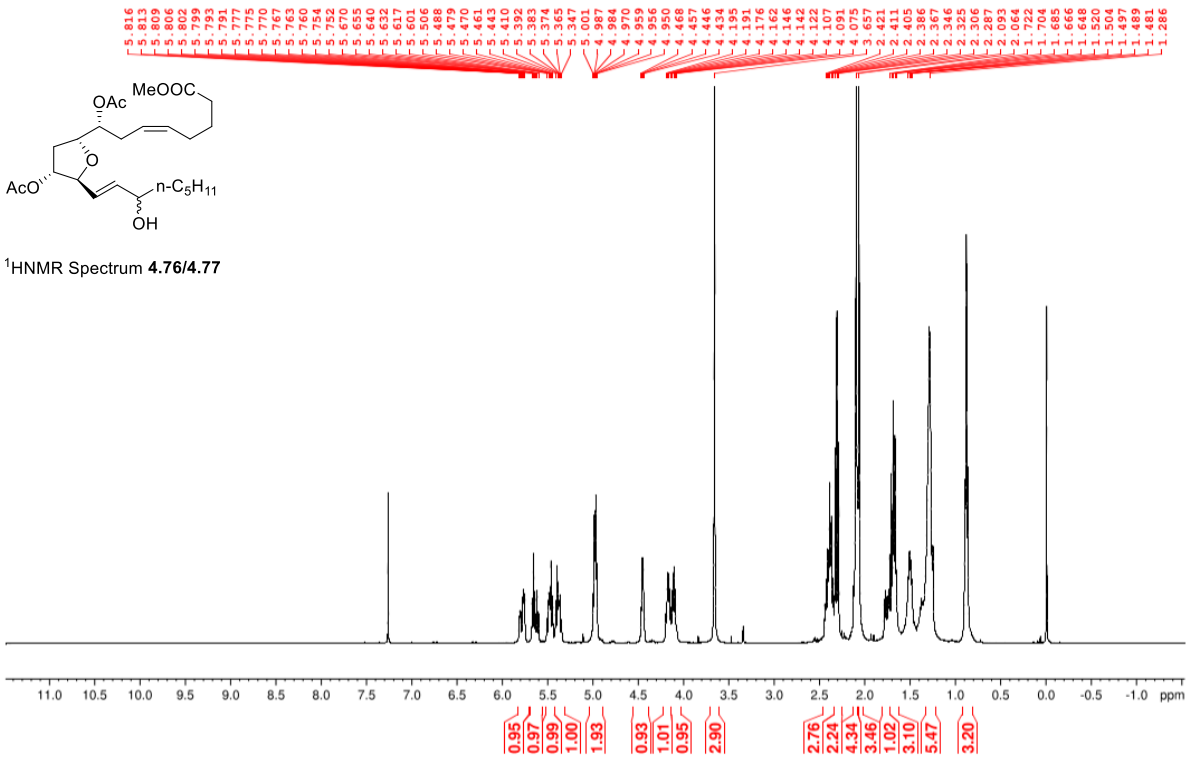

Figure A.58 ^1H NMR (400 MHz, $CDCl_3$) of **4.76/77**.

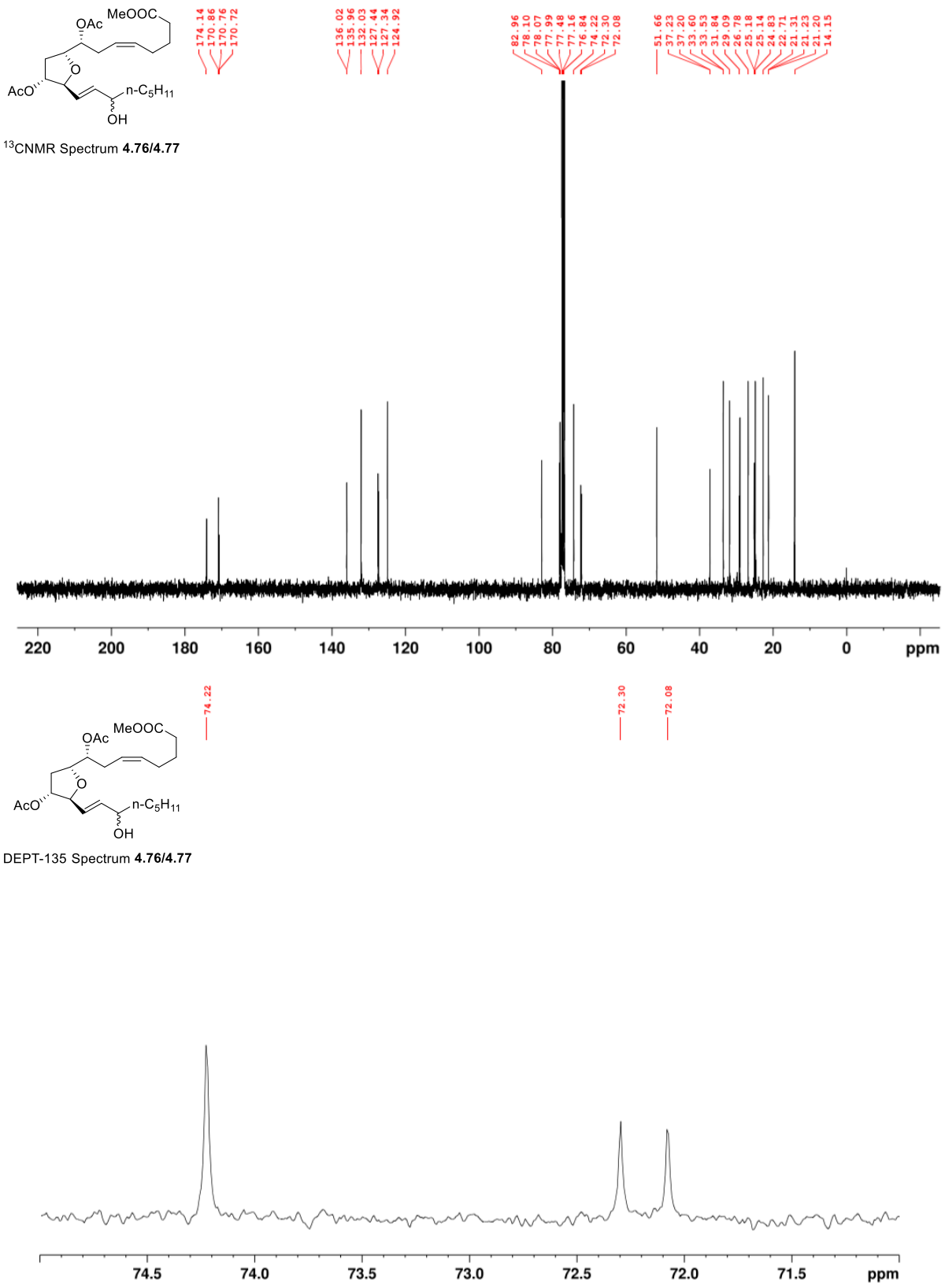

Figure A.59 ^{13}C NMR (100 MHz, $CDCl_3$) of **4.76/77** and ^{13}C NMR (100 MHz, $CDCl_3$) of **4.69/70** 71-75 ppm showing two distinct diastereomeric alcohols (72.3 and 72.1 ppm).

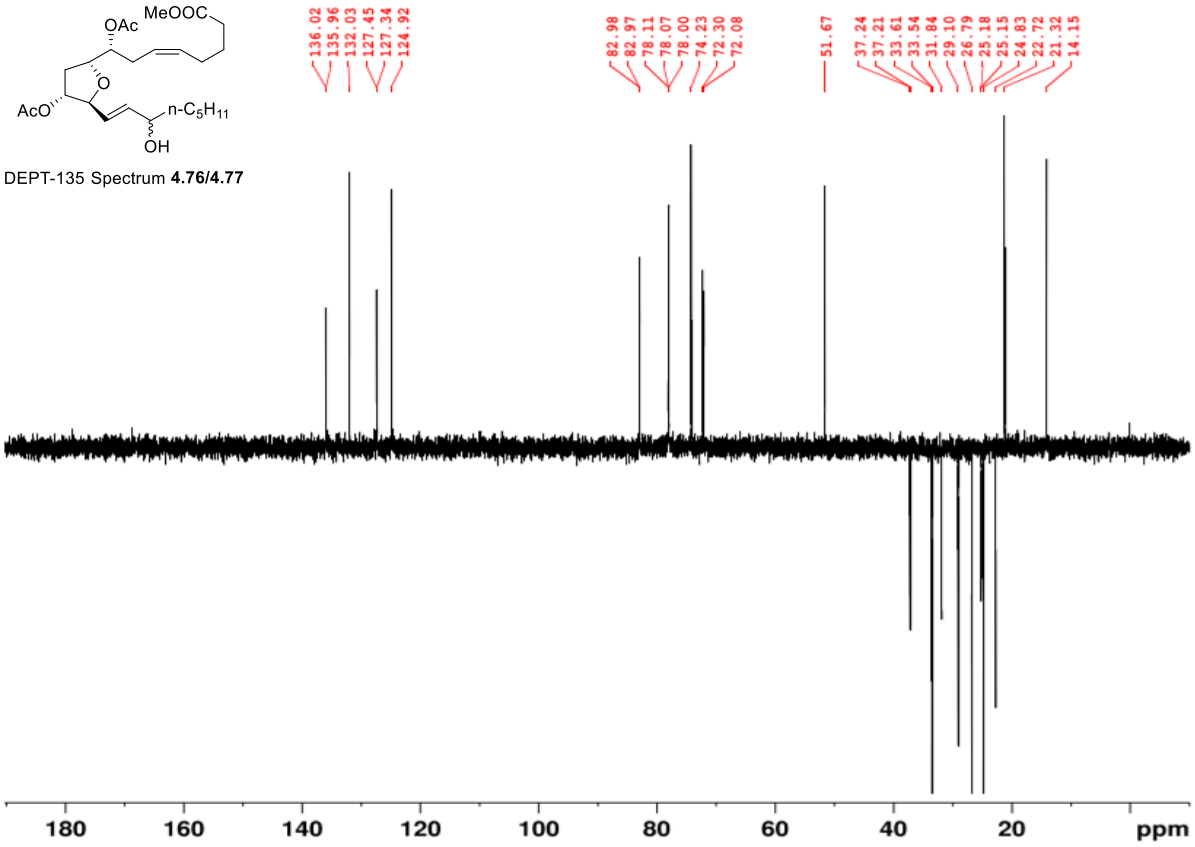

Figure A.60 DEPT-135 (100MHz, $CDCl_3$) of **4.76/77**.

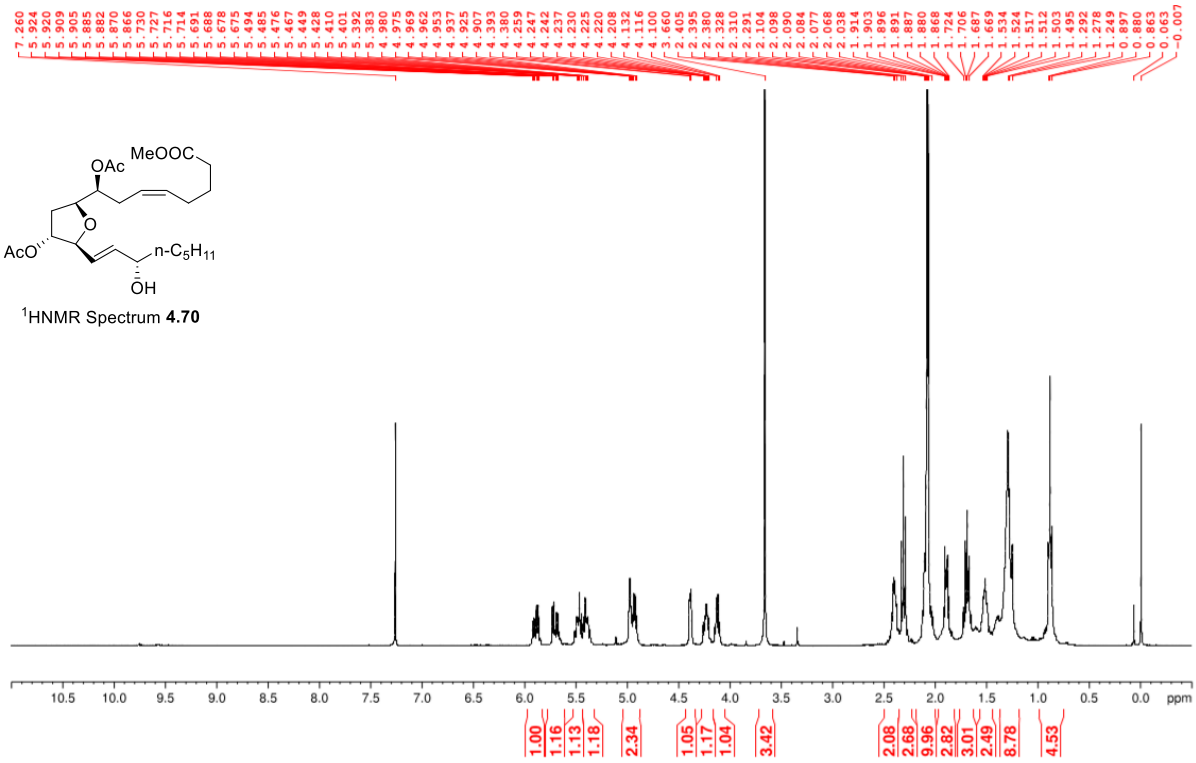

Figure A.61 ^{1}H NMR (400 MHz, $CDCl_3$) of **4.70**.

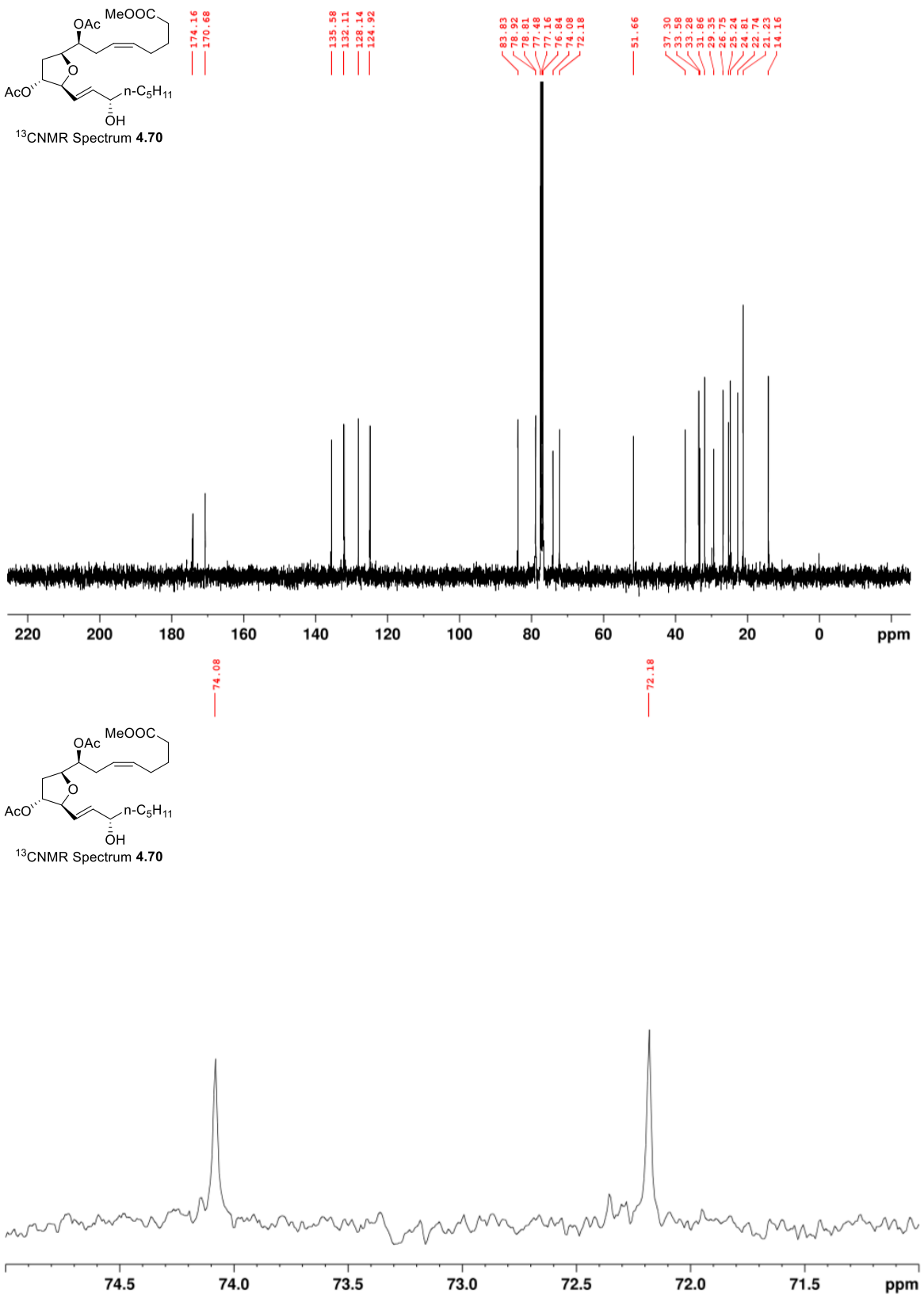

Figure A.62 ^{13}C NMR (100 MHz, $CDCl_3$) of **4.70** and ^{13}C NMR (100 MHz, $CDCl_3$) of **4.70** 71-75 ppm showing a single diastereomeric alcohol (74.1 and 72.2).

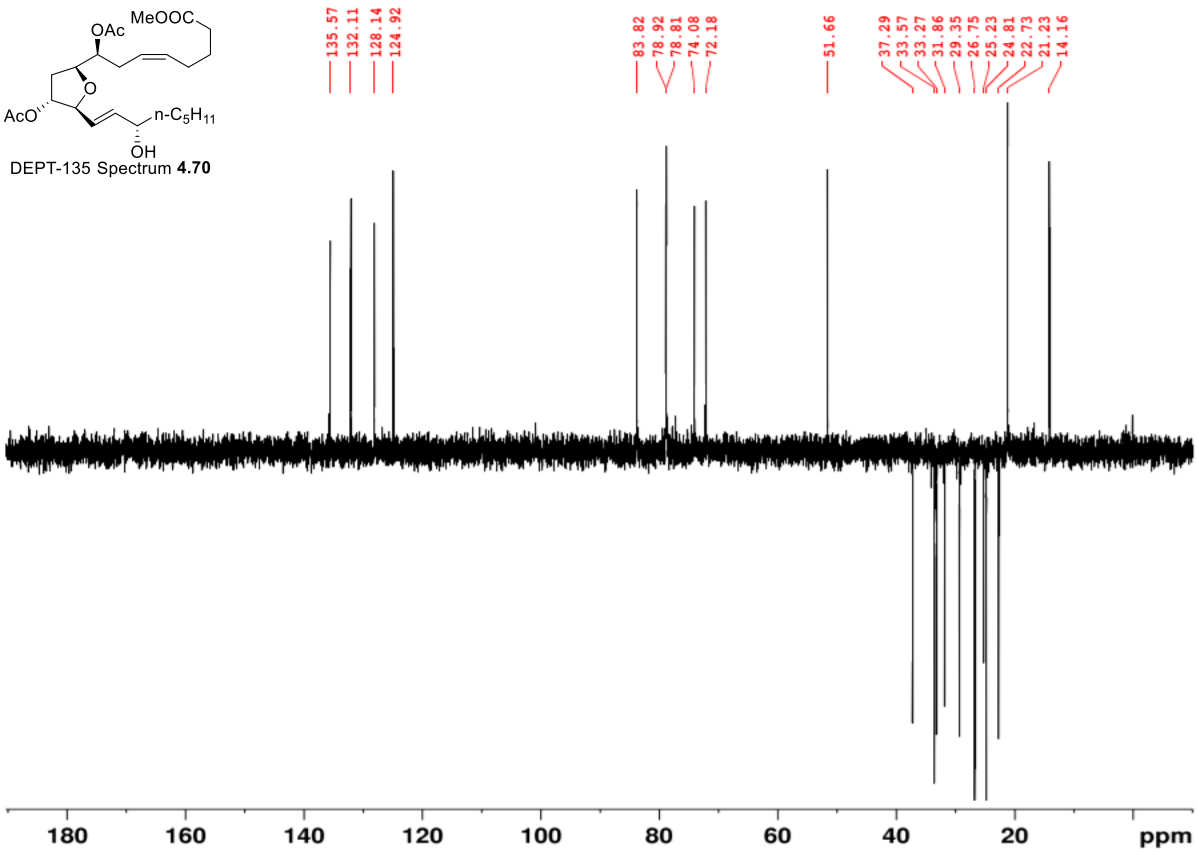

Figure A.63 DEPT-135 (100MHz, $CDCl_3$) of **4.70**.

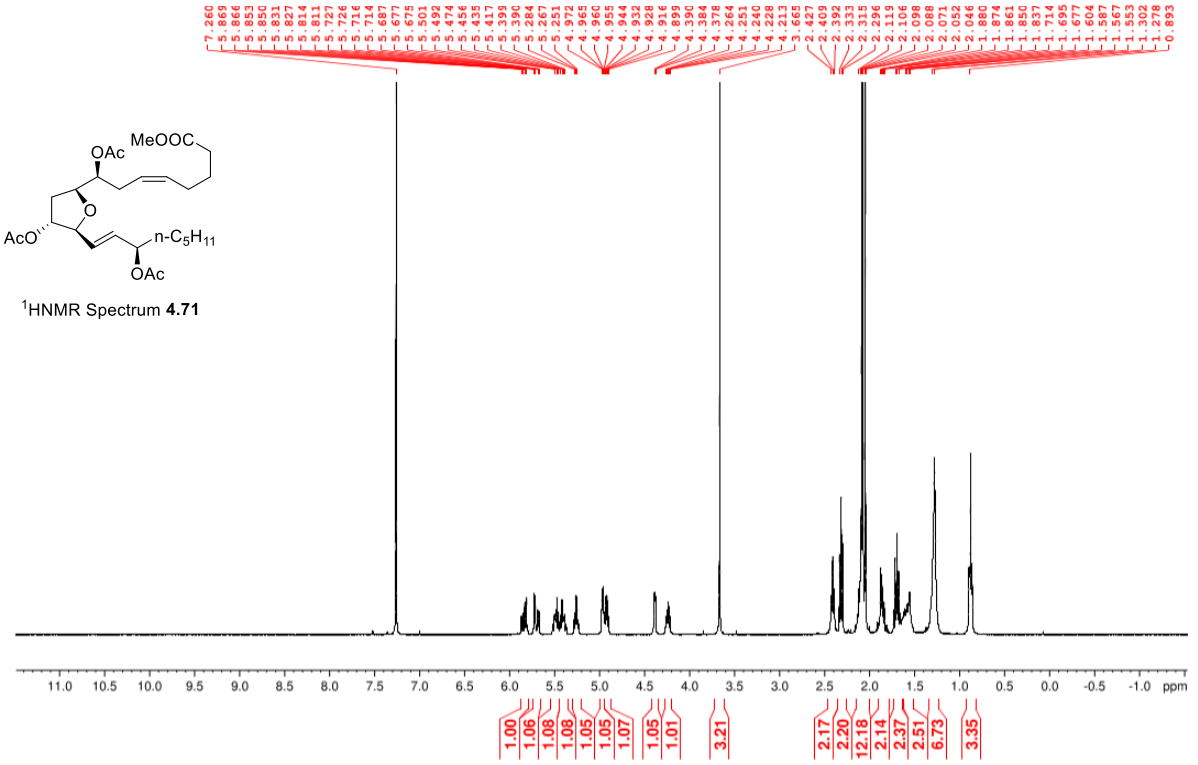

Figure A.64 ^{1}H NMR (400 MHz, $CDCl_3$) of **4.71**.

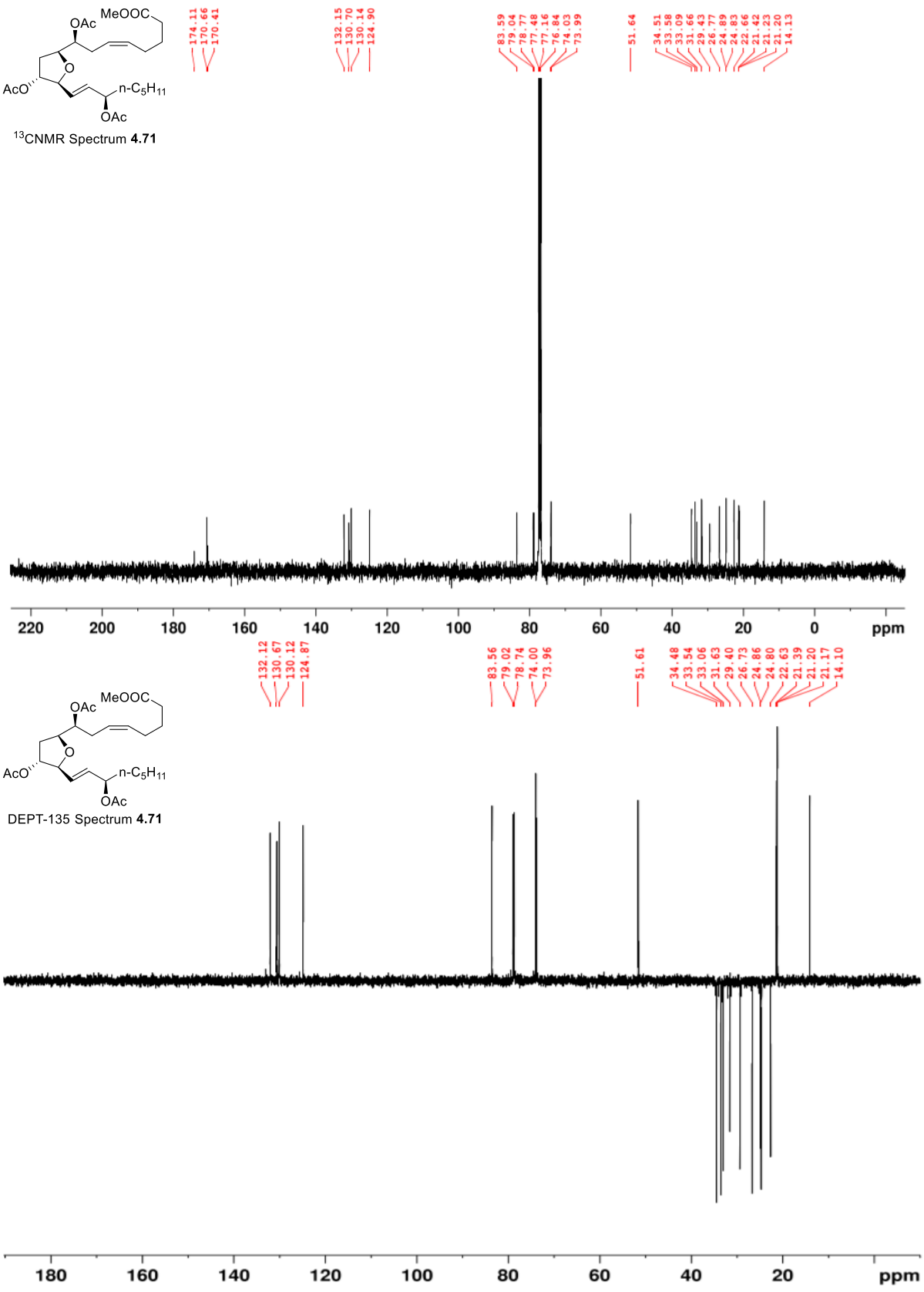

Figure A.65 ^{13}C NMR (100 MHz, $CDCl_3$) and DEPT-135 (100MHz, $CDCl_3$) of **4.71**.

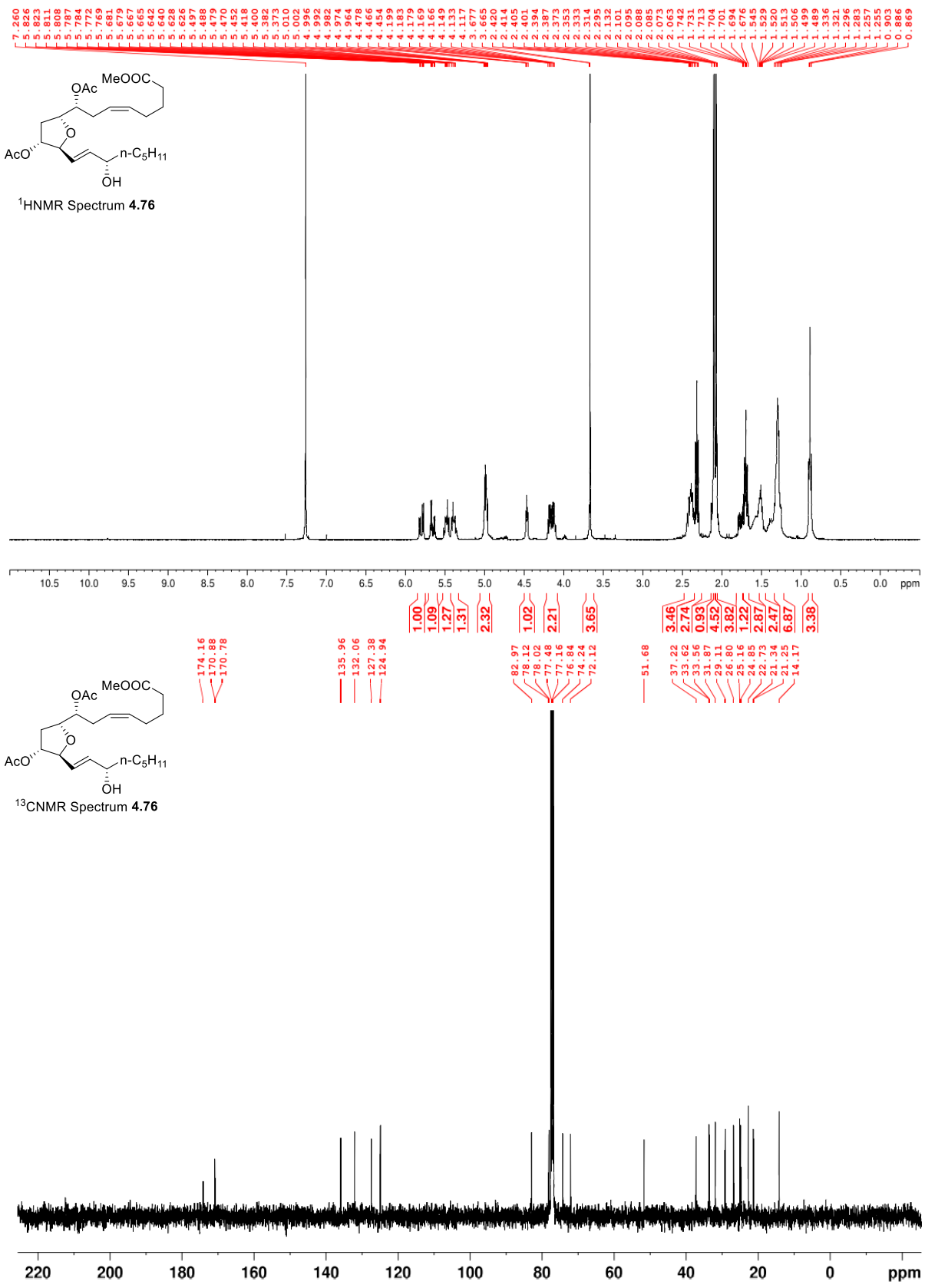

Figure A.66 ^{1}H NMR (400 MHz, $CDCl_3$) and ^{13}C NMR (100 MHz, $CDCl_3$) of **4.76**.

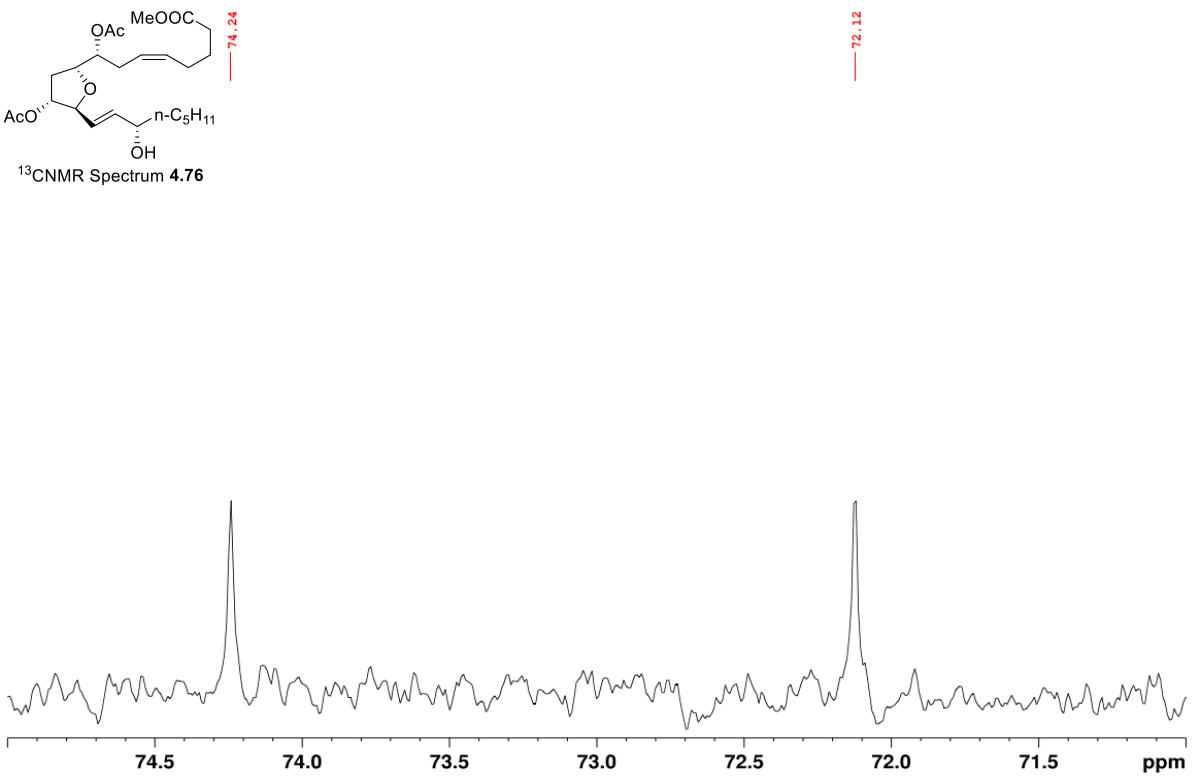

Figure A.67 ^{13}C NMR (100 MHz, $CDCl_3$) of **4.76** 71-75 ppm showing a single diastereomeric alcohol (74.2 and 72.1).

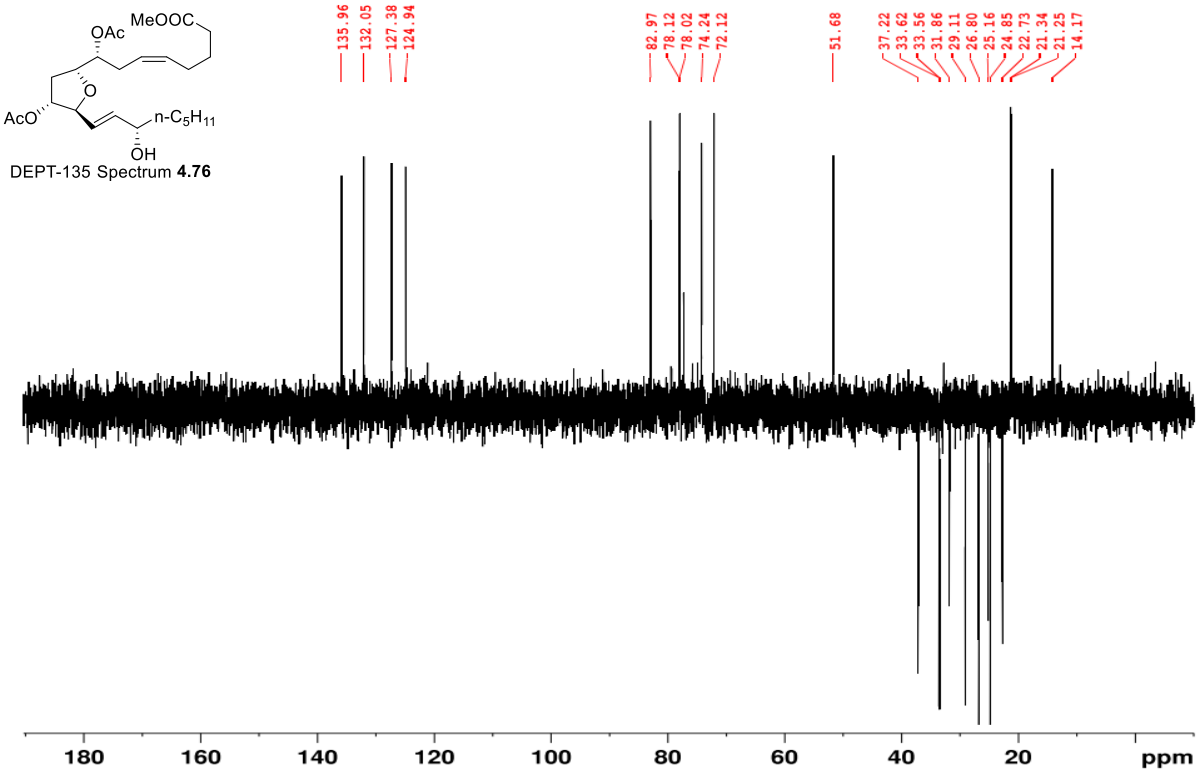

Figure A.68 DEPT-135 (100MHz, $CDCl_3$) of **4.76**.

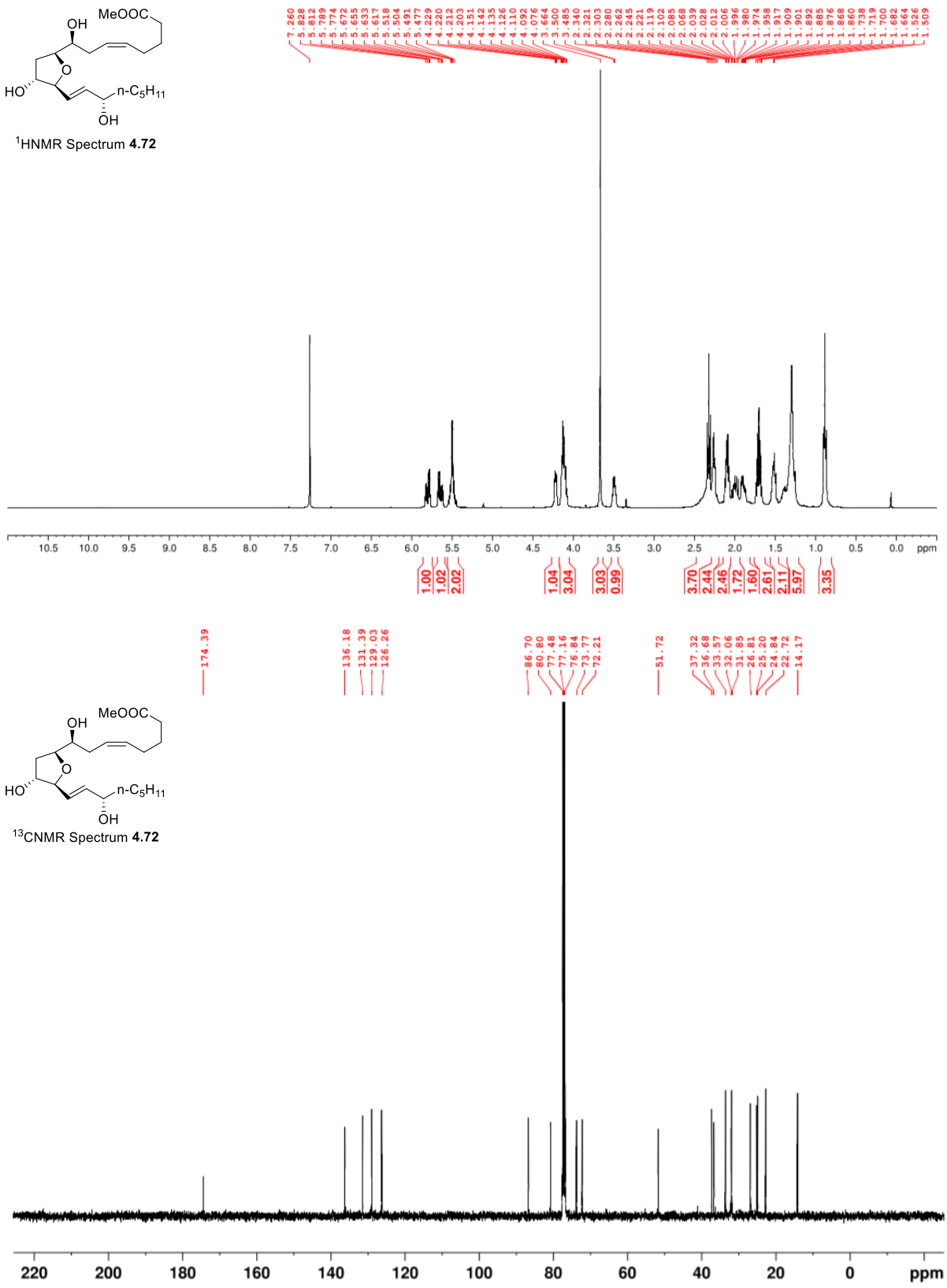

Figure A.69 ^{1}H NMR (400 MHz, $CDCl_3$) and ^{13}C NMR (100 MHz, $CDCl_3$) of **4.72**.

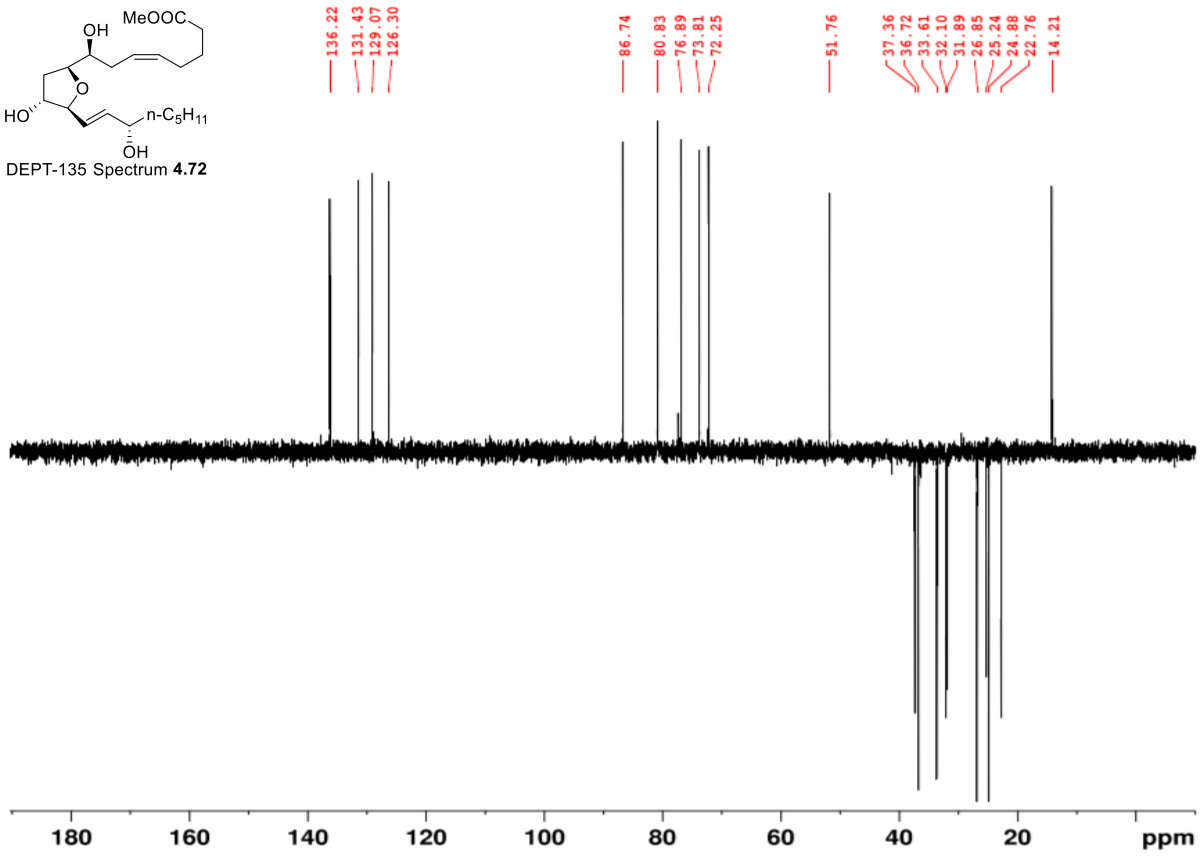

Figure A.70 DEPT-135 (100MHz, $CDCl_3$) of **4.72**.

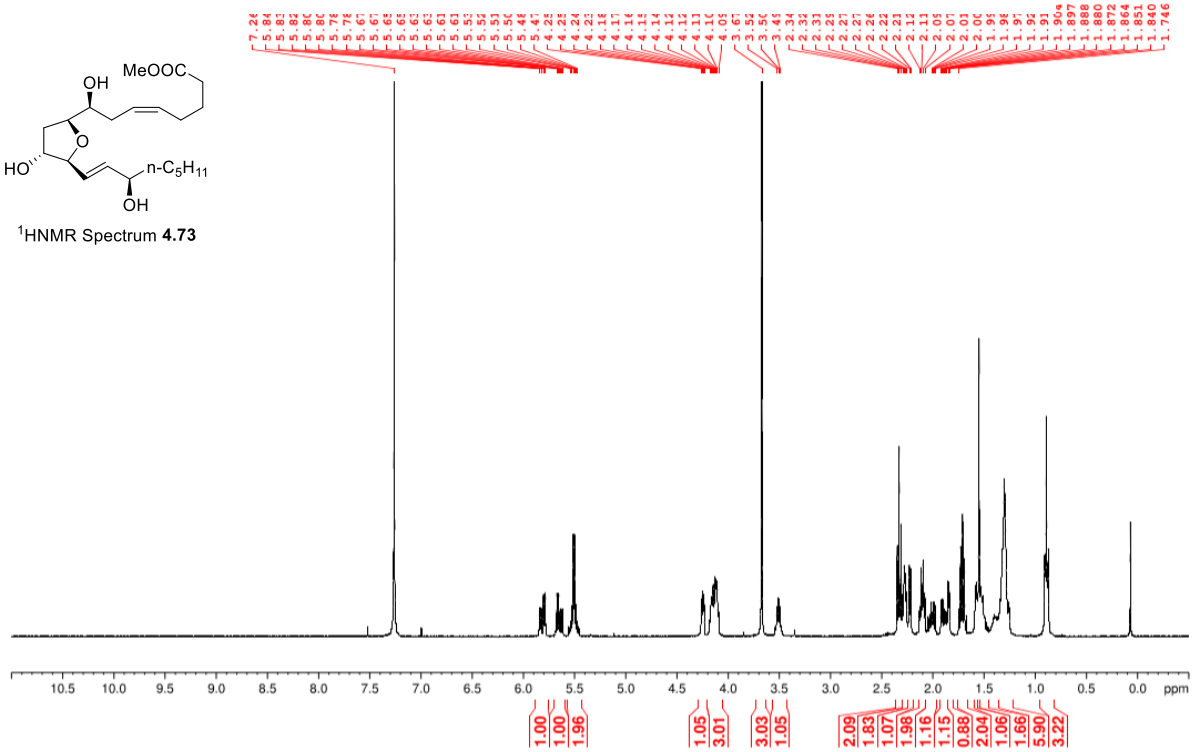

Figure A.71 ^{1}H NMR (400 MHz, $CDCl_3$) of **4.73**.

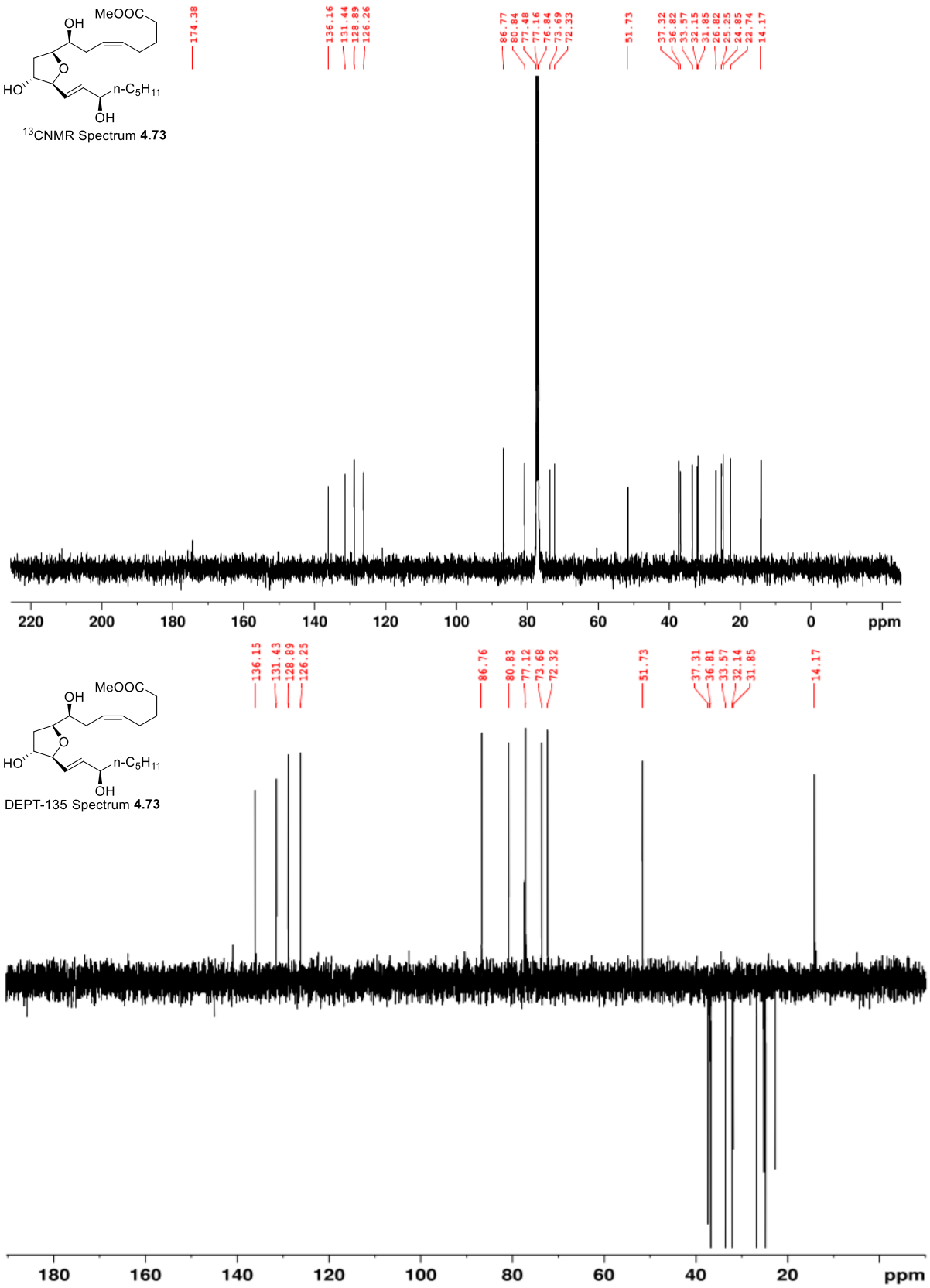

Figure A.72 ^{13}C NMR (100 MHz, $CDCl_3$) and DEPT-135 (100MHz, $CDCl_3$) of **4.73**.

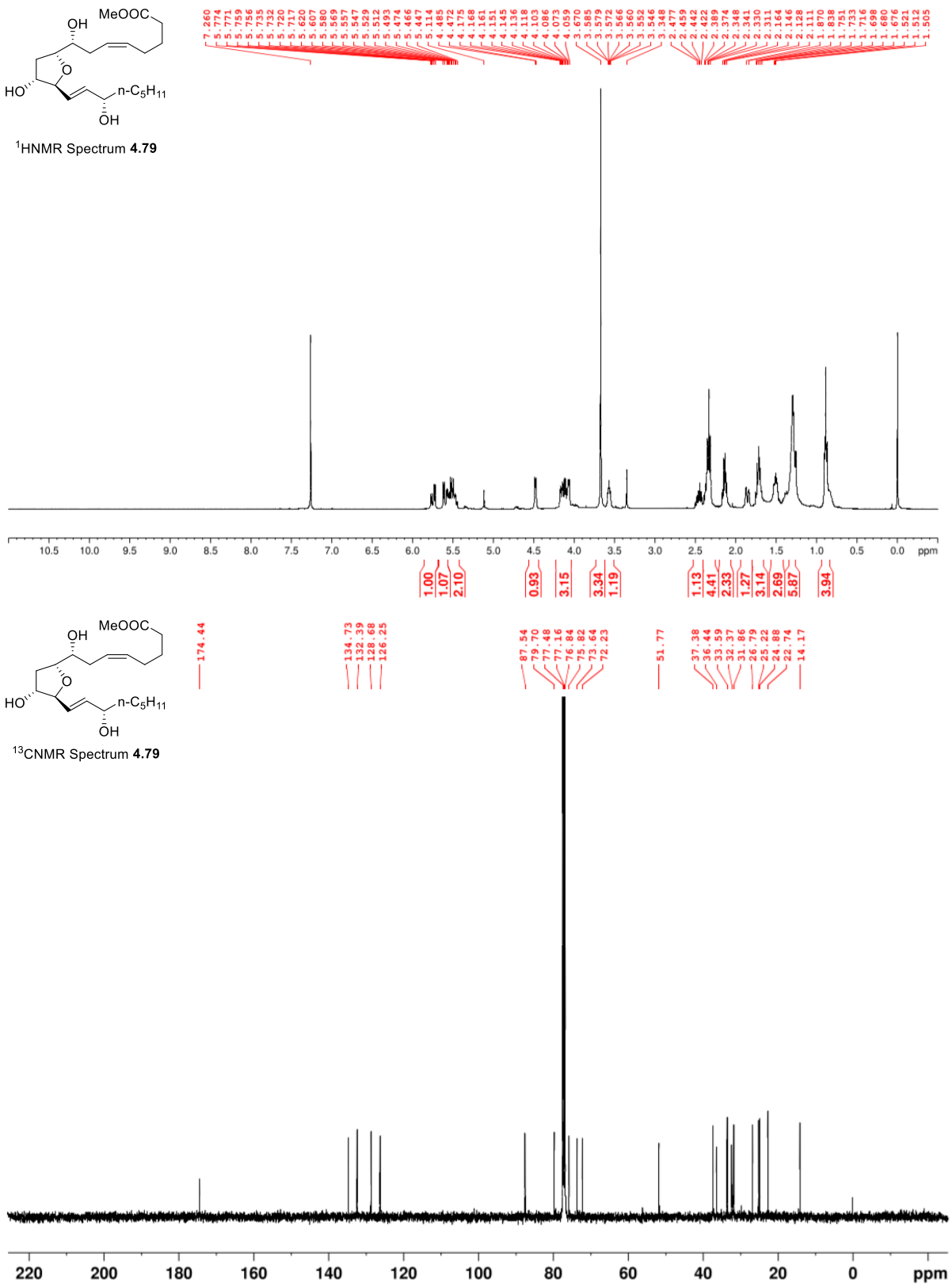

Figure A.73 ^{1}H NMR (400 MHz, $CDCl_3$) and ^{13}C NMR (100 MHz, $CDCl_3$) of **4.79**.

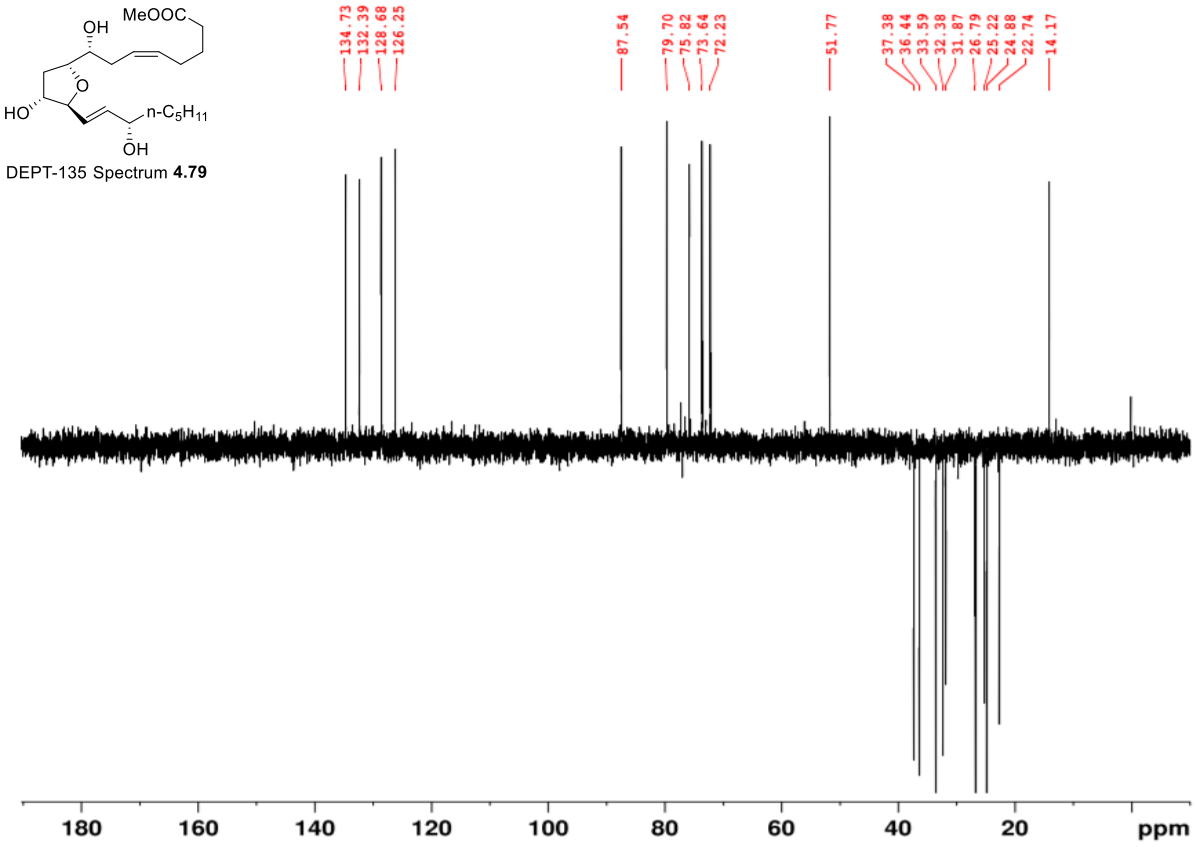

Figure A.74 DEPT-135 (100MHz, $CDCl_3$) of **4.79**.

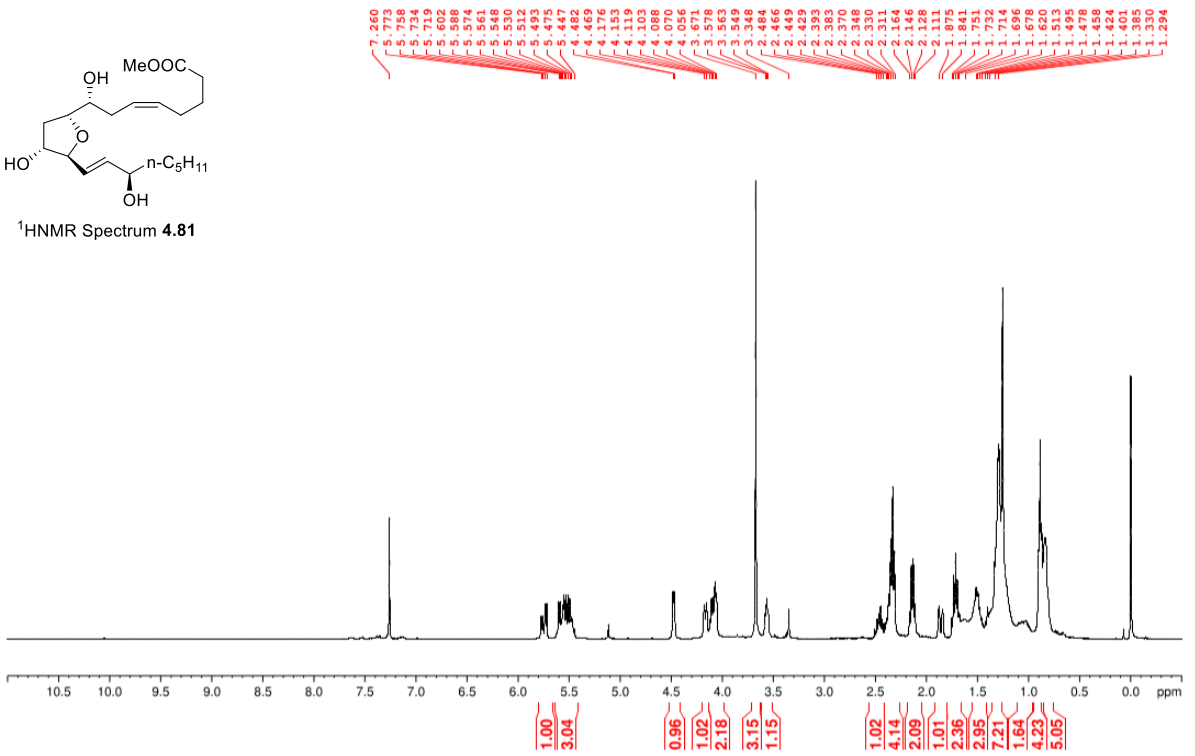

Figure A.75 ^{1}H NMR (400 MHz, $CDCl_3$) of **4.81**.

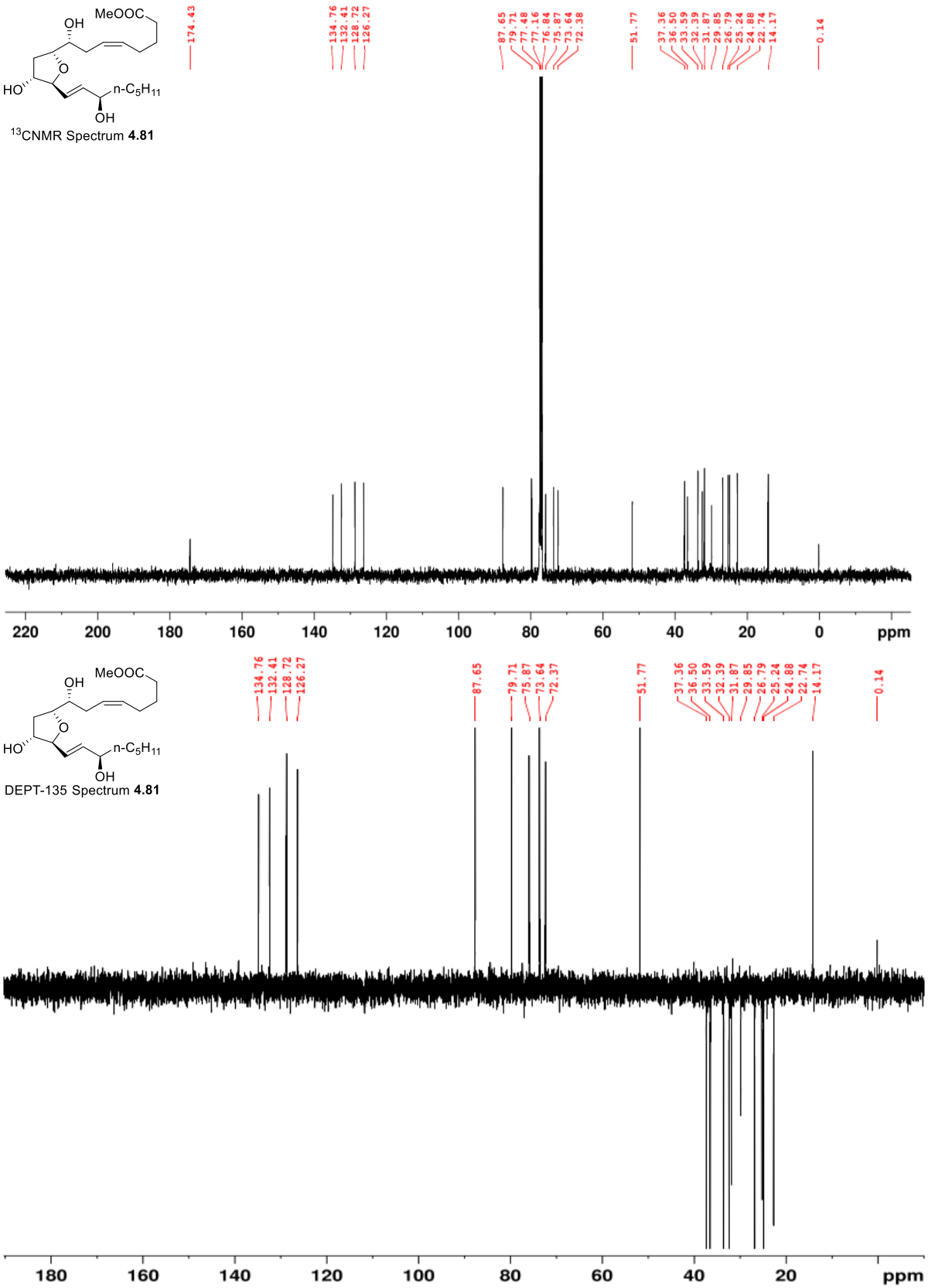

Figure A.76 ^{13}C NMR (100 MHz, $CDCl_3$) and DEPT-135 (100MHz, $CDCl_3$) of **4.81**.

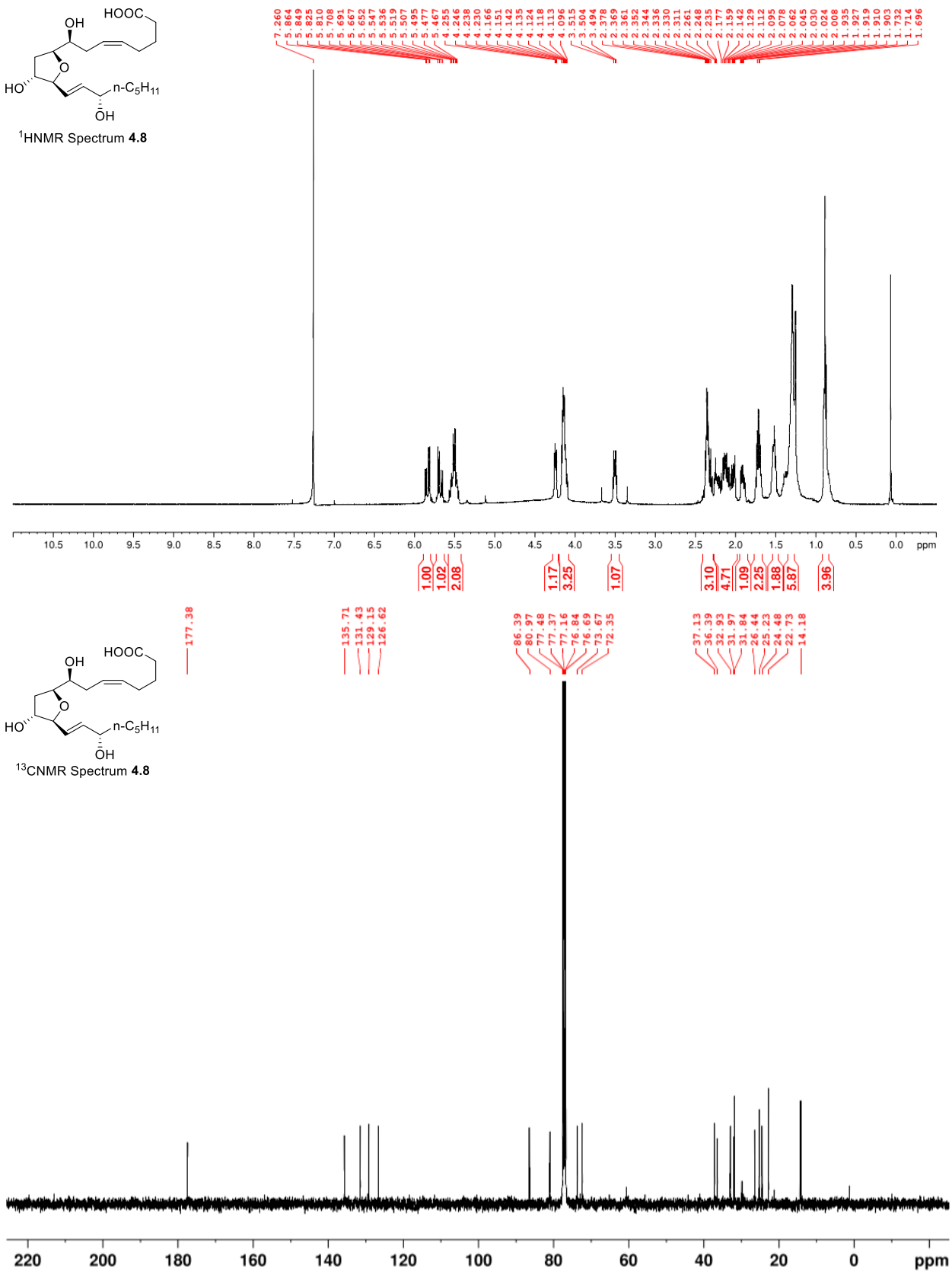

Figure A.77 ^{1}H NMR (400 MHz, $CDCl_3$) and ^{13}C NMR (100 MHz, $CDCl_3$) of **4.8**.

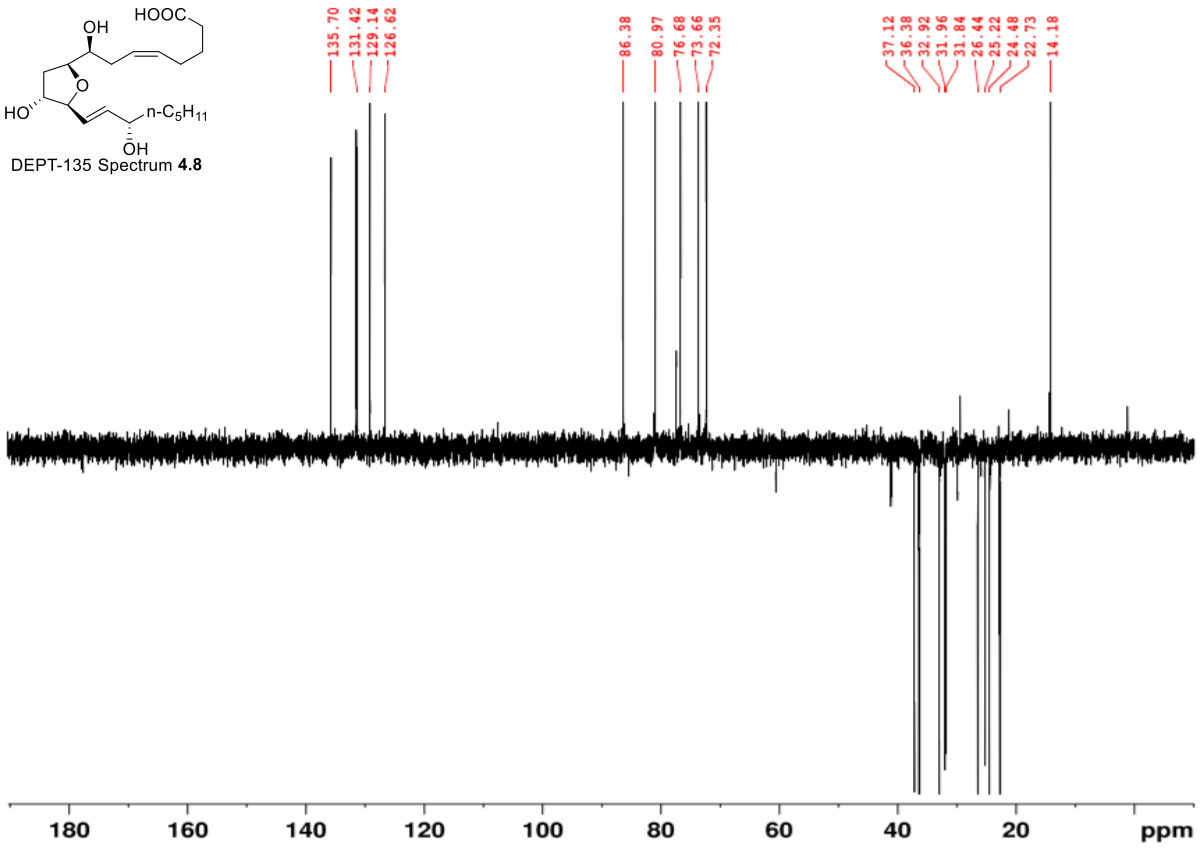

Figure A.78 DEPT-135 (100MHz, $CDCl_3$) of **4.82**.

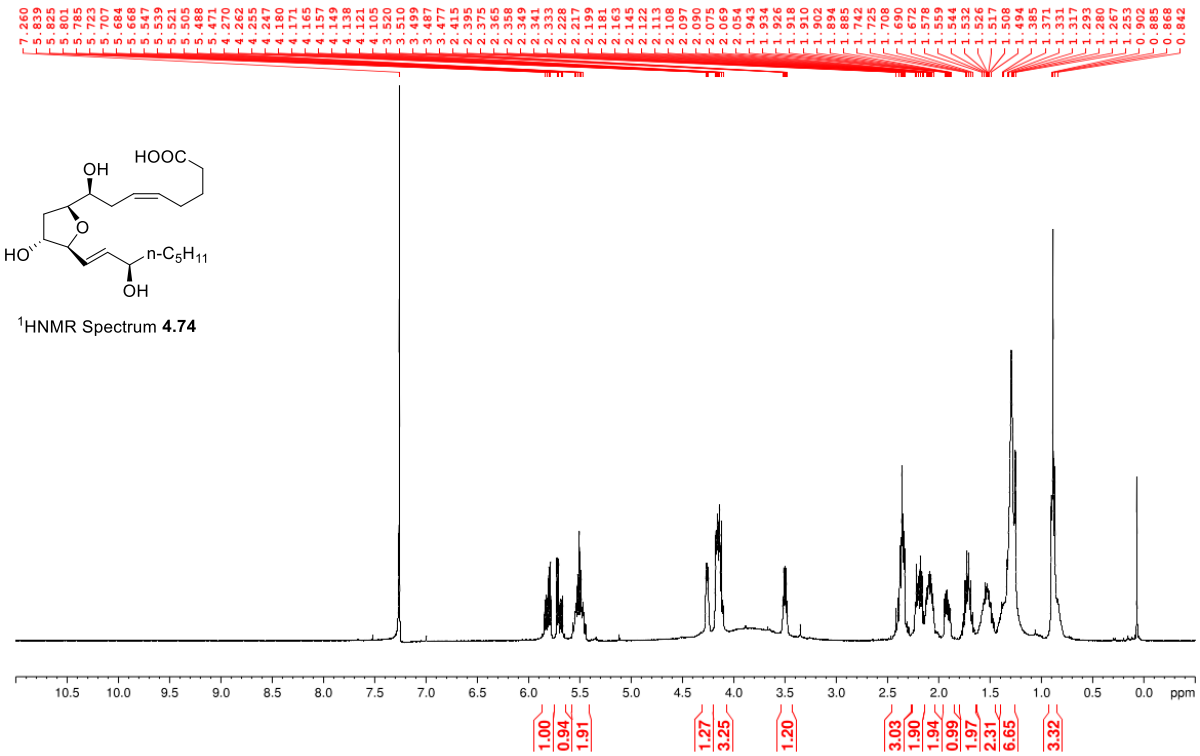

Figure A.79 ^{1}H NMR (400 MHz, $CDCl_3$) of **4.74**.

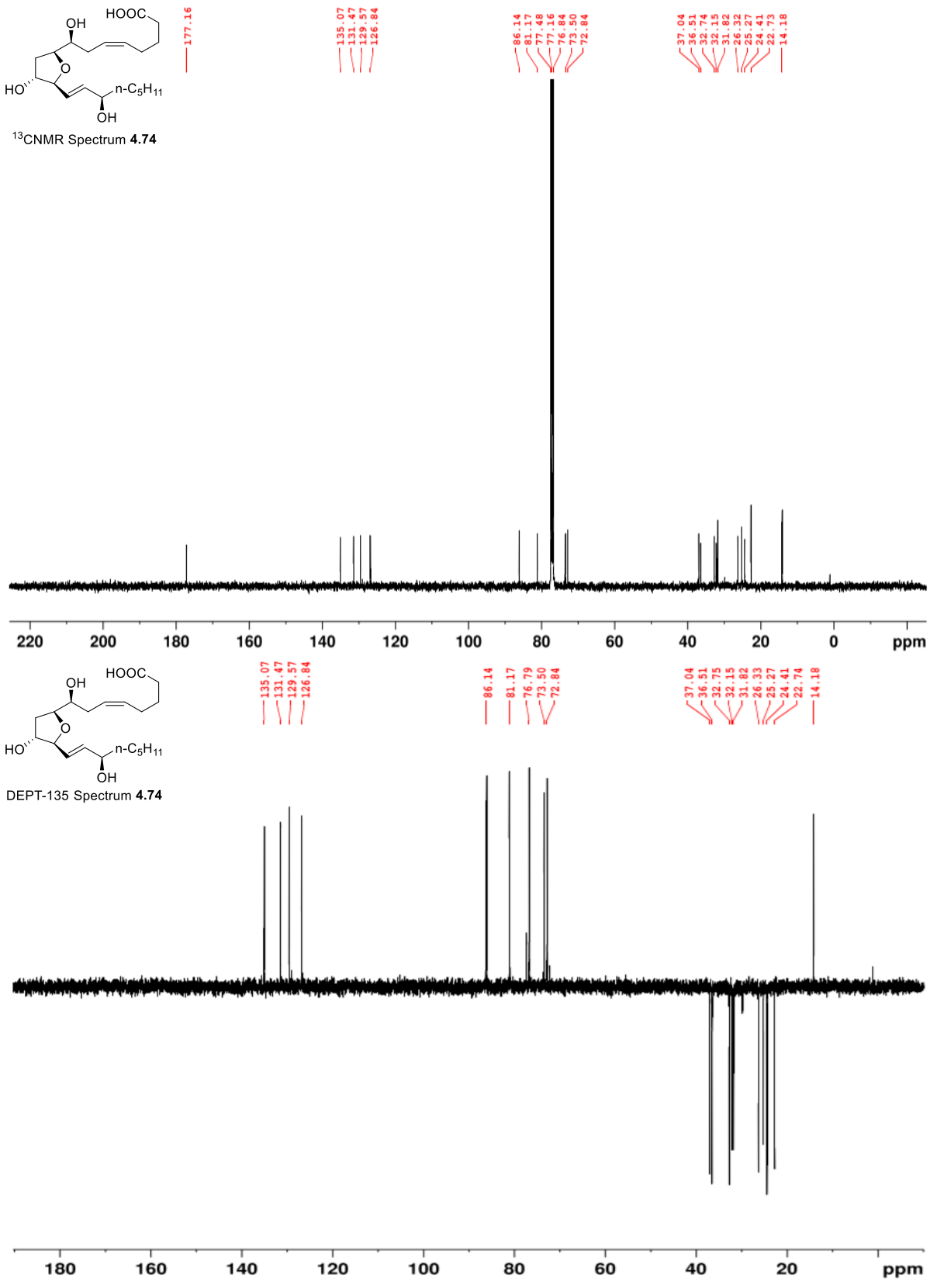

Figure A.80 ^{13}C NMR (100 MHz, $CDCl_3$) and DEPT-135 (100MHz, $CDCl_3$) of **4.74**.

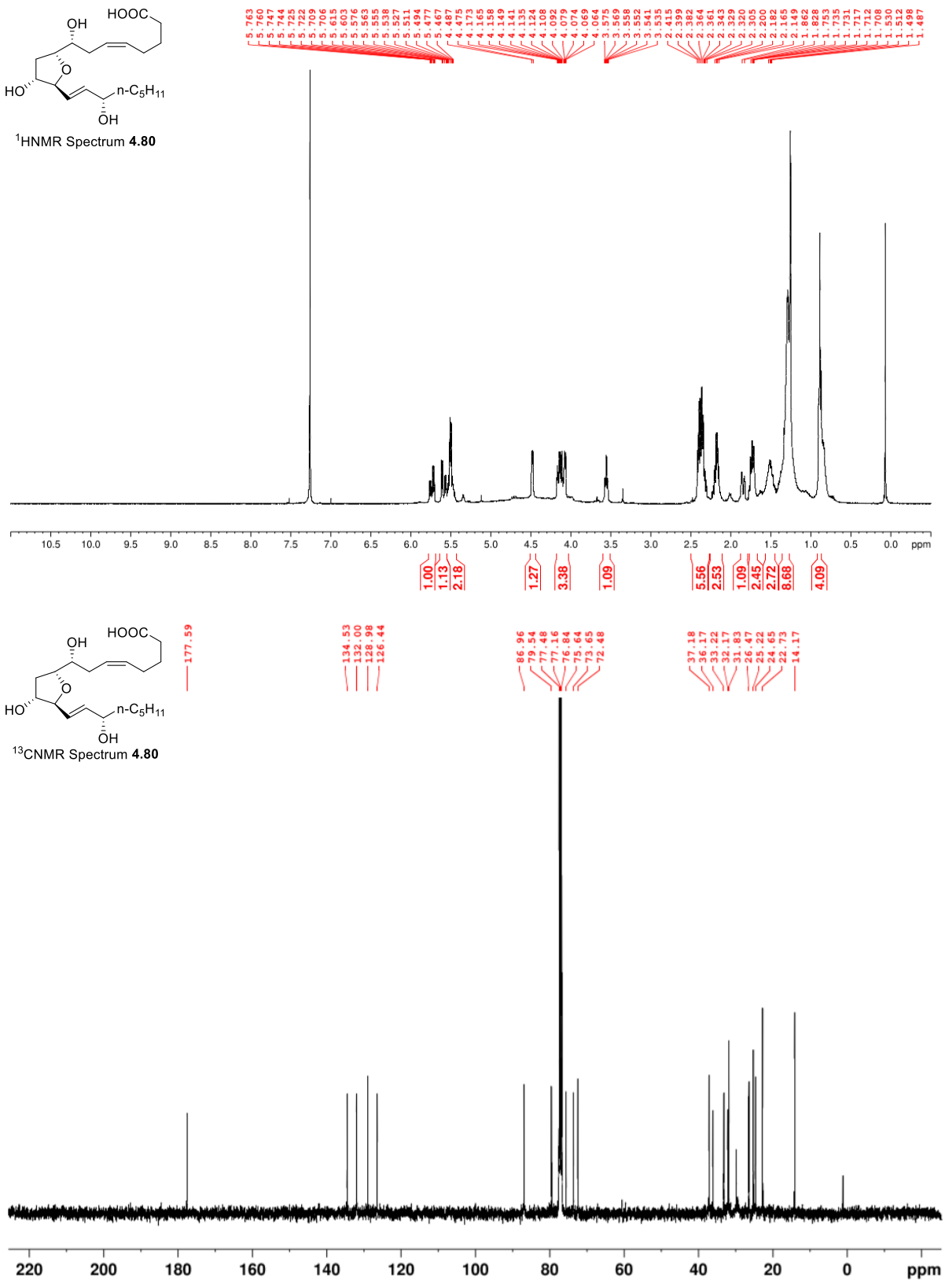

Figure A.81 ^{1}H NMR (400 MHz, $CDCl_3$) and ^{13}C NMR (100 MHz, $CDCl_3$) of **4.80**.

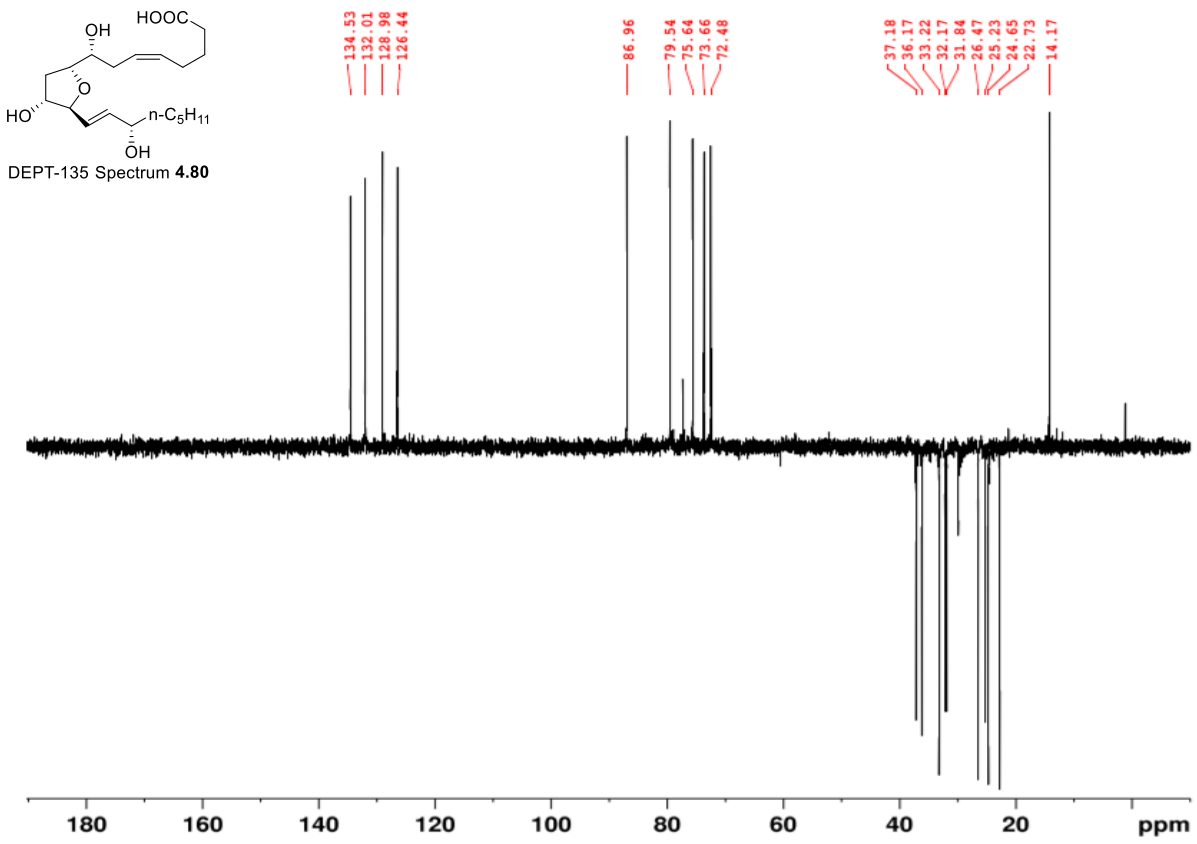

Figure A.82 DEPT-135 (100MHz, $CDCl_3$) of **4.80**.

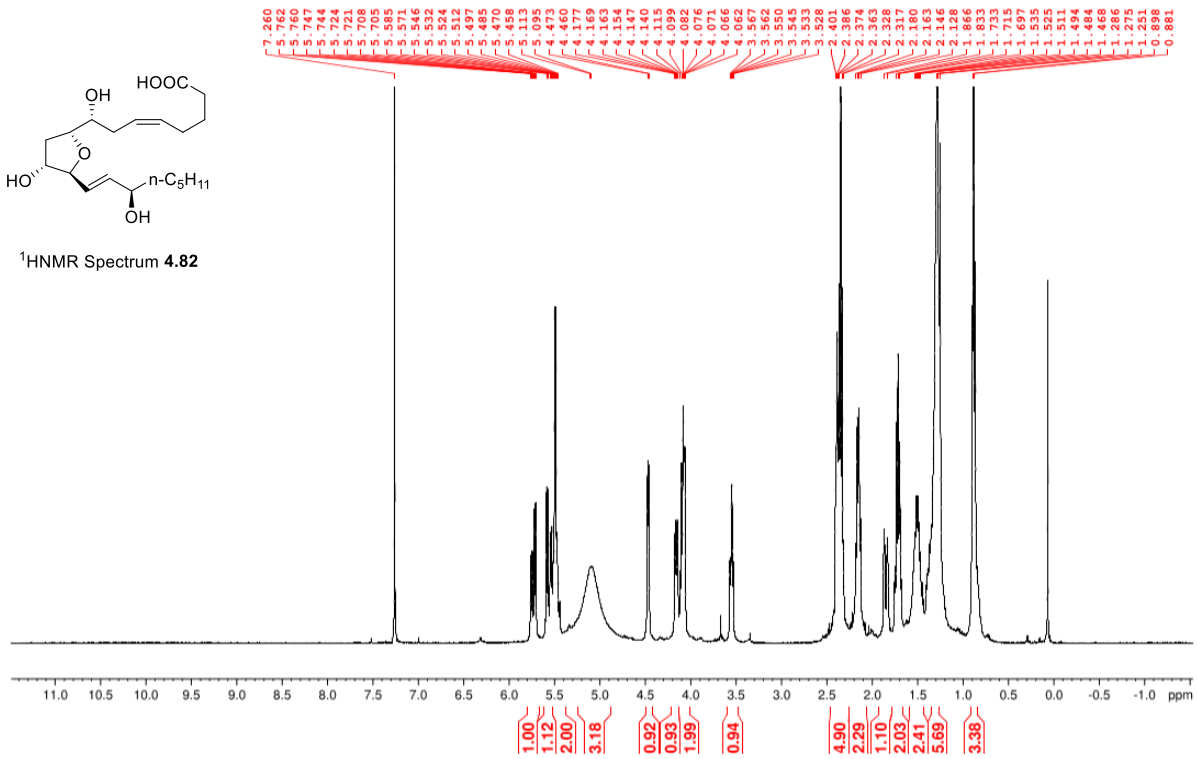

Figure A.83 ^{1}H NMR (400 MHz, $CDCl_3$) of **4.82**.

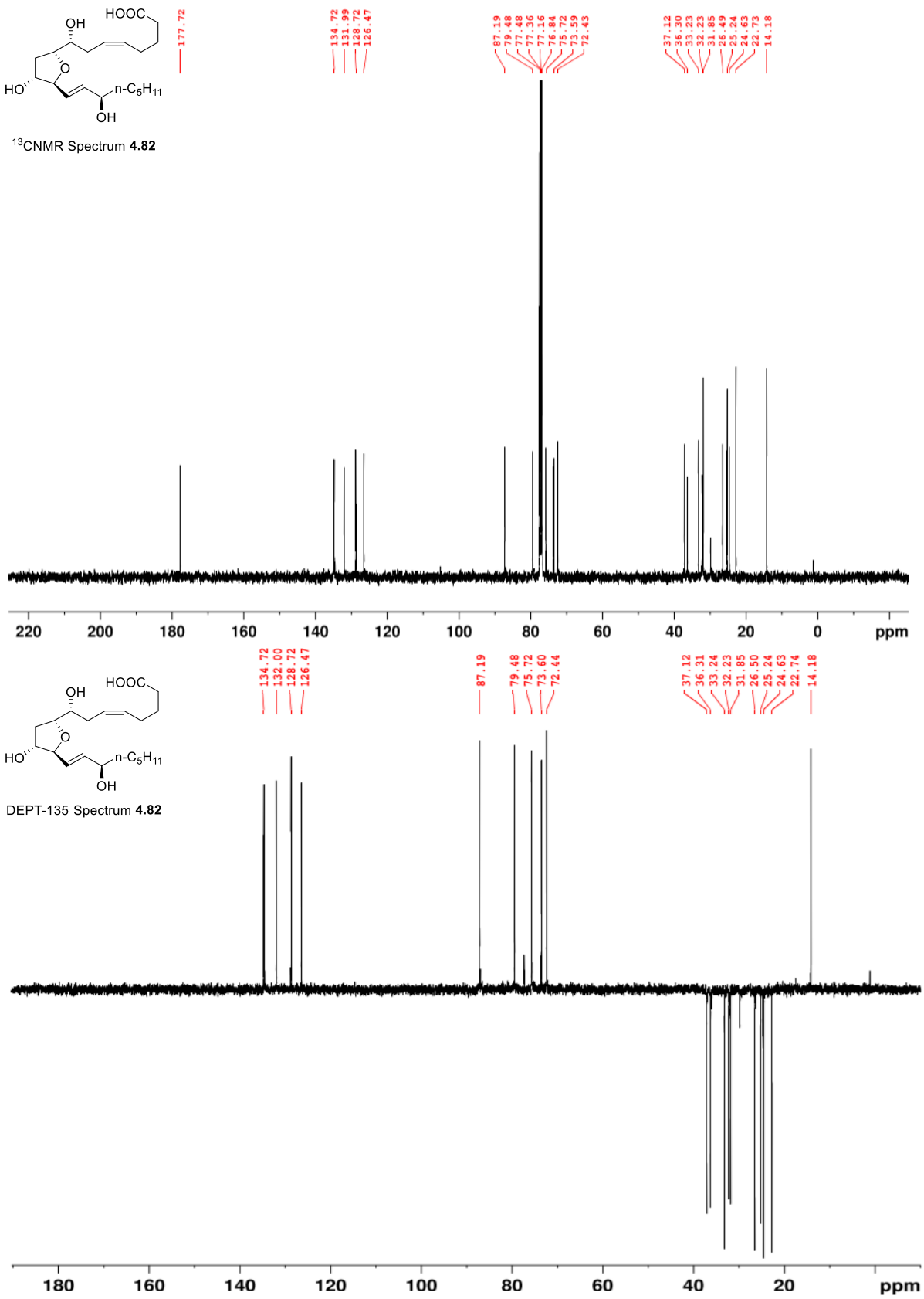

Figure A.84 ^{13}C NMR (100 MHz, $CDCl_3$) and DEPT-135 (100MHz, $CDCl_3$) of **4.82**.

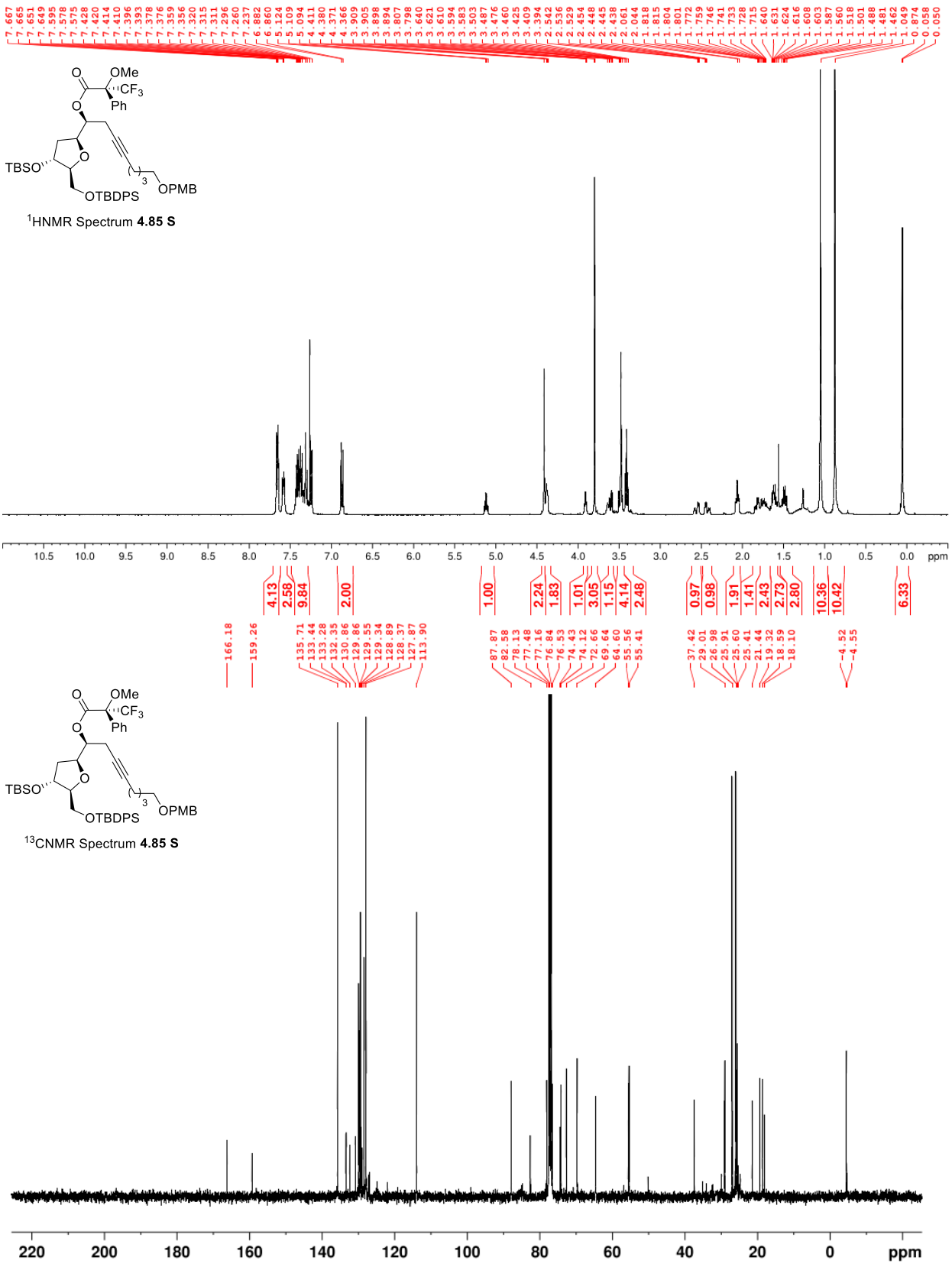

Figure A.85 ^{1}H NMR (400 MHz, $CDCl_3$) and ^{13}C NMR (100 MHz, $CDCl_3$) of **4.85 S**.

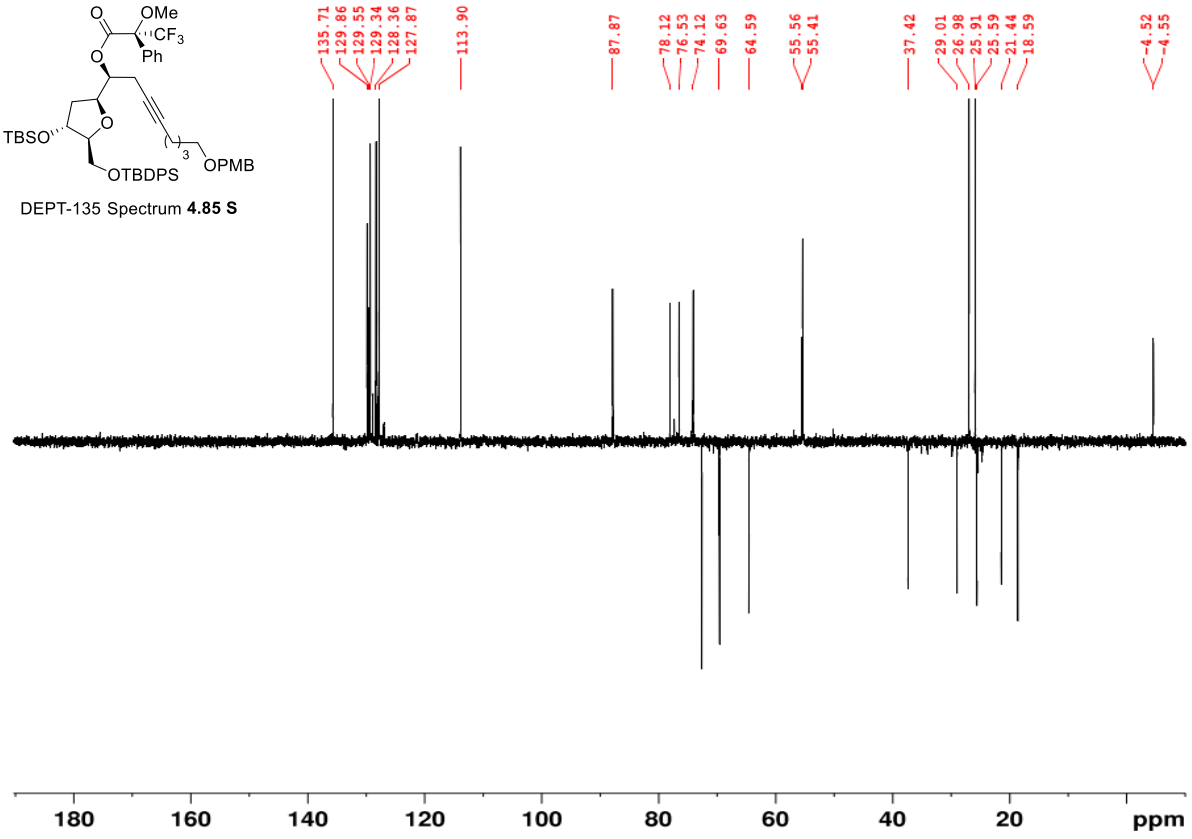

Figure A.86 DEPT-135 (100MHz, $CDCl_3$) of **4.85 S**.

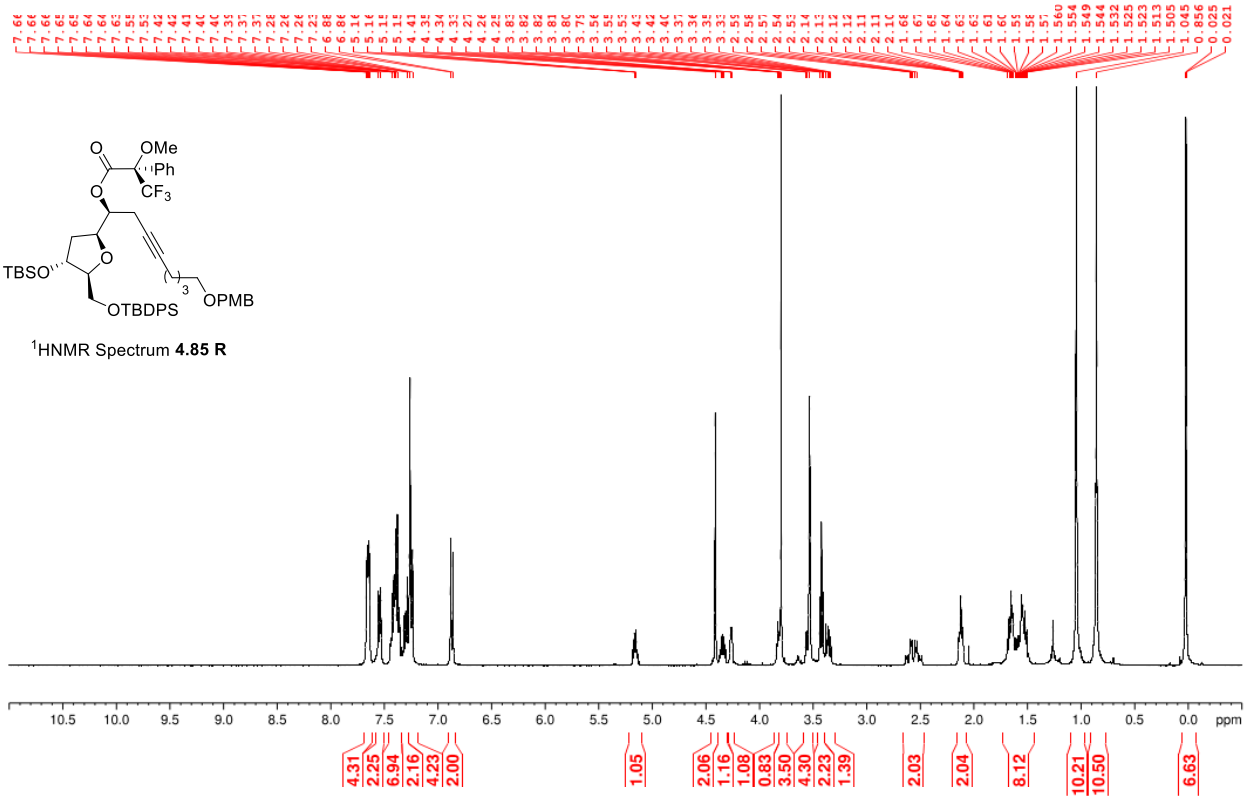

Figure A.87 ^{1}H NMR (400 MHz, $CDCl_3$) of **4.85 R**.

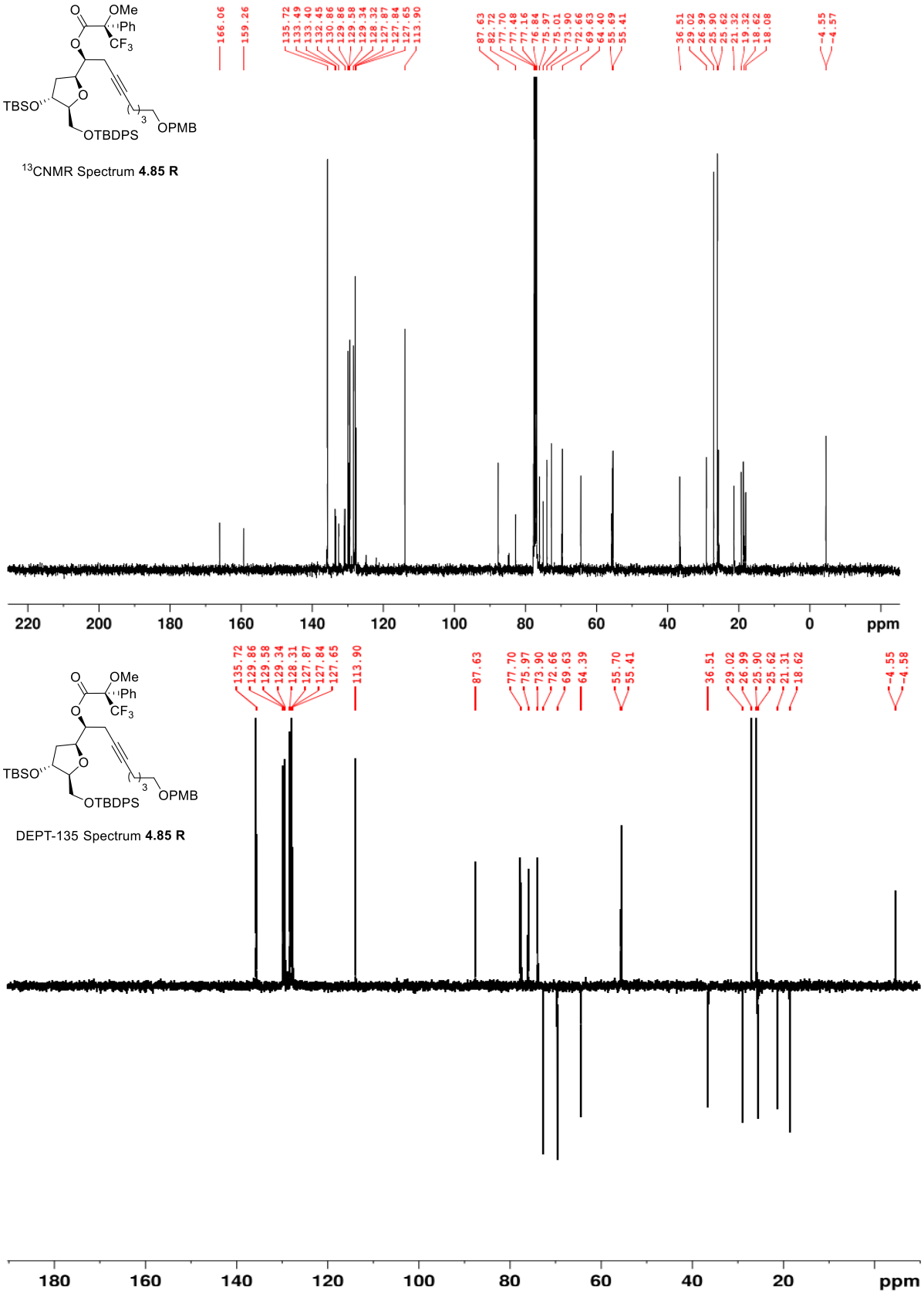

Figure A.88 ^{13}C NMR (100 MHz, $CDCl_3$) and DEPT-135 (100MHz, $CDCl_3$) of **4.85 R**.

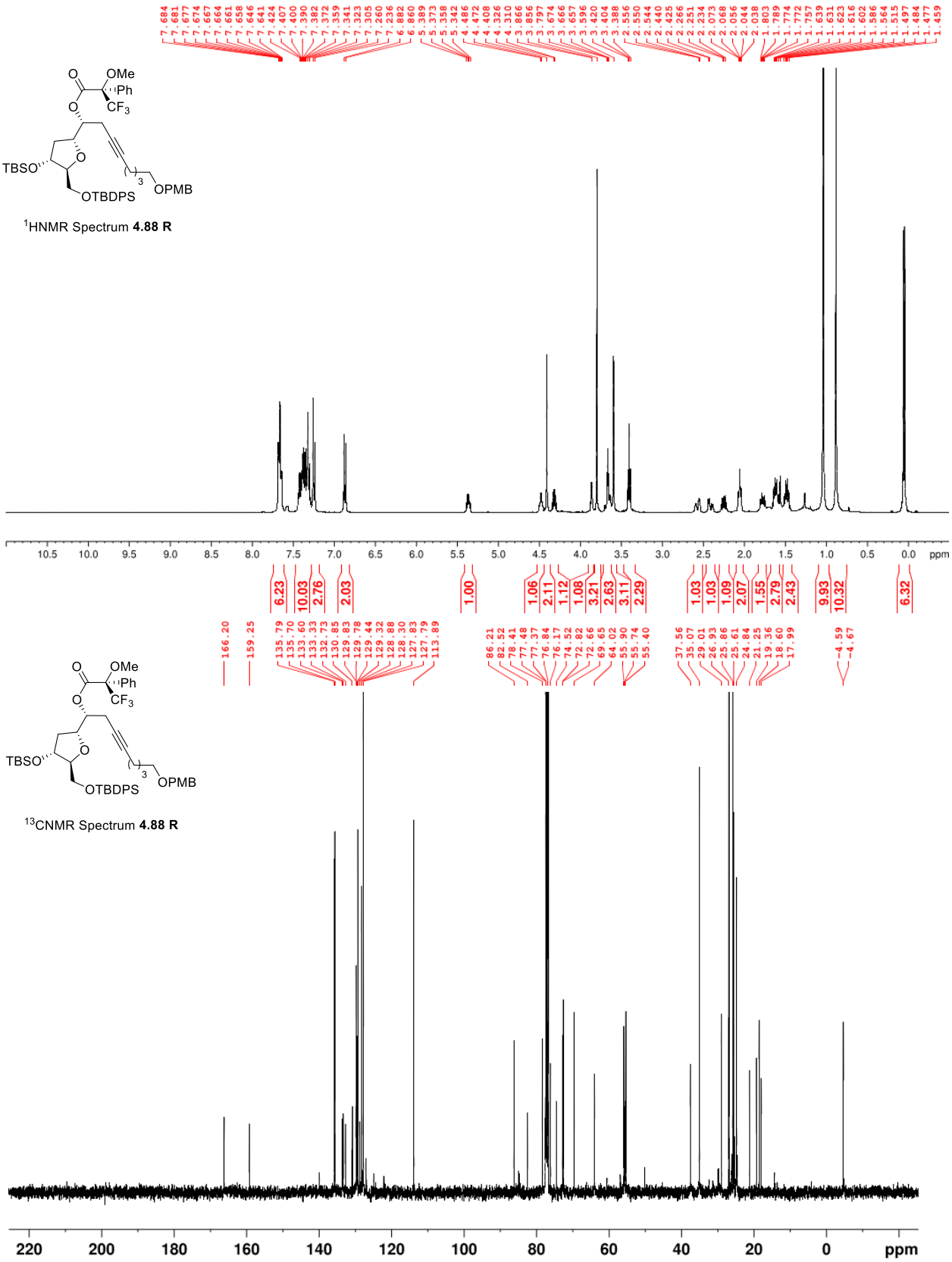

Figure A.89 ^{1}H NMR (400 MHz, $CDCl_3$) and ^{13}C NMR (100 MHz, $CDCl_3$) of **4.88 R**.

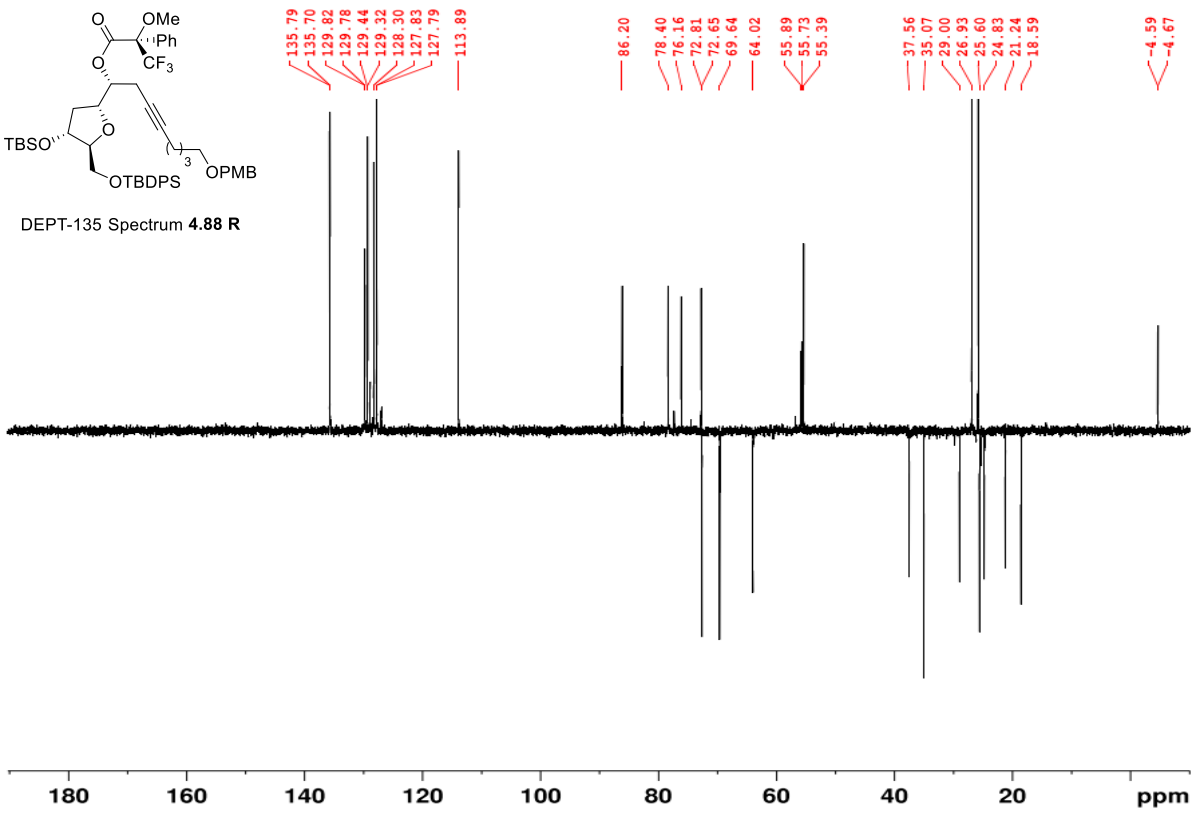

Figure A.90 DEPT-135 (100MHz, $CDCl_3$) of **4.88 R**.

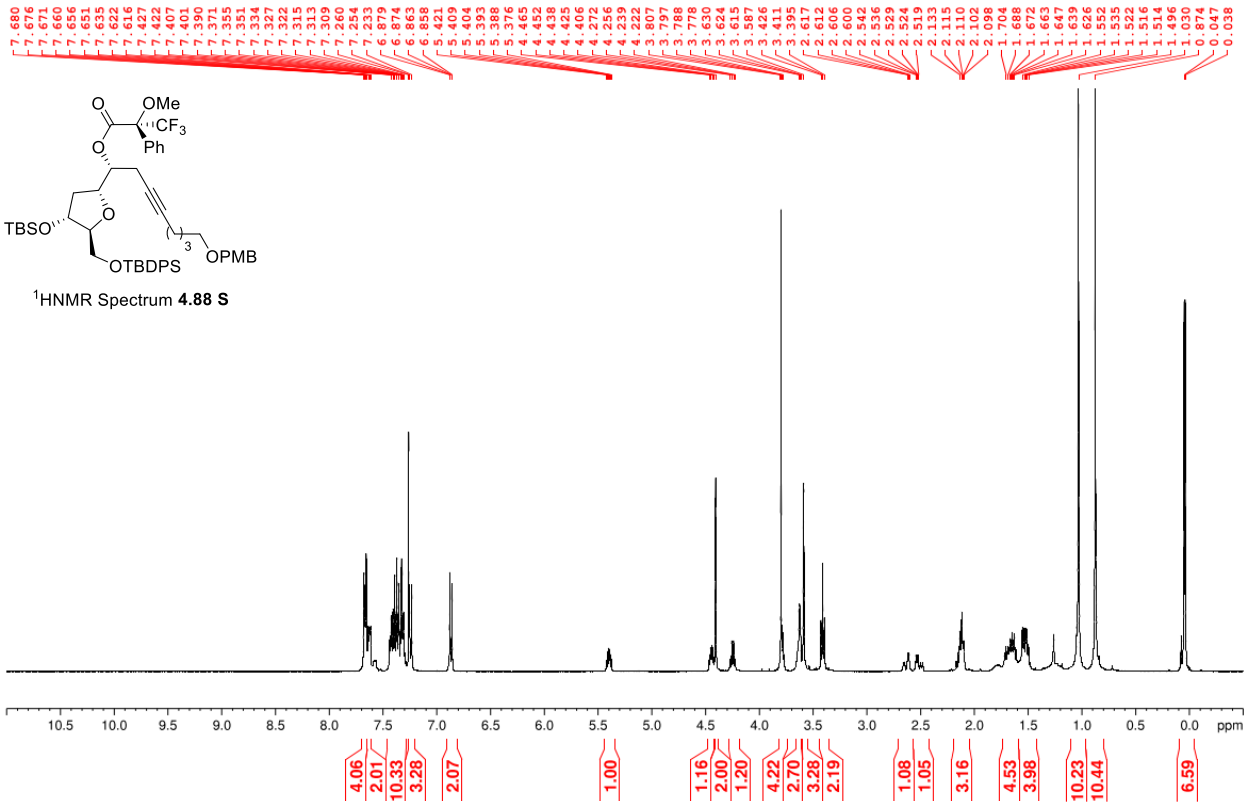

Figure A.91 ^{1}H NMR (400 MHz, $CDCl_3$) of **4.88 S**.

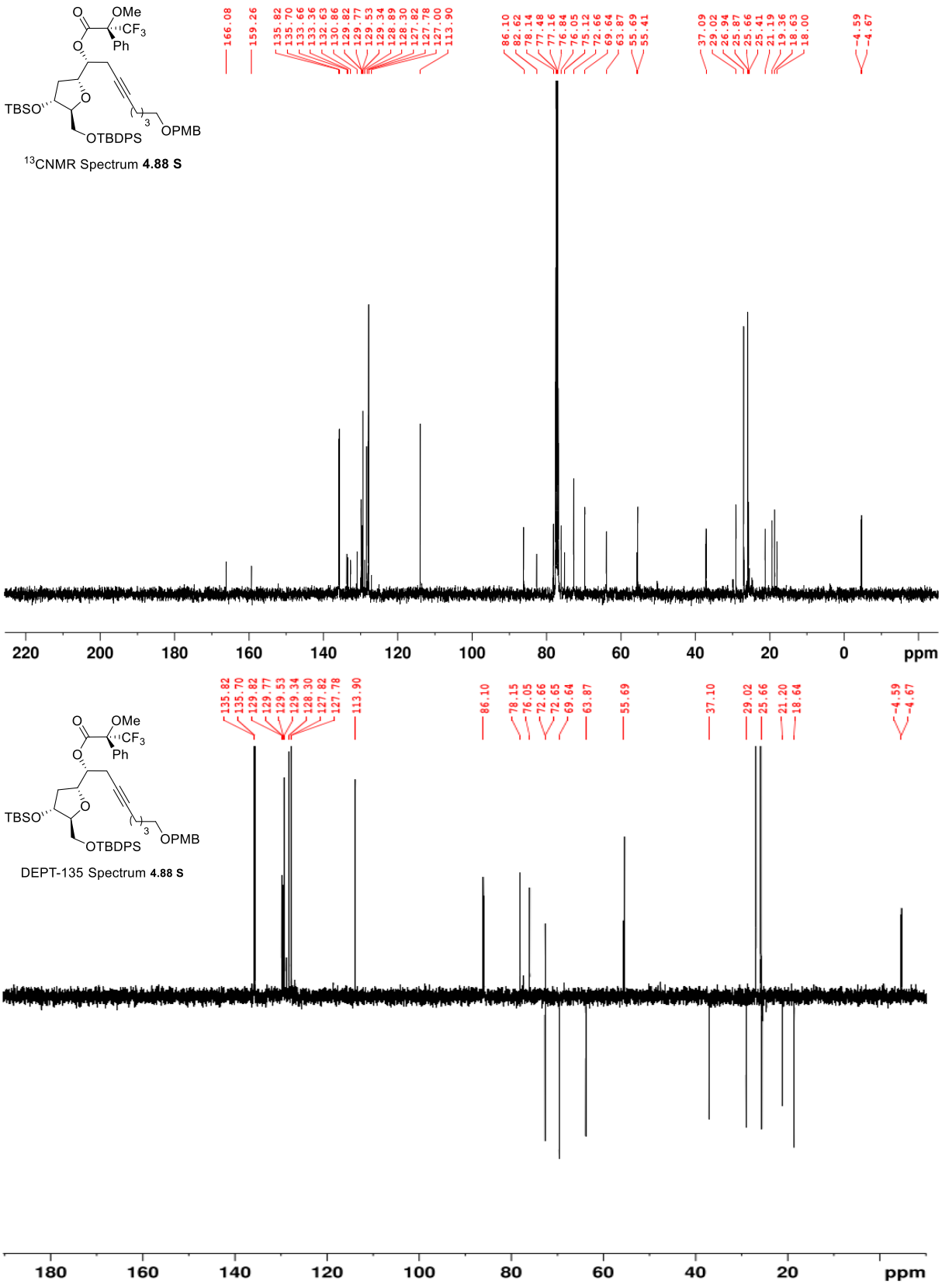

Figure A.92 ^{13}C NMR (100 MHz, $CDCl_3$) and DEPT-135 (100MHz, $CDCl_3$) of **4.88 S**.

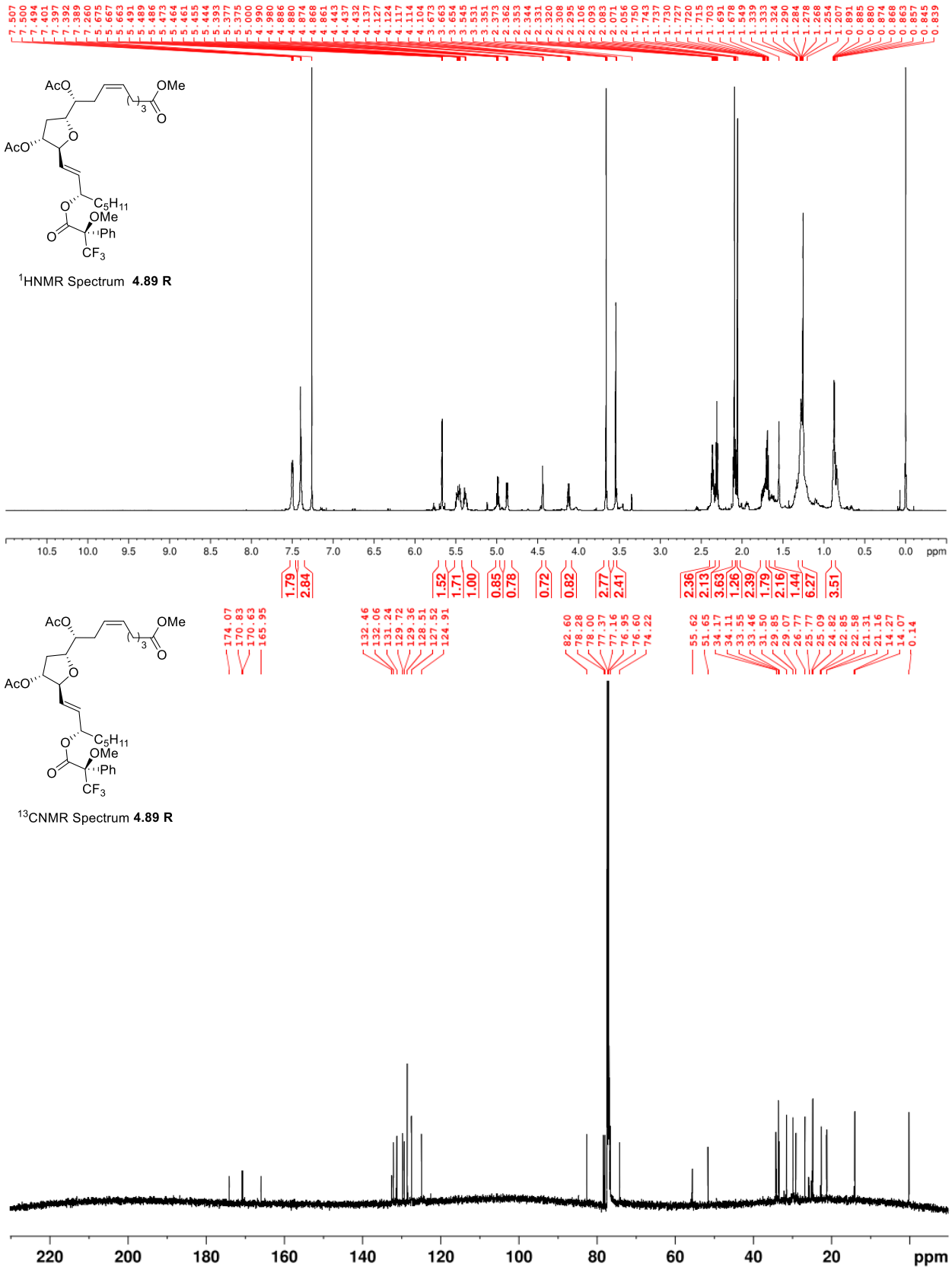

Figure A.93 ^{1}H NMR (600 MHz, $CDCl_3$) and ^{13}C NMR (125 MHz, $CDCl_3$) of **4.89 R**.

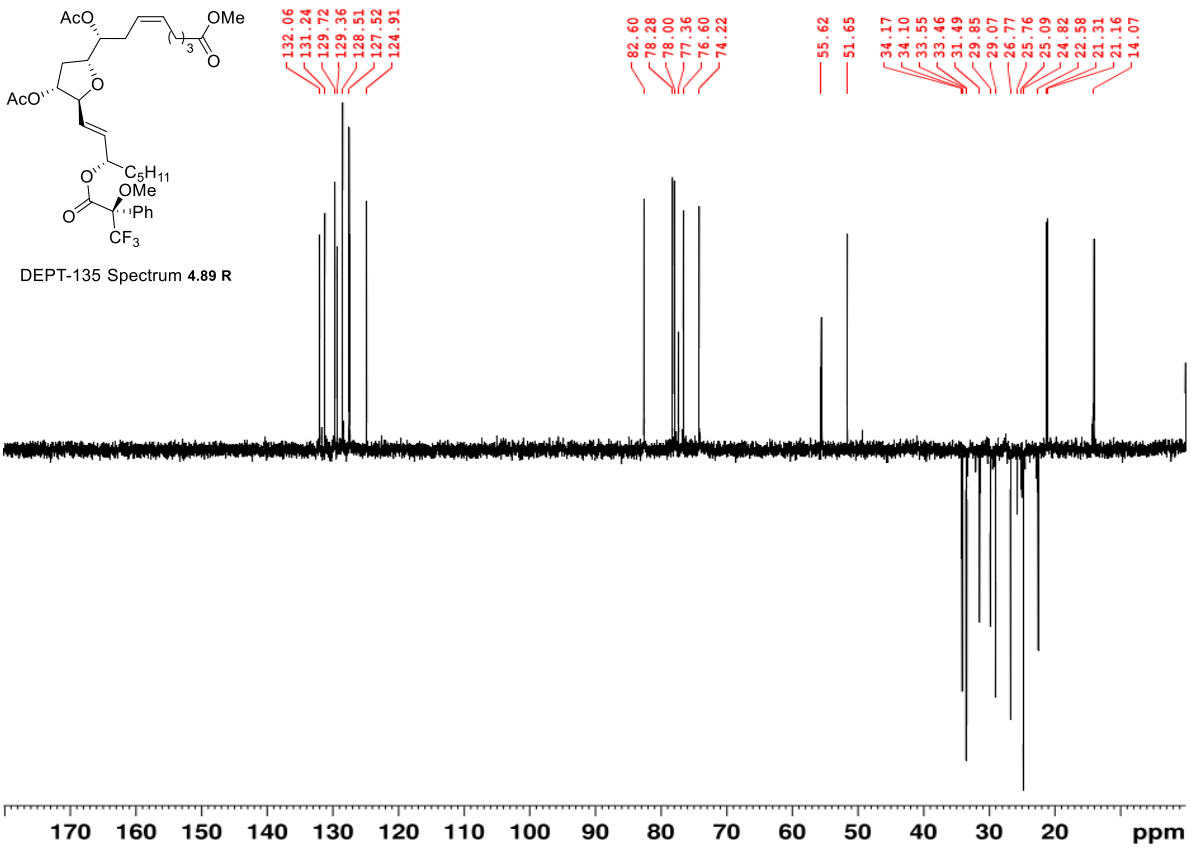

Figure A.94 DEPT-135 (125 MHz, $CDCl_3$) of **4.89 R**.

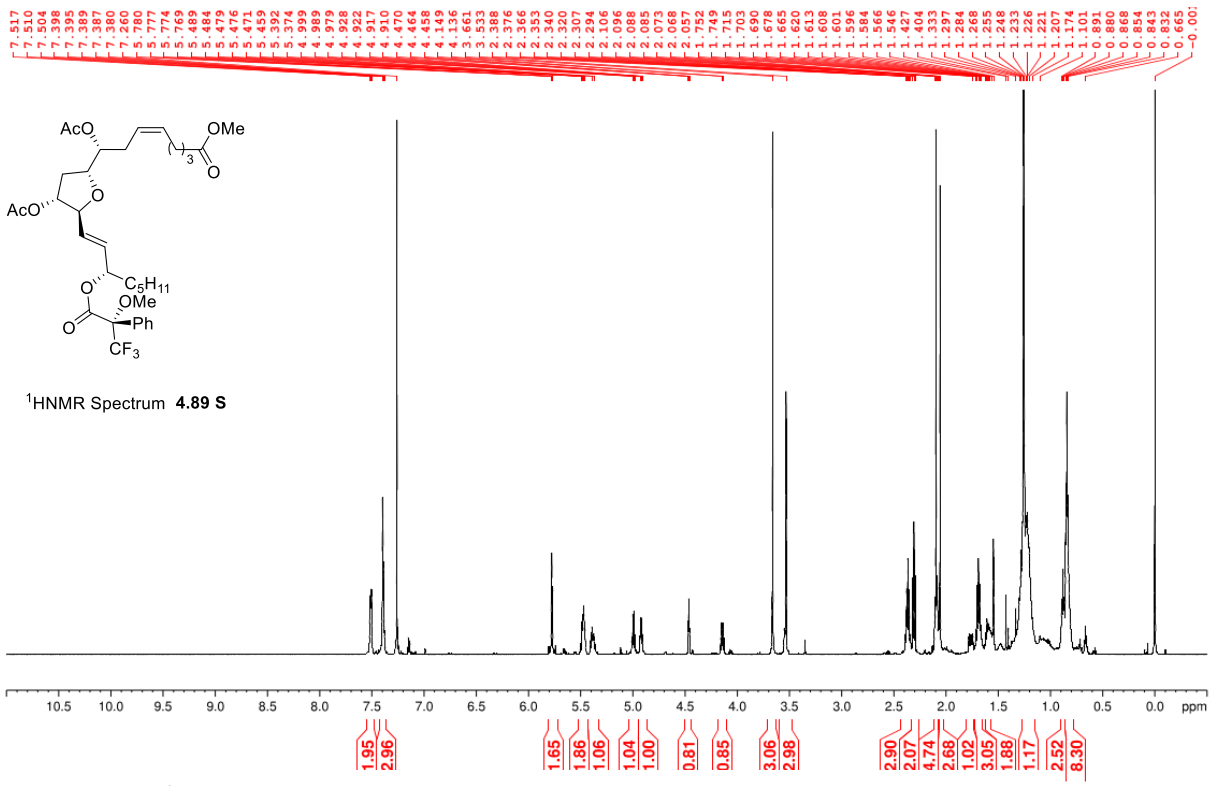

Figure A.95 ^{1}H NMR (600 MHz, $CDCl_3$) of **4.89 S**.

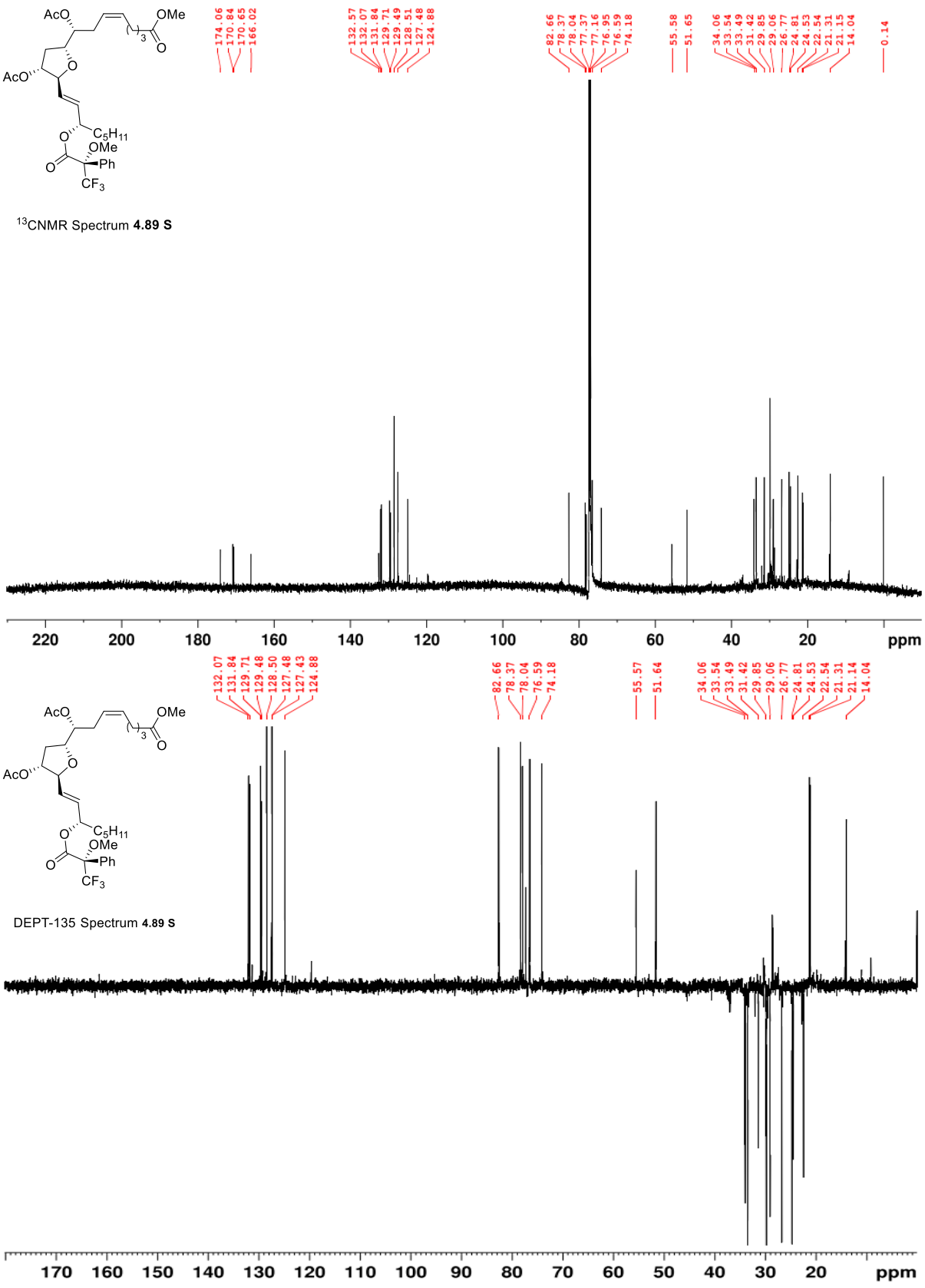

Figure A.96 ^{13}C NMR (125 MHz, $CDCl_3$) and DEPT-135 (125 MHz, $CDCl_3$) of **4.89 S**.